EVALUATION OF CORROSION PROTECTION SYSTEMS AND TESTING METHODS FOR CONVENTIONAL REINFORCING STEEL

By

Bin Ge
David Darwin
Carl E. Locke, Jr.
JoAnn Browning

A Report on Research Sponsored by

THE NATIONAL SCIENCE FOUNDATION

Research Grant No. CMS-9812716

THE KANSAS DEPARTMENT OF TRANSPORTATION
Contract Nos. C1131 and C1281

Structural Engineering and Engineering Materials
SM Report No. 73

THE UNIVERSITY OF KANSAS CENTER FOR RESEARCH

April 2004

ABSTRACT

The performance of several corrosion protection systems for conventional reinforcing steel are evaluated. These include a lower water-cement ratio, two different corrosion-inhibiting admixtures, Rheocrete (an organic corrosion inhibitor) and DCI-S (an inorganic corrosion inhibitor), and an alternative deicer CMA (calcium magnesium acetate).

The systems are evaluated using rapid macrocell tests developed at the University of Kansas, as well as two bench-scale techniques, the Southern Exposure (SE) and cracked beam (CB) tests, that are generally accepted in United States practice. Macrocell tests are conducted on bars symmetrically embedded in a mortar cylinder. Specimens are exposed to a simulated concrete pore solution with 1.6 molar ion concentration of sodium chloride. For the bench-scale tests, a 6.04 m ion concentration deicer solution is ponded on the top of both SE and CB specimens. The performance of the systems using the rapid macrocell tests and bench-scale tests is also compared.

The results indicate that in a salt environment, based on the SE and rapid tests, the higher water-cement ratio, the higher corrosion rate and the more negative the anode corrosion potential. Based on the SE tests, both inhibitors used in this study, Rheocrete and DCI-S, significantly reduce the corrosion rate of the steel. In the CB tests, however, neither a low water-cement ratio nor the corrosion inhibitors protect the reinforcing steel.

The results also indicate that in a CMA environment, for SE tests and CB tests, corrosion rates were extremely low. CMA, however, causes concrete to undergo severe surface deterioration in both tests. For the rapid macrocell tests, no conclusion

can be drawn because of corrosion that occurred on the exposed portion of the steel in the specimens.

The rapid macrocell test appears to provide an efficient method for evaluation steel performance in uncracked concrete exposed to a salt environment.

Key Words: chlorides; concrete; corrosion; corrosion testing; reinforcing bars

ACKNOWLEDGEMENTS

This report is based on research performed by Bin Ge in partial fulfillment of the requirements for the MSCE degree from the University of Kansas. Funding for this research was provided by the National Science Foundation, under NSF Grant No. CMS-9812716, and the Kansas Department of Transportation, under Contract Nos. C1131 and C1281. Additional support for this research was provided by Dupont Corporation, 3M Corporation, and LRM Industries. Oversight for the project was provided by Dan Scherschligt of the Kansas Department of Transportation.

TABLE OF CONTENTS

LIST OF TABLES

LIST OF FIGURES

CHAPTER 1

INTRODUCTION

1.1 General

The corrosion of reinforcing steel causes many highway structures in the United States to deteriorate before their design life is attained. One of the biggest causes of this problem is the use of deicing salts to keep the decks clear of ice and snow. In the United States, approximately 10 million tons of salt are applied per year to highways (Broomfield 1997). In 1979, the cost of bridge repairs in the federal-aid system due to corrosion damage was estimated to 6.3 billion dollars (Locke 1986). The Strategic Highway Research Program estimated that the cost of rehabilitation of chloride induced deteriorated bridge decks in the United States was $20 billion in 1986 and increasing at a rate of $500 million annually.

The need for cost-effective systems to protect reinforcing steel against corrosion is clear. Methods used to lengthen the service life of reinforced concrete include cathodic protection systems, epoxy coatings of reinforcing steel, lower water-cement ratio, corrosion inhibitors, alternative deicing materials, etc. Cathodic protection systems require constant monitoring to ensure effectiveness and, depending upon the application, may be maintenance intensive and expensive to install. Epoxy coating of steel became the corrosion prevention method of choice in the late 1970's. However, studies in recent years have begun to question the long-term efficacy of epoxy coating systems for providing corrosion durability. The research presented in this report addresses evaluating the following corrosion protection methods: lower water-cement ratio, corrosion inhibitors (Rheocrete and DCI-S) and alternative deicing material (calcium magnesium acetate).

1.2 Background and Literature Review

1.2.1 Background

Generally speaking, steel is well protected from corrosion when embedded in concrete. The concrete cover can provide a barrier to prevent ingress of moisture, oxygen, acidic gases and aggressive anions. More importantly, the cement paste in the concrete provides an alkaline environment that protects steel against corrosion. This corrosion resistance is due to a passivating or protective iron-oxide film that forms on the steel. The film is stable in the highly alkaline concrete environment (pH of 12.5 to 13.8) (Jones 1992). If the pH of the concrete pore solution is lowered, for example, by carbonation, due to the penetration of CO_2 in the concrete, or indirectly, due to the presence of aggressive ions, like Cl^-, found in deicing salts and seawater, the iron-oxide film becomes unstable and corrosion will occur. Since the volume of the corrosion products is four to six times larger than that of iron, the surrounding concrete cracks when the expansive pressure exceeds the tensile strength of concrete. Structural problems may arise due to the loss of bond between the steel and concrete or the reduced cross-sectional area of the steel.

1.2.2 Electrochemistry

The corrosion process is electrochemical in nature. Corrosion of steel in concrete is accompanied by a flow of electrons between anodic and cathodic areas on a metal surface. Four components are necessary for the development of a corrosion cell: (1) sufficient dissolved oxygen is required for reaction at the cathodic sites, (2) moisture is required to maintain low electrical resistivity in the concrete between the

Measurements have indicated that carbonation usually results in the reduction of the pH of the pore water to values below 9.5. Passive protection is lost once the pH drops below 11.5. Corrosion problems related to carbonation involve poor concrete quality, low concrete cover, and old age.

1.2.4 Chlorides

The depassivation mechanism due to chloride attack is different than occurs due to carbonation. Chlorides act as catalysts in the corrosion process when there is a sufficient concentration at the steel surface to break down the passive layer. Chlorides are not consumed, but help to break down the passive oxide layer on the steel and allow the corrosion process to proceed quickly. The reactions are as following:

$$Fe^{2+} + 4Cl^- \rightarrow (FeCl_4)^{2-} \quad (1.8)$$

$$(FeCl_4)^{2-} + 2H_2O \rightarrow Fe(OH)_2 + 2H^+ + 4Cl^- \quad (1.9)$$

To initiate corrosion, a "threshold" level of chlorides needs to present. In 1962, it was reported that the required minimum concentration of chloride in concrete immediately surrounding steel to initiate corrosion, the chloride corrosion threshold, is 0.15% *soluble* chloride, by weight of cement (Lewis 1962). For typical bridge deck concrete with a cement factor of 7, this is equivalent to 0.025% *soluble* chloride, by weight of concrete, or 0.59 kg *soluble* chloride per cubic meter of concrete. Subsequent research at FHWA laboratories estimated the corrosion threshold to be 0.033% *total* chloride, by weight of concrete. There are indications that the chloride corrosion threshold can vary between concrete in different bridges, depending on the type of cement and mix design used, which can affect the concentrations of tricalcium aluminate (C_3A) and hydroxyl ion (OH^-) in the concrete. In fact, it has been suggested that because of the role that hydroxyl ions play in protecting steel from corrosion, it is

anode and the cathode, and (3) anodes and (4) cathodes must develop on either a macro or micro scale to create a corrosion cell. Microcells may occur within millimeters, while the anodes and cathodes in a macrocell may be up to several meters apart. In a corrosion cell, iron corrodes or oxidizes at anodic sites to form ferrous iron with the release of two electrons:

$$Fe \rightleftarrows Fe^{2+} + 2e^{-} \quad (1.1)$$

Electrons flow through the steel to combine with oxygen and water at the cathode to form hydroxyl ions:

$$H_2O + \tfrac{1}{2} O_2 + 2e^{-} \rightleftarrows 2OH^{-} \quad (1.2)$$

Hydroxyl ions then combine with a ferrous ion at the anode to form ferrous hydroxide:

$$Fe^{2+} + 2OH^{-} \rightarrow Fe(OH)_2 \quad (1.3)$$

The ferrous hydroxide can react to form ferric hydroxide $Fe(OH)_3$ and hydrated ferric oxide or rust:

$$4Fe(OH)_2 + O_2 + 2H_2O \rightarrow 4Fe(OH)_3 \quad (1.4)$$

$$2Fe(OH)_3 \rightarrow Fe_2O_3 \cdot H_2O + 2H_2O \quad (1.5)$$

1.2.3 Carbonation

The term carbonation refers to the penetration of atmospheric carbon dioxide into the concrete matrix. Since dissolution of carbon dioxide in water gives rise to a weak (carbonic) acid, continuing diffusion of the gas into the concrete will result in the progressive neutralization and subsequent acidification of the pore water. This reaction occurs as:

$$CO_2 + H_2O \rightarrow H_2CO_3 \quad (1.6)$$

$$H_2CO_3 + Ca(OH)_2 \rightarrow CaCO_3 + 2H_2O \quad (1.7)$$

more appropriate to express the corrosion threshold in terms of the ratio of chloride to hydroxyl ion content, $[Cl^-]/[OH^-]$. Passivity is lost when $[Cl^-]/[OH^-]$ exceeds 0.6 (Hausmann 1967).

1.3 Corrosion Potential and Corrosion Rates

Corrosion potential is a thermodynamic property that indicates whether a metal in a given environment will have a tendency to corrode. The corrosion potential of steel in concrete is usually measured using a suitable reference electrode - 'half cell', either placed in contact with the surface of the structure or embedded within it. ASTM C 867 specifies that the measurement of the corrosion potential of steel in concrete be made with respect to a copper/copper sulfate half cell. However, it is more common to measure potentials in the laboratory using a saturated calomel electrode. Therefore, the criteria for corrosion of steel in concrete for both electrodes are given in Table1.1.

Corrosion rate is an indicator of how fast the metal will deteriorate. There are various ways to measure the corrosion rate of steel in concrete, including AC impedance, electrochemical noise and linear polarization-resistance. Linear polarization-resistance is the most suitable technique for measuring the corrosion rate of steel in concrete (Broomfield 1997). Linear polarization-resistance measurements use a noncorroding counter electrode and a reference electrode to establish a polarization curve by imposing a range of potentials on the metal and measuring the corresponding corrosion currents using a potentiostat. A portion of the polarization curve will exhibit a linear relationship, usually over a range of ±10 mV. The slope of the linear region is proportional to the resistance of the metal. The corrosion current density is then obtained by the equation:

$$I_{corr} = B/R_p \qquad (1.10)$$

where B is a constant (in concrete, B equals to 26 to 52 mV depending upon the passive or active condition of the steel) and R_p is the polarization resistance ($k\Omega \cdot cm^2$). Criteria relating linear polarization measurements to deterioration rates, similar to the ASTM C 876 criteria for half cell potentials, have been published (Broomfield et al. 1993). The major limitation of the linear polarization-resistance measurement is that the instantaneous corrosion rate may change with temperature, relative humidity and other factors. Therefore, measurements must be taken under different conditions to estimate the integrated corrosion.

An alternative approach to the linear polarization-resistance technique, which can monitor long-term corrosion performance, is macrocell corrosion rate measurement. The macrocell corrosion rate is determined by measuring the voltage drop across a resistor through which the macrocell corrosion current is flowing. The voltage drop is transformed to a corrosion rate using Faraday's law (Jones 1992):

$$r = ia/(nFD) \qquad (1.11)$$

where: r macrocell corrosion rate (thickness loss per unit time)

i current density (amperes/cm^2 or coulombs/cm^2.sec)

a atomic weight (55.84 g for iron)

n number of ion equivalents exchanged (For $Fe^{2+} = 2$)

F Faraday's constant (96500 amp-sec/equivalent)

D density of metal (7.87 g/cm^3 for steel)

For current density (i) in $\mu A/cm^2$,

$$r = 11.59i \ (\mu m/yr) \qquad (1.12)$$

Balance – Denver Instruments TR4102 Digital Scale;

Mortar Mixer – Model N-50, manufactured by Hobart Co.

2.2.2 Materials and Reagents

Reinforcing Steel – ASTM A 615 No. 16 (No. 5) reinforcing steel bars;

Cement – Type I portland cement;

Sand – ASTM C 778 graded Ottawa sand;

Epoxy Coating – Herberts O'Brien™ 7-1870 Nap-Guard Rebar Patch Kit;

Battery Grease – NCP-2 battery corrosion preventative spray, manufactured by Noco Co.;

Container – Consolidated Plastics company Inc. 178 x 191 mm (7 x 7½ in., diameter x height), 4.5 liter plastic container with lid;

Agar – Agar high gel strength [9002-18-0], manufactured by Sigma Chemical Co.;

NaCl – Fisher Scientific;

CMA (calcium magnesium acetate) – CMA100 deicer, manufactured by Cryotech Deicing Technology Co.;

NaOH- Fisher Scientific;

KOH - Fisher Scientific;

DCI-S – An inorganic corrosion inhibitor, consisting of calcium nitrite and a retarder, manufactured by W.R. Grace & Co.;

Rheocrete 222+ – An organic corrosion inhibitor, an aqueous mixture of amines and esters, manufactured by Master Builders, Inc.;

Rheobuild 3000FC – High range water reducing admixture, manufactured by Master Builders, Inc.;

Tube – Fisher Scientific Flexible clear plastic tubing, inner diameter 6.4 mm (1/4 in.), outer diameter 9.5 mm (3/8 in.) and wall thickness 1.6 mm (1/16 in.).

2.2.3 Mixture Design

Seven mortar mixtures are used in this study, as shown in Table 2.1.

2.2.4 Test Preparation

Specimen Fabrication - "Lollipop" style specimens are used in the rapid tests (Fig. 2.1). The specimen is 152 mm (6 in.) long and consists of a 127 mm (5 in.) long No. 16 [No.5] reinforcing bar symmetrically embedded 76 mm (3 in.) into a 30 mm (1.18 in.) diameter mortar cylinder. The mortar cylinder is 102 mm (4 in.) long and provides a 7 mm cover over the reinforcing bar.

1. *Preparation of Reinforcing Bar* – The reinforcing bars are cut to a length of 127 mm (5 in.). One end is drilled and tapped to receive a 10-24 x 9.5 mm (3/8 in.) screw to provide an electrical connection. The bar is then cleaned with acetone to remove oil, grease, and dirt. To prevent crevice corrosion of the steel at the interface between the steel and the surrounding mortar, two coats epoxy in a 15 mm (0.6 in.) wide band are applied around the bar, 70 mm (2.75 in.) from the nontapped end of the bar. Each layer of epoxy is allowed to dry for 4 hours at room temperature. The epoxy is mixed and applied following the manufacturer's instructions. The adhesion between steel and epoxy is achieved by sandblasting the region to be coated to remove mill scale prior to coating. Duct tape is used to prevent other parts of the specimen from being accidentally sandblasted in the process.

2. *Molding of Test Specimens* – The mold for the specimen is made from standard

commercial materials that are available at the local hardware store. The specimen mold and mold container are shown in Fig. 2.2.

The mold consists of the following items, as identified in Fig. 2.2:

A. No. 6.5 Rubber Stopper (Laboratory grade)

   A 16 mm (0.625 in.) diameter hole is drilled into the center of the stopper.

B. 25 mm (1 in.) to 25 mm (1 in.) PVC Fitting (ASTM D 2466), internal diameter 33 mm (1.3 in.)

   At one end of the fitting, the external diameter is machined down to a 41 mm (1.60 in.) so that it will fit into connector, D.

C. No. 9 Rubber Stopper (Laboratory grade)

   A 16 mm (0.625 in.) diameter hole is drilled into the center of the stopper.

D. 32 mm (1.25 in.) to 32 mm (1.25 in.) PVC Fitting (ASTM D 2466), internal diameter 42 mm (1.65 in.)

E. 1 in. PVC Pipe (ASTM D 2466), internal diameter 30 mm (1.18 in.)

   The pipe is cut into 102 mm (4 in.) lengths and sliced longitudinally along one side through its thickness.

F. Two Pieces of CCA Treated Wood: 51 mm (2 in.) x 203 mm (8 in.) x 381 mm (15 in.)

   The bottom piece has eight holes on the top surface centered two wide and four deep. Each hole is 52 mm (2 in.) in diameter and 6 mm (0.25 in.) deep.

The top piece has eight holes centered two wide and four deep. Each hole is 33 mm (1-5/16 in.) in diameter through half of the thickness of the wood piece, and 25 mm (1 in.) in diameter through the other half. Six holes are drilled through the thickness of the top and bottom pieces to receive 6 mm (0.25 in.) diameter threaded rod.

G. Six Threaded Rods: 6 mm (0.25 in.) x 305 mm (12 in.)

Each rod has one nut, one wing nut, and two washers.

Assembly of the mold is explained in the following steps (this assembly procedure is taken from Martinez et al. (1990)):

a. The tapped end of the prepared reinforcing bar is inserted through the hole of the small rubber stopper, A, beginning at the widest end of the stopper. The distance between the untapped end and the rubber stopper is 76 mm (3 in.).

b. The rubber stopper is inserted in the machined end of the small connector, B. The widest end of the small rubber stopper has to be in contact with the shoulder (an integral ring) on the internal surface of the small connector.

c. The large rubber stopper, C, is inserted in the cut end of the larger connector, D, until it makes contact with the shoulder on the inside surface of the connector.

d. The turned end of the small connector, B, is inserted in the free end of the large connector, D. At the same time, the tapped end of the reinforcing bar is inserted through the hole of the large rubber stopper, C.

e. The longitudinal slice along the side of the PVC pipe, E, is taped with masking tape. The pipe is then inserted in the free end of the small connector.

f. The assembled mold is placed between the wooden boards, F, in the holes provided. The threaded rods, G, are then inserted between the wooden boards. The rods are used to hold the molds together and center the reinforcing bar by tightening or loosening the nuts on the rods.

3. *Casting* – The mortar is mixed following the procedures in ASTM C 305. The specimens are cast in three layers. Each layer is rodded 25 times with a 3.2 mm (0.125 in.) diameter 305 mm (12 in.) long rod, and vibrated on a vibrating table at amplitude of 0.15 mm (0.006 in.) and a frequency of 60 Hz for 30 sec.

4. *Curing* – The specimens are cured for 24 hours in the molds at room temperature and then removed from the molds and placed in a curing tank containing lime-saturated water at a temperature of 23.3 ± 1.1°C (74 ± 2°F) for 13 days. The total curing time is two weeks.

Mortar Fill – The mortar fill, which consists of the same mixture as used in the test specimen, is cast in a 25 mm (1 in.) thick layer using a metal cookie sheet as the form. The fill is cast in the same time as the specimen. After one day, the mortar is broken into pieces and stored until the time of test.

Concrete Pore Solution – The constituents in the pore solution are based on the analysis of Fazammehr (1985). For this study, one liter of simulated pore solution contains 974.8 g of distilled water, 16.50 g of KOH, 17.55 g of NaOH.

Deicer Pore Solution – 1.6 molal ion concentration of deicer is used in this study, which consists of 45.6 g of NaCl or 100 g of CMA for each liter of pore solution.

Salt Bridge – A salt bridge consists a conductive gel in a flexible tube. The gel is made with 4.5 grams of agar, 30 grams of potassium chloride (KCl), and 100 grams of distilled water, enough to produce 4 salt bridges with a total length of 1.8 m (6 ft). The constituents are mixed together and heated over a hot plate at 200°C (400°F) for 2 minutes and then siphoned into four flexible latex tubes, each 0.45 m (1.5 ft) long. The salt bridges are then placed in boiling water for one hour to finish the gel process. The gel in the tube must be continuous, without interruption by air bubbles.

Terminal Box – A terminal box is constructed to ease the process of taking electrical measurements for a large number of test specimens. Six pairs of binding posts are attached to the top of the box. A 10-ohm resistor is connected across each pair of posts.

Air Scrubber – Compressed air is used to supply oxygen to the cathode solution. An air scrubber is used to remove carbon dioxide from compressed air, since CO_2 lowers the pH of the pore solution. The air scrubber consists of a 19 liter (5 gallon) plastic container filled with 1M NaOH solution. More NaOH is added, as needed, to maintain the pH of the solution at least 12.5.

2.2.5 Test Set Up and Data Collection

After 14 days, the specimen is taken from the curing tank and its surface is thoroughly dried using compressed air. A copper wire is then attached to the top end of the specimen with a 6 mm (0.25 in.) 10-24 steel screw, and the connection is covered with epoxy. After the epoxy is dry, the mortar is cleaned from the exposed reinforcing steel if there is any. Battery grease is then applied to this bare section of the bar.

The test requires two plastic containers. The anode is assembled by placing one specimen inside a container, along with crushed mortar fill and a simulated pore solution containing a deicer. The cathode is assembled by placing two specimens in a second container, along with crushed mortar fill and a simulated pore solution. Ionic conductivity is established between the solutions in the two containers using a salt bridge. Scrubbed air is bubbled into the liquid surrounding the cathode to insure an adequate supply of oxygen. The anode and cathode specimens are connected to two biding posts that are connected by a 10-ohm resistor. A schematic of the test setup is shown in Fig. 2.3.

The voltage across the 10-ohm resistor and the corrosion potential of the anode and cathode are measured once a day for the first week and once a week after that. To measure the corrosion potentials of the anode and the cathode, an open electrical circuit is obtained by disconnecting the wires from the binding posts. After two hours, readings are taken by connecting one lead from a digital voltmeter to the binding post corresponding to the bar in question and the other lead to a standard calomel electrode immersed in the solution.

Rapid tests are typically run for 15 weeks. During the test period, any rust that forms on the bare portion of the specimen is removed and battery grease is reapplied.

When each test is set up, the specimens are checked to ensure that quality is consistent. The anode specimens are those have minimal cracks and pores based on visual inspection. Specimens not used as anodes are used as the cathodes.

2.2.6 Tests Performed

For this study, 94 rapid tests were performed. The material combinations and the number of specimens cast are given in Table 2.2, where the M stands for

macrocell test, NO for no inhibitor, RH for Rheocrete 222+, DC for DCI-S, 50, 45, 35 for water-cement ratio 0.50, 0.45, 0.35 respectively, N for NaCl and C for CMA.

2.3 Bench-Scale Tests

The Southern Exposure (SE) and the cracked beam (CB) tests are used to evaluate the corrosion resistance of conventional steel in concrete for two different water-cement ratios, with and without corrosion inhibitors, and different deicing solutions. During the tests, the macrocell corrosion rate, corrosion potential, and mat-to-mat resistance between the anode and the cathode bars are measured.

2.3.1 Apparatus

Calomel electrode – Fisher Scientific Standard Pre-filled Calomel Reference Electrode;

Copper-Copper Sulfate electrode – MCM Electrode RE-5, manufactured by McMiller Co.;

Millivoltmeter – Hewlett-Packard 3456A Digital Voltmeter;

AC Ohm meter – Hewlett-Packard 4338A Milliohmmeter;

Balance – Denver Instruments TR4102 Digital Scale;

Concrete mixer – Lancaster Counter Current Batch Mixer, manufactured by Lancaster Iron works, Inc.

2.3.2 Materials and Reagents

Reinforcing Steel – ASTM A 615 No. 16 (No. 5) reinforcing steel bars;

Cement – Type I portland cement;

Coarse Aggregate – bulk specific gravity ssd = 2.58, absorption dry = 2.27%, unit weight = 1.54 kg/m^3 (95.9 lb/ft^3), 19 mm (3/4 in.) nominal maximum size;

Fine Aggregate – bulk specific gravity ssd = 2.60, absorption dry = 0.78%, fineness modulus = 2.51;

Epoxy Coating – Ceilcote 615 Ceilgard, manufactured by Ceilcote Co.

NaCl – Fisher Scientific;

CMA – CMA100 deicer, manufactured by Cryotech Deicing Technology Co.;

DCI-S – An inorganic corrosion inhibitor, consisting of calcium nitrite and retarder, manufactured by W.R. Grace & Co.;

Rheocrete 222+ – An organic corrosion inhibitor, an aqueous mixture of amines and esters, manufactured by Master Builders, Inc.;

Air Entraining Agent (AE)– Vinsol Rison, from Master Builders Inc.;

Silicone Caulk – The caulk, 100 percent silicone manufactured by Macklenburg-Duncan.

2.3.3 Mixture Design

The mixture designs used in this study are shown in Table 2.3.

2.3.4 Test preparation

Specimen fabrication - The SE specimen (Fig. 2.4) consists of a small slab containing two mats of reinforcing steel. The slab is 178 mm (7 in.) thick by 305 mm (12 in.) square. The top mat of steel consists of two bars; the bottom mat consists of four bars. A dam is cast around the top surface at the same time when the specimen is cast. The CB specimen (Fig. 2.4) is half the width of the SE specimen, with one bar

on top and two bars on the bottom. A dam is also cast around the top surface of the specimen. "Cracks" are formed in the specimen using a 0.30 mm thick stainless steel shim, cast into the concrete and removed 24 hours after casting. The "crack" leaves a direct path to the top reinforcing steel.

1. *Preparation of Reinforcing Bar* – Each reinforcing bar is cut to a length of 305 mm (12 in.). Both ends of the bar are drilled and tapped for a 10-24 threaded bolt to a depth of 13 mm (0.5 in.). The bar is then cleaned in an acetone bath to remove oil, grease, and dirt.

2. *Mold Assembly* – The molds are made so that the specimen is cast upside down. Each mold is made out of 19 mm (0.75 in.) thick plywood and consists of four sides and a bottom. A beveled rectangular piece of wood that is slightly smaller than the bottom is bolted to the bottom to create a dam in the edge of the specimen. The five pieces are fastened with clamps and the inside corners are sealed with caulk. Small holes, drilled in two side molds, are used to support the reinforcing bars using bolts. A slot is cut in the bottom of each CB mold so that a 0.30 mm thick stainless steel shim can be inserted, creating a uniform crack in the final beam. The wood forming material is coated with mineral oil for ease in removing the specimen.

3. *Casting* – Concrete is mixed in accordance with the requirements for mechanical mixing in ASTM C 192. The specimens are cast in two layers. Each layer is vibrated on a vibrating table at an amplitude of 0.15 mm (0.006 in.) and a frequency of 60 Hz for 30 sec. The second layer is finished with a wooden float.

4. *Curing* – After the specimens are cast, the specimens are cured in their mold for 24 hours at room temperature. The specimens are then removed from

the molds and cured in a plastic bag with distilled water for 48 hours at room temperature. The shims in the CB specimens are removed prior to placement in the bag. The specimens are removed from the bag at the age of 3 days and air cured for 25 days at room temperature, when the corrosion tests begin.

5. *Epoxy and Wiring* – One day before testing begins, copper wires are used to connect the top and bottom steel to the exterior binding post on the terminal box. Two coats of concrete epoxy are applied to all four sides of the specimen and the dam. The epoxy is mixed and applied according to manufacturer's recommendations.

Deicer Solution – 6.04 molal ion concentration deicer solutions are used in this study. They are listed in Table 2.4.

Terminal Box – A terminal box is constructed to ease the process of taking electrical measurements for a large number of test specimens. Six pairs of binding posts are attached to the top of the box. A 10-ohm resistor is connected across each pair of posts.

Heating Tent [This description is adapted from Senecal et al. (1995)]– The heating tent is designed to be mobile and can hold 6 SE and 6 CB specimens at once. The tent is an oblong structure, 1.2 m (3.5 feet) high, 1.33 m (4 feet) wide, and 2.67 m (8 feet) long. The roof and ends are made of 19 mm (0.75 in.) thick plywood and are connected together by six 2.67 m (8 feet) studs. The sides of the tent are covered in two layers of plastic, separated by a 25 mm (1 in.) dead space. Three heating lamps (250 watts) are evenly spaced along the roof of the tent. When the tent is placed over the specimens, the lamps are 4450 mm (18 in.) above the specimens. A thermostat with a temperature probe senses the temperature within the tent and maintains a temperature range of 38°C±1.5° (100°F±3°F).

2.3.5 Test Set up and Data Collection

The test procedure is the same for both the SE and CB tests. The specimens are placed on wooden skids to allow for air circulation under the specimens. The top and bottom mats are connected to separate biding posts. The posts are connected by a 10-ohm resistor (Fig. 2.4). The specimens are subjected to alternative wetting and drying cycles designed to accelerate the corrosion process. A cycle consists of:

a. Ponding-drying cycle: Four days of ponding with a 6.04 molal ion concentration deicer solution at room temperature (the specimens are covered with plastic to reduce evaporation). Three days of drying at 38°C±1.5° (100°F±3°F) (the specimens are under a tent). This cycle is repeated for 12 weeks.

b. Ponding cycle: Twelve weeks of continuous ponding with a 6.04 molal ion concentration deicer solution at room temperature (the specimens are covered with plastic).

The two cycles are repeated four times, with a total test period of 96 weeks.

On the fourth day of each cycle, the voltage drop across the resistor, the mat-to-mat resistance and the corrosion potentials of both mats are measured. The voltage drop is measured first. The mat-to mat resistance, which is the resistance between the two layers of reinforcing steel, is then measured using an AC Ohm meter. To measure the mat-to-mat resistance, the circuit must be broken. The corrosion potentials of both mats of steel are taken after the macrocell has been disconnected for 2 hours. During the ponding-drying cycle, the corrosion potential is taken immediately after the deicer solution is removed. The CSE test procedure described in ASTM C 876 is used.

During the ponding cycle, corrosion potential is obtained by immersing a standard calomel electrode in the solution.

2.3.6 Tests Performed

For this study, 36 SE tests and 27 CB tests were performed. The material combinations and the number of specimens cast are given in Table 2.5.

CHAPTER 3

RESULTS AND EVALUATION

This chapter presents results of the tests described in Chapter 2 and an evaluation of those results. The chapter is divided into three sections, covering (1) the results of the rapid tests, (2) the results of the bench-scale tests, and (3) a comparison of the two test methods.

3.1 Rapid Tests

This section summarizes the results of the rapid macrocell tests. The results are based on the average test results, with individual tests shown in Figures A1.a through A19.f of Appendix A. Test series are identified as follows:

M = Macrocell tests

No = No inhibitor

RH = Rheocrete 222^{+}

DC = DCI-S

50, 40, 35 = water-cement ratios 0.50, 0.40, 0.35, respectively

N, C = NaCl and CMA (calcium magnesium acetate), respectively

In some tests, the corrosion rates appear to be negative; that is, the cathode, rather than the anode, appears to be corroding. This occurred in the early stages of small number of tests. In those cases, the corrosion rate is not used to determine the average corrosion rate.

During the tests, the specimens are checked periodically. Any rust on the exposed portion of the reinforcing bars is removed and battery grease is reapplied to the bars. In some cases, the corrosion potential and the corrosion rate shift significantly after the rust is removed. An example is shown in Fig. A5: On day 63,

rust was removed from specimen M-RH 35 NaCl-4 after the readings were taken. Figure A5.a shows that the anode corrosion potential (with respect to an SCE) shifted from –0.56 V to –0.31 V. Figure A5.e shows that the corrosion rate dropped from 8.0 to 0.9 μm/yr. As demonstrated by this example, the corrosion of the exposed portion of the steel dominated the corrosion performance of some of the specimens.

An inspection of the specimens indicated that the mortar in some of the lollipop specimens contained surface cracks. To determine the effect of the cracks on the behavior of the specimens, macrocell tests were performed with specimens clad in mortar with water-cement ratios of 0.50, 0.45, and 0.35 and exposed to NaCl. For each water-cement ratio, two batches in which the specimens were not cracked and one batch in which the specimens contained surface cracks were evaluated. The results of these tests are shown in Figs. 3.1 through 3.6. For each water-cement ratio, the corrosion rate is actually lowest for the specimens containing cracks. At water-cement ratios 0.50 and 0.35, the average corrosion potential of the specimens with the cracked mortar is least negative. For a water-cement ratio of 0.45, the corrosion potential of the cracked specimens is the most negative.

These comparisons show that the presence of the small cracks in the surface of the specimens does not measurably affect the test results.

The balance of this section describes the appearance of the specimens and the influence of water-cement ratio, deicer solution, and corrosion inhibitors.

3.1.1 Appearance of Specimens

The specimens were inspected at the completion of the 105-day test period. Rust was found on the exposed portion of the reinforcing bars in most anode

specimens, as shown in Fig. 3.7, while no rust was found on the exposed portion of the reinforcing bars in the cathode specimens (Fig. 3.8).

The mortar was removed from the bars for further inspection. Most anode specimens without corrosion inhibitors had rust on the steel that had been covered by the mortar, as shown in Fig. 3.9. No rust was visible on the mortar-covered portion of anode specimens when the mortar contained corrosion inhibitors (Fig. 3.10); this was the case for the covered portion of the reinforcing bars in all cathode specimens (Fig. 3.11).

3.1.2 Effect of Water-Cement Ratio

The results of the tests to evaluate the effect of water-cement ratio on corrosion behavior are shown in Figs. 3.12 through 3.23. For each comparison, the figures are paired, showing average corrosion rate and average corrosion potential, respectively. Overall, as expected, the specimens with the lower water-cement ratio mortar exhibited the lower corrosion rate, although there were some exceptions.

For the specimens exposed to NaCl in which the mortar did not contain a corrosion inhibitor, the average corrosion rates at 15 weeks for water-cement ratios 0.50, 0.45, and 0.35 are 4.3 μm/yr, 5.5 μm/yr, and 1.8 μm/yr, respectively (Fig 3.12). The average corrosion rate for the specimens with w/c = 0.50, however, is much higher than the other two specimens from week 2 through week 11 (14 through 77 days). As shown in Fig. 3.13, the average corrosion potential of the anode specimens becomes progressively more negative as the water-cement ratio increases. For the specimens cast with corrosion inhibitors (Figs. 3.14 through 3.17), the corrosion rate is higher and corrosion potential is more negative for a water-cement ratio of 0.45 than for a water-cement ratio of 0.35. The results for specimens exposed to CMA are

shown in Figs. 3.18 through 3.23. For these specimens, there is no clear correlation between corrosion performance and water-cement ratio. In fact, it appears that the specimens with the higher water-cement ratios perform better. In all likelihood, these results, including the relatively high measured corrosion rates (1 to 2 μm/yr), are due to corrosion on the exposed portion of the bars. This observation strongly suggests that the specimen design should be modified so that no portion of the reinforcing bar is exposed.

3.1.3 Effect of Deicer Solutions

The corrosion performance of specimens with water-cement ratios of 0.45 and 0.35 with and without corrosion inhibitors is compared in Figs. 3.24 through 3.29. The results are not particularly useful due to the dominance of the effect of corrosion on the exposed portion of the bars, especially for the specimens exposed to CMA. The only observation that can be made is that, for these specimens, the corrosion rate at the conclusion of the tests (105 days) is higher for specimens in NaCl for a water-cement ratio of 0.45 and higher with the specimens exposed to CMA for water-cement ratio of 0.35. As will be shown for the bench-scale tests, bars exposed to CMA exhibit very little corrosion. Therefore, no valid conclusions can be drawn for this portion of the research based on the macrocell test specimens.

3.1.4 Effect of Corrosion Inhibitors

The corrosion rates of reinforcing steel for specimens in which the mortar contained no corrosion inhibitor or contained Rheocrete 222$^+$ or DCI-S are shown in Figs. 3.30 through 3.33.

Figure 3.30 compares the corrosion rates of the bars in mortar with a water-cement ratio of 0.45 exposed to NaCl. Throughout the tests, the specimens without a corrosion inhibitor corrode at a significantly higher rate than those with a corrosion inhibitor. At the end of the tests, for a water-cement ratio of 0.45, the average corrosion rate for specimens without inhibitors is 5.6 μm/yr, compared with values of 1.5 and 1.25 for specimens containing Rheocrete 222^{+} and specimens containing DCI-S, respectively. Similar behavior, but at lower corrosion rates, is obtained for specimens fabricated with a water-cement ratio of 0.35, as shown in Fig. 3.31.

As might be expected from earlier comparisons for specimens containing CMA, no conclusions can be drawn because of the poor quality of the data.

3.2 Bench-Scale Tests

This section summarizes the results of the bench-scale tests. As described in Chapter 2, the test period is 96 weeks. For each set of comparisons, average results for corrosion rate, mat-to-mat resistance, and the corrosion potential for the top mat (anode) and bottom mat (cathode) are shown. As done for the rapid macrocell tests, this section describes the visual appearance of these specimens at the conclusion of the tests and the influence of water-cement ratio, deicer exposure, and corrosion inhibitors.

3.2.1 Appearance of Specimens

At the end of the test period, some Southern Exposure specimens and all cracked beam specimens exposed to NaCl exhibited corrosion products on the upper surface, as shown in Figs. 3.34 and 3.35, respectively. Southern Exposure specimens

with a water-cement ratio of 0.45 exposed to NaCl and without inhibitors exhibited surface cracking, even in cases in which rust was not visible, as shown in Fig. 3.36.

The concrete was removed to allow the bars to be inspected. The top layer of bars for most Southern Exposure and all cracked beam specimens exposed to salt exhibited corrosion (Fig. 3.37). The bottom layer of bars exhibited corrosion only for specimens without inhibitors with a water-cement ratio of 0.45 exposed to salt (Fig. 3.38). No corrosion was observed for Southern Exposure or cracked beam specimens exposed to CMA. On the negative side, however, CMA caused severe deterioration of the concrete surface, resulting in the exposure of the coarse aggregate, as shown in Fig. 3.39. The damage is likely due to a decrease in pH caused by the CMA and may also be the result of the crystallization of CMA in the concrete pores due to the ponding and drying cycles.

3.2.2 Effect of Water-Cement Ratio

The effects of water-cement ratio on the corrosion rate, mat-to-mat resistance, and corrosion potential for Southern Exposure specimens and cracked beam specimens subjected to NaCl are shown in Figs. 3.40 through 3.51 and 3.52 through 3.63, respectively. The figures show that, for the Southern Exposure specimens, the use of the lower water-cement ratio results in a significantly lower corrosion rate; whereas for the cracked beam specimens, the corrosion rate is largely independent of the water-cement ratio.

For the Southern Exposure specimens without corrosion inhibitors, the corrosion rate at the end of 96 weeks is 1.2 μm/yr for a water-cement ratio of 0.35 compared to 3.8 μm/yr for a water-cement ratio of 0.45 (Fig. 3.40). The mat-to-mat resistance is similar for the two water-cement ratios up through about 40 weeks,

higher for a water-cement ratio of 0.45 from 40 through 80 weeks, and about the same from week 80 through the end of the test (Fig. 3.41). As shown in Figs. 3.42 and 3.43, the corrosion potential is significantly more negative for the higher water-cement ratio specimens for both the top and bottom mats of steel, showing the effect of the greater permeability of the concrete.

Similar observations can be made for the material containing Rheocrete 222$^+$ (Figs. 3.38-3.47) and DCI-S (Figs. 3.48-3.51), except that the corrosion rates are significantly lower than observed for the specimens without corrosion inhibitors.

Comparisons for the cracked beam specimens are shown in Figs. 3.52 through 3.63. As pointed out earlier, the corrosion rates are nearly independent of water-cement ratio, as might be expected, since the salt solution has direct access to the top bars. With some exceptions, the results are similar to those for the Southern Exposure specimens in terms of corrosion rate, mat-to-mat resistance, and corrosion potential of the top bars. For specimens without inhibitors, the mat-to-mat resistance drops beginning in week 78 and the corrosion potential is significantly more negative for the bottom bars for specimens with a water-cement ratio of 0.45 than for those with a water-cement ratio of 0.35 during the same period. The drop in the mat-to-mat resistance is likely due to cracking caused by the deposition of additional corrosion products.

At 96 weeks, the corrosion rate is zero for the cracked beam specimens containing Rheocrete 222$^+$ with a water-cement ratio of 0.35 (Fig. 3.56) and 5 μm/yr for the matching specimens with a water-cement ratio of 0.45. Through 84 weeks, however, the corrosion rates are nearly identical.

For the cracked beam specimens containing DCI-S (Figs. 3.60-3.63), at both water-cement ratios, the corrosion rates are very similar through 56 weeks and at 96

weeks, although the *lower* water-cement ratio specimens exhibit a higher corrosion rate between week 56 and week 91.

3.2.3 Effect of Deicer Solutions

The effects of NaCl and CMA on the corrosion rate for Southern Exposure specimens with and without corrosion inhibitors and water-cement ratios of 0.45 and 0.35 are shown in Figs. 3.64 through 3.87 and for cracked beam specimens with and without corrosion inhibitors and a water-cement ratio of 0.45 in Figs. 3.88 through 3.99.

Across the board, CMA causes no measurable corrosion in either the Southern Exposure or cracked beam specimens. Specimens subjected to NaCl, however, not only exhibit measurable corrosion rates, but more negative corrosion potentials than do the specimens exposed to CMA. Overall, the mat-to-mat resistances of specimens exposed to NaCl and CMA are similar, as shown in Figs. 3.73, 3.81, and 3.85, although this is not true in every case. For example, the mat-to-mat resistance of the specimens exposed to CMA is significantly higher than that of the specimens exposed to NaCl in some tests (shown in Figs. 3.63 and 3.89), while the opposite is true in others (Fig. 3.77).

3.2.4 Effect of Corrosion Inhibitors

The effect of corrosion inhibitors is shown in Figs. 3.100 through 3.107 and in Figs. 3.108 through 3.115 for Southern Exposure and cracked beam specimens, respectively, exposed to NaCl.

As shown in Fig. 3.100, at a water-cement ratio of 0.45, there is little difference in the corrosion rate of the specimens containing the two corrosion inhibitors (average corrosion rate of about 0.5 μm/yr throughout the test period). The specimens without a corrosion inhibitor corrode at about 4 μm/yr. The mat-to-mat

resistance is similar through week 76, when it drops markedly for the specimens without a corrosion inhibitor, probably indicating the formation of a crack due to tensile stresses caused by the corrosion products that, in turn, provides a low-resistance path between the top and bottom mats of steel. The average corrosion potentials of the specimens without a corrosion inhibitor are uniformly more negative than for the specimens containing a corrosion inhibitor (Figs. 3.102 and 3.103).

Similar observations for corrosion rate, mat-to-mat resistance, and corrosion potential can be made for the specimens with a water-cement ratio of 0.35, except that the corrosion rates are much lower (0.1 μm/yr for specimens containing Rheocrete 222$^+$ or DCI-S and a maximum of 2.0 μm/yr for specimens without a corrosion inhibitor), as shown in Fig. 3.104. At the lower water-cement ratio, the mat-to-mat resistances are similar throughout the test period (Fig. 3.105). As shown in Fig. 3.106, at a water-cement ratio of 0.35, the top bars in the specimens containing Rheocrete 222$^+$ remain passive throughout the test period, while those containing DCI-S lose their passivity during the final six weeks. The specimens without a corrosion inhibitor actively corrode, beginning about week 50. Figure 3.107 shows that the bottom bars in the specimens containing a corrosion inhibitor remain passive throughout the test period; whereas, the bottom bars in the specimens without a corrosion inhibitor exhibit active corrosion on occasion.

In contrast to the Southern Exposure specimens, the presence of a direct path for the deicer chemical to the top bars in the cracked beam specimens results in corrosion performance that is not improved by a corrosion inhibitor. The specimens with a water-cement ratio of 0.45, with or without a corrosion inhibitor, exhibit corrosion rates between 0 and 7.0 μm/yr during the final 70 weeks of the test, as shown in Fig. 3.108. For a water-cement ratio of 0.35, the specimens corrode at rates

between 1.0 and 5.0 throughout most of the test, although the specimens containing DCI-S corrode at very high rates between week 46 and week 92, as shown in Fig. 3.112. Overall, the mat-to-mat resistances and corrosion potentials of specimens with and without a corrosion inhibitor are similar, with two exceptions: At a water-cement ratio of 0.45, the bottom bars in specimens without a corrosion inhibitor become active during the tests, as do the specimens at a water-cement ratio of 0.35 containing Rheocrete 222^{+}.

3.3 COMPARISON OF DIFFERENT TEST METHODS

This section compares the results obtained for the rapid macrocell, Southern Exposure, and cracked beam tests for specimens exposed to NaCl. For specimens exposed to CMA, the comparison is impractical because of the dominance of the effect of corrosion on the exposed portion of the bars in rapid macrocell tests, while CMA causes no measurable corrosion in bench-scale tests. The comparisons are made based on the corrosion rate at the end of the test (15 weeks for the macrocell test and 96 weeks for the bench scale tests) and the total corrosion loss during the test period. Because there also can be large fluctuations in the corrosion rate during the last several weeks of the bench scale tests, they are also compared based on the average corrosion rates between 41 and 60 weeks. In each case, the comparisons are made based on the average for all of the specimens in a given series.

As shown in Fig. 3.116, at the end of the tests, the higher the corrosion rate in the rapid macrocell tests, the higher the corrosion rate in the SE tests. The correlation appears to be approximately linear. As shown in Fig. 3.117, the same is true when the corrosion rate at 15 weeks in the rapid macrocell tests is compared to the average corrosion rate for weeks 41 to 60 in the SE tests. The correlation, however, does not

appear to be as good. As shown in Fig. 3.118, at the end of the tests, the larger the corrosion total loss in the rapid macrocell tests, the larger the corrosion total loss in the SE tests. In this case, the relationship is relatively smooth, but not linear, with the total corrosion loss exhibited by the SE specimen without inhibitors being significantly greater than would be predicted based on the rapid macrocell results and the relative performance of the other specimens. Overall, the rapid macrocell tests appear to provide a good prediction of the SE tests, although the corrosion on the exposed portion of the bars in rapid macrocell tests makes them less reliable than the bench-scale tests.

Figures 3.119, 3.120 and 3.121 compare the CB and rapid macrocell tests. Figures 3.122, 3.123 and 3.124 compare the CB and SE tests. In contrast to the correlation between the rapid macrocell tests and the SE tests, the CB tests do not correlate well with either test. The reason is that the salt solution has direct access to the top bars for the CB tests, resulting in the corrosion rates that are nearly independent of the concrete properties (water-cement ratio or corrosion inhibitor). Thus, no clear relationship between the results of the CB and rapid macrocell tests or between the results of the CB and SE tests is observed for the systems evaluated in this study.

Overall, considering the relatively short test period (15 weeks), the rapid macrocell test appears to provide an efficient method for evaluating steel performance in uncracked concrete exposed to a salt environment. The rapid macrocell tests within each group, however, were less consistent than the bench-scale tests due to the effect of corrosion on the exposed portion of the bars. Changes in the test, however, such as completely enclosing the bars in mortar, should improve the reliability of the rapid macrocell tests.

CHAPTER 4
CONCLUSIONS AND RECOMMENDATIONS

4.1 Summary

The performance of several corrosion protection systems for conventional reinforcing steel are evaluated using rapid macrocell tests developed at the University of Kansas, plus two bench-scale techniques, the Southern Exposure (SE) and cracked beam (CB) tests, that are generally accepted in United States practice. Macrocell corrosion rate and corrosion potential are measured for both rapid macrocell and bench-scale tests. Macrocell mat-to-mat resistance is measured only for bench-scale tests. Corrosion protection is provided though the use of a lower water-cement ratio, two different corrosion-inhibiting admixtures, Rheocrete (an organic corrosion inhibitor) and DCI-S (an inorganic corrosion inhibitor), and an alternative deicer CMA (calcium magnesium acetate). The study involves 94 rapid macrocell test specimens, 36 SE test specimens and 27 CB test specimens. Correlation between the test methods is evaluated.

4.2 Conclusions

The following conclusions are based on the test results and analyses presented in this report.

1. In a salt environment, based on the SE and rapid macrocell tests, the higher the water-cement ratio, the higher the corrosion rate and the more negative the anode corrosion potential. In the CB tests, however, a low water-cement ratio provides no advantage in protecting the reinforcing steel.

2. Based on the SE tests, both inhibitors used in this study, Rheocrete and DCI-S, significantly reduce the corrosion rate of the steel in a salt environment. Based on the CB tests, however, Rheocrete and DCI-S provide no advantage compared to concrete without an inhibitor in protecting against corrosion in cracked concrete. For the rapid macrocell tests, no conclusion can be drawn because of corrosion of the exposed portion of the steel in the specimens.
3. In a CMA environment, for SE tests and CB tests, corrosion rates are extremely low. CMA, however, causes concrete to deteriorate in both tests. For the rapid macrocell tests, no conclusion can be drawn because of corrosion on the exposed portion of the steel in the specimens.
4. For rapid macrocell tests, the presence of the small cracks in the surface of the specimens does not measurably affect the test results.
5. Considering the relatively short test period, the rapid macrocell test appears to provide an efficient method for the evaluation of corrosion performance in uncracked concrete exposed to a salt environment.

4.3 Recommendations for future study

1. Field tests of corrosion protection systems should be implemented to evaluate the applicability of the laboratory tests.
2. Rapid macrocell test procedures should be improved to minimize the corrosion of exposed part of the specimen by decreasing the moisture around the exposed potion of the specimen or covering all the steel with mortar.

3. A 6.04 molal ion concentration CMA ponding solution was used in this study, which caused deterioration of concrete. Concrete behavior in the field when subjected to CMA should be studied.
4. The presence of chloride ions in concrete is the main reason for corrosion of reinforcing steel. For this reason, the chloride content of the concrete in the SE specimens should be measured periodically to establish the chloride corrosion threshold for the corrosion protection systems.

REFERENCES

ASTM C 192-90a. (1994). "Standard practice for Making and Curing Concrete Test Specimens in the Laboratory," *1994 Annual Book of ASTM Standards*, American Society for Testing and Materials, Philadelphia, PA, Vol. 4.02, pp. 113-119.

ASTM C 876-91. (1994). "Standard Test Method for Half-Cell Potentials of Uncoated Reinfocing Steel in Concrete," *1994 Annual Book of ASTM Standards*, American Society for Testing and Materials, Philadelphia, PA, Vol. 4.02, pp. 432-437.

Axelsson, H., Darwin, D., and Locke, C. E, Jr. (1999). "Influence of Adhesion at Steel/Mortar Interface on Corrosion Characteristics of Reinforcing Steel," *SL Report* 99-4, University of Kansas Center for Research, Lawrence, Kansas, 55 pp.

Broomfield, J.P., Rodriguez, J., Ortega, L. M., and Garcia, A. M., (1993). "Corrosion Rate Measurement and Life Prediction for Reinforced concrete Structures," *Proceedings of the Structural Faults and Repair-93*, University of Edinburgh, Scotland, Vol. 2, pp. 155-164.

Broomfield, J.P. (1997). *Corrosion of steel in concrete: understanding, investigation, and repair.*, E & FN Spon, London, 240 pp.

Farzammehr, H. (1985). "Pore Solution Analysis of Sodium Chloride and Calcium Chloride Containing Cement Pastes," *Master of Science Thesis*, University of Oklahoma, Norman, OK, 101 pp.

Jones, D. A., (1992). *Principles and Prevention of Corrosion.*, Macmillan Publishing Company, New York, 568 pp.

Hausmann, D. A. (1967). "Steel Corrosion in Concrete - How Does it Occur?", Material Protection, Nov., pp. 19-23.

Lewis, D. A. (1962), "Some Aspects of the Corrosion of Steel in Concrete." *Proceeding of the First International Congress on Metallic Corrosion*, London, pp. 547-555.

Locke, C. E. (1986). "Corrosion of Steel in Portland Cement Concrete: Fundamental Studies," *Corrosion Effect of Stray Currents and the Techniques for Evaluating Corrosion of Rebars in Concrete*, ASTM STP 906, American Society for Testing and Materials, Philadelphia, pp. 5-14.

Martinez, S. L., Darwin, D., McCabe, S. L., and Locke, C. E. (1990). "Rapid Test for Corrosion Effects of Deicing Chemicals in Reinforced Concrete," *SL Report* 90-4, University of Kansas Center for Research, Lawrence, KS, Aug., 61 pp.

McDonald, D. B., Pfeifer, D. W., Krauss, P., and Sherman, M. R. (1994). "Test Methods for New Breeds of Reinforcing Bars," *Corrosion and Corrosion Protection of Steel in Concrete*, Vol. II, July, pp. 1155-1171.

Pfeifer, D. W., Landgren, R. J., and Zoob, A. (1987). "Protective Systems for New Prestressed and Substructure Concrete," *Report* No. FHWA/RD-86/193, Federal Highway Administration, McLean, VA, April, 133 pp.

Ulig, H. H., and Revie, R. R. (1985). *Corrosion and Corrosion Control: An Introduction to Corrosion Science and Engineering*, John Wiley & Sons, New York, 441 pp.

Table 1.1 Criteria for corrosion of steel in concrete for different standard half cells (ASTM C 876)

Copper/Copper Sulfate	Calomel	Corrosion Condition
> -200 mV	> -126 mV	Low (10% risk of corrosion)
-200 mV to -350 mV	-126 mV to -276 mV	Indeterminate corrosion risk
-350 mV to -500 mV	-276 mV to -426 mV	High (>90% risk of corrosion)
< -500 mV	< -426 mV	Severe corrosion

Table 1.2 Criteria for corrosion rate of steel in concrete

Corrosion Rate I_{corr} ($\mu A/cm^2$)	Corrosion Condition
< 0.1	Passive condition
0.1 to 0.5	Low to moderate corrosion
0.5 to 1.0	Moderate to high corrosion
> 1.0	High corrosion rate

Table 2.1 Mixture design for rapid test specimens

Mixture ID	w/c *	Cement (g)	Sand (g)	Distilled water (g)	Rheocrete 222+ (ml)	DCI-S (ml)
M-NO50	0.50	800	1600	400	-	-
M-NO45	0.45	889	1526	400	-	-
M-RH45	0.45	889	1526	396	5.9	-
M-DC45	0.45	889	1526	389	-	17.6
M-NO35	0.35	1143	1315	400	-	-
M-RH35	0.35	1143	1315	396	6.0	-
M-DC35	0.35	1143	1315	389	-	17.9

* Water in the inhibitor is included in the water-cement ratio

Table 2.2 Rapid tests performed

Test ID and specimen numbers	Corrosion inhibitor*	w/c	Deicer solution	Number of tests	Anode**
M-NO50N-1~M-NO50N-5	-	0.50	NaCl	5	selected
M-NO50N-6~M-NO50N-10	-	0.50	NaCl	5	selected
M-NO50N-11~M-NO50N-15	-	0.50	NaCl	5	unselected
M-NO45N-1~M-NO45N-5	-	0.45	NaCl	5	selected
M-NO45N-6~M-NO45N-10	-	0.45	NaCl	5	selected
M-NO45N-11~M-NO45N-15	-	0.45	NaCl	5	unselected
M-NO45C-1~M-NO45N-5	-	0.45	NaCl	5	selected
M-RH45N-1~M-RH45N-5	RH	0.45	NaCl	5	selected
M-RH45C-1~M-RH45C-5	RH	0.45	CMA	5	selected
M-DC45N-1~M-DC45N-5	DC	0.45	NaCl	5	selected
M-DC45C-1~M-DC45C-5	DC	0.45	CMA	5	selected
M-NO35N-1~M-NO35N-5	-	0.35	NaCl	5	selected
M-NO35N-6~M-NO35N-10	-	0.35	NaCl	5	selected
M-NO35N-11~M-NO35N-14	-	0.35	NaCl	4	unselected
M-NO35C-1~M-NO35C-5	-	0.35	CMA	5	selected
M-RH35N-1~M-RH35N-5	RH	0.35	NaCl	5	selected
M-RH35C-1~M-RH35C-5	RH	0.35	CMA	5	selected
M-DC35N-1~M-DC35N-5	DC	0.35	NaCl	5	selected
M-DC35C-1~M-DC35C-5	DC	0.35	CMA	5	selected

* DC = DCI - S
RH = Rheocrete 222+

** The selected anode specimens are those have minimal cracks and pores based on visual inspection. Specimens not used as anodes are used as the cathodes.

Table 2.3 Mixture design for bench scale test specimens

Mixture ID	w/c	Water (kg/m^3)	Cement (kg/m^3)	Coarse Aggregate (kg/m^3)	Fine Aggregate (kg/m^3)	AE (ml/m^3)	Rheocrete 222+ (ml/m^3)	DCI-S (ml/m^3)	S.P. (ml/m^3)
B-NO45	0.45	158	351	864	842	90	-	-	-
B-RH45	0.45	154	349	864	851	225	5000	-	-
B-DC45	0.45	145	342	864	848	88	-	15000	-
B-NO35	0.35	153	438	862	764	80	-	-	750
B-RH35	0.35	155	448	864	751	250	5000	-	760
B-DC35	0.35	147	445	864	761	85	-	15000	800

Table 2.4 6.04 molal deicer solution content

	Distilled water (g)	NaCl (g)	CMA (g)
Salt solution for SE	600	105	-
Salt solution for CB	300	52.5	-
CMA solution for SE	508.3	-	191.7
CMA solution for CB	254.1	-	95.9

Table 2.5 Bench scale tests performed

Material Combination	Number of Tests Using Salt Solution	Number of Tests Using CMA Solution
A 615 steel, w/c = 0.45, no inhibitors	3 SEs and 3 CBs	3 SEs and 3 CBs
A 615 steel, w/c = 0.35, no inhibitors	3 SEs and 3 CBs	3 SEs
A 615 steel, w/c = 0.45, with RH	3 SEs and 3 CBs	3 SEs and 3 CBs
A 615 steel, w/c = 0.35, with RH	3 SEs and 3 CBs	3 SEs
A 615 steel, w/c = 0.45, with DC	3 SEs and 3 CBs	3 SEs and 3 CBs
A 615 steel, w/c = 0.35, with DC	3 SEs and 3 CBs	3 SEs

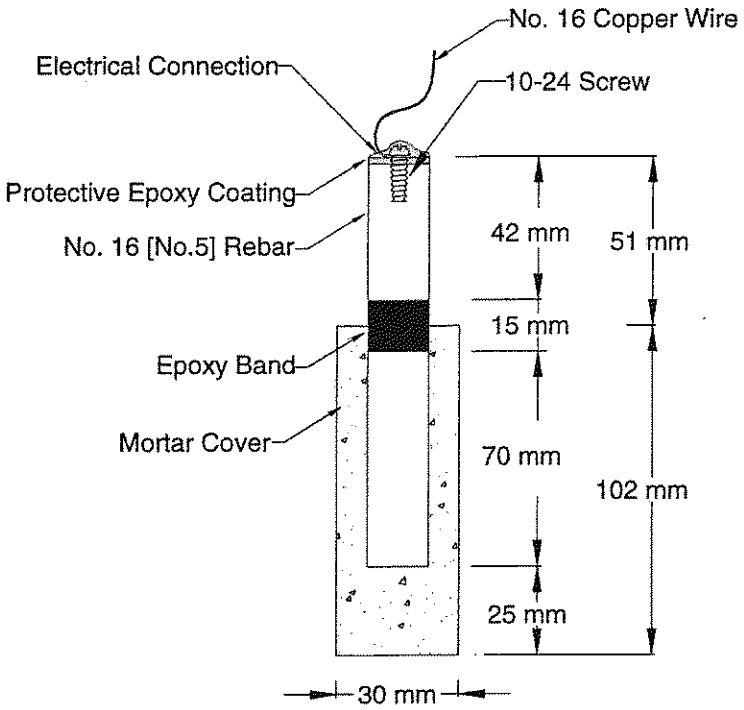

Figure 2.1 Cross Section of Rapid Test Specimen

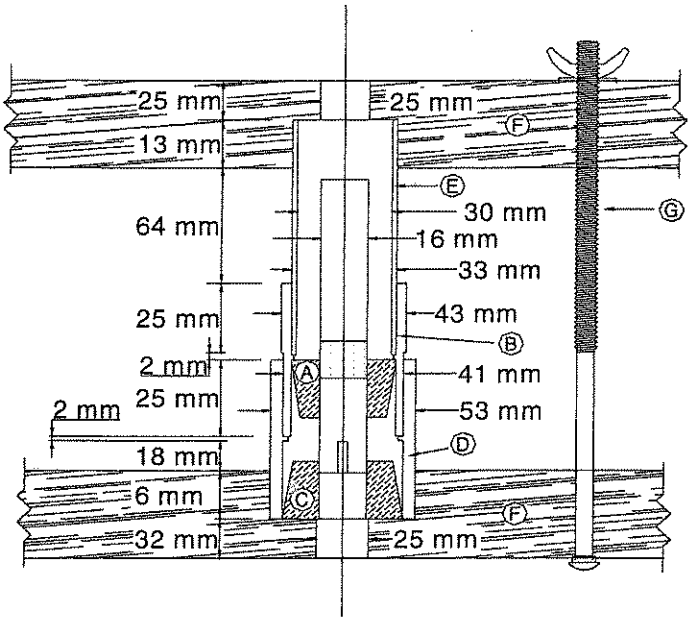

Figure 2.2 Cross Section of Mold for Rapid Test

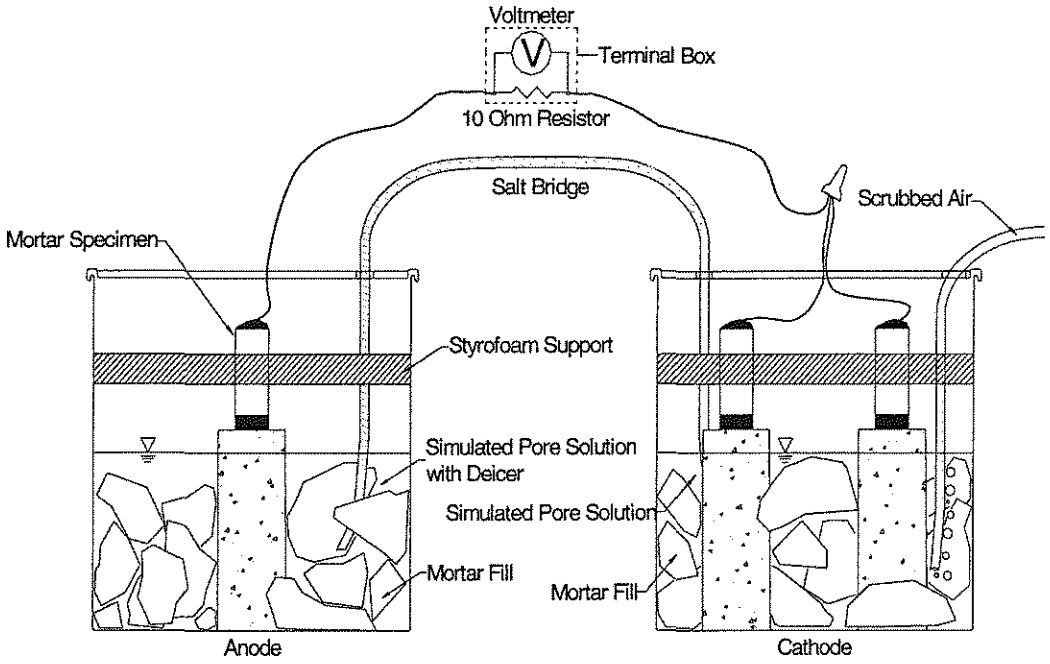

Figure 2.3 Schematic of Rapid Macrocell Test

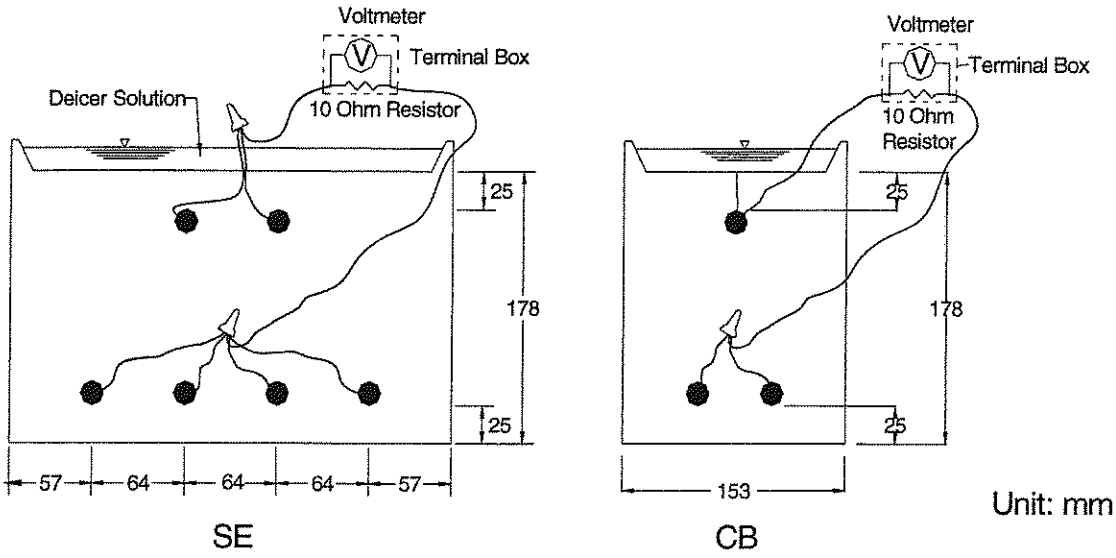

Figure 2.4 Schematic of SE and CB Specimens

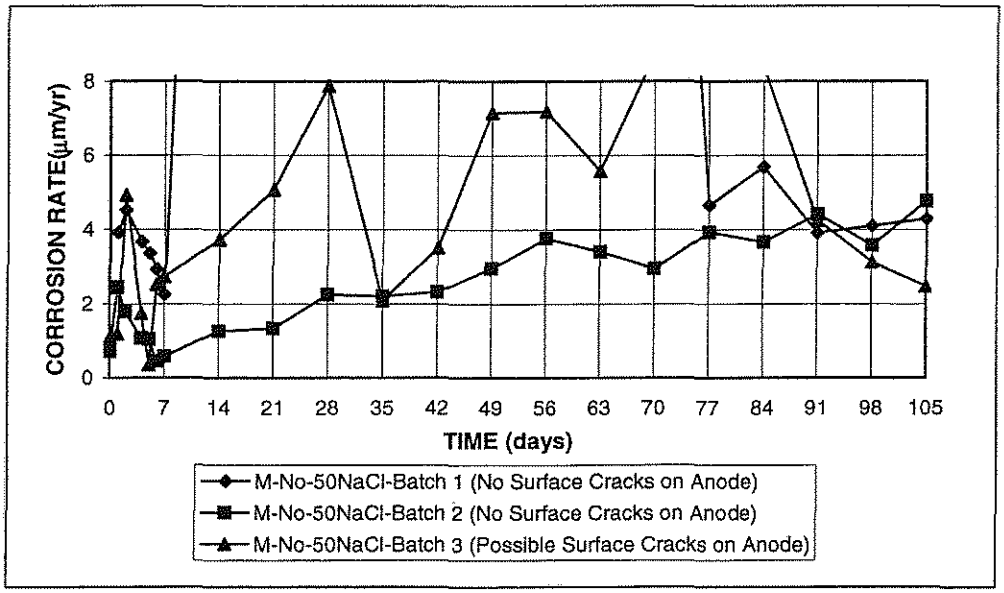

Figure 3.1 Macrocell test: Average corrosion rate for different batch; w/c=0.5; no inhibitors; 1.6 m ion NaCl in simulated concrete pore solution

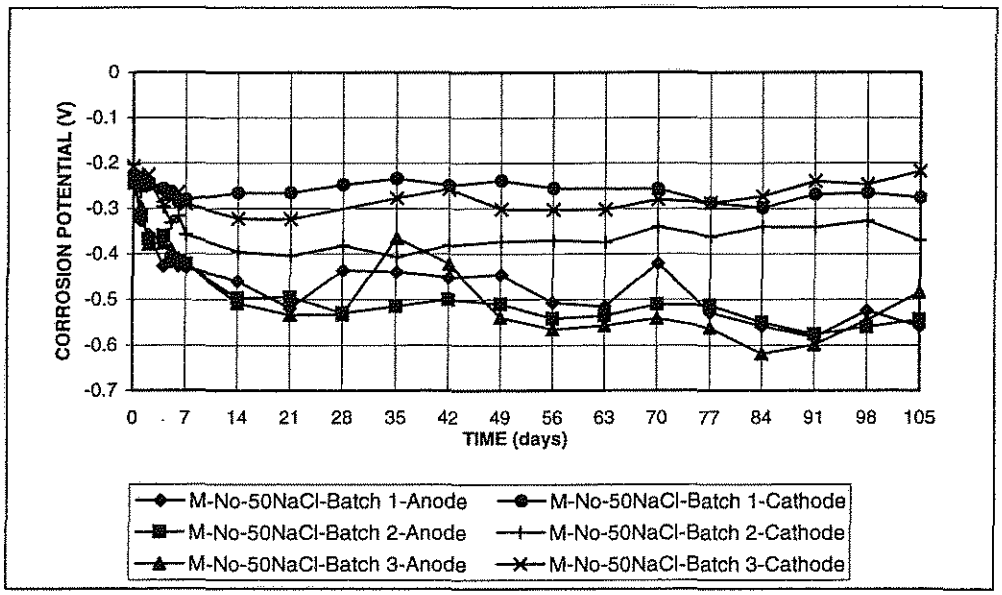

Figure 3.2 Macrocell test: Average corrosion potential with respect to saturated calomel electrode for different batch; w/c=0.5; no inhibitors; 1.6 m ion NaCl in simulated concrete pore solution

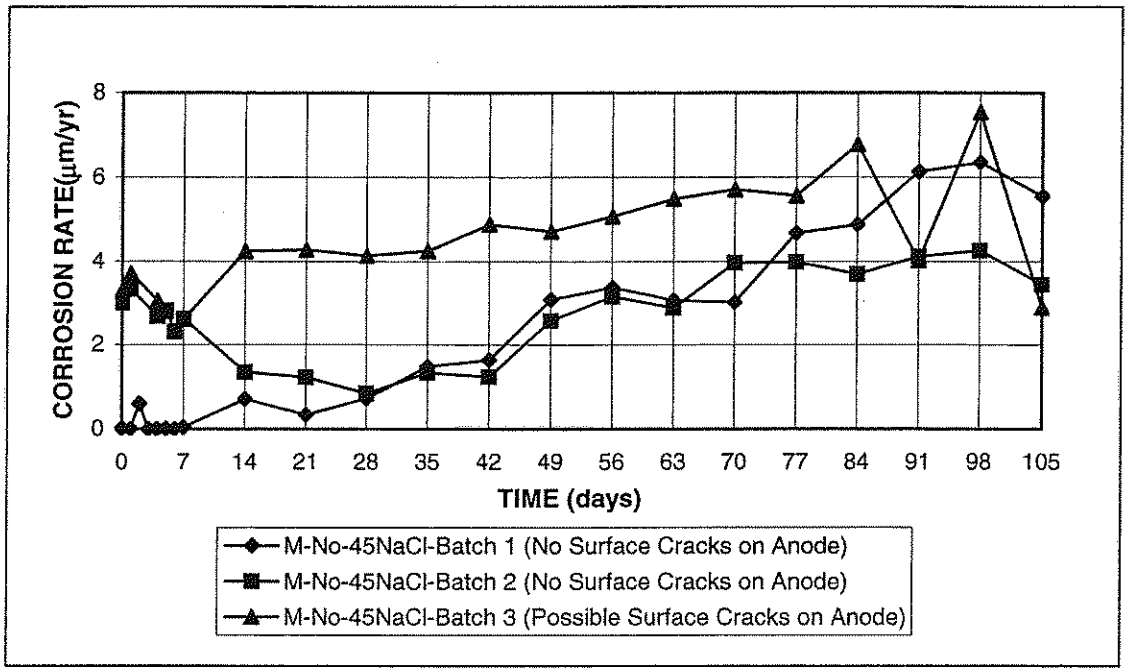

Figure 3.3 Macrocell test: Average corrosion rate for different batch; w/c=0.45; no inhibitors; 1.6 m ion NaCl in simulated concrete pore solution

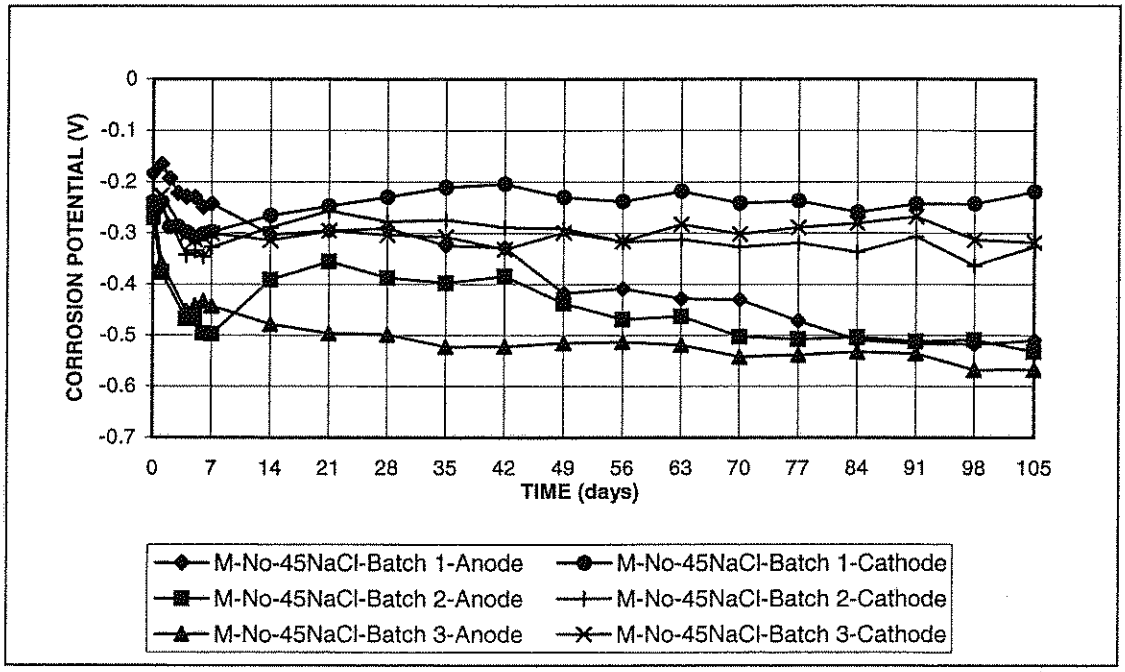

Figure 3.4 Macrocell test: Average corrosion potential with respect to saturated calomel electrode for different batch; w/c=0.45; no inhibitors; 1.6 m ion NaCl in simulated concrete pore solution

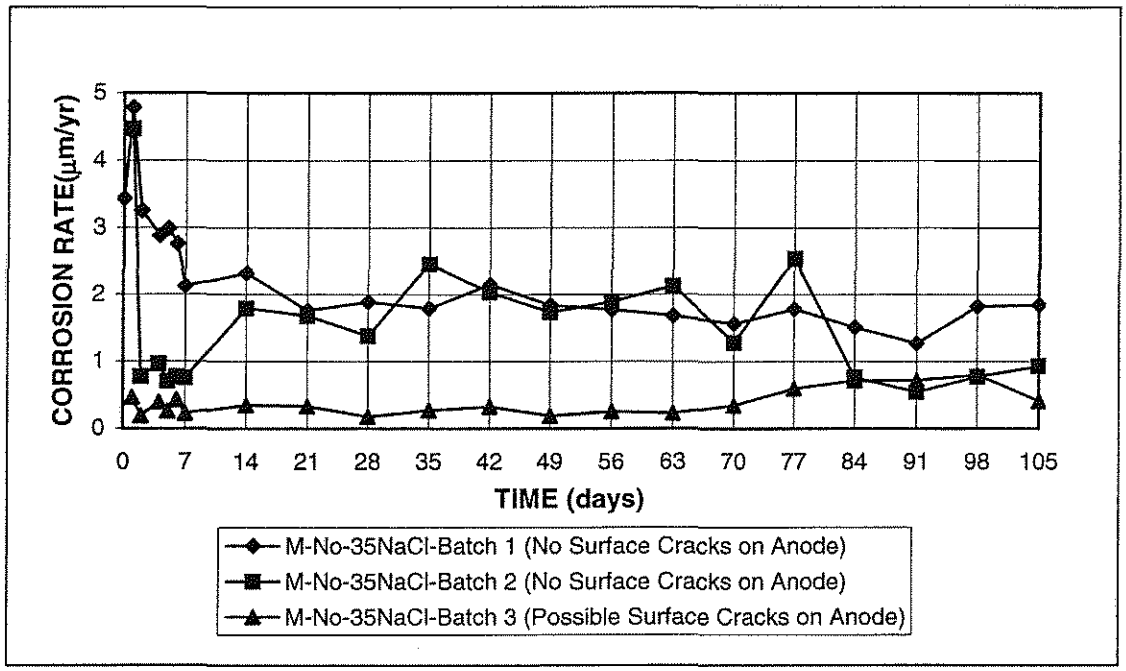

Figure 3.5 Macrocell test: Average corrosion rate for different batch; w/c=0.35; no inhibitors; 1.6 m ion NaCl in simulated concrete pore solution

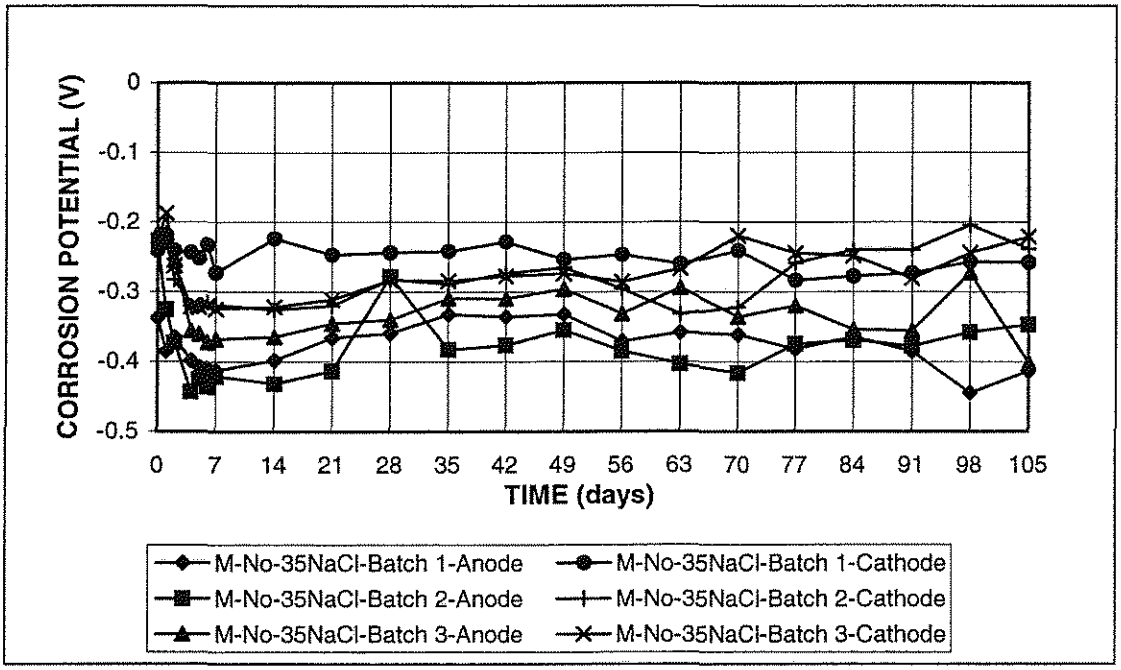

Figure 3.6 Macrocell test: Average corrosion potential with respect to saturated calomel electrode for different batch; w/c=0.35; no inhibitors; 1.6 m ion NaCl in simulated concrete pore solution

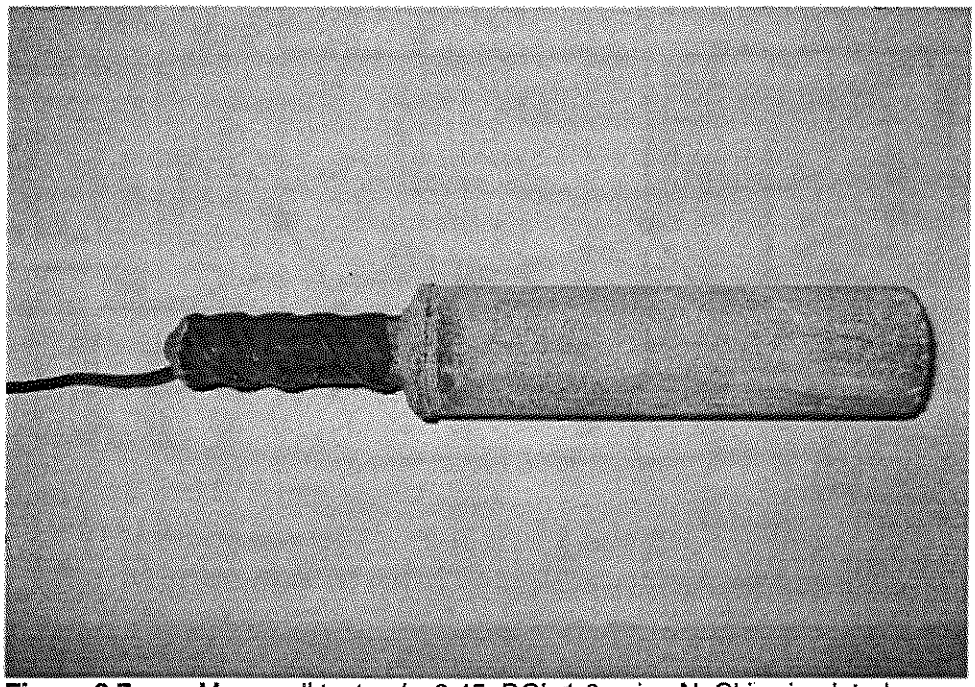

Figure 3.7 Macrocell test: w/c=0.45; DCI; 1.6 m ion NaCl in simulated concrete pore solution; anode of specimen #3.

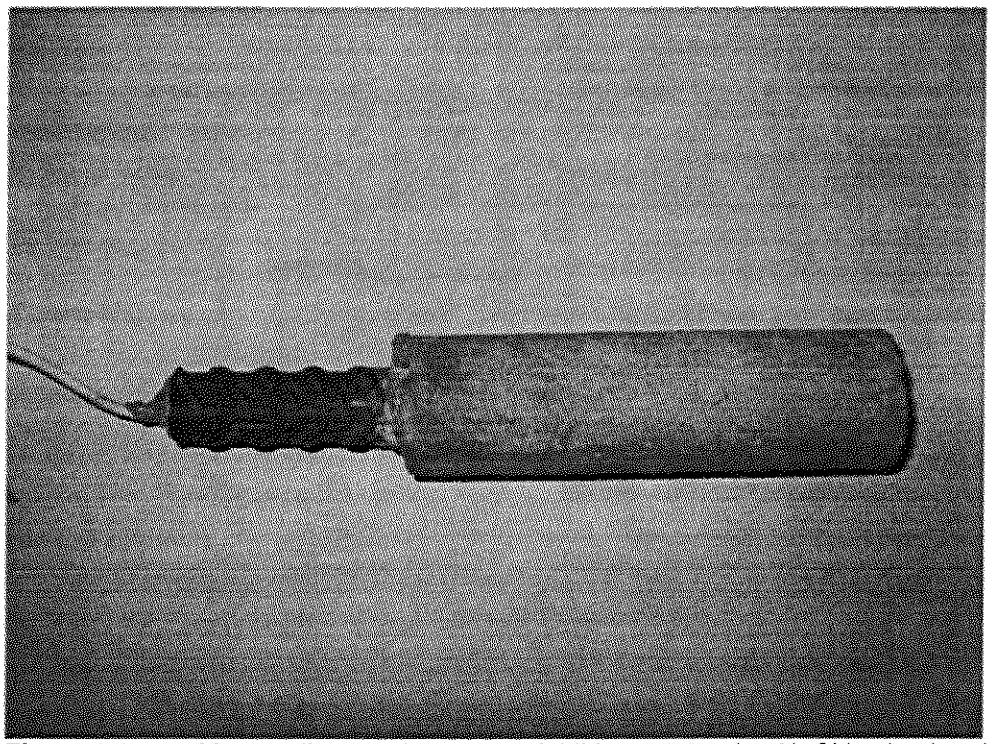

Figure 3.8 Macrocell test: w/c=0.35; no inhibitors; 1.6 m ion NaCl in simulated concrete pore solution; one of cathodes of specimen #1.

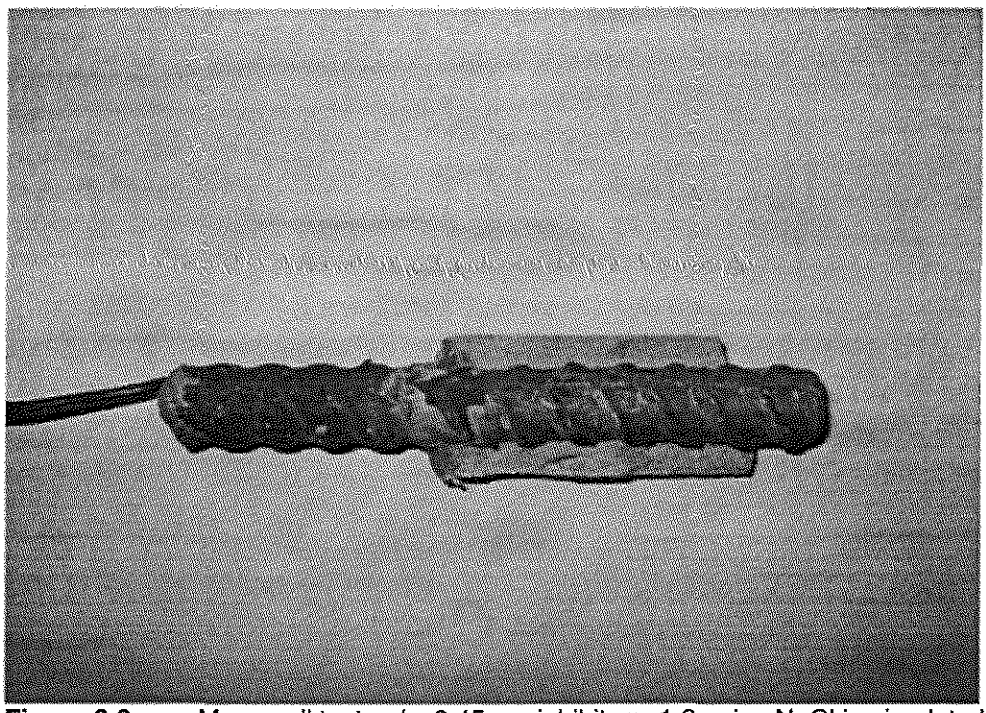

Figure 3.9 Macrocell test: w/c=0.45; no inhibitors; 1.6 m ion NaCl in simulated concrete pore solution; anode of specimen #1.

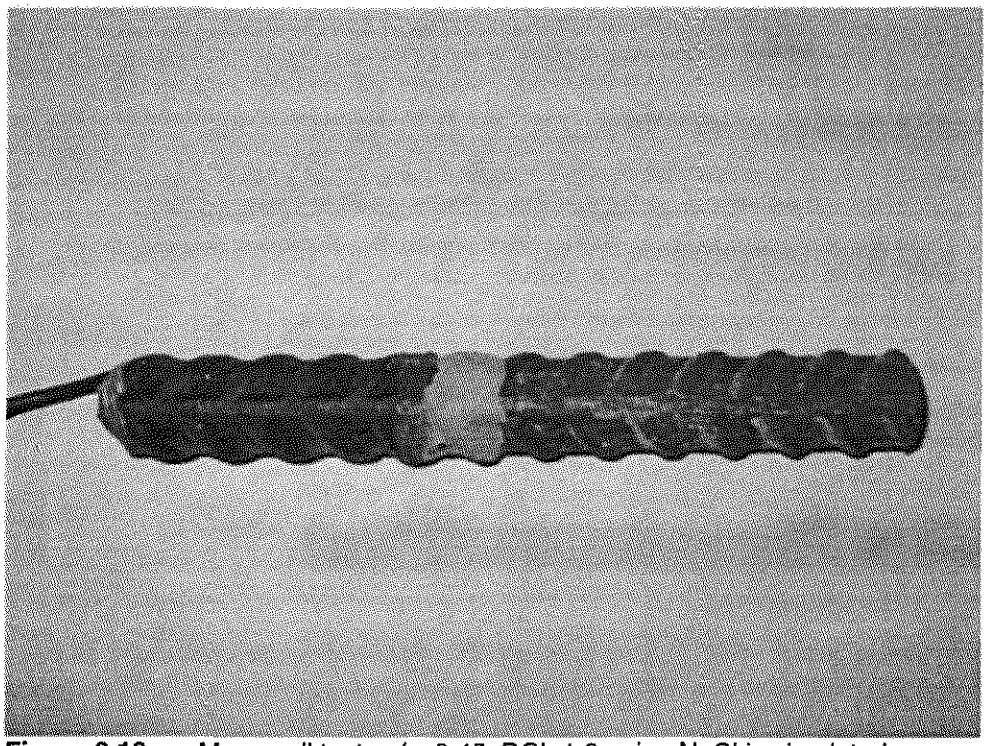

Figure 3.10 Macrocell test: w/c=0.45; DCI; 1.6 m ion NaCl in simulated concrete pore solution; anode of specimen #2.

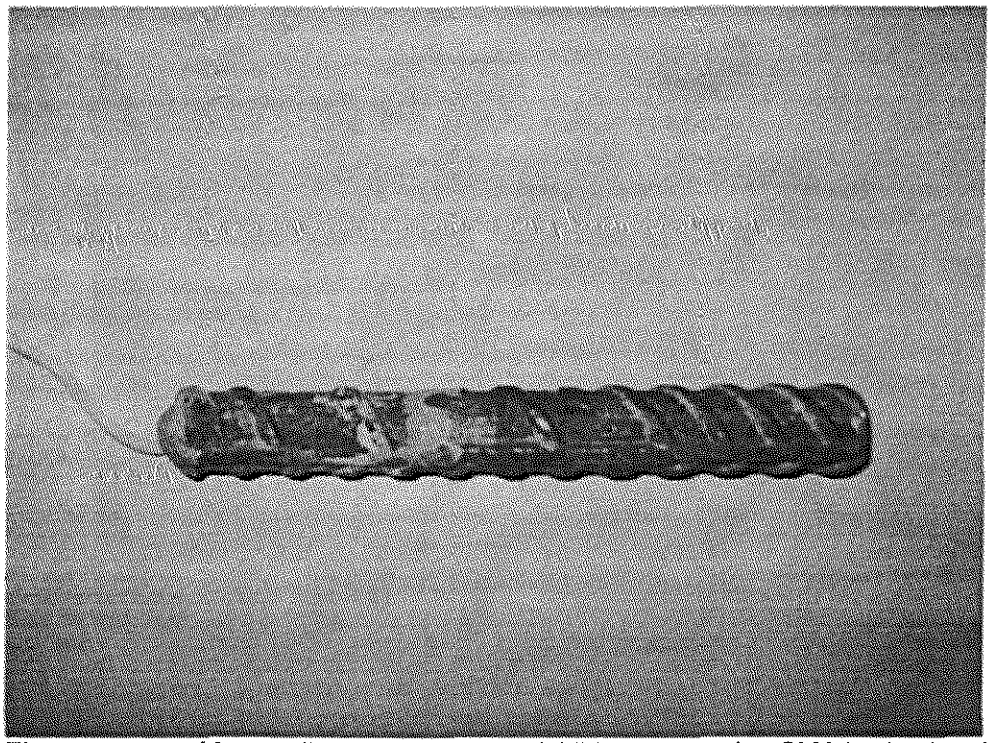

Figure 3.11 Macrocell test: w/c=0.45; no inhibitors; 1.6 m ion CMA in simulated concrete pore solution; one of cathodes of specimen #4.

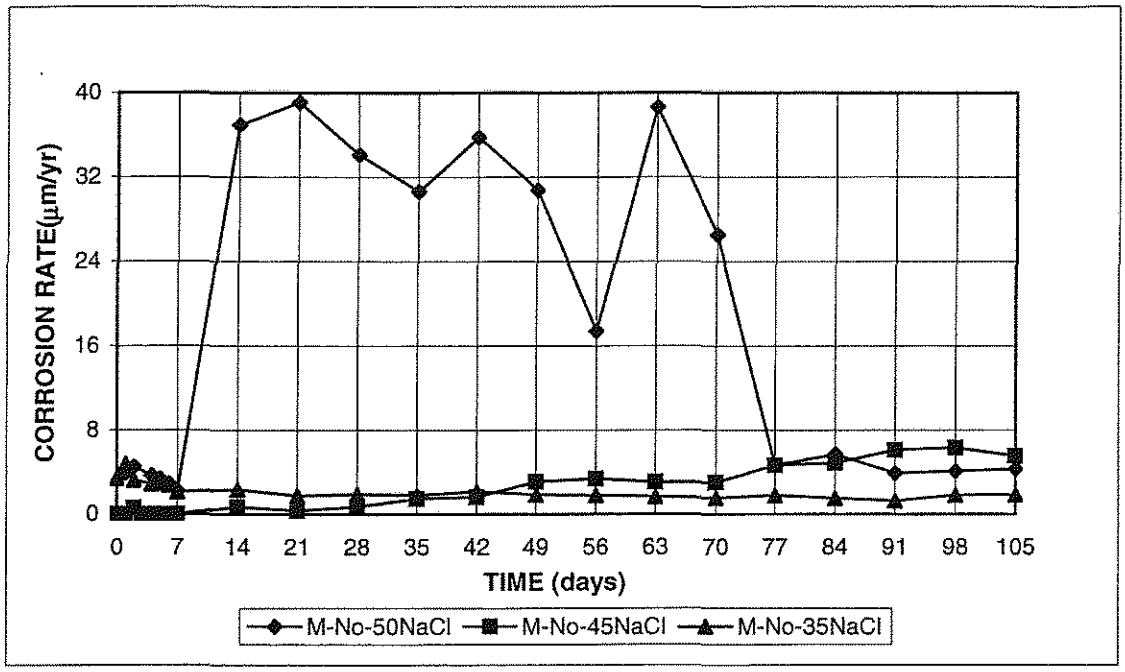

Figure 3.12 Macrocell test: Average corrosion rate for different water-cement ratio; no inhibitors; 1.6 m ion NaCl in simulated concrete pore solution

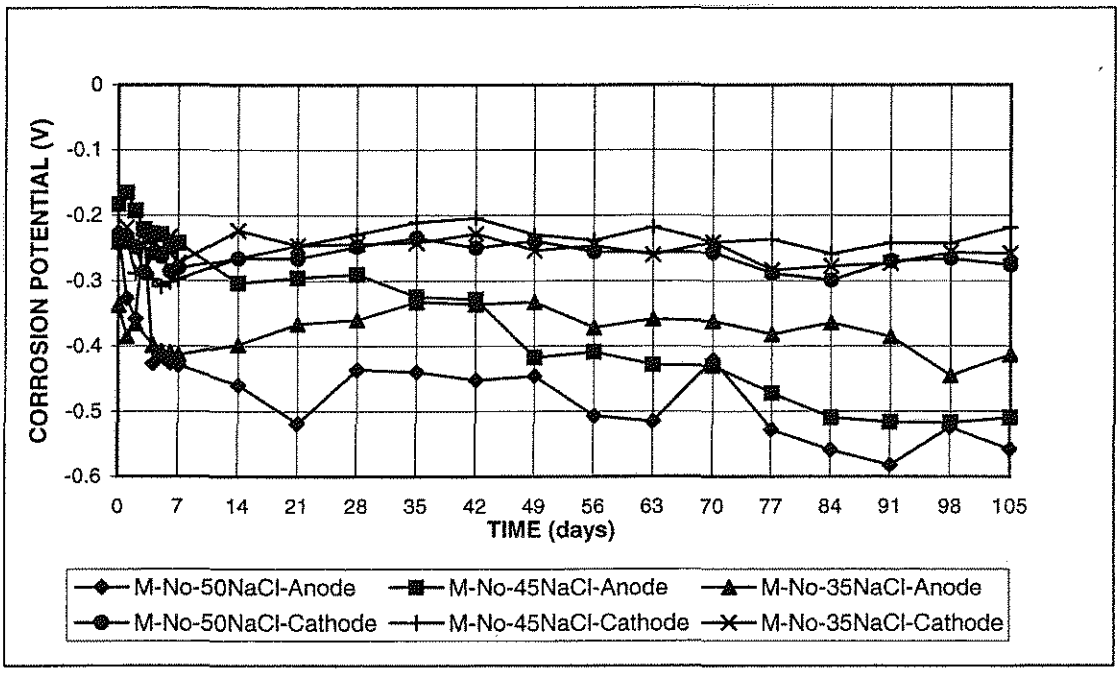

Figure 3.13 Macrocell test: Average corrosion potential with respect to saturated calomel electrode for different water-cement ratio; no inhibitors; 1.6 m ion NaCl in simulated concrete pore solution

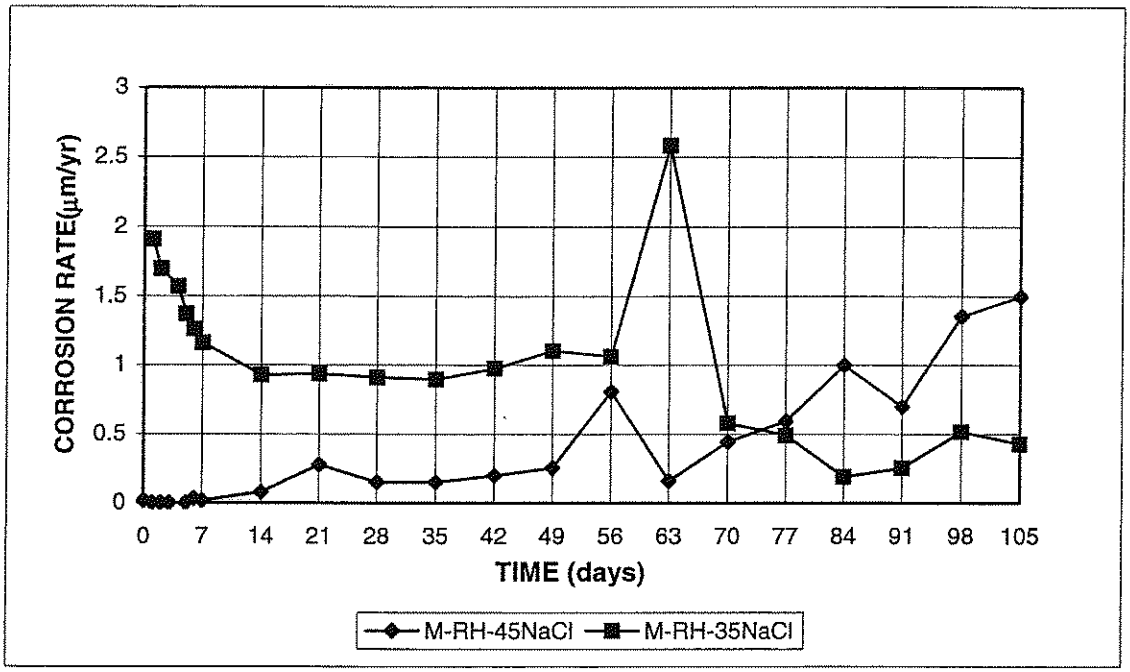

Figure 3.14 Macrocell test: Average corrosion rate for different water-cement ratio; Rheocrete; 1.6 m ion NaCl in simulated concrete pore solution

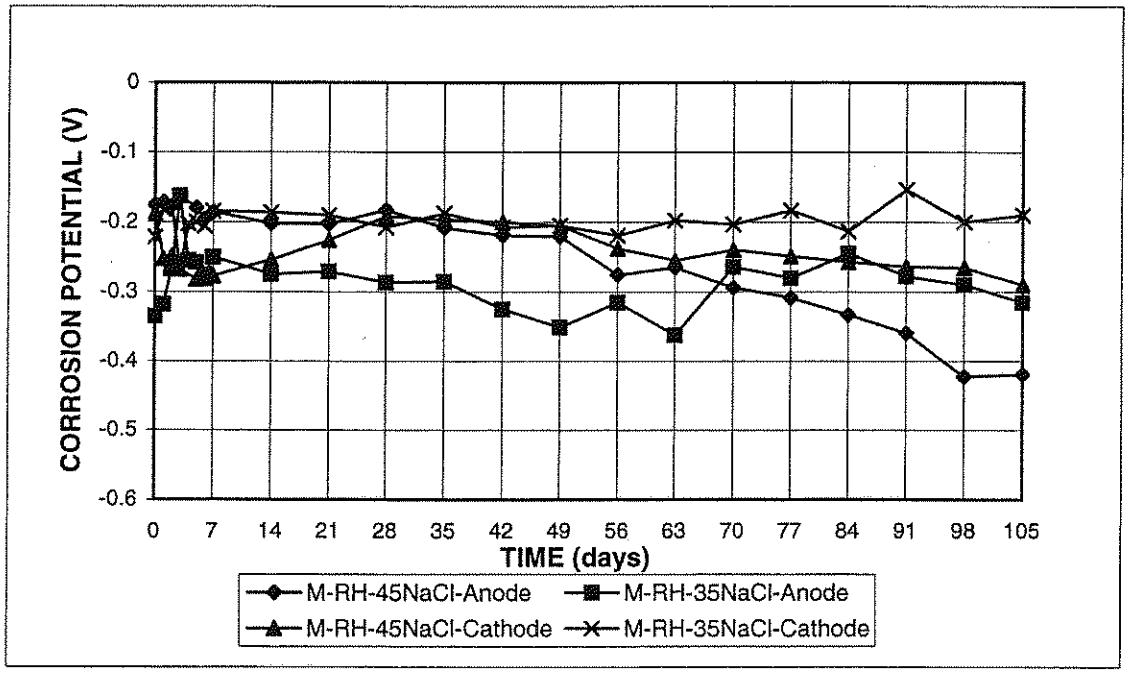

Figure 3.15 Macrocell test: Average corrosion potential with respect to saturated calomel electrode for different water-cement ratio; Rheocrete; 1.6 m ion NaCl in simulated concrete pore solution

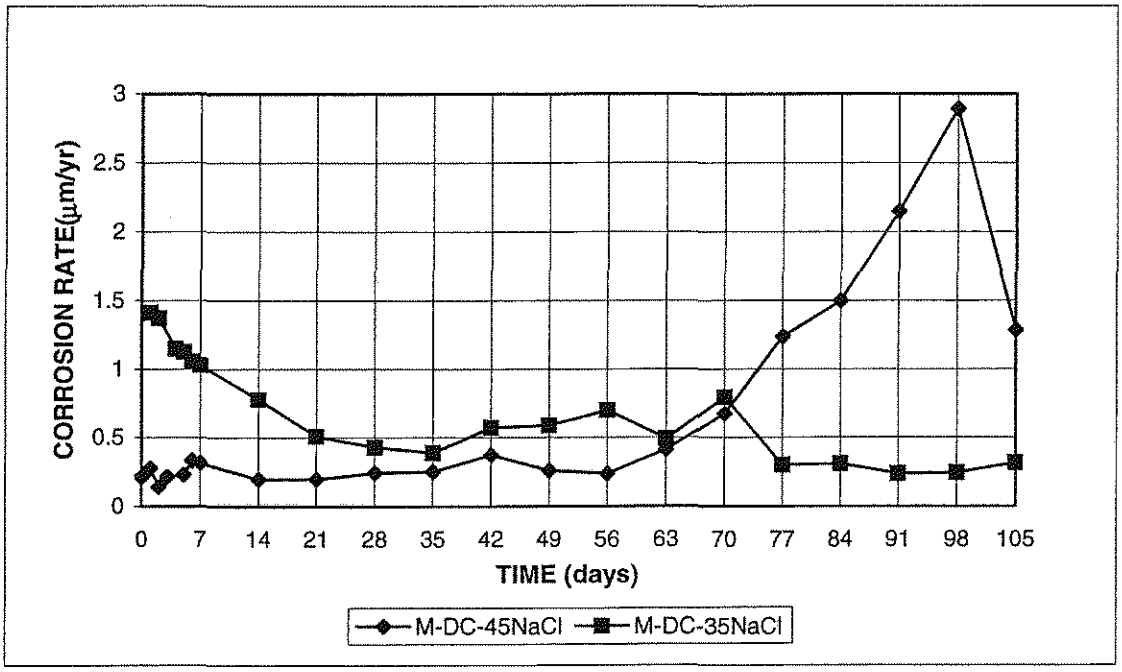

Figure 3.16 Macrocell test: Average corrosion rate for different water-cement ratio; DCl; 1.6 m ion NaCl in simulated concrete pore solution

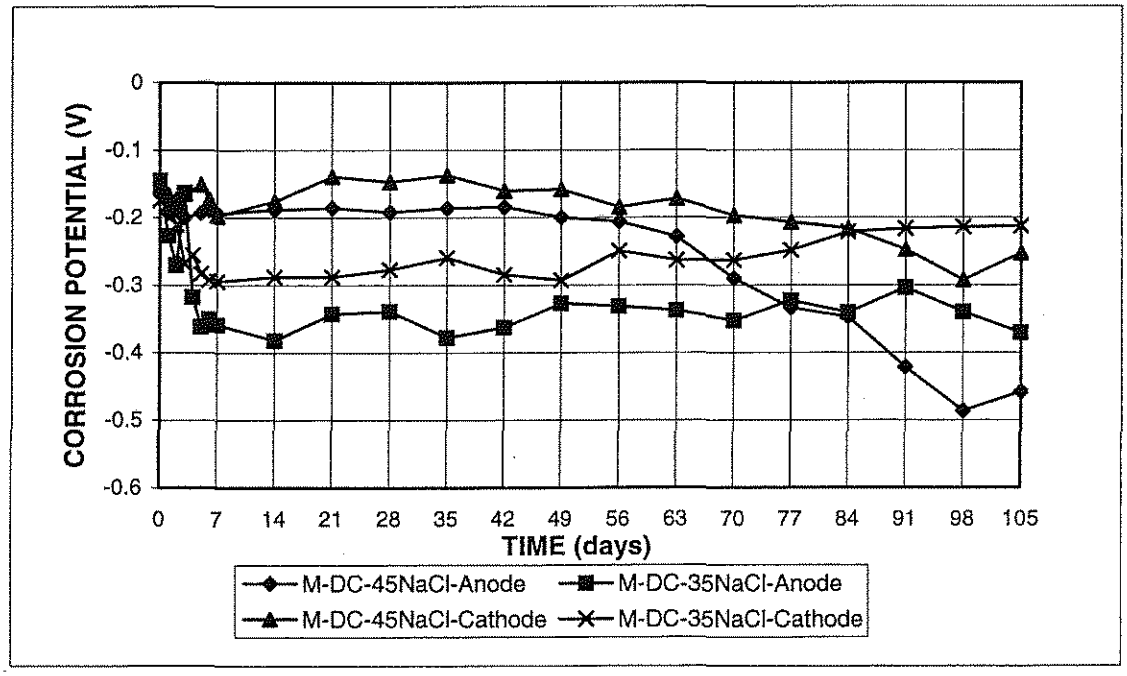

Figure 3.17 Macrocell test: Average corrosion potential with respect to saturated calomel electrode for different water-cement ratio; DCl; 1.6 m ion NaCl in simulated concrete pore solution

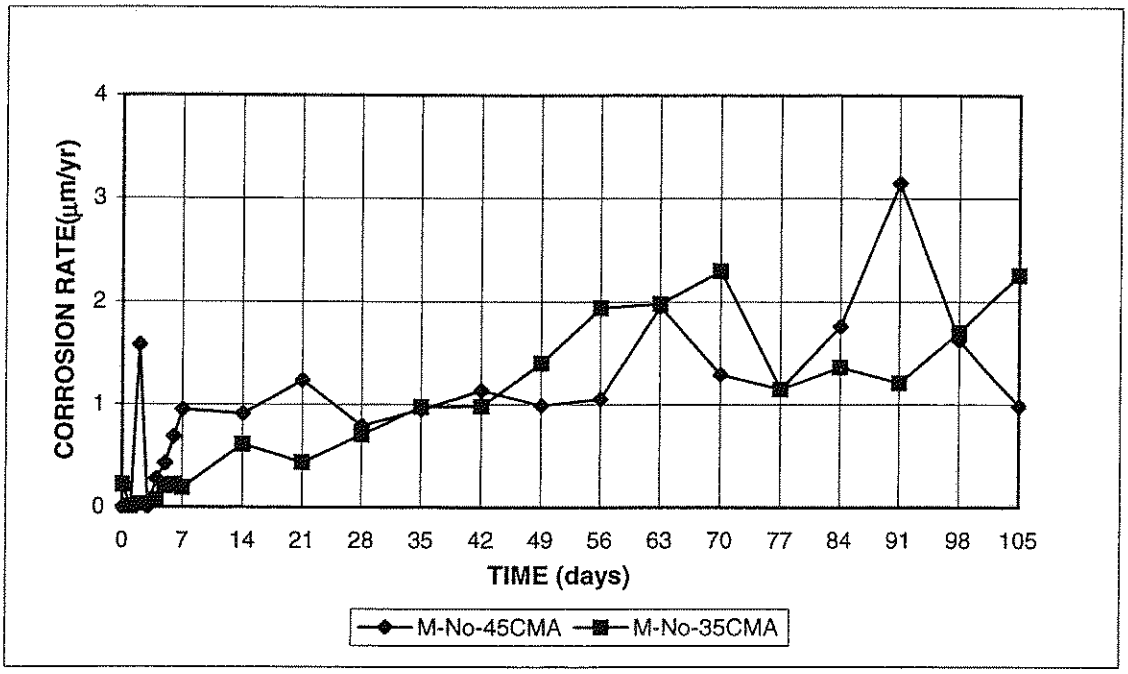

Figure 3.18 Macrocell test: Average corrosion rate for different water-cement ratio; no inhibitors; 1.6 m ion CMA in simulated concrete pore solution

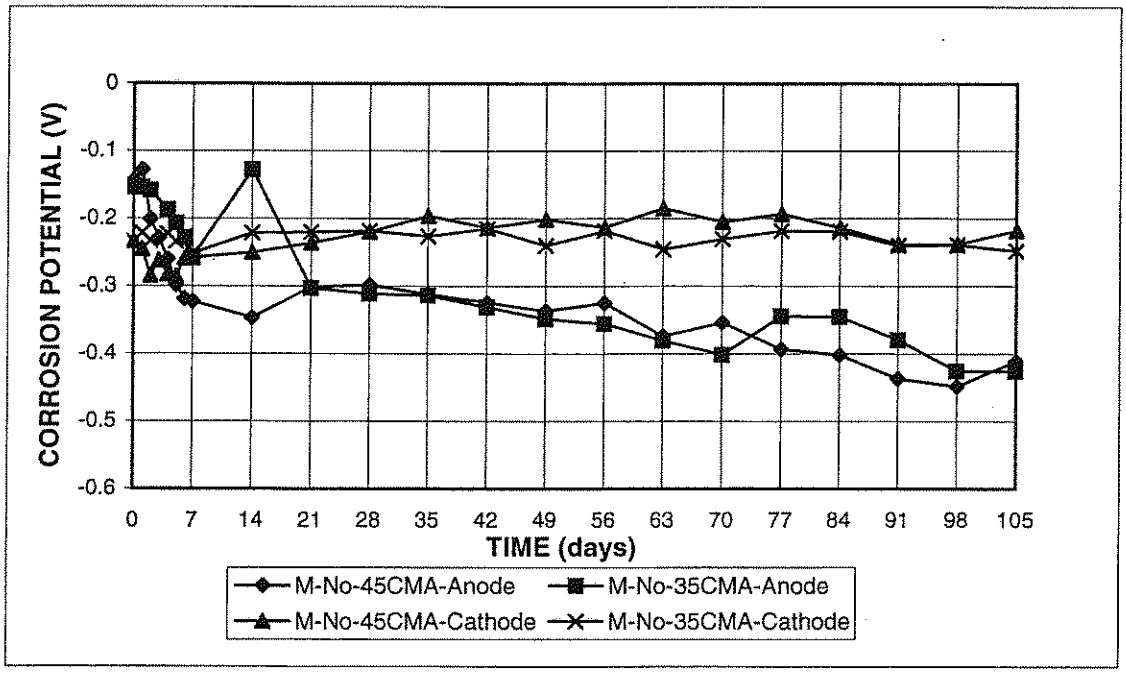

Figure 3.19 Macrocell test: Average corrosion potential with respect to saturated calomel electrode for different water-cement ratio; no inhibitors; 1.6 m ion CMA in simulated concrete pore solution

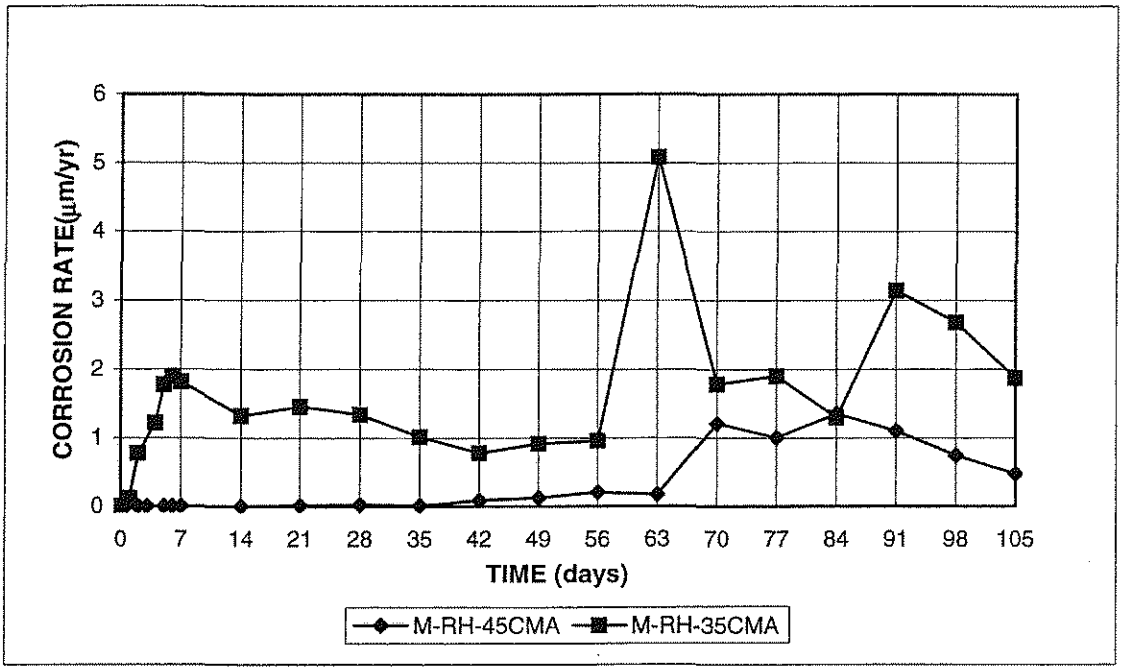

Figure 3.20 Macrocell test: Average corrosion rate for different water-cement ratio; Rheocrete; 1.6 m ion CMA in simulated concrete pore solution

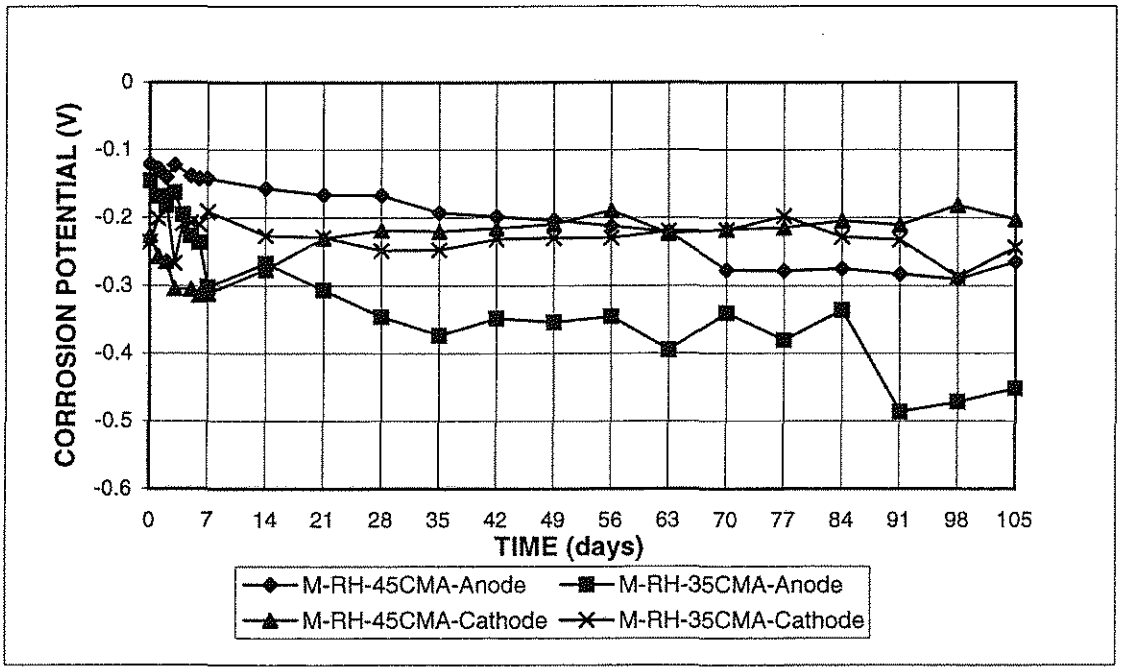

Figure 3.21 Macrocell test: Average corrosion potential with respect to saturated calomel electrode for different water-cement ratio; Rheocrete; 1.6 m ion CMA in simulated concrete pore solution

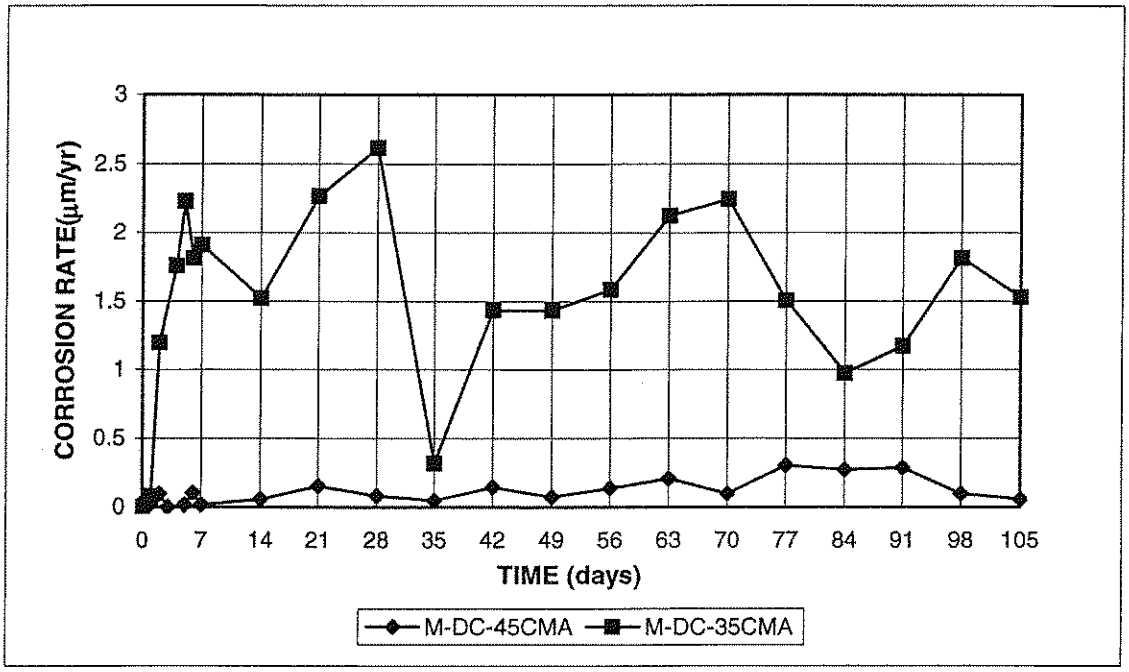

Figure 3.22 Macrocell test: Average corrosion rate for different water-cement ratio; DCI; 1.6 m ion CMA in simulated concrete pore solution

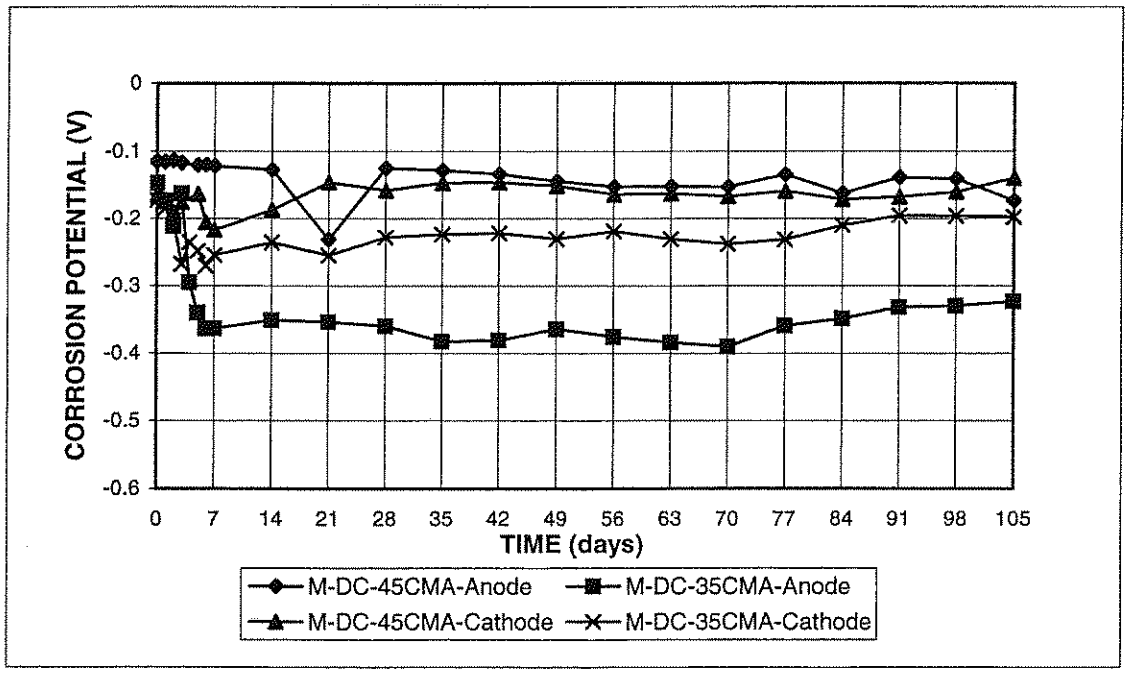

Figure 3.23 Macrocell test: Average corrosion potential with respect to saturated calomel electrode for different water-cement ratio; DCI; 1.6 m ion CMA in simulated concrete pore solution

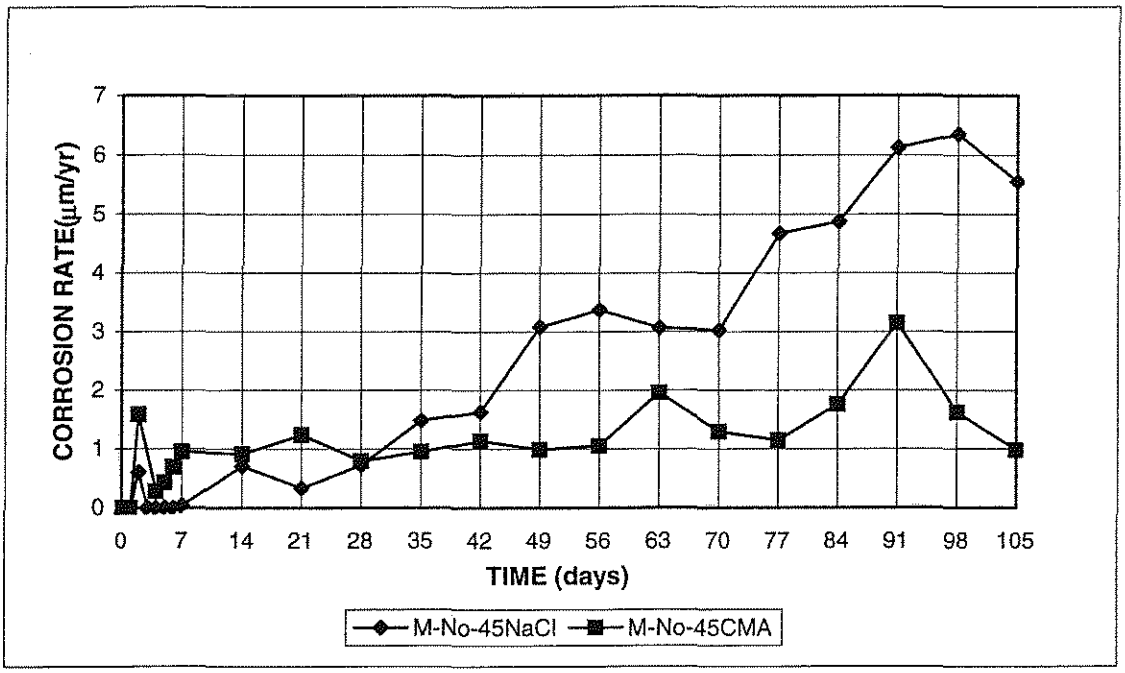

Figure 3.24 Macrocell test: Average corrosion rate for different deicer solution; no inhibitors; w/c=0.45; 1.6 m ion NaCl or CMA in simulated concrete pore solution

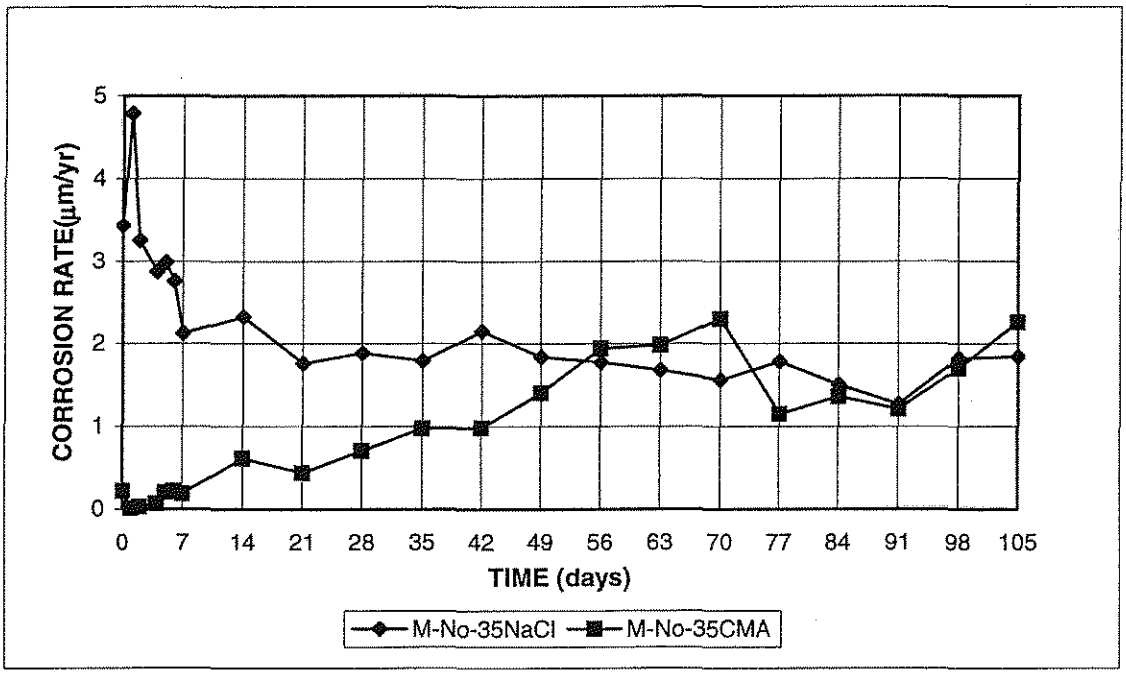

Figure 3.25 Macrocell test: Average corrosion rate for different deicer solution; no inhibitors; w/c=0.35; 1.6 m ion NaCl or CMA in simulated concrete pore solution

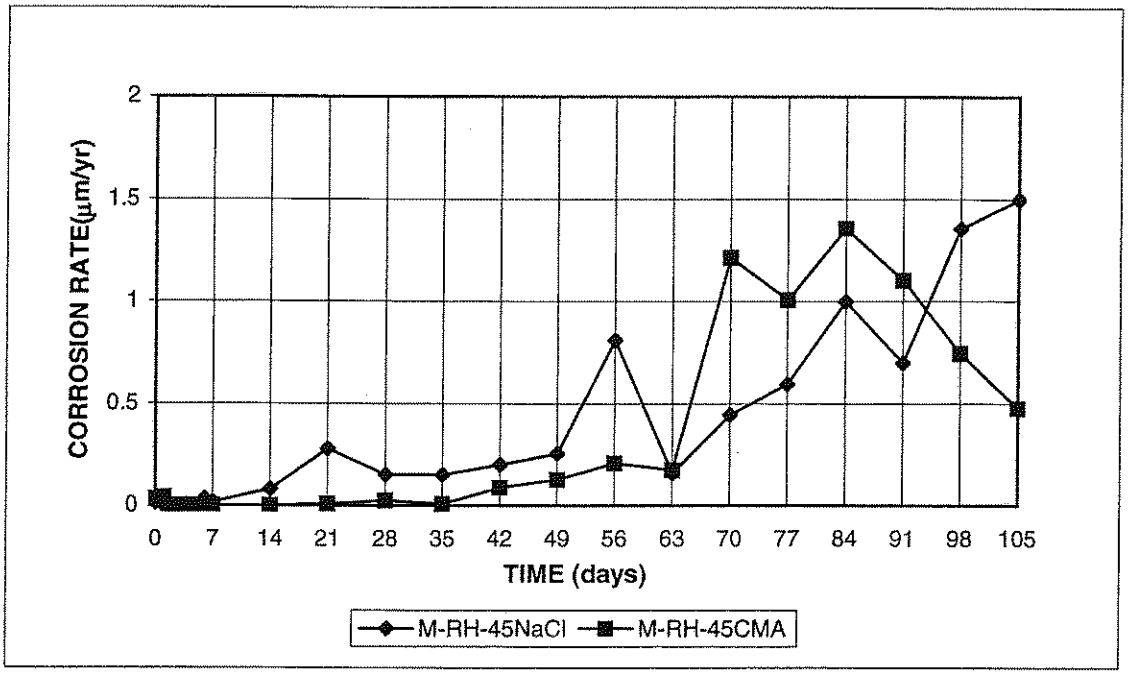

Figure 3.26 Macrocell test: Average corrosion rate for different deicer solution; Rheocrete; w/c=0.45; 1.6 m ion NaCl or CMA in simulated concrete pore solution

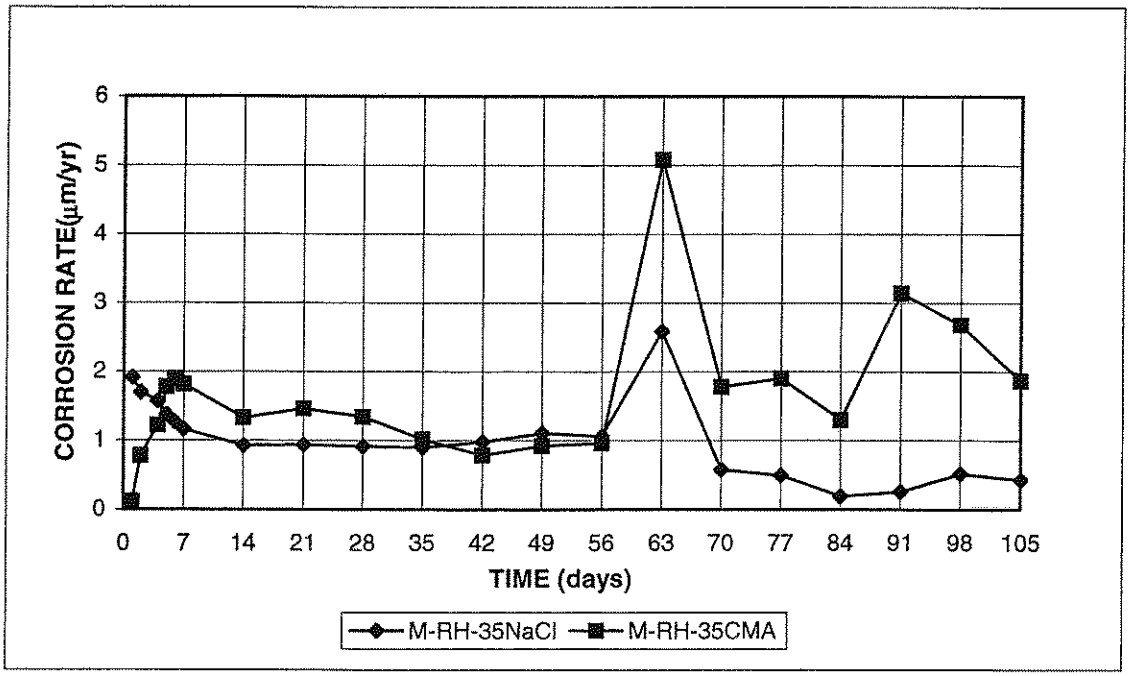

Figure 3.27 Macrocell test: Average corrosion rate for different deicer solution; Rheocrete; w/c=0.35; 1.6 m ion NaCl or CMA in simulated concrete pore solution

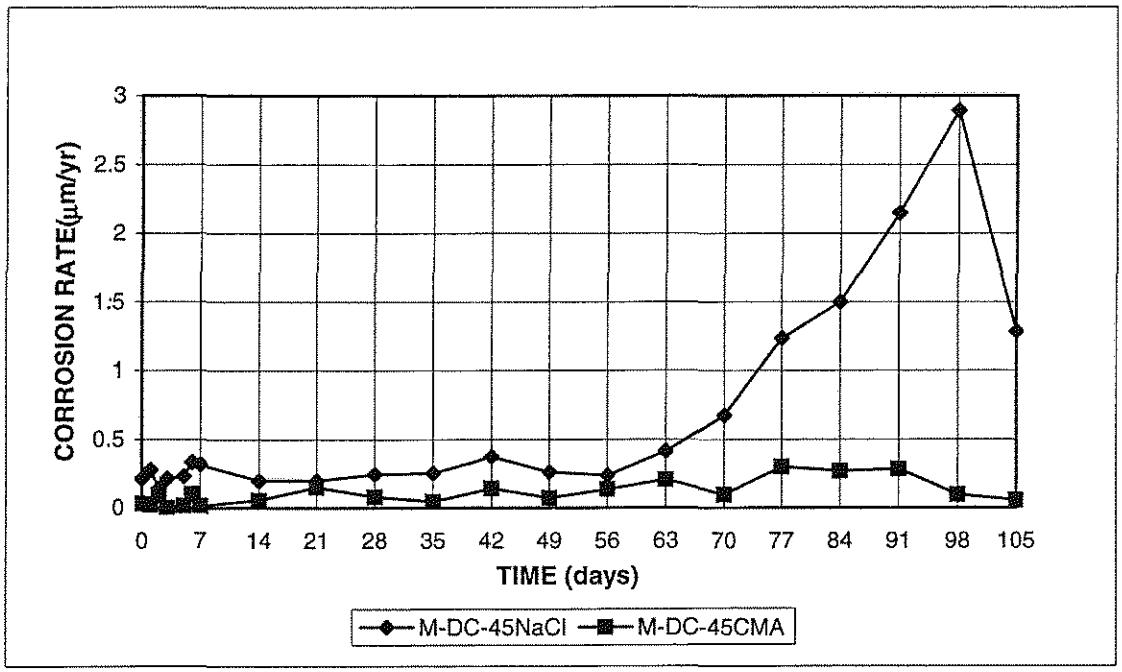

Figure 3.28 Macrocell test: Average corrosion rate for different deicer solution; DCI; w/c=0.45; 1.6 m ion NaCl or CMA in simulated concrete pore solution

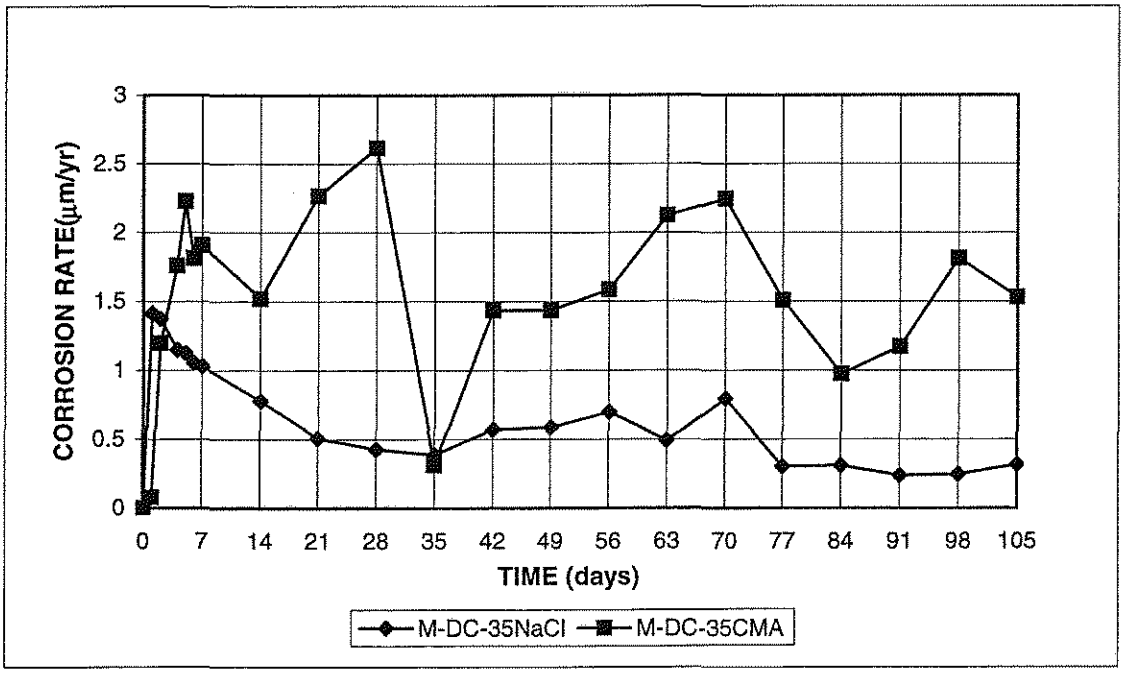

Figure 3.29 Macrocell test: Average corrosion rate for different deicer solution; DCI; w/c=0.35; 1.6 m ion NaCl or CMA in simulated concrete pore solution

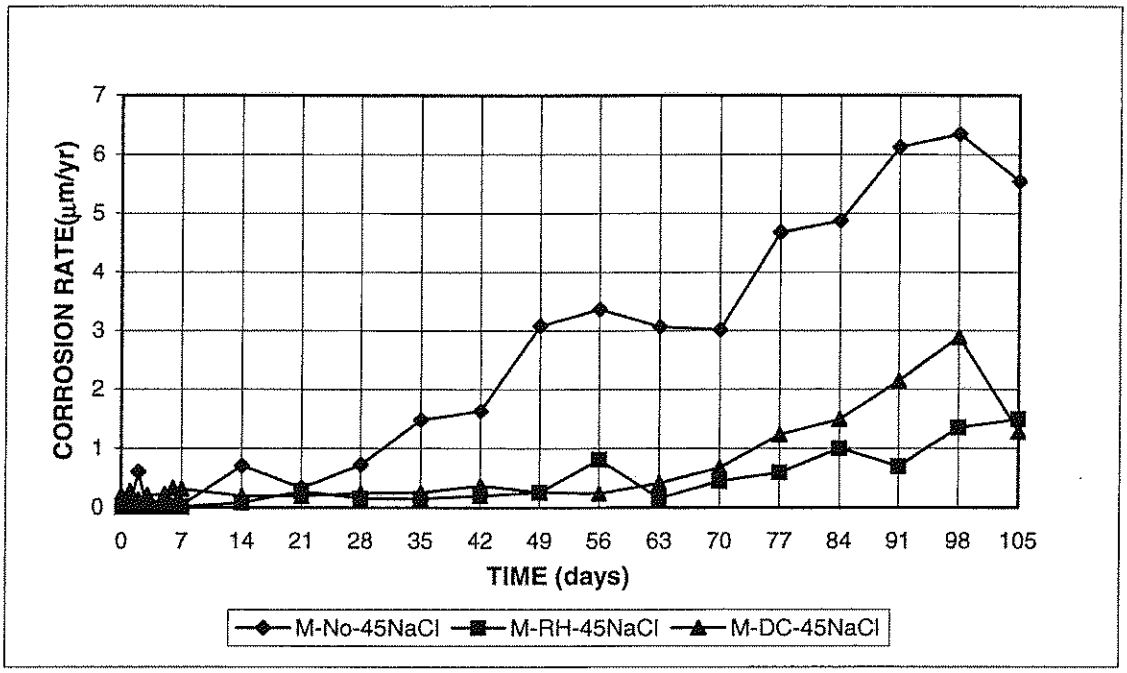

Figure 3.30 Macrocell test: Average corrosion rate with or without inhibitors; w/c=0.45; 1.6 m ion NaCl in simulated concrete pore solution

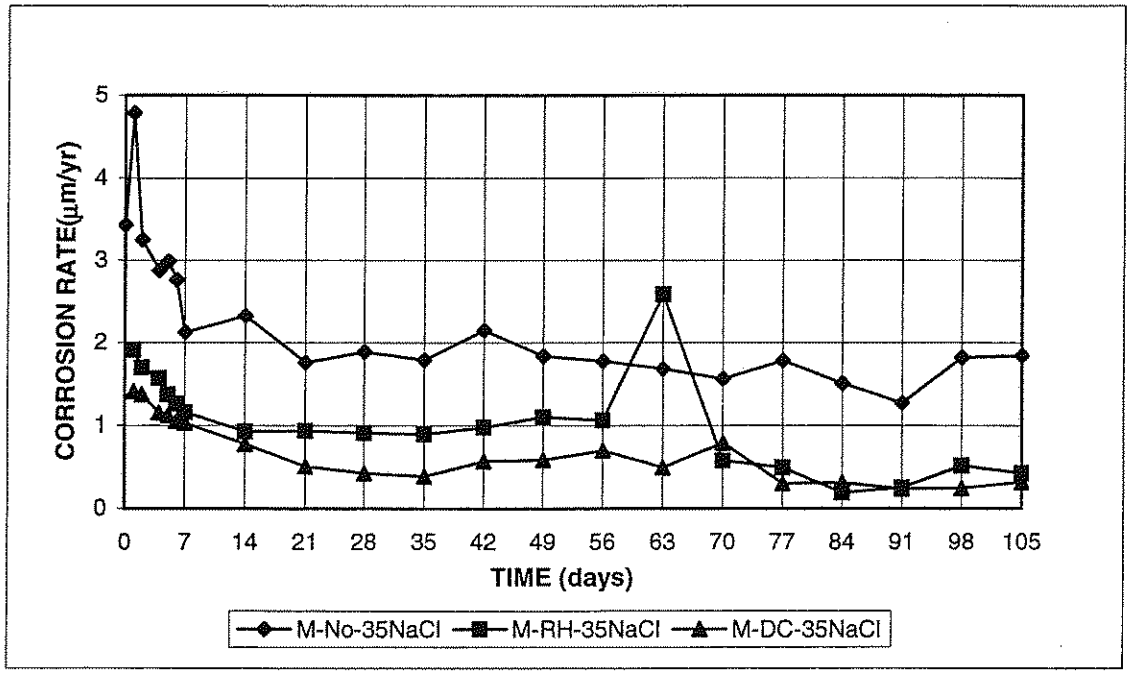

Figure 3.31 Macrocell test: Average corrosion rate with or without inhibitors; w/c=0.35; 1.6 m ion NaCl in simulated concrete pore solution

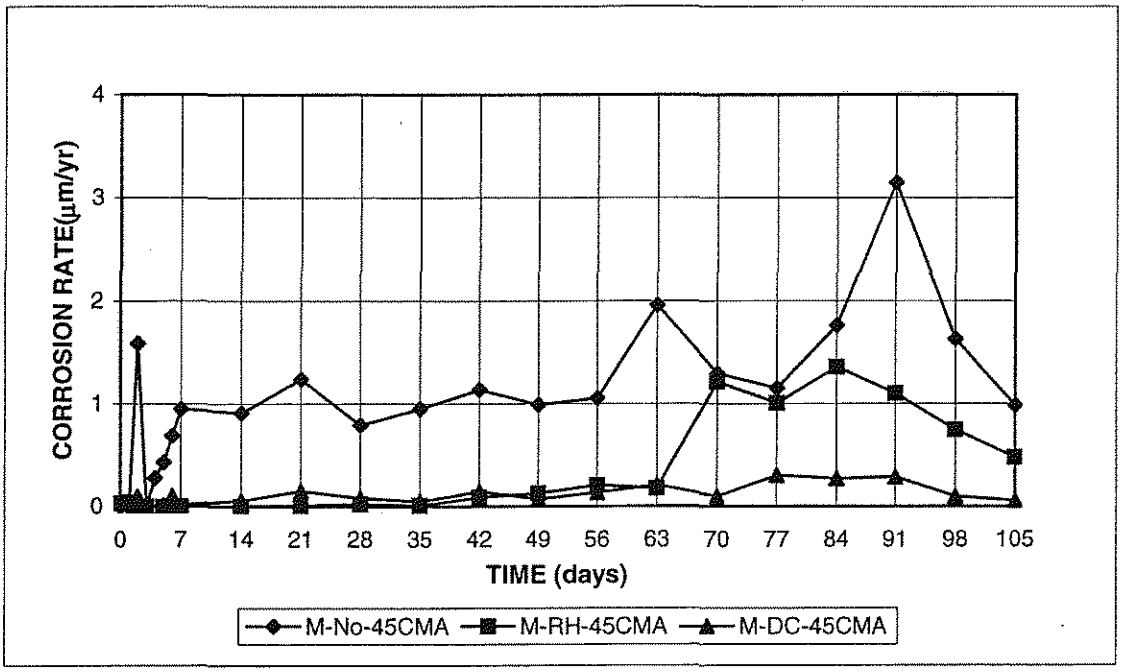

Figure 3.32 Macrocell test: Average corrosion rate with or without inhibitors; w/c=0.45; 1.6 m ion CMA in simulated concrete pore solution

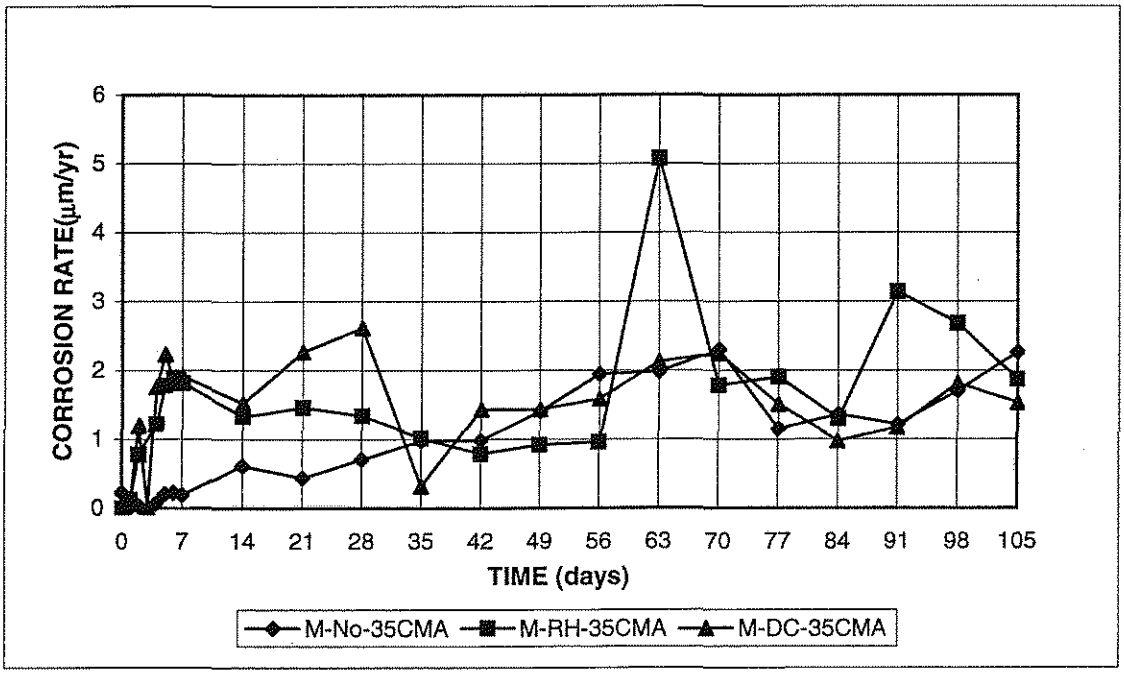

Figure 3.33 Macrocell test: Average corrosion rate with or without inhibitors; w/c=0.35; 1.6 m ion CMA in simulated concrete pore solution

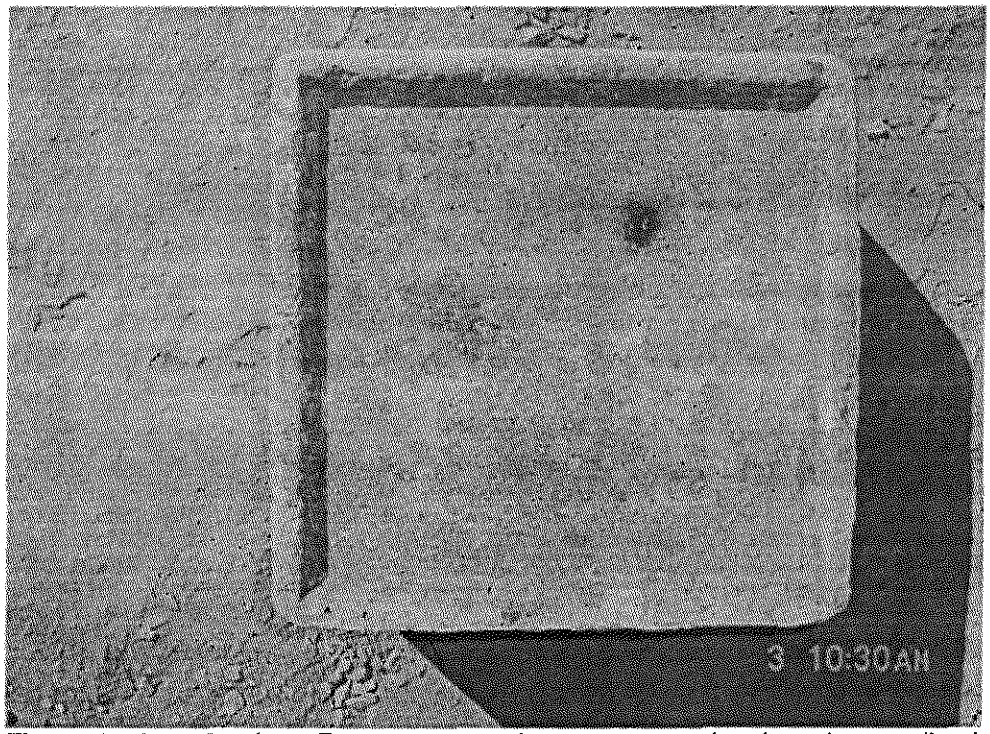

Figure 3.34 Southern Exposure test: w/c=0.45, conventional steel, normalized, no inhibitors, 6.04 m ion NaCl, specimen #3

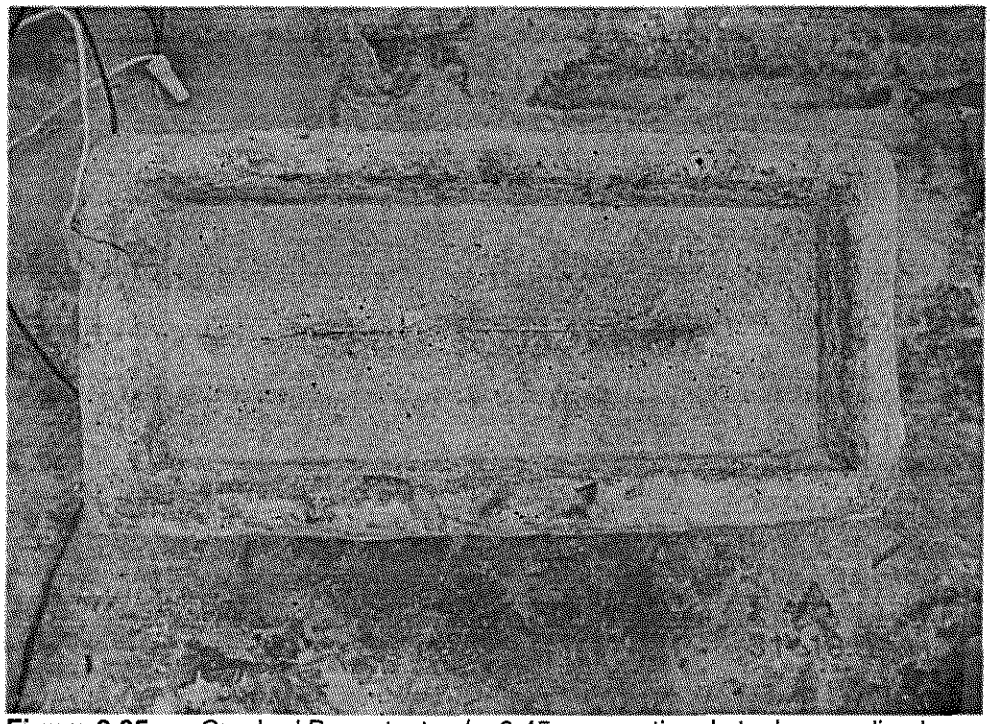

Figure 3.35 Cracked Beam test: w/c=0.45, conventional steel, normalized, rheocrete, 6.04 m ion NaCl, specimen #1

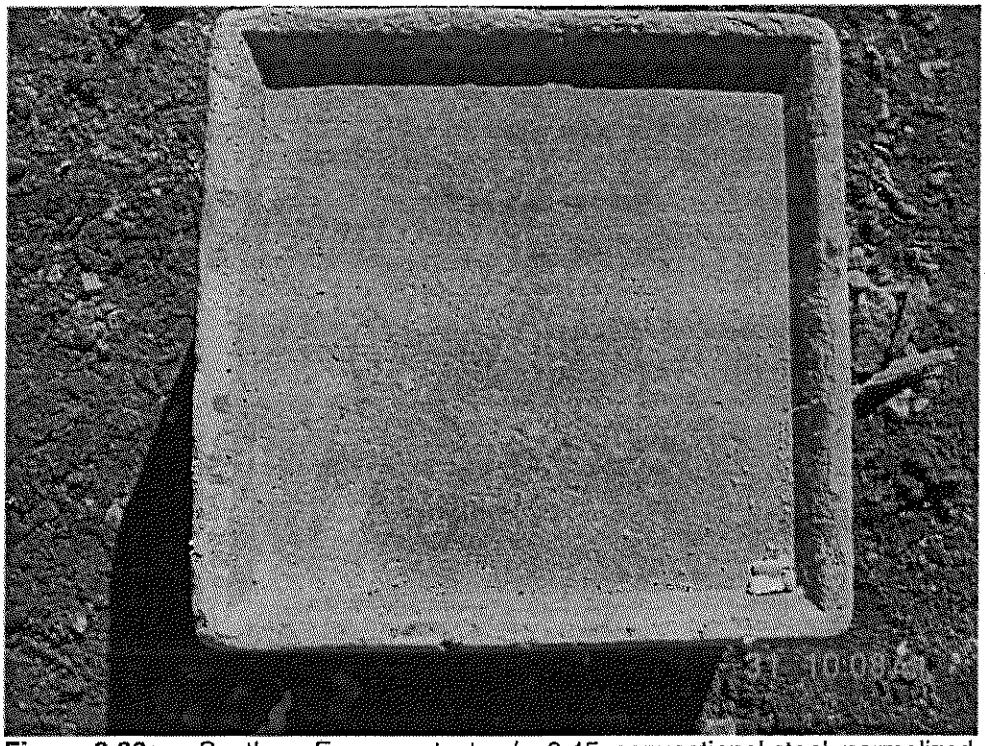

Figure 3.36 Southern Exposure test: w/c=0.45, conventional steel, normalized, no inhibitors, 6.04 m ion NaCl, specimen #2

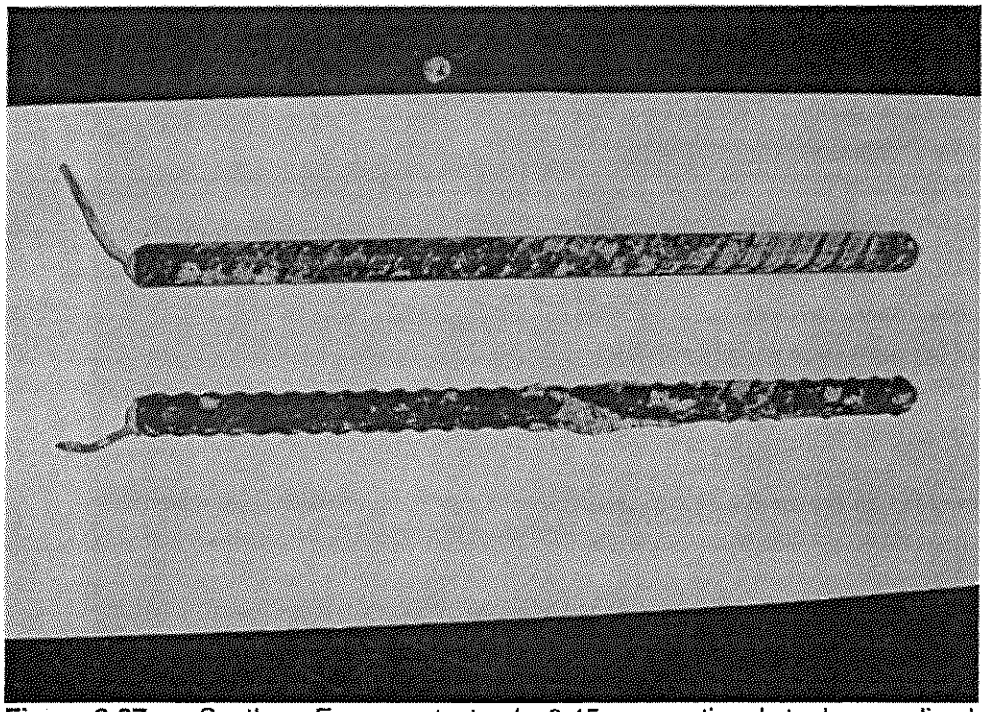

Figure 3.37 Southern Exposure test: w/c=0.45, conventional steel, normalized, rheocrete, 6.04 m ion NaCl, specimen #1, top mat

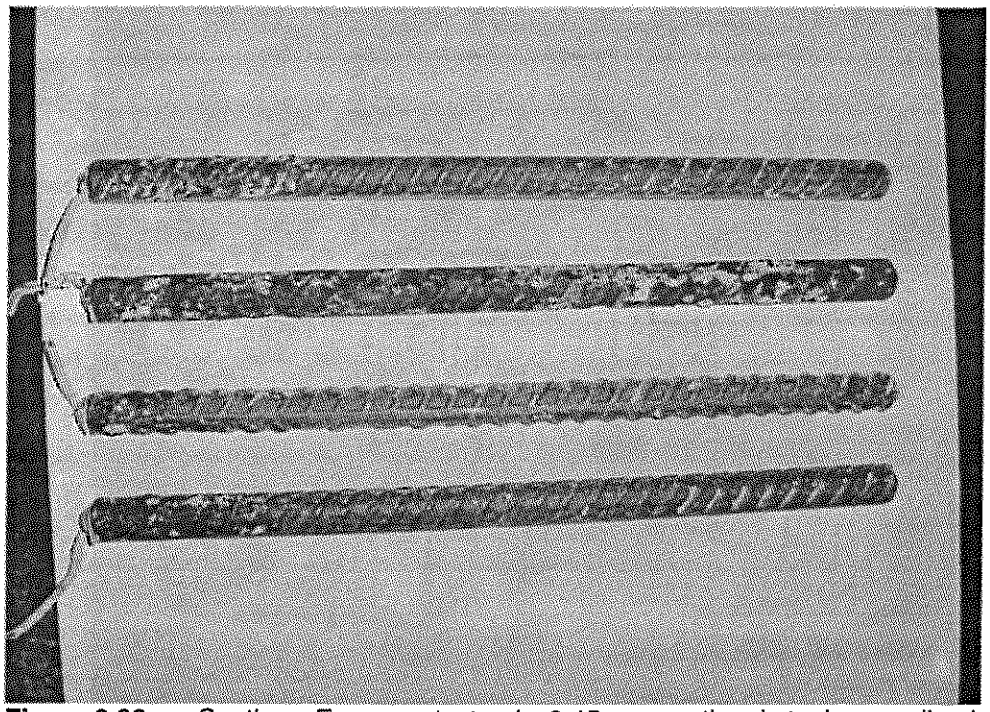

Figure 3.38 Southern Exposure test: w/c=0.45, conventional steel, normalized, no inhibitors, 6.04 m ion NaCl, specimen #3, bottom mat

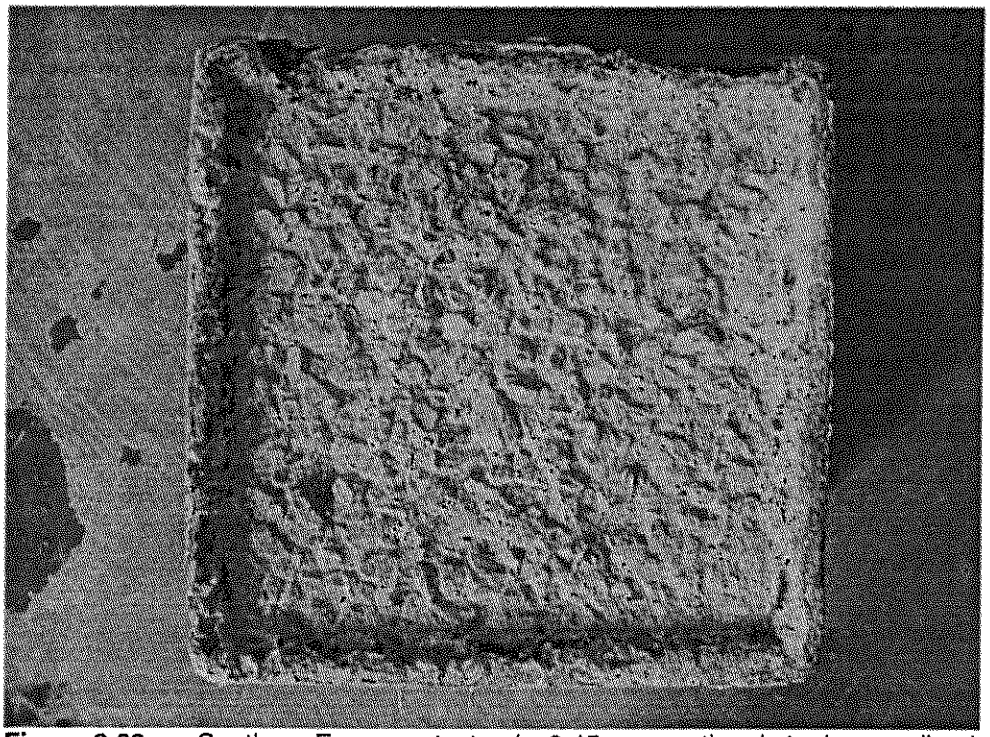

Figure 3.39 Southern Exposure test: w/c=0.45, conventional steel, normalized, rheocrete, 6.04 m ion CMA, specimen #1

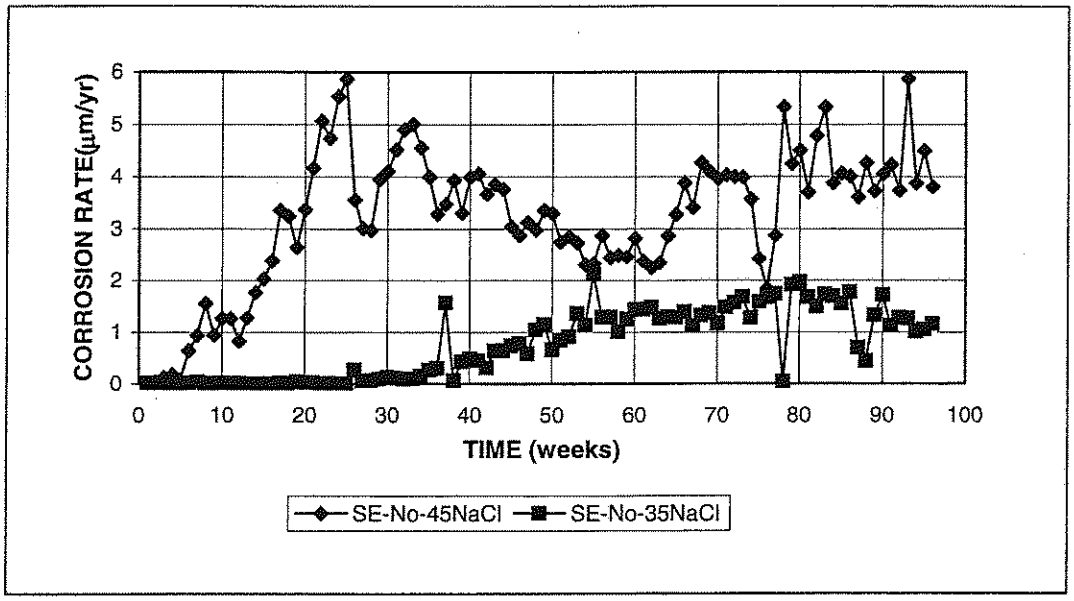

Figure 3.40 Southern Exposure test: Average corrosion rate for different water cement ratio, coventional steel, normalized, no inhibitors, 6.04 m ion NaCl

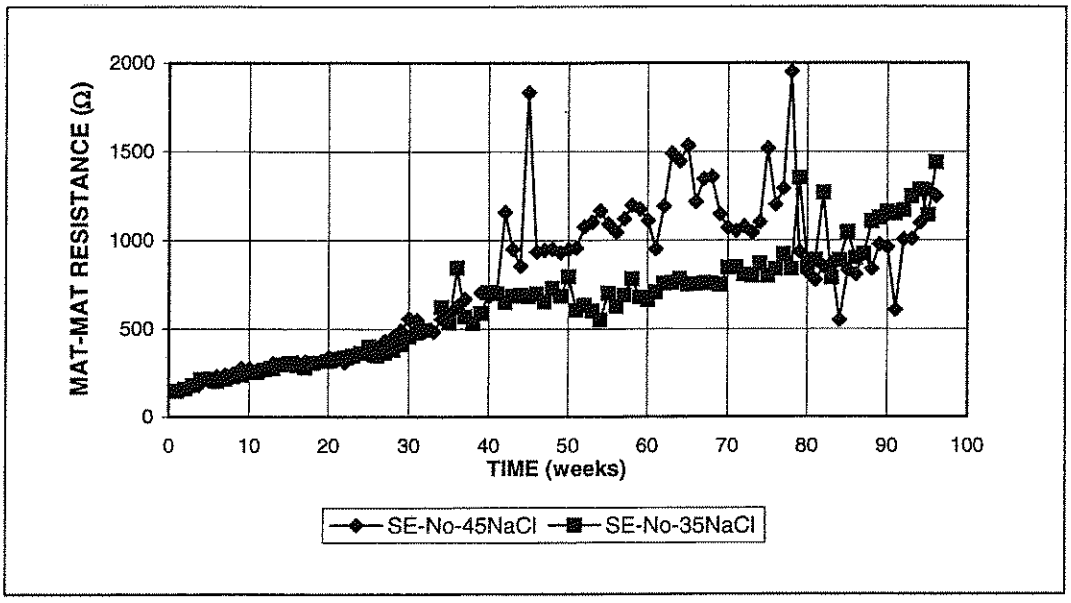

Figure 3.41 Southern Exposure test: Average mat-to-mat resistance for different water cement ratio, coventional steel, normalized, no inhibitors, 6.04 m ion NaCl

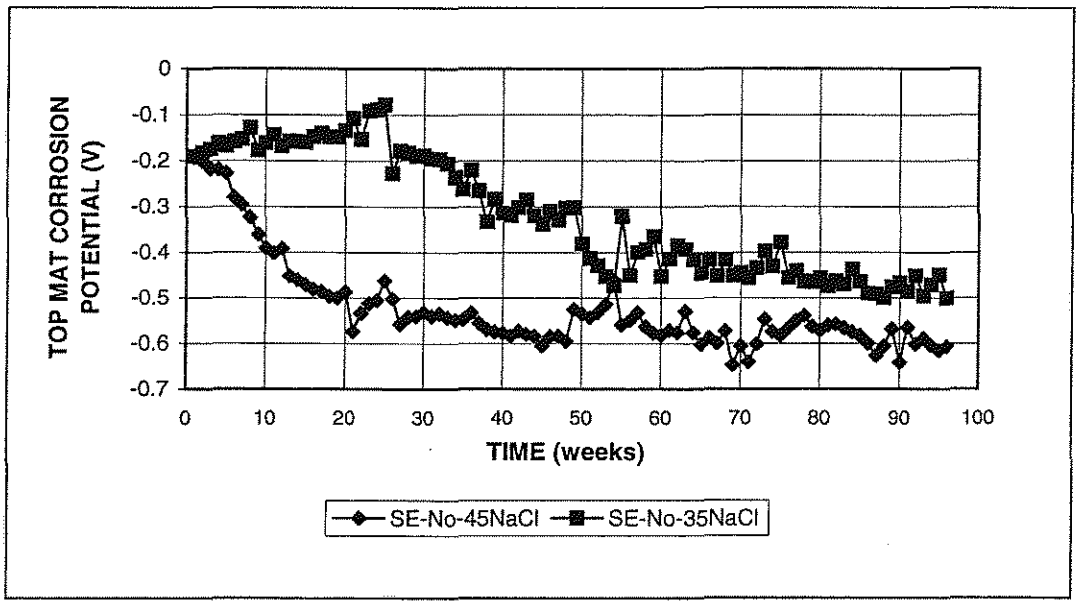

Figure 3.42 Southern Exposure test: Average corrosion potential with respect to copper-copper sulfate electrode. Top mat, different water cement ratio, coventional steel, normalized, no inhibitors, 6.04 m ion NaCl

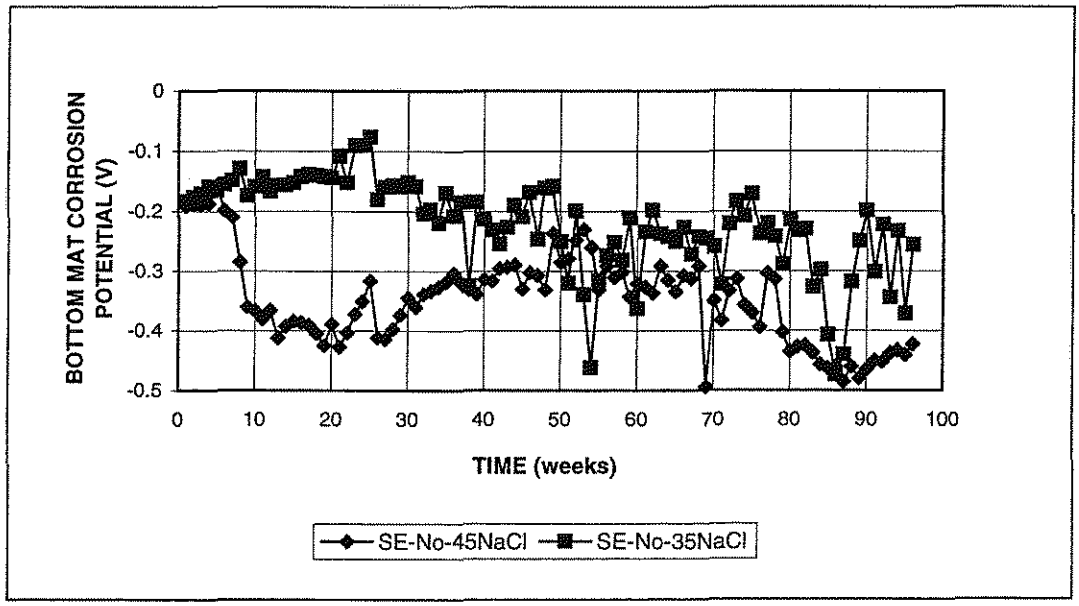

Figure 3.43 Southern Exposure test: Average corrosion potential with respect to copper-copper sulfate electrode. Bottom mat, different water cement ratio, coventional steel, normalized, no inhibitors, 6.04 m ion NaCl

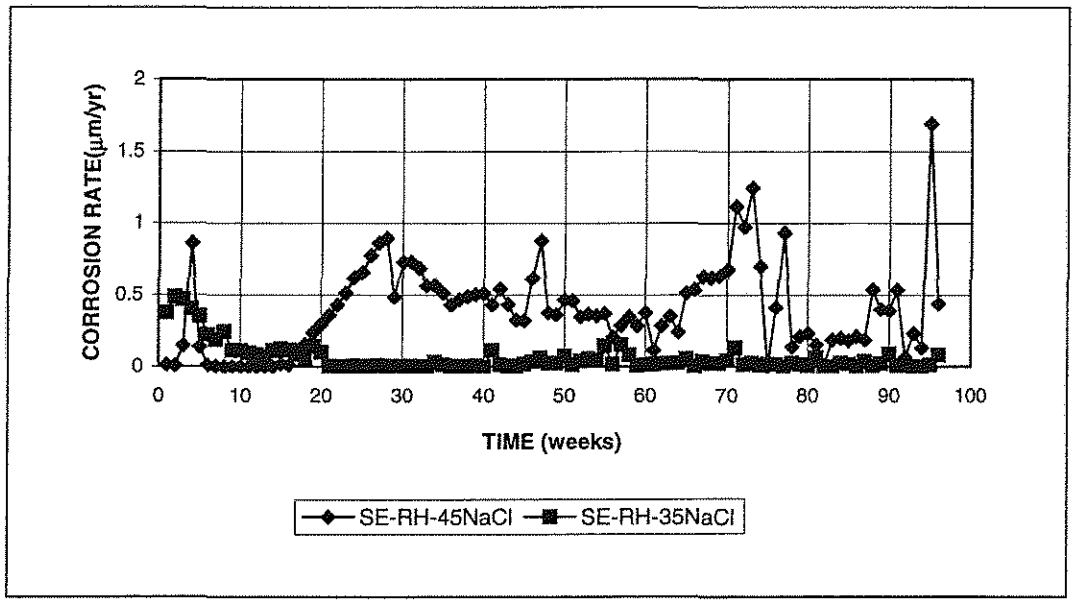

Figure 3.44 Southern Exposure test: Average corrosion rate for different water cement ratio, coventional steel, normalized, Rheocrete, 6.04 m ion NaCl

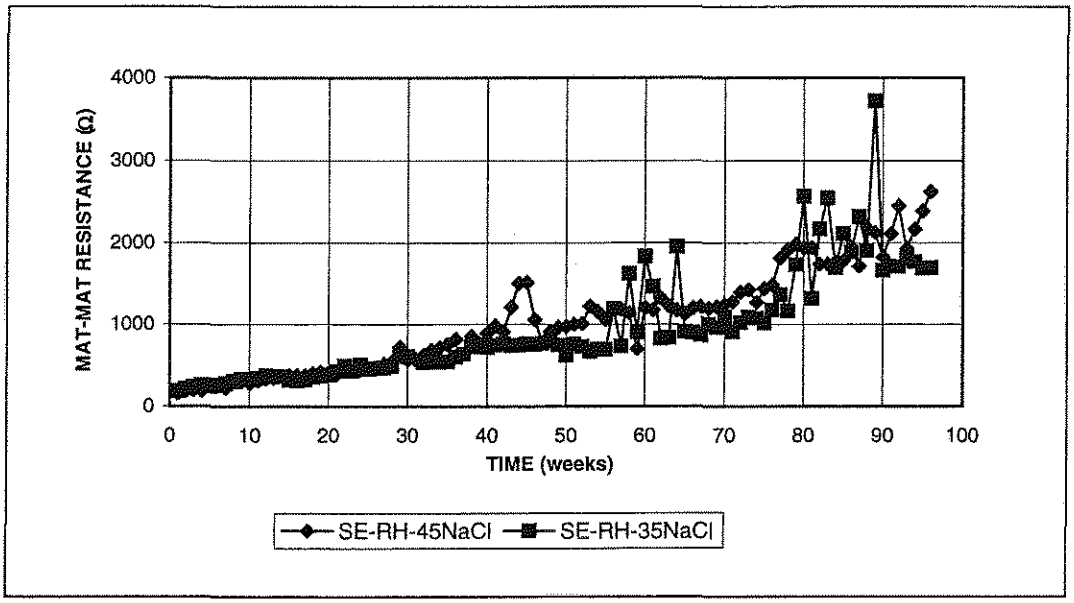

Figure 3.45 Southern Exposure test: Average mat-to-mat resistance for different water cement ratio, coventional steel, normalized, Rheocrete, 6.04 m ion NaCl

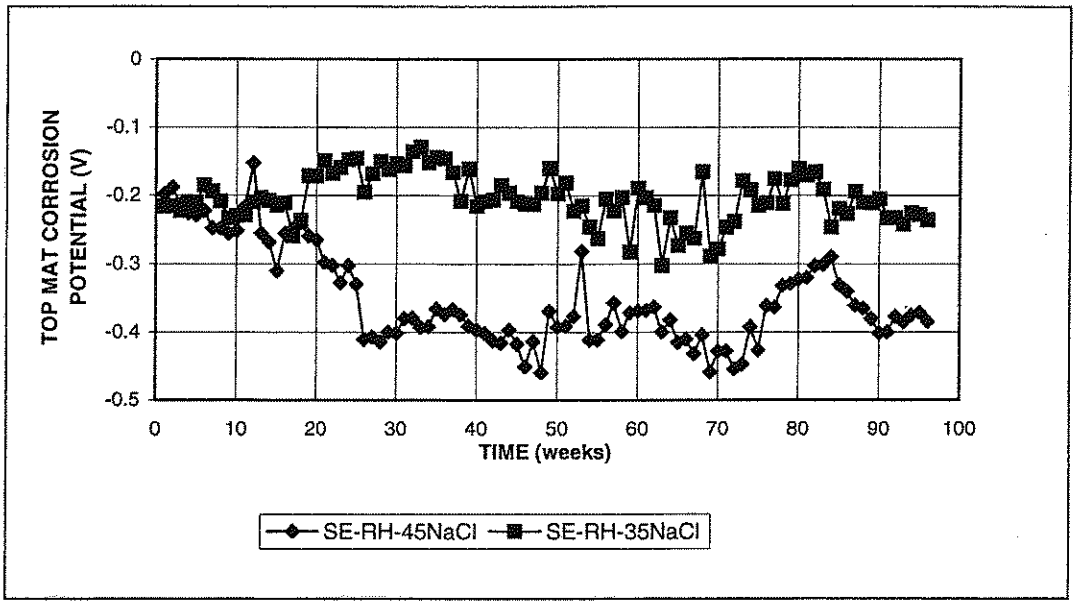

Figure 3.46 Southern Exposure test: Average corrosion potential with respect to copper-copper sulfate electrode. Top mat, different water cement ratio, coventional steel, normalized, Rheocrete, 6.04 m ion NaCl

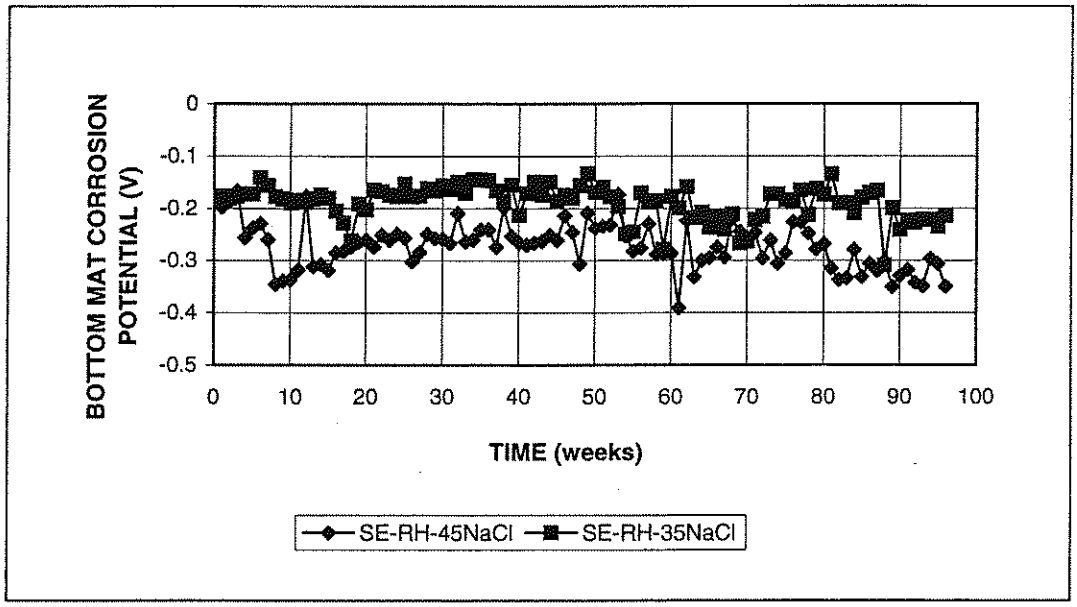

Figure 3.47 Southern Exposure test: Average corrosion potential with respect to copper-copper sulfate electrode. Bottom mat, different water cement ratio, coventional steel, normalized, Rheocrete, 6.04 m ion NaCl

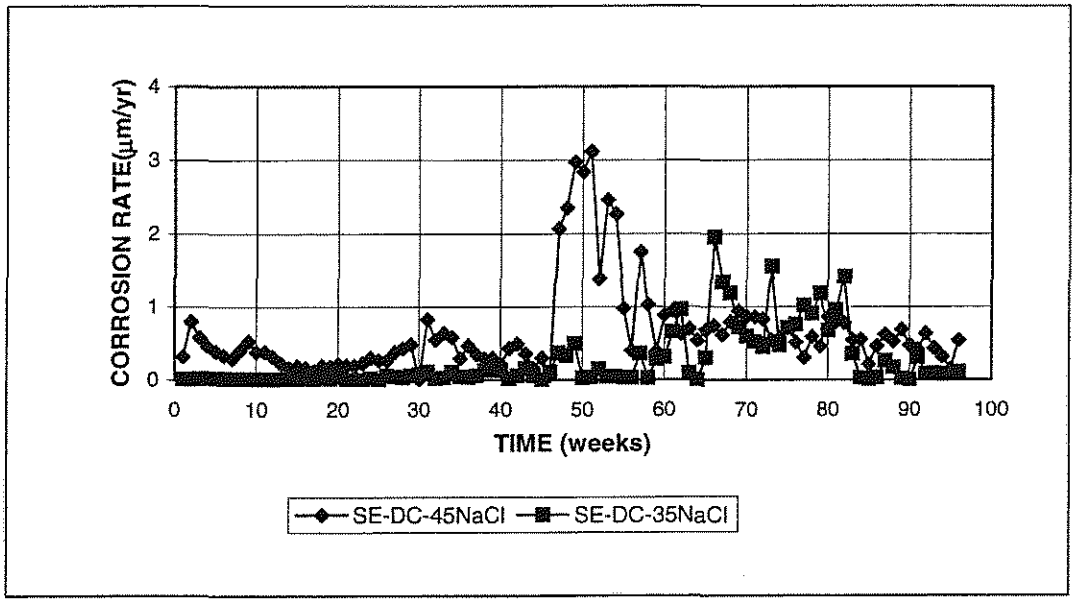

Figure 3.48 Southern Exposure test: Average corrosion rate for different water cement ratio, coventional steel, normalized, DCI, 6.04 m ion NaCl

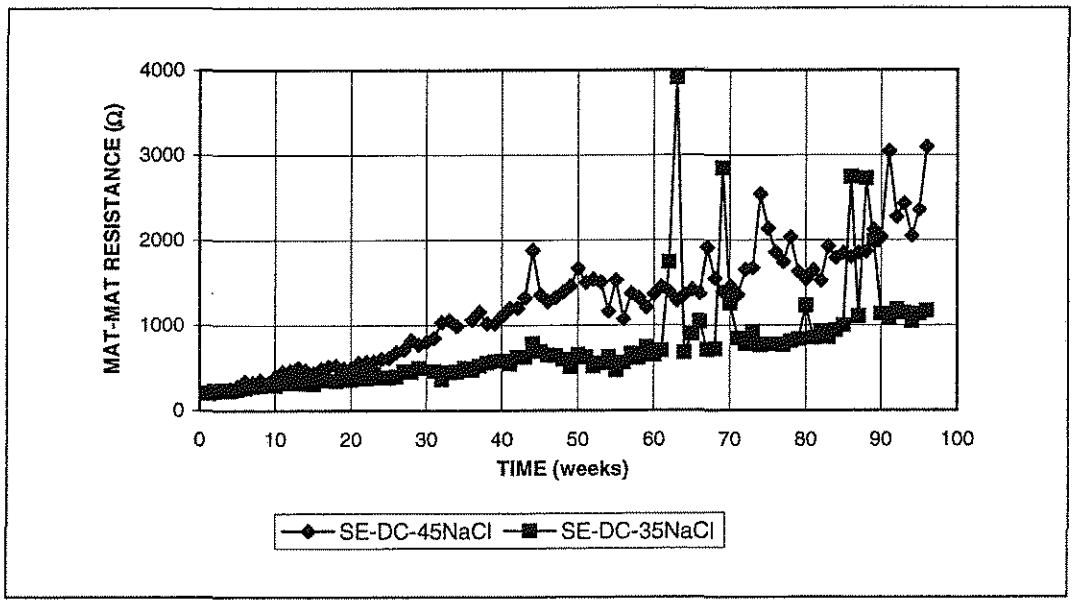

Figure 3.49 Southern Exposure test: Average mat-to-mat resistance for different water cement ratio, coventional steel, normalized, DCI, 6.04 m ion NaCl

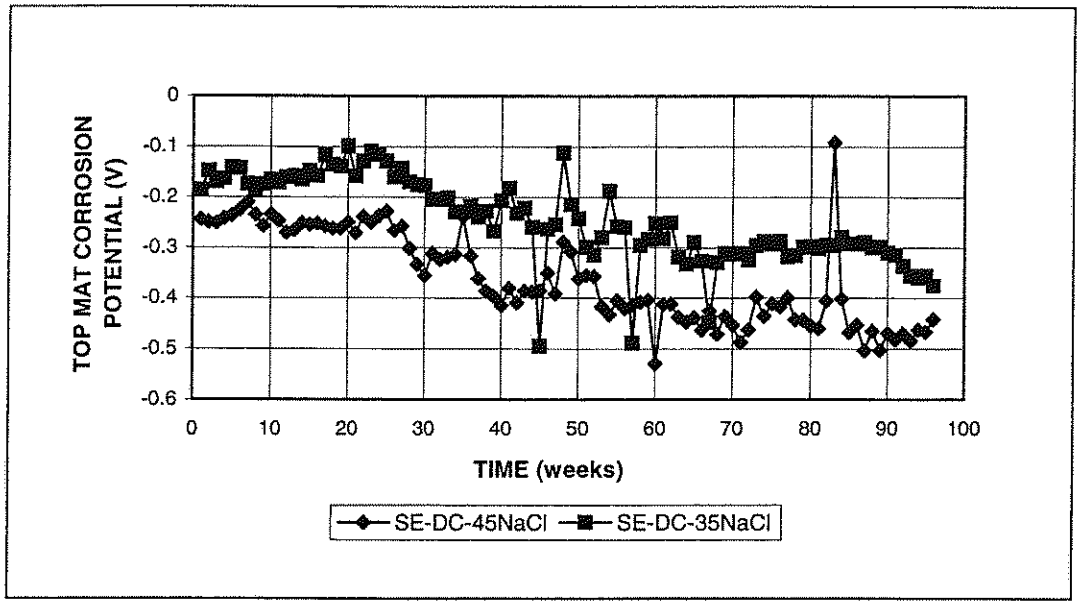

Figure 3.50 Southern Exposure test: Average corrosion potential with respect to copper-copper sulfate electrode. Top mat, different water cement ratio, coventional steel, normalized, DCl, 6.04 m ion NaCl

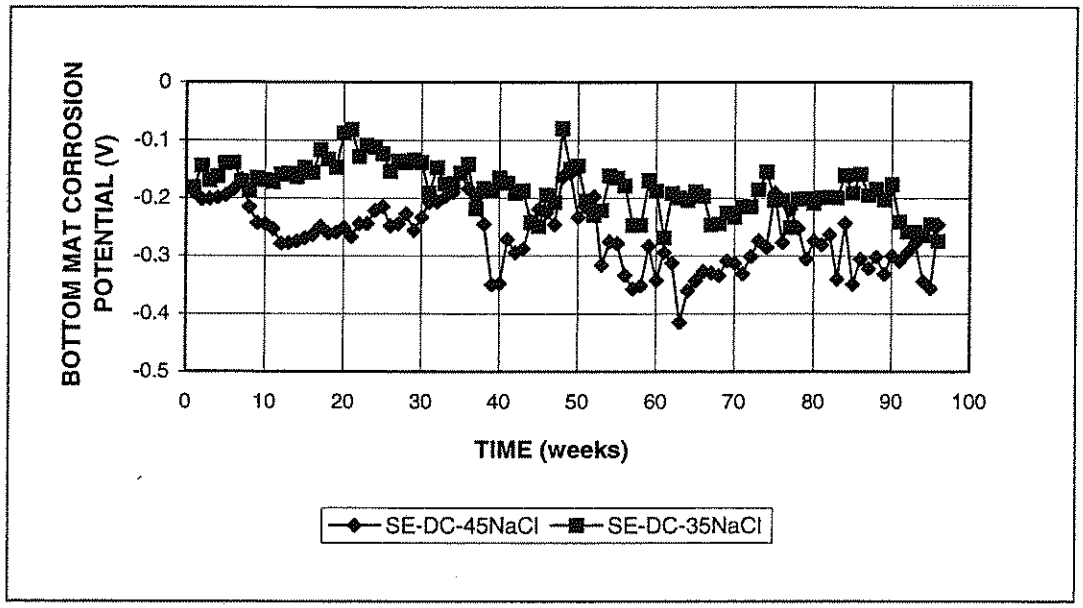

Figure 3.51 Southern Exposure test: Average corrosion potential with respect to copper-copper sulfate electrode. Bottom mat, different water cement ratio, coventional steel, normalized, DCl, 6.04 m ion NaCl

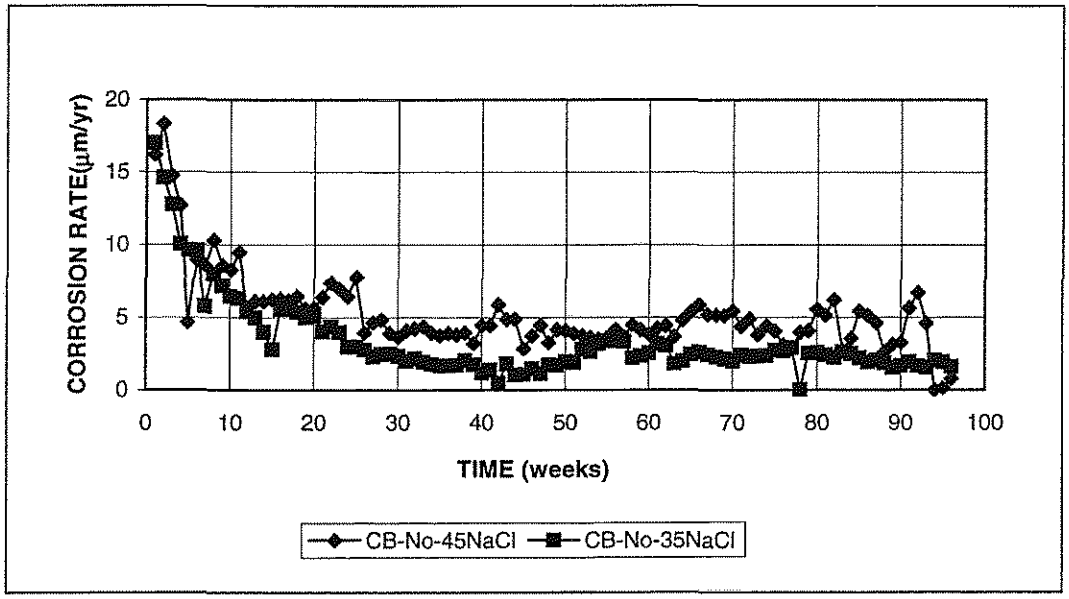

Figure 3.52 Cracked Beam test: Average corrosion rate for different water cement ratio, coventional steel, normalized, no inhibitors, 6.04 m ion NaCl

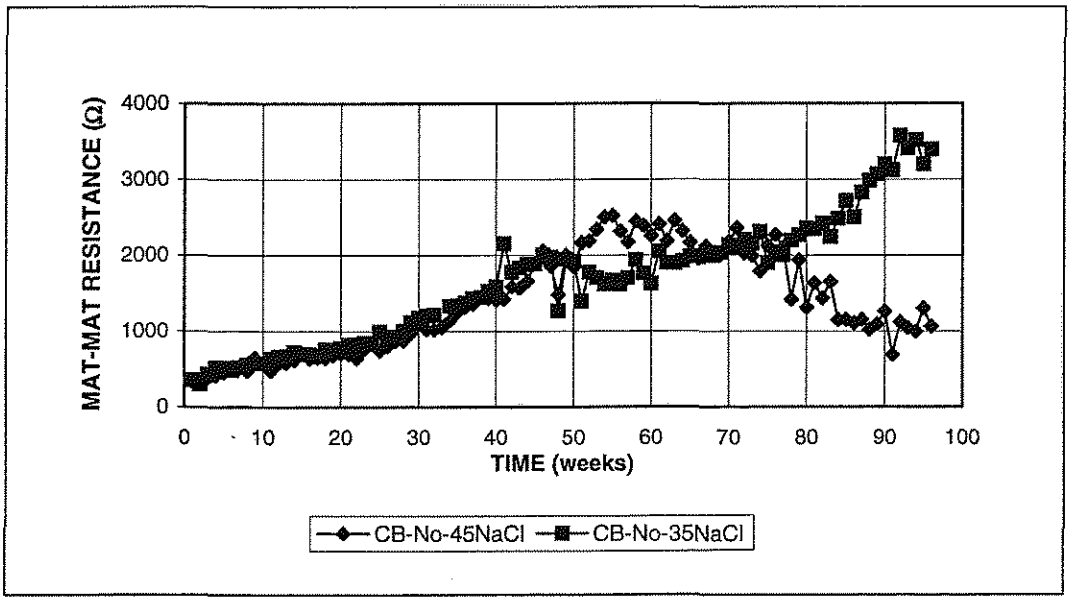

Figure 3.53 Cracked Beam test: Average mat-to-mat resistance for different water cement ratio, coventional steel, normalized, no inhibitors, 6.04 m ion NaCl

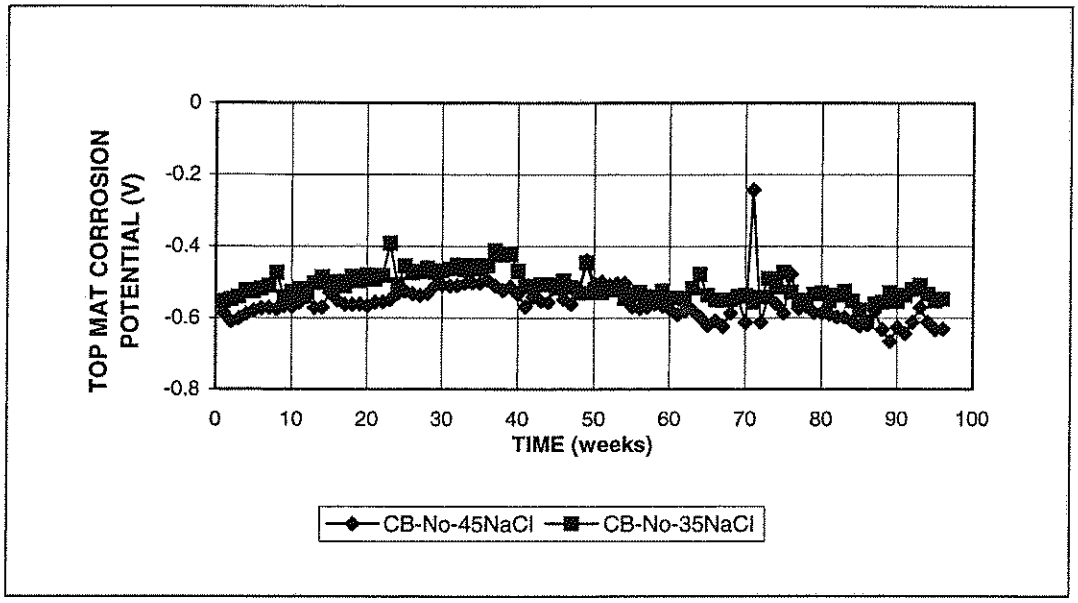

Figure 3.54 Cracked Beam test: Average corrosion potential with respect to copper-copper sulfate electrode. Top mat, different water cement ratio, coventional steel, normalized, no inhibitors, 6.04 m ion NaCl

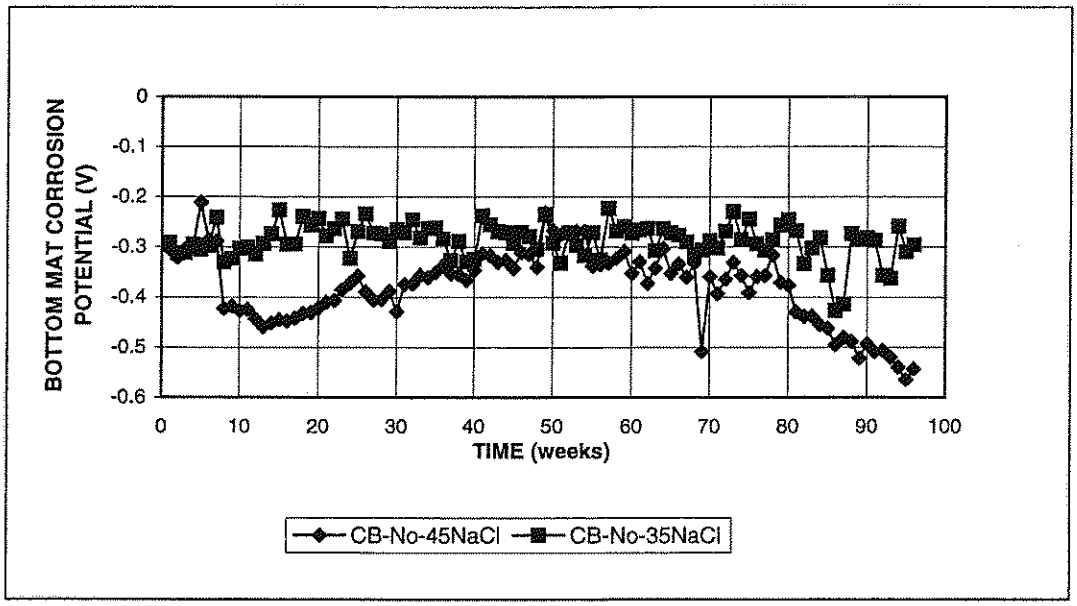

Figure 3.55 Cracked Beam test: Average corrosion potential with respect to copper-copper sulfate electrode. Bottom mat, different water cement ratio, coventional steel, normalized, no inhibitors, 6.04 m ion NaCl

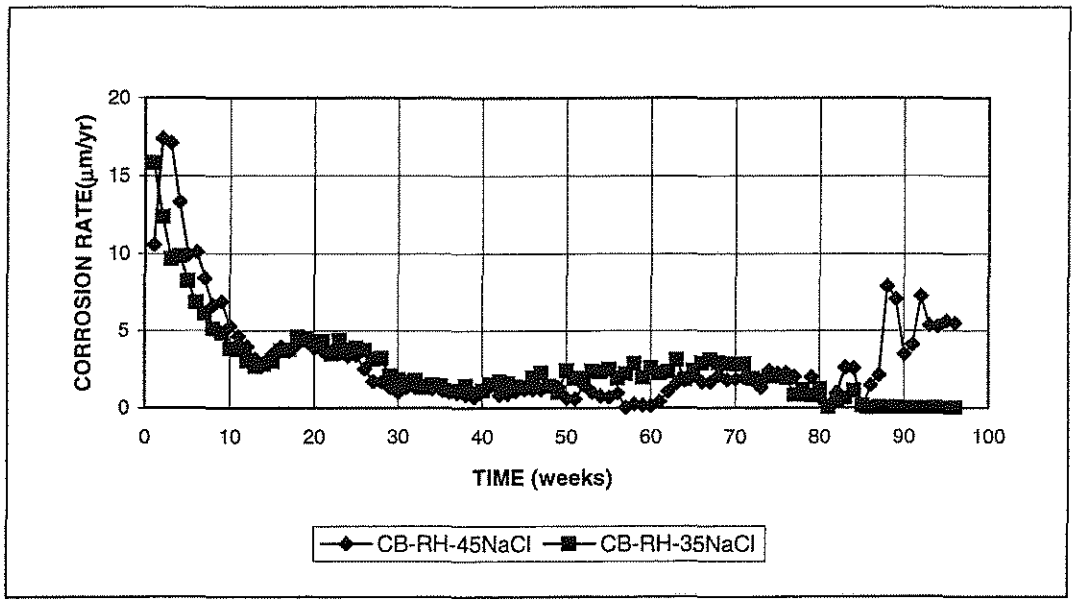

Figure 3.56 Cracked Beam test: Average corrosion rate for different water cement ratio, coventional steel, normalized, Rheocrete, 6.04 m ion NaCl

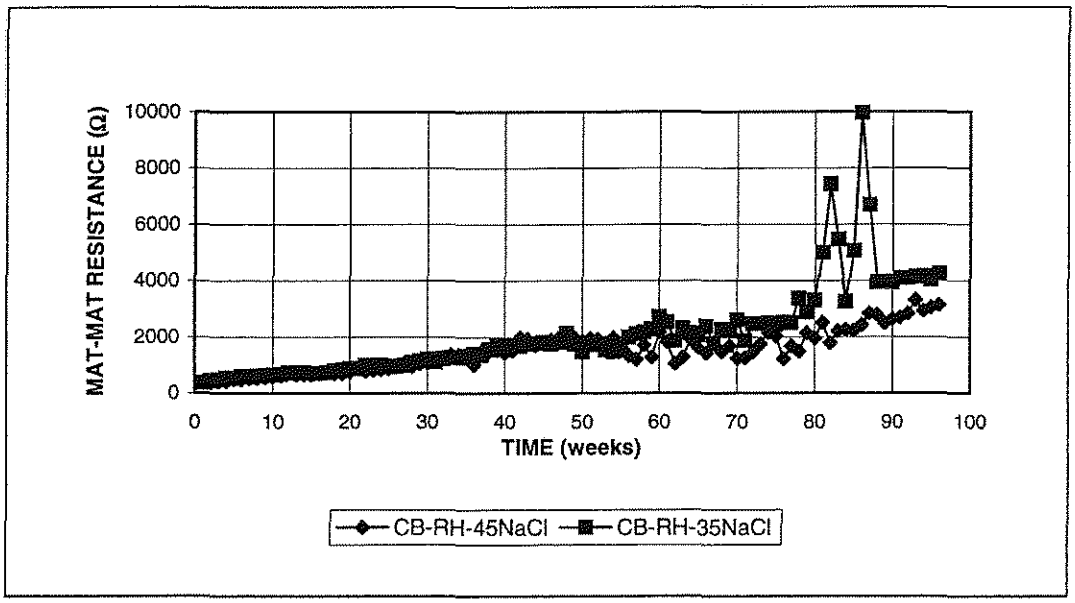

Figure 3.57 Cracked Beam test: Average mat-to-mat resistance for different water cement ratio, coventional steel, normalized, Rheocrete, 6.04 m ion NaCl

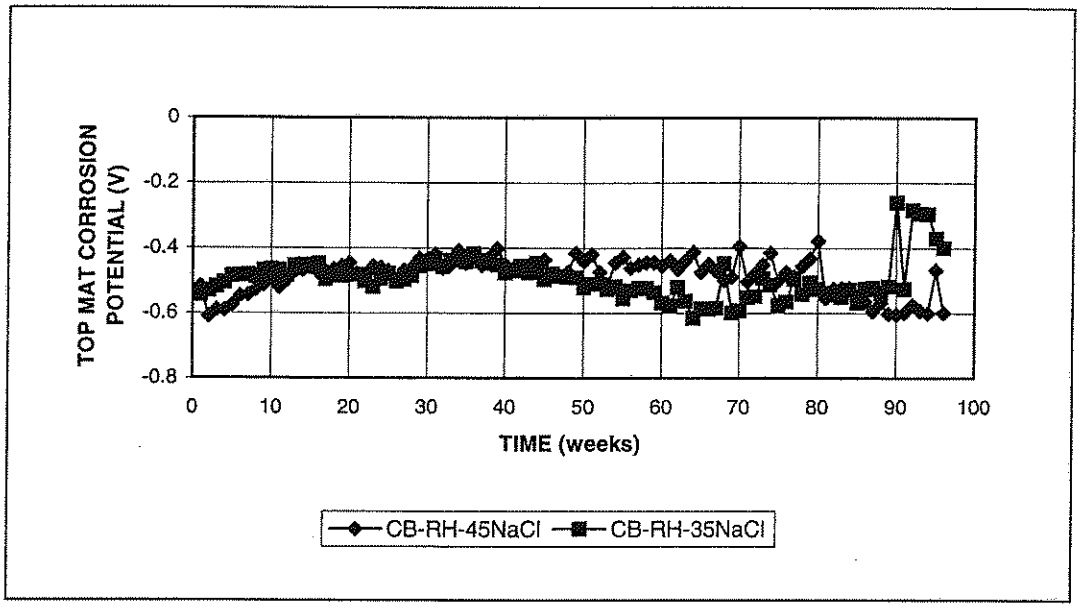

Figure 3.58 Cracked Beam test: Average corrosion potential with respect to copper-copper sulfate electrode. Top mat, different water cement ratio, coventional steel, normalized, Rheocrete, 6.04 m ion NaCl

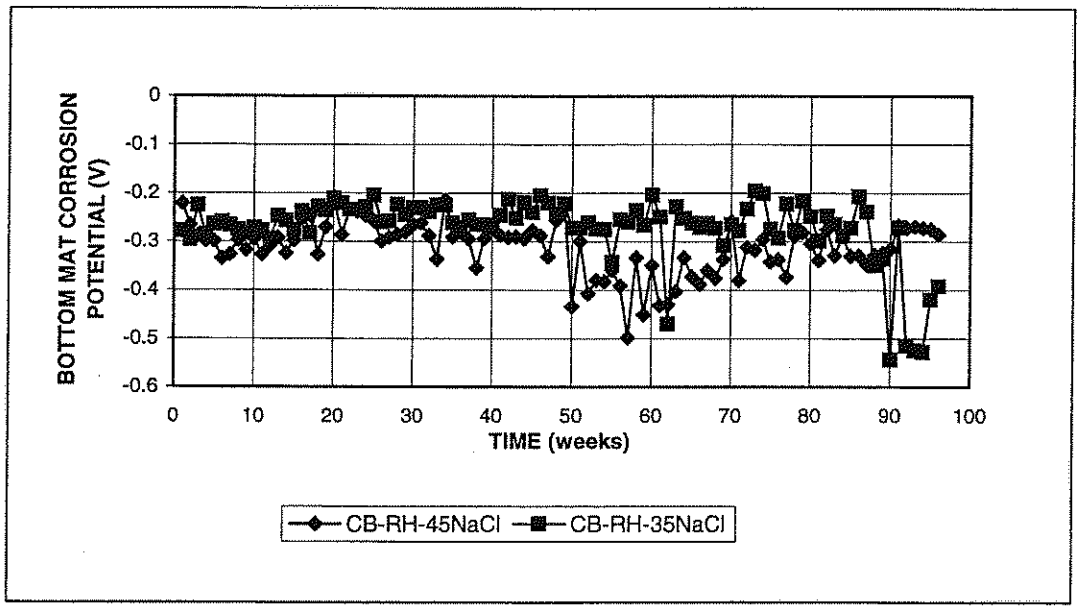

Figure 3.59 Cracked Beam test: Average corrosion potential with respect to copper-copper sulfate electrode. Bottom mat, different water cement ratio, coventional steel, normalized, Rheocrete, 6.04 m ion NaCl

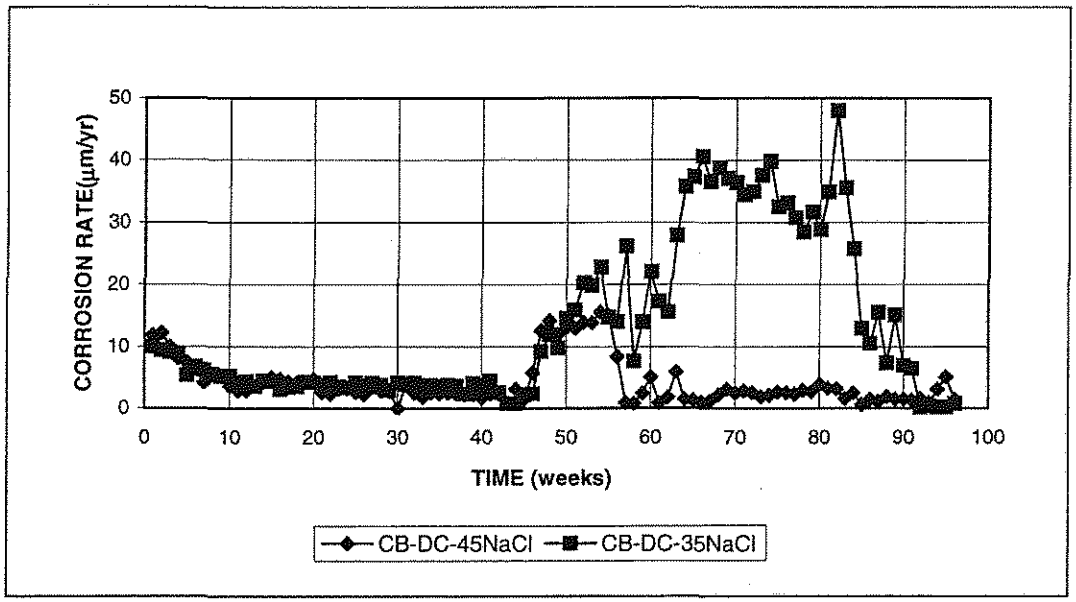

Figure 3.60 Cracked Beam test: Average corrosion rate for different water cement ratio, coventional steel, normalized, DCI, 6.04 m ion NaCl

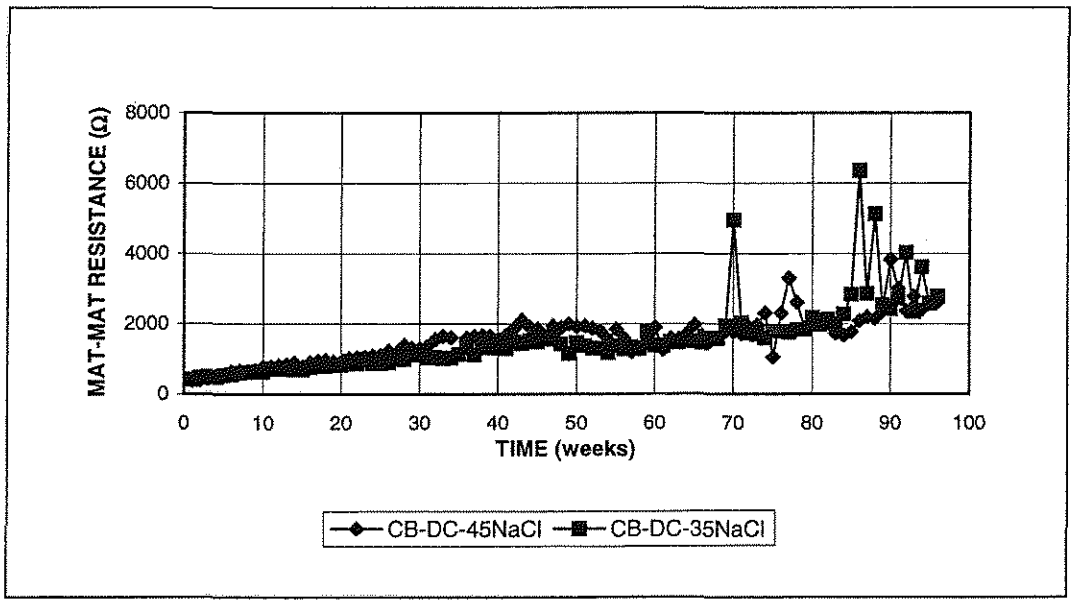

Figure 3.61 Cracked Beam test: Average mat-to-mat resistance for different water cement ratio, coventional steel, normalized, DCI, 6.04 m ion NaCl

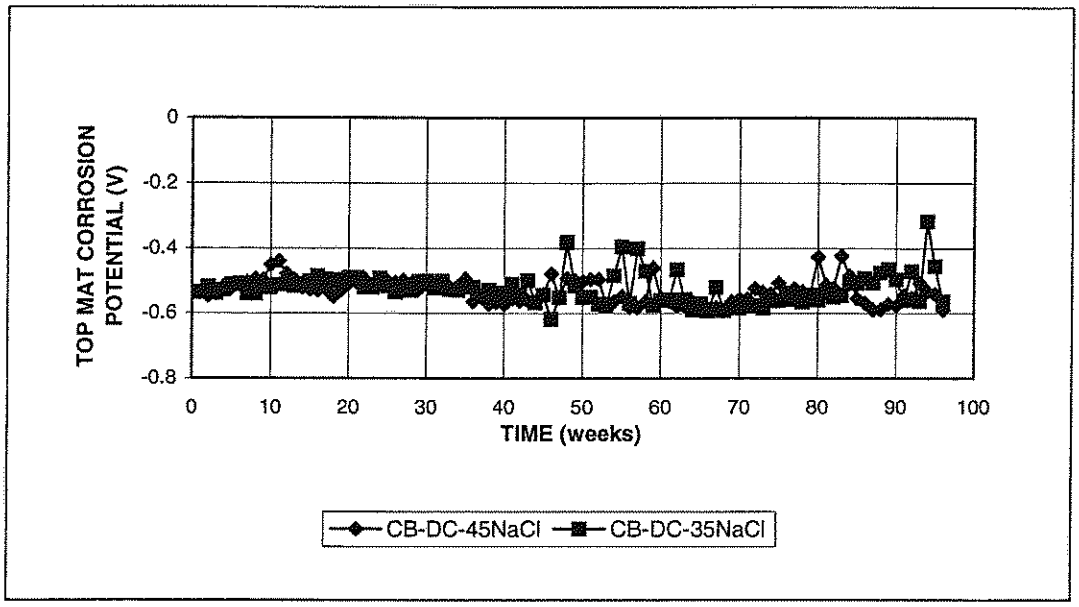

Figure 3.62 Cracked Beam test: Average corrosion potential with respect to copper-copper sulfate electrode. Top mat, different water cement ratio, coventional steel, normalized, DCI, 6.04 m ion NaCl

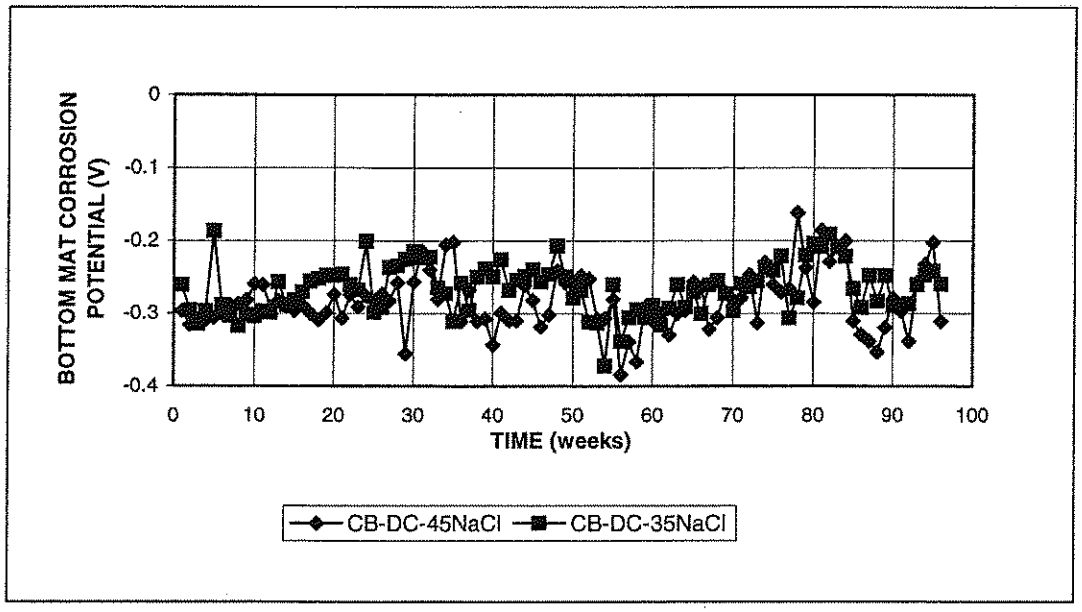

Figure 3.63 Cracked Beam test: Average corrosion potential with respect to copper-copper sulfate electrode. Bottom mat, different water cement ratio, coventional steel, normalized, DCI, 6.04 m ion NaCl

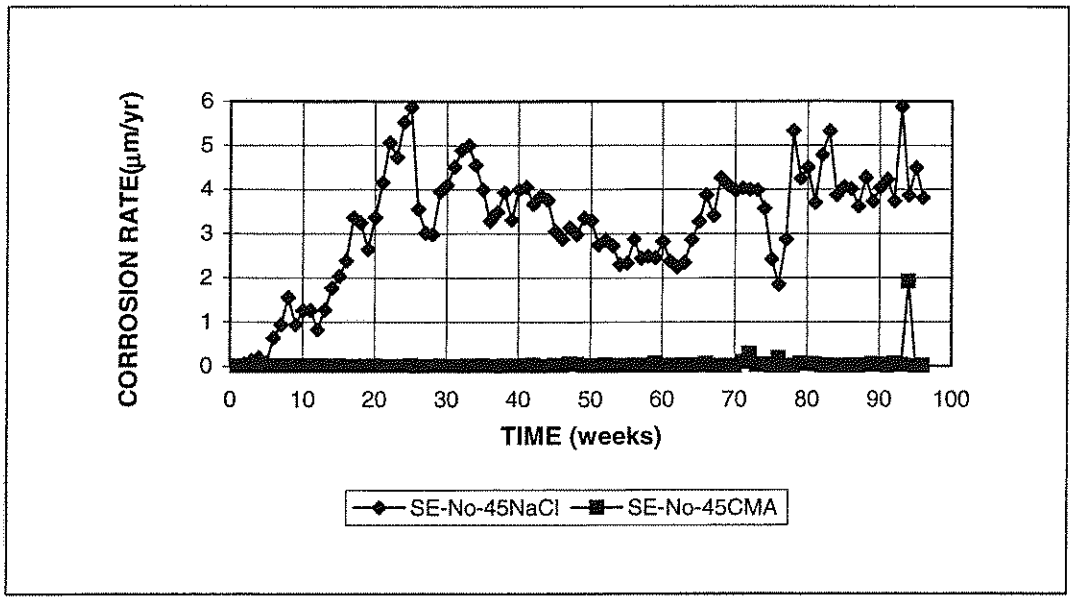

Figure 3.64 Southern Exposure test: Average corrosion rate for different deicer solution, coventional steel, normalized, w/c=0.45, no inhibitors, 6.04 m ion NaCl or CMA

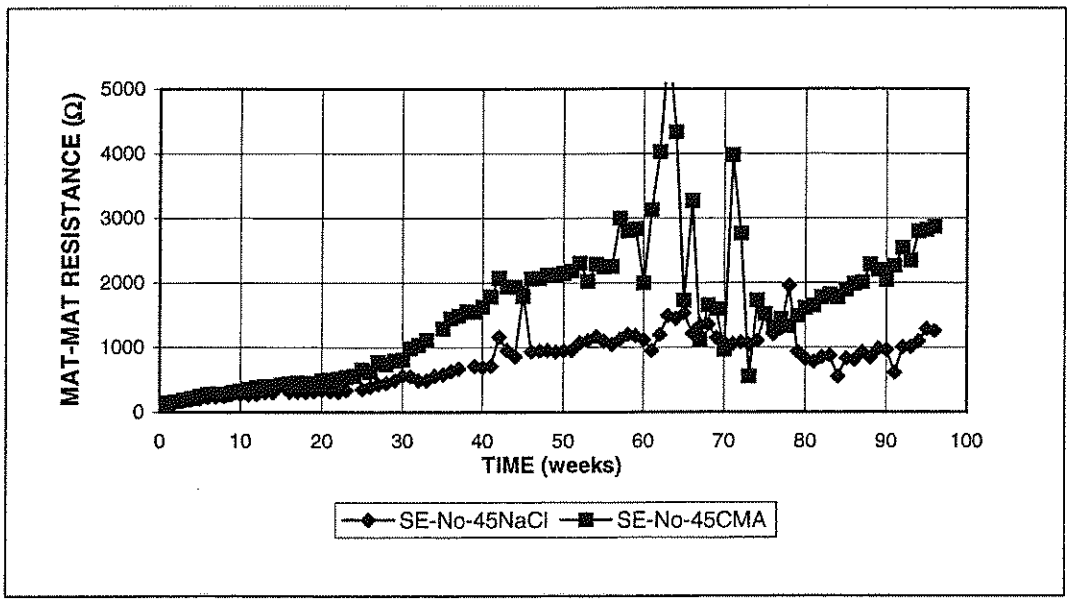

Figure 3.65 Southern Exposure test: Average mat-to-mat resistance for different deicer solution, coventional steel, normalized, w/c=0.45, no inhibitors, 6.04 m ion NaCl or CMA

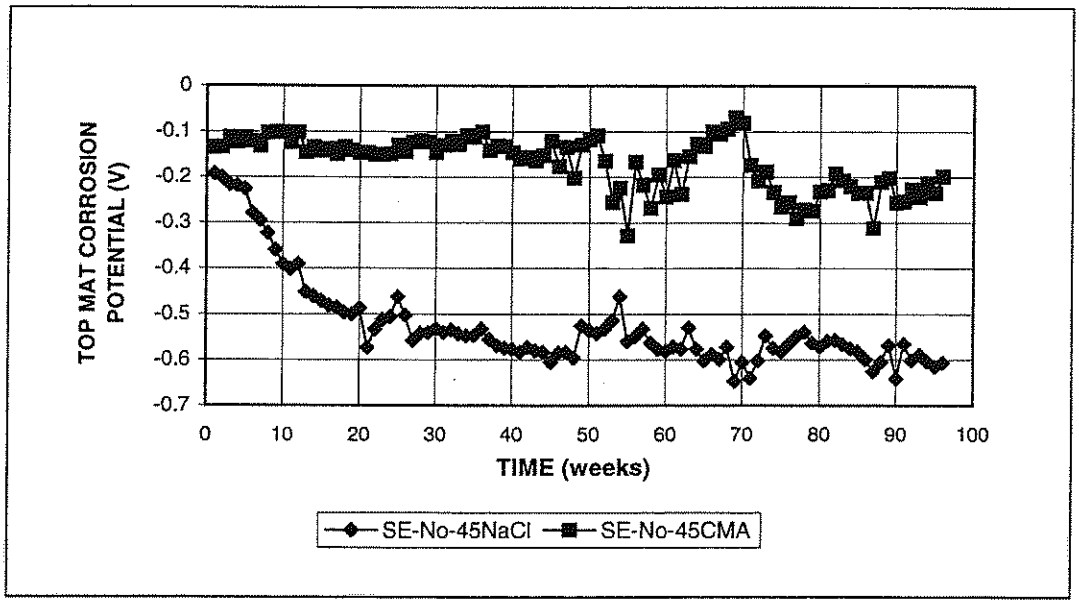

Figure 3.66 Southern Exposure test: Average corrosion potential with respect to copper-copper sulfate electrode. Top mat, different deicer solution, coventional steel, normalized, w/c=0.45, no inhibitors, 6.04 m ion NaCl or CMA

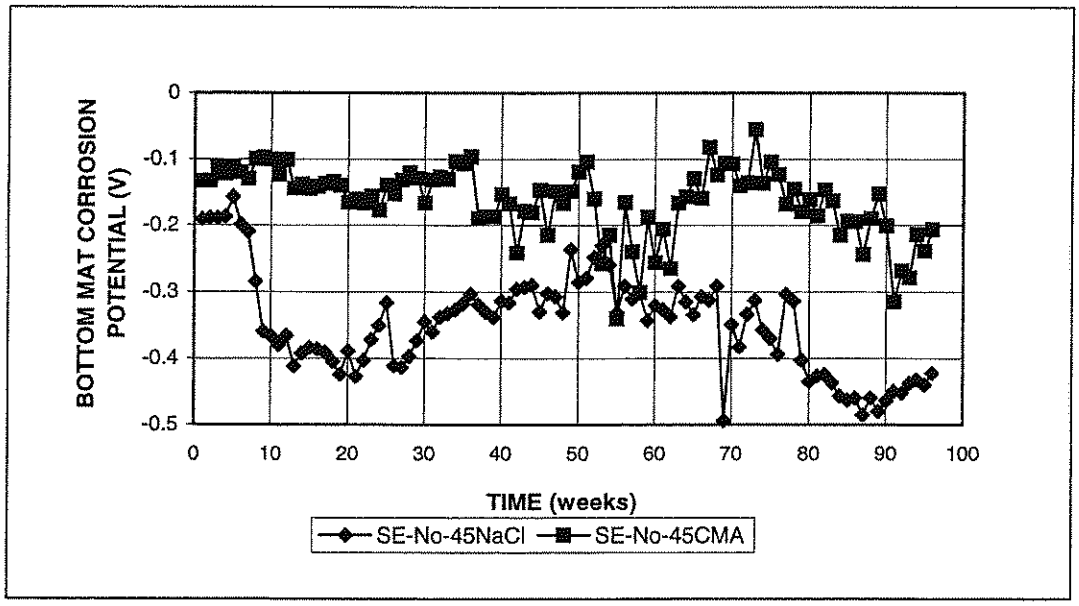

Figure 3.67 Southern Exposure test: Average corrosion potential with respect to copper-copper sulfate electrode. Bottom mat, different deicer solution, coventional steel, normalized, w/c=0.45, no inhibitors, 6.04 m ion NaCl or CMA

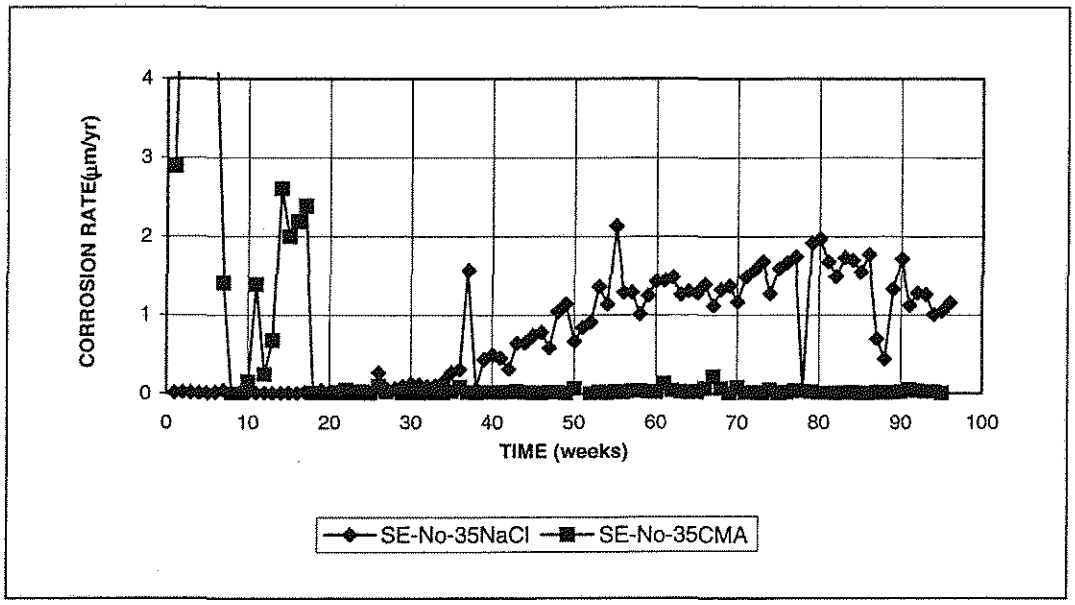

Figure 3.68 Southern Exposure test: Average corrosion rate for different deicer solution, coventional steel, normalized, w/c=0.35, no inhibitors, 6.04 m ion NaCl or CMA

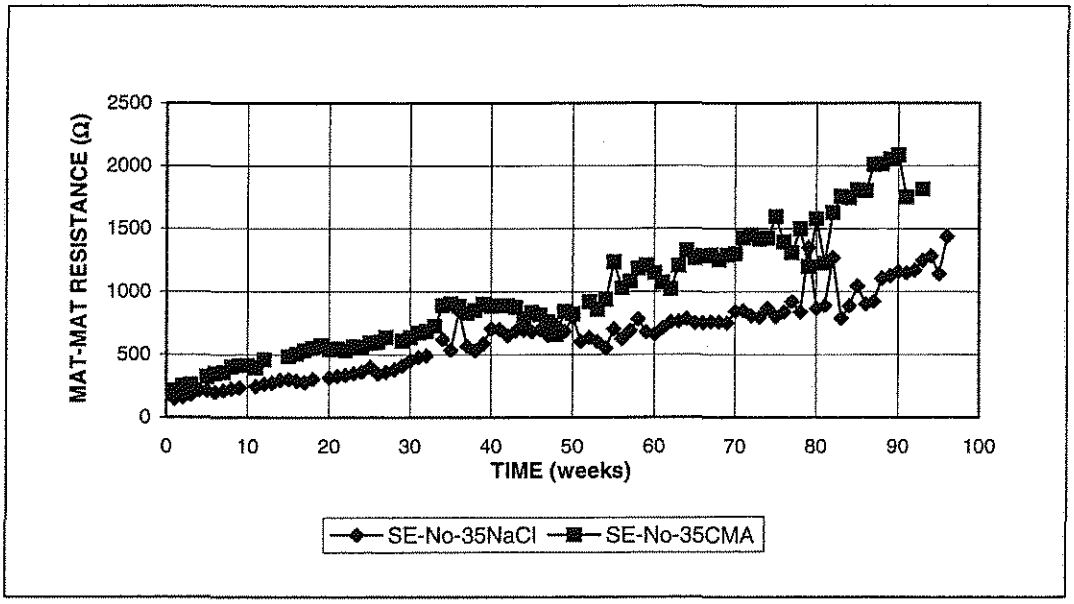

Figure 3.69 Southern Exposure test: Average mat-to-mat resistance for different deicer solution, coventional steel, normalized, w/c=0.35, no inhibitors, 6.04 m ion NaCl or CMA

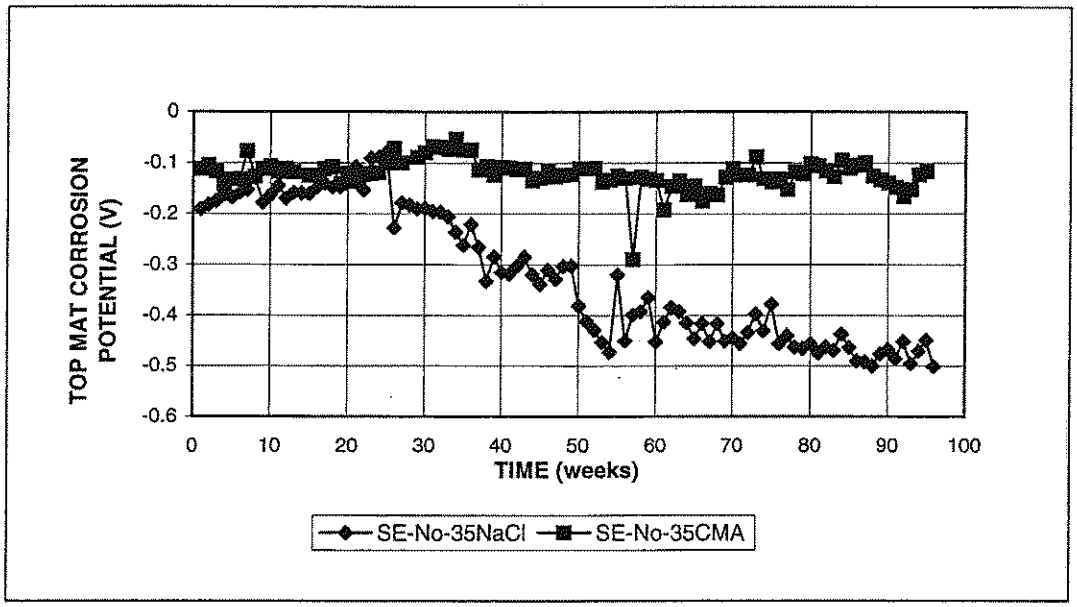

Figure 3.70 Southern Exposure test: Average corrosion potential with respect to copper-copper sulfate electrode. Top mat, different deicer solution, coventional steel, normalized, w/c=0.35, no inhibitors, 6.04 m ion NaCl or CMA

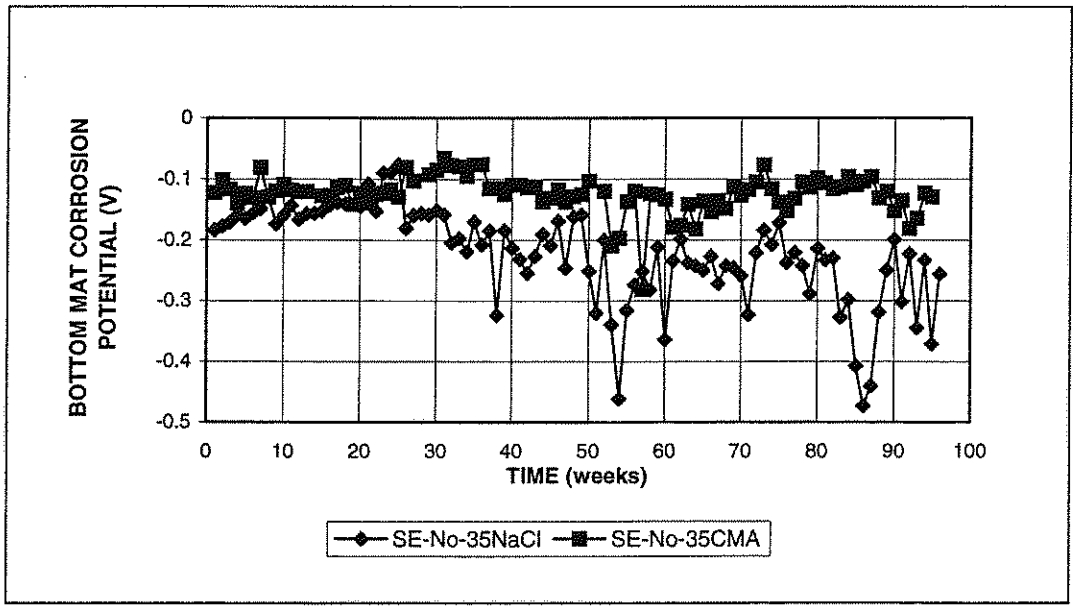

Figure 3.71 Southern Exposure test: Average corrosion potential with respect to copper-copper sulfate electrode. Bottom mat, different deicer solution, coventional steel, normalized, w/c=0.35, no inhibitors, 6.04 m ion NaCl or CMA

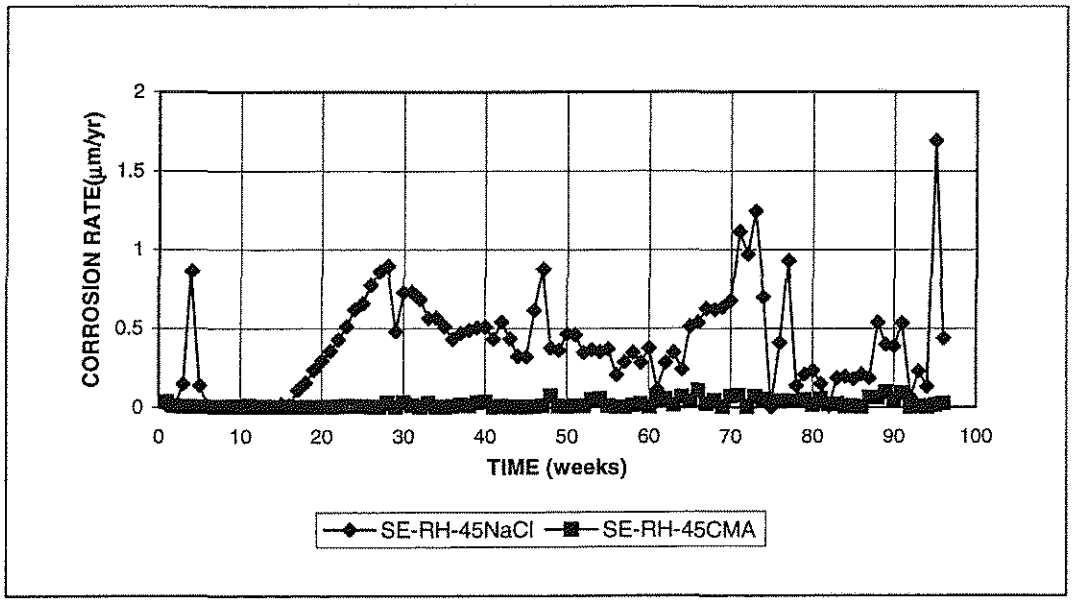

Figure 3.72 Southern Exposure test: Average corrosion rate for different deicer solution, coventional steel, normalized, w/c=0.45, Rheocrete, 6.04 m ion NaCl or CMA

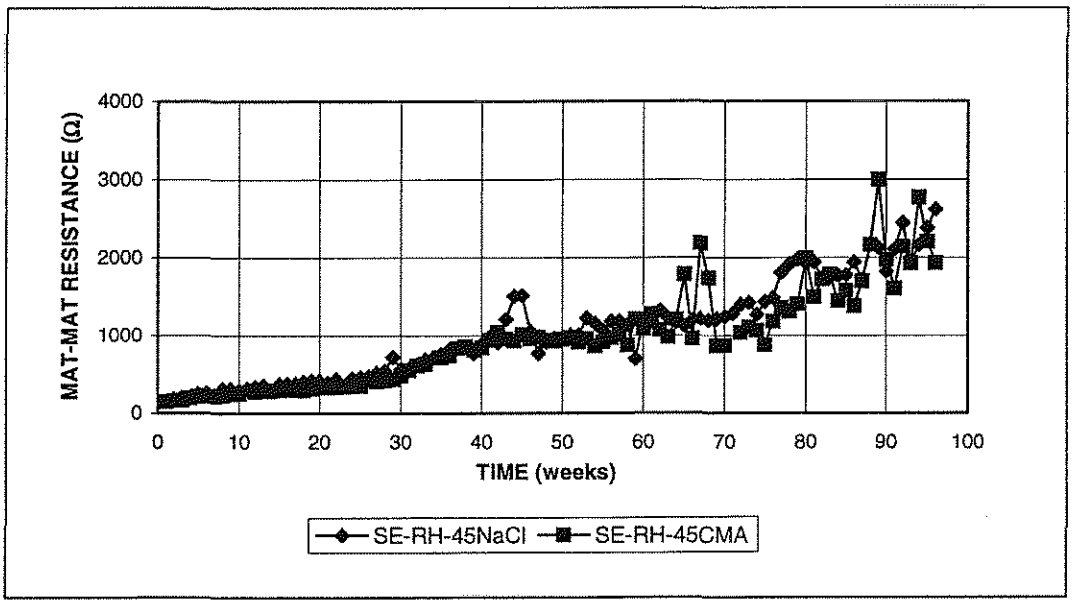

Figure 3.73 Southern Exposure test: Average mat-to-mat resistance for different deicer solution, coventional steel, normalized, w/c=0.45, Rheocrete, 6.04 m ion NaCl or CMA

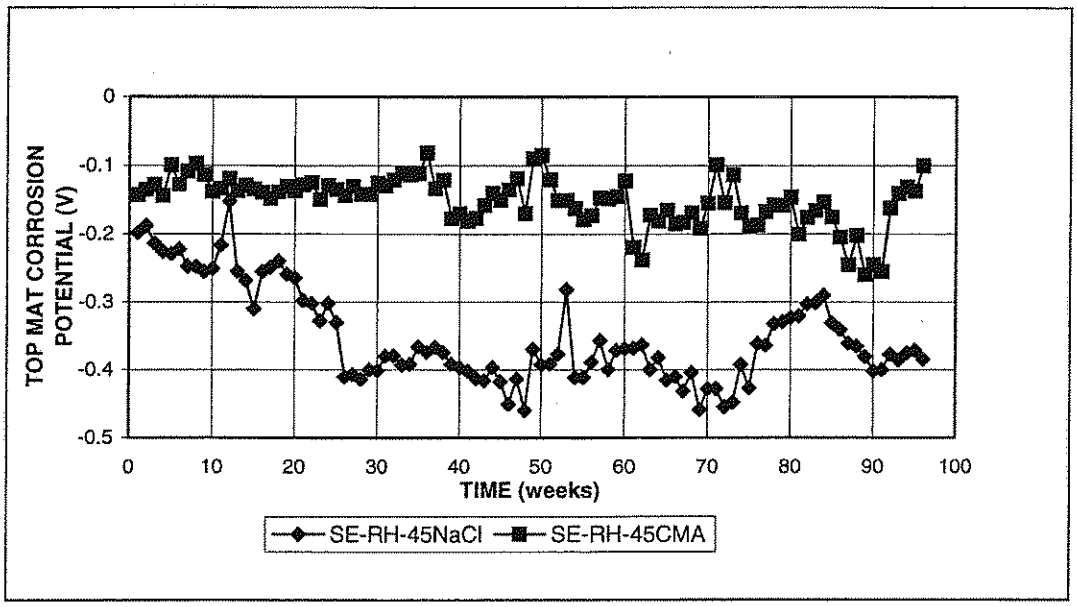

Figure 3.74 Southern Exposure test: Average corrosion potential with respect to copper-copper sulfate electrode. Top mat, different deicer solution, coventional steel, normalized, w/c=0.45, Rheocrete, 6.04 m ion NaCl or CMA

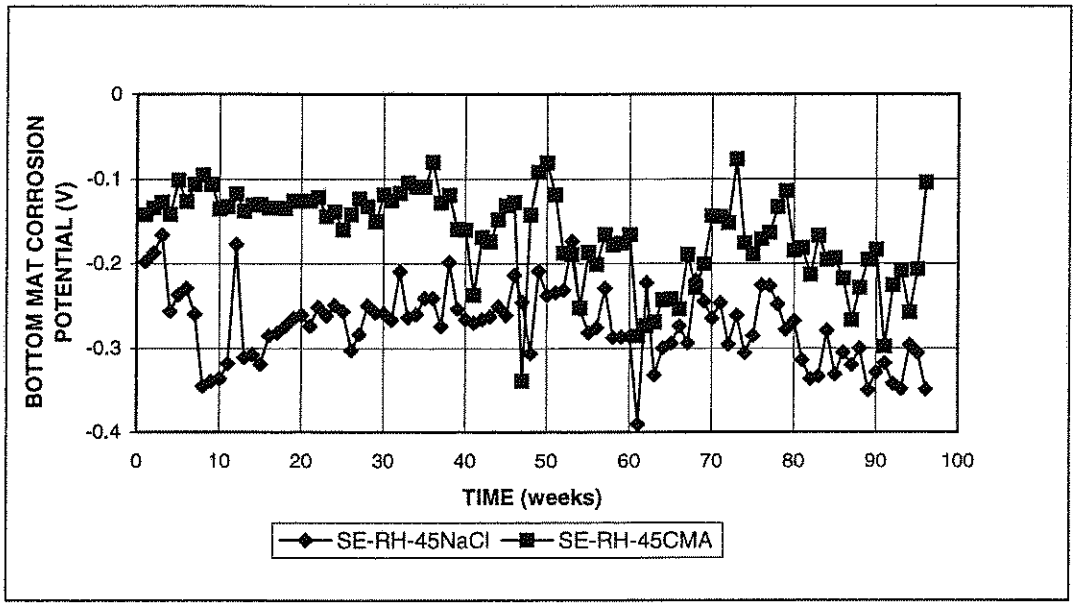

Figure 3.75 Southern Exposure test: Average corrosion potential with respect to copper-copper sulfate electrode. Bottom mat, different deicer solution, coventional steel, normalized, w/c=0.45, Rheocrete, 6.04 m ion NaCl or CMA

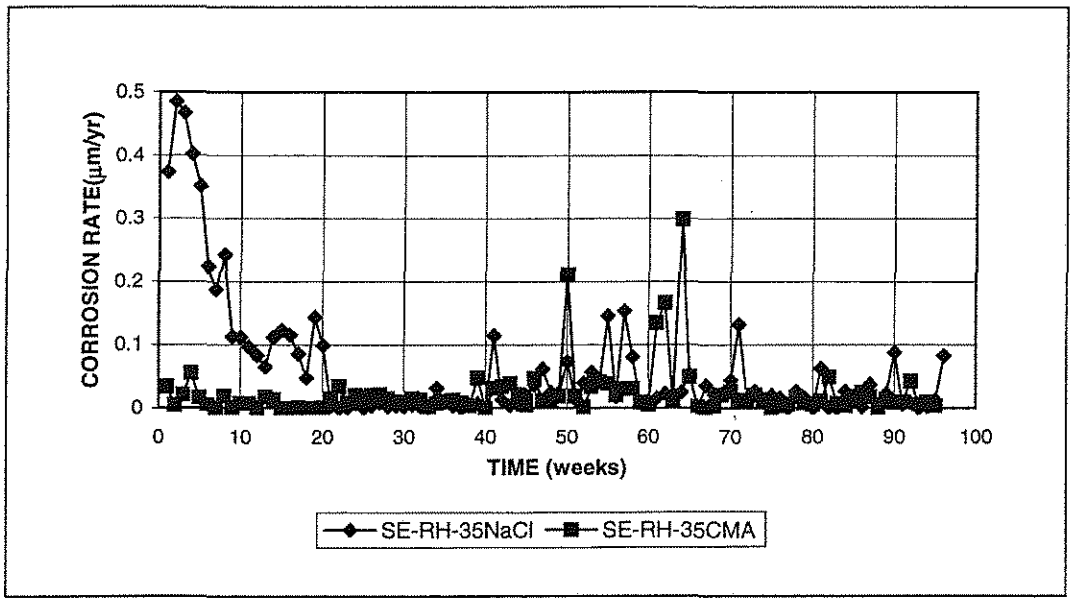

Figure 3.76 Southern Exposure test: Average corrosion rate for different deicer solution, coventional steel, normalized, w/c=0.35, Rheocrete, 6.04 m ion NaCl or CMA

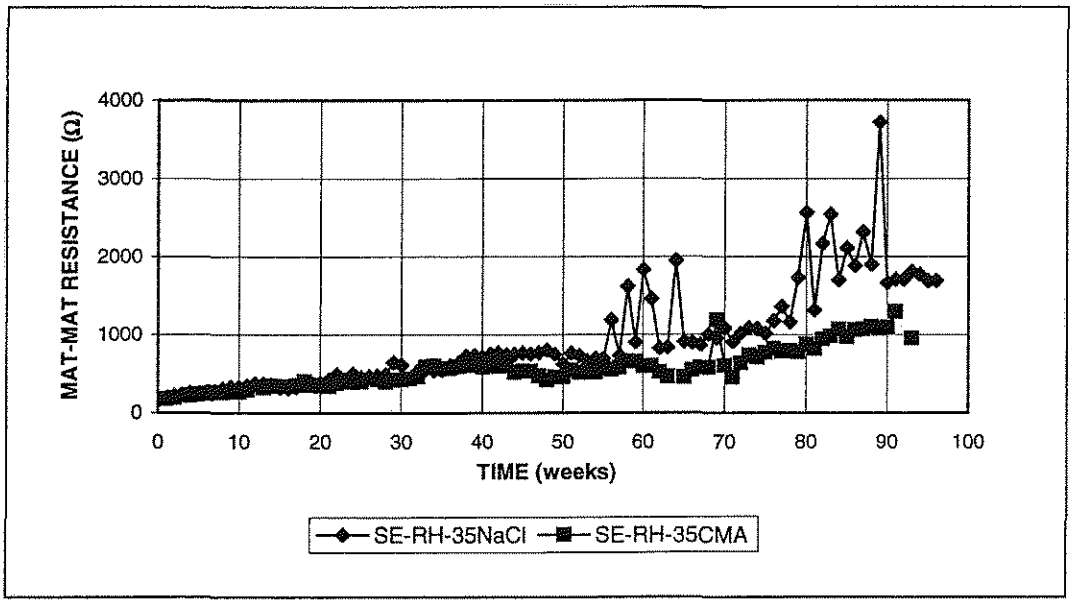

Figure 3.77 Southern Exposure test: Average mat-to-mat resistance for different deicer solution, coventional steel, normalized, w/c=0.35, Rheocrete, 6.04 m ion NaCl or CMA

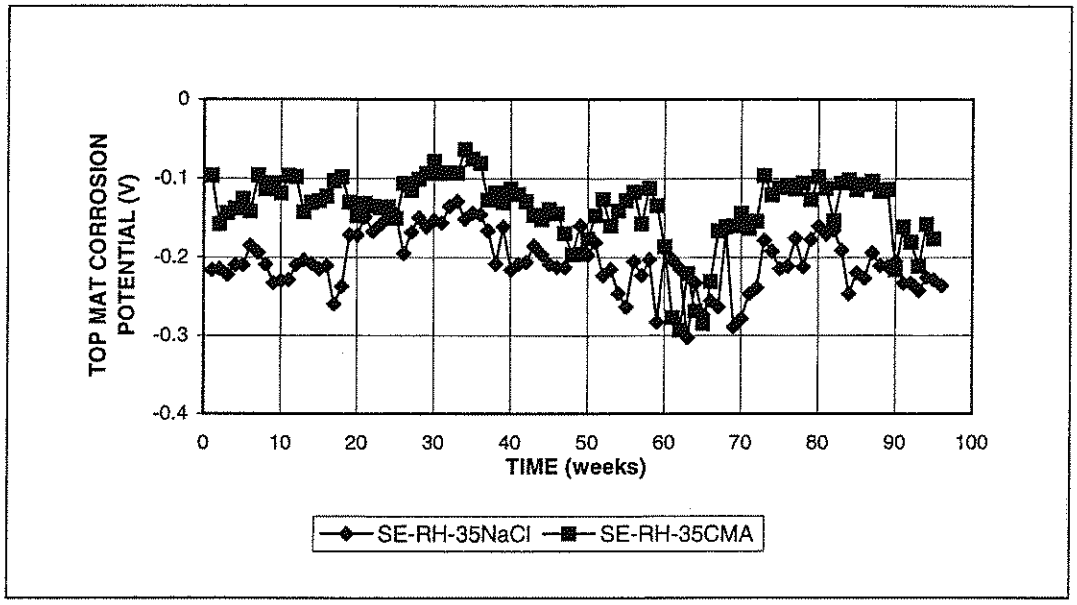

Figure 3.78 Southern Exposure test: Average corrosion potential with respect to copper-copper sulfate electrode. Top mat, different deicer solution, coventional steel, normalized, w/c=0.35, Rheocrete, 6.04 m ion NaCl or CMA

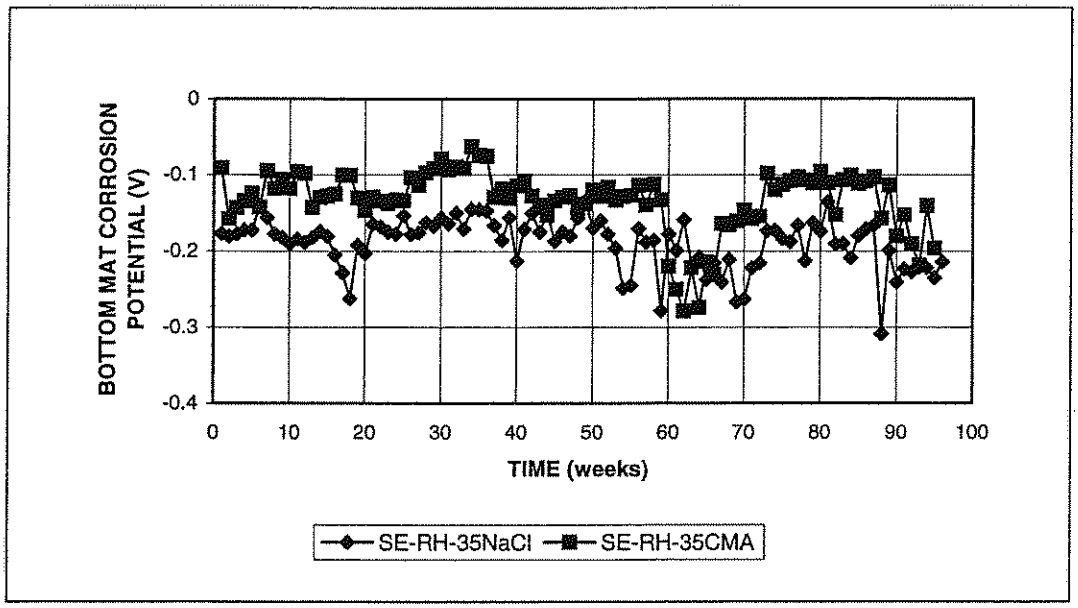

Figure 3.79 Southern Exposure test: Average corrosion potential with respect to copper-copper sulfate electrode. Bottom mat, different deicer solution, coventional steel, normalized, w/c=0.35, Rheocrete, 6.04 m ion NaCl or CMA

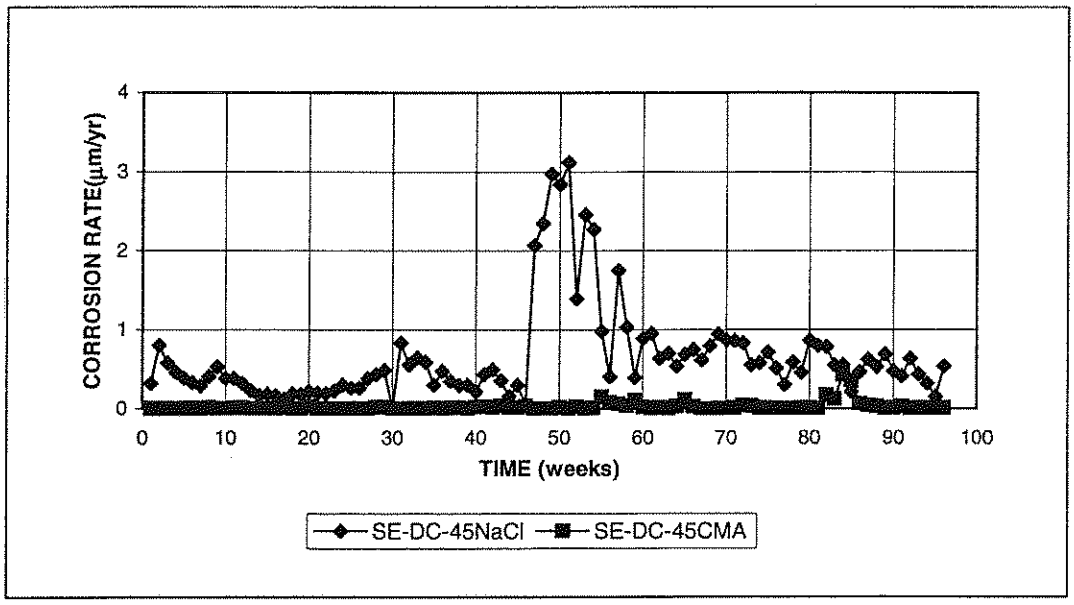

Figure 3.80 Southern Exposure test: Average corrosion rate for different deicer solution, coventional steel, normalized, w/c=0.45, DCI, 6.04 m ion NaCl or CMA

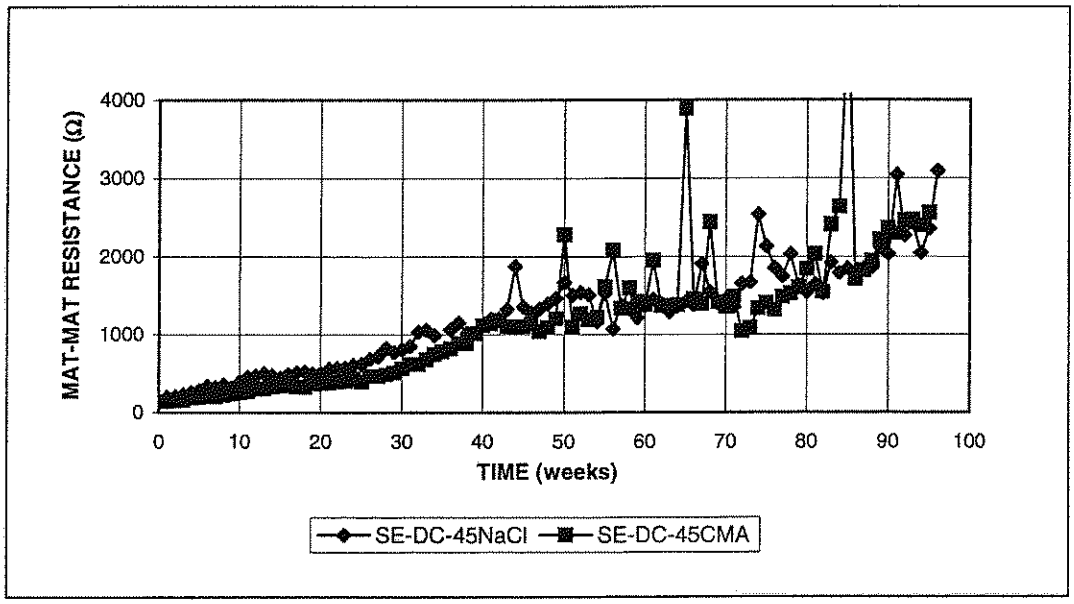

Figure 3.81 Southern Exposure test: Average mat-to-mat resistance for different deicer solution, coventional steel, normalized, w/c=0.45, DCI, 6.04 m ion NaCl or CMA

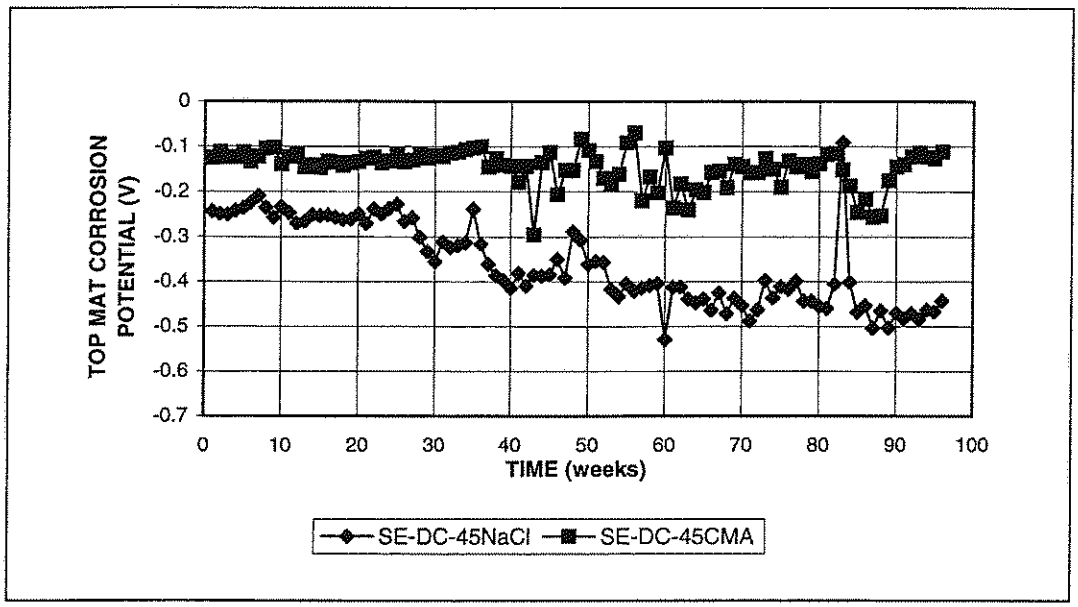

Figure 3.82 Southern Exposure test: Average corrosion potential with respect to copper-copper sulfate electrode. Top mat, different deicer solution, coventional steel, normalized, w/c=0.45, DCI, 6.04 m ion NaCl or CMA

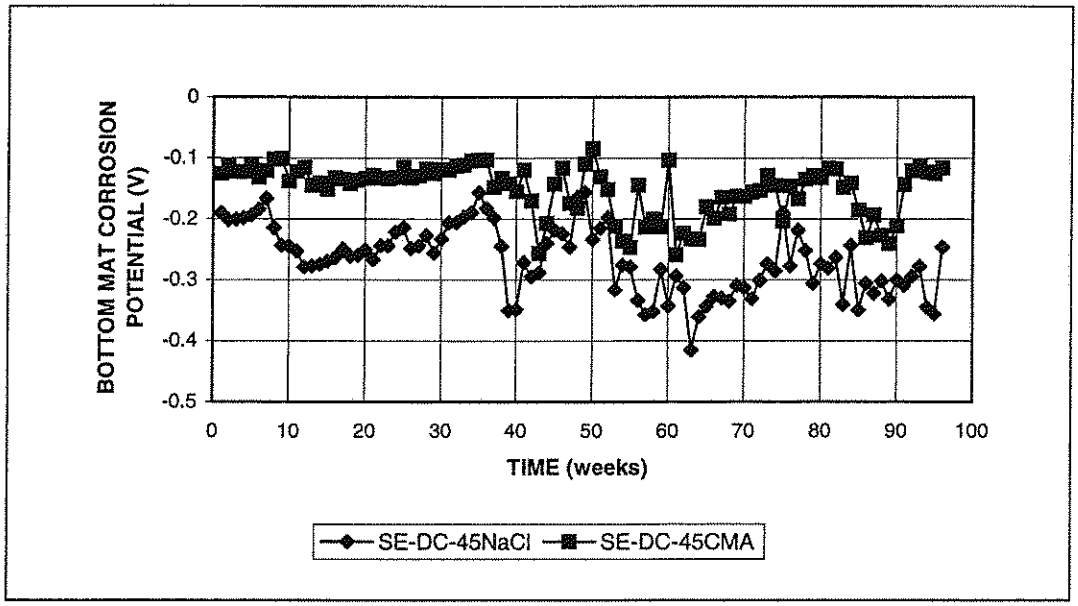

Figure 3.83 Southern Exposure test: Average corrosion potential with respect to copper-copper sulfate electrode. Bottom mat, different deicer solution, coventional steel, normalized, w/c=0.45, DCI, 6.04 m ion NaCl or CMA

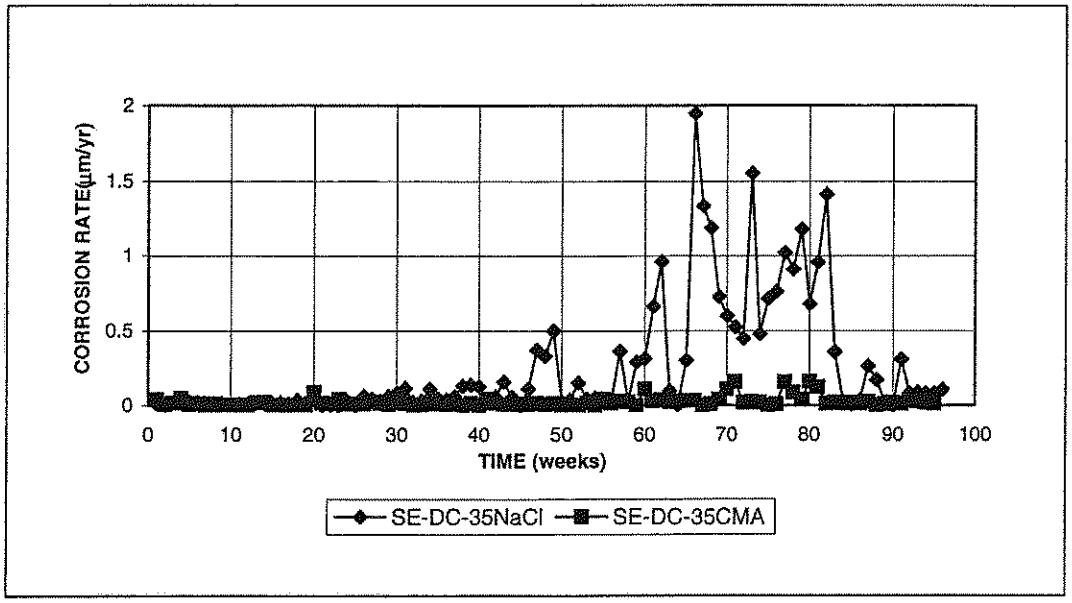

Figure 3.84 Southern Exposure test: Average corrosion rate for different deicer solution, coventional steel, normalized, w/c=0.35, DCI, 6.04 m ion NaCl or CMA

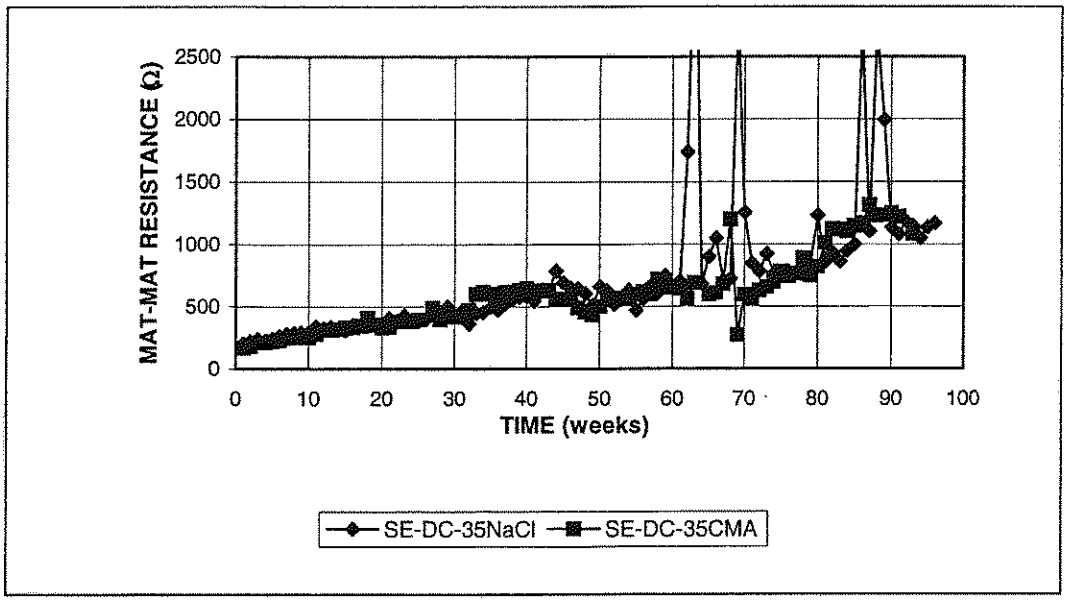

Figure 3.85 Southern Exposure test: Average mat-to-mat resistance for different deicer solution, coventional steel, normalized, w/c=0.35, DCI, 6.04 m ion NaCl or CMA

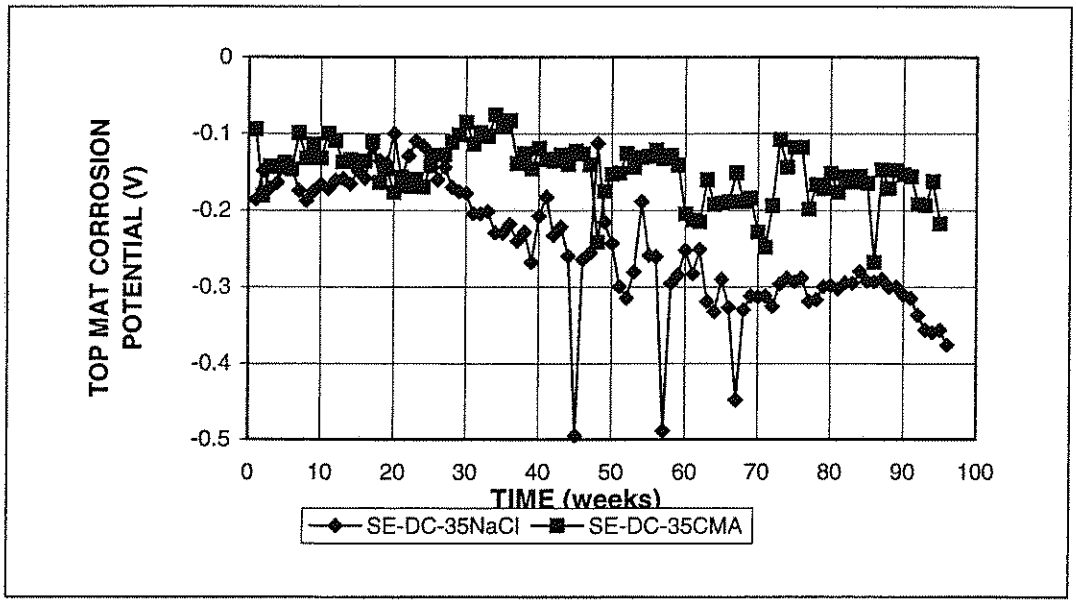

Figure 3.86 Southern Exposure test: Average corrosion potential with respect to copper-copper sulfate electrode. Top mat, different deicer solution, coventional steel, normalized, w/c=0.35, DCI, 6.04 m ion NaCl or CMA

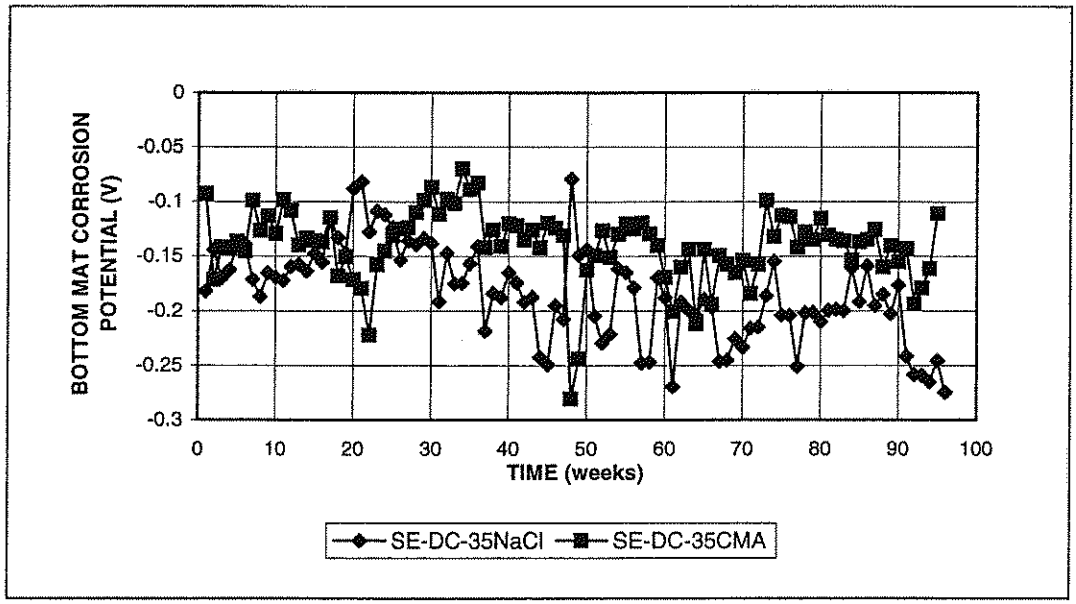

Figure 3.87 Southern Exposure test: Average corrosion potential with respect to copper-copper sulfate electrode. Bottom mat, different deicer solution, coventional steel, normalized, w/c=0.35, DCI, 6.04 m ion NaCl or CMA

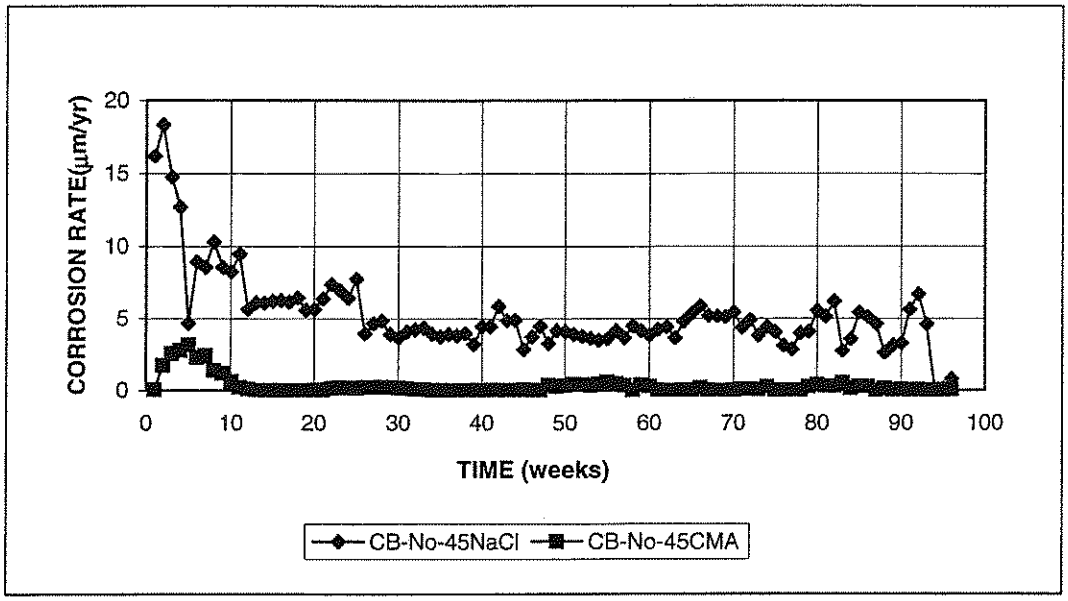

Figure 3.88 Cracked Beam test: Average corrosion rate for different deicer solution, coventional steel, normalized, no inhibitors, w/c=0.45, 6.04 m ion NaCl or CMA

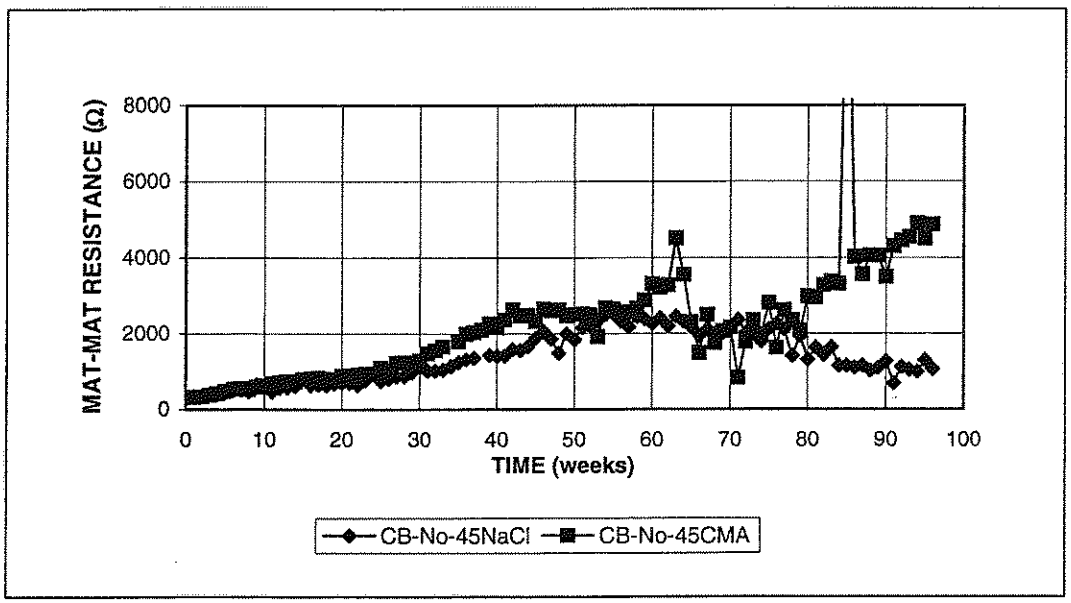

Figure 3.89 Cracked Beam test: Average mat-to-mat resistance for different deicer solution, coventional steel, normalized, no inhibitors, w/c=0.45, 6.04 m ion NaCl or CMA

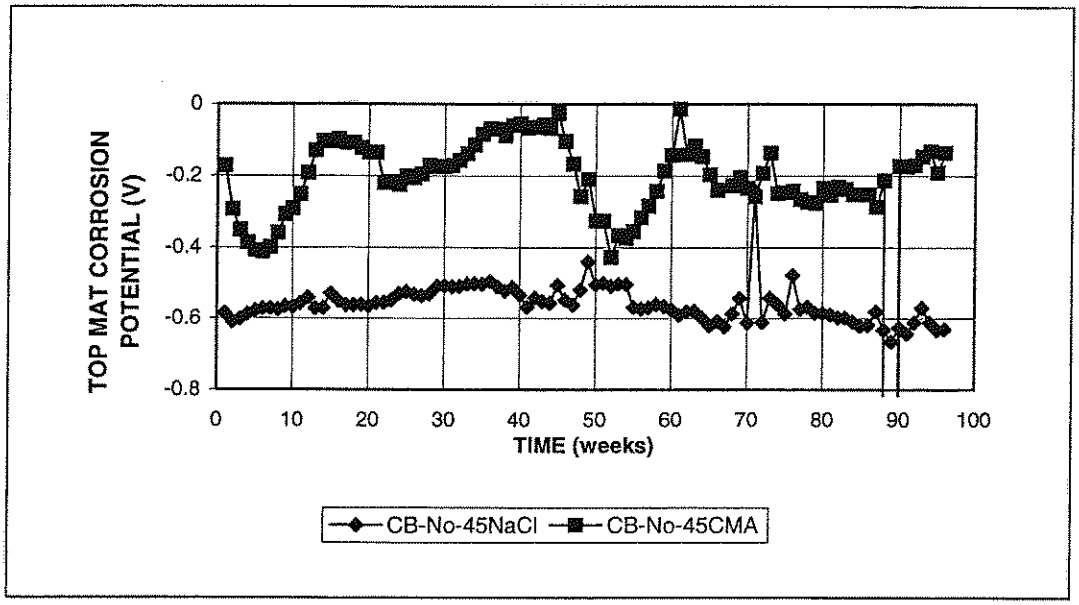

Figure 3.90 Cracked Beam test: Average corrosion potential with respect to copper-copper sulfate electrode. Top mat, different deicer solution, coventional steel, normalized, no inhibitors, w/c=0.45, 6.04 m ion NaCl or CMA

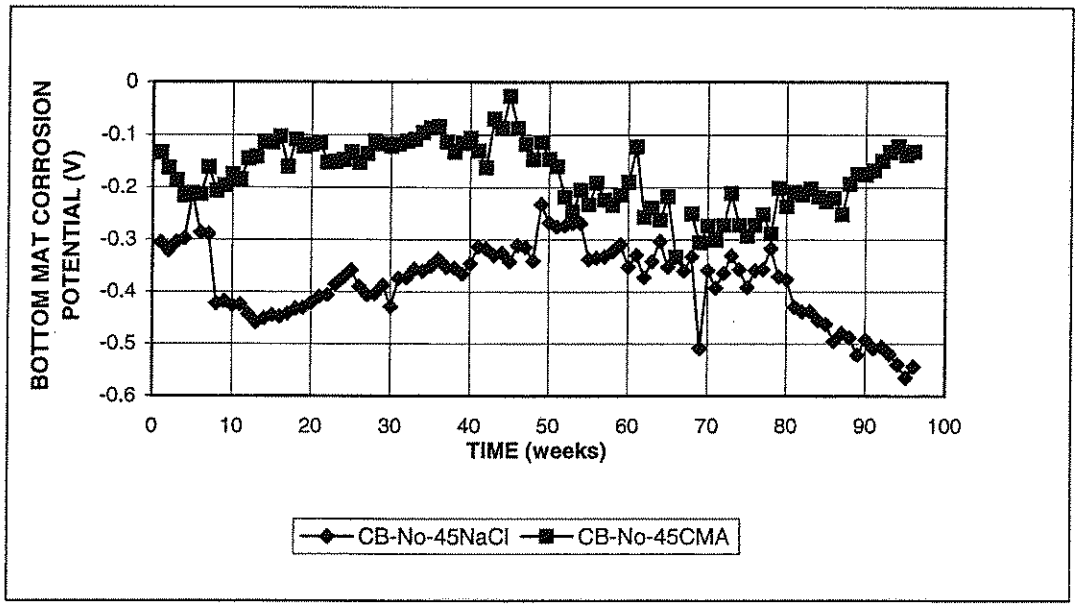

Figure 3.91 Cracked Beam test: Average corrosion potential with respect to copper-copper sulfate electrode. Bottom mat, different deicer solution, coventional steel, normalized, no inhibitors, w/c=0.45, 6.04 m ion NaCl or CMA

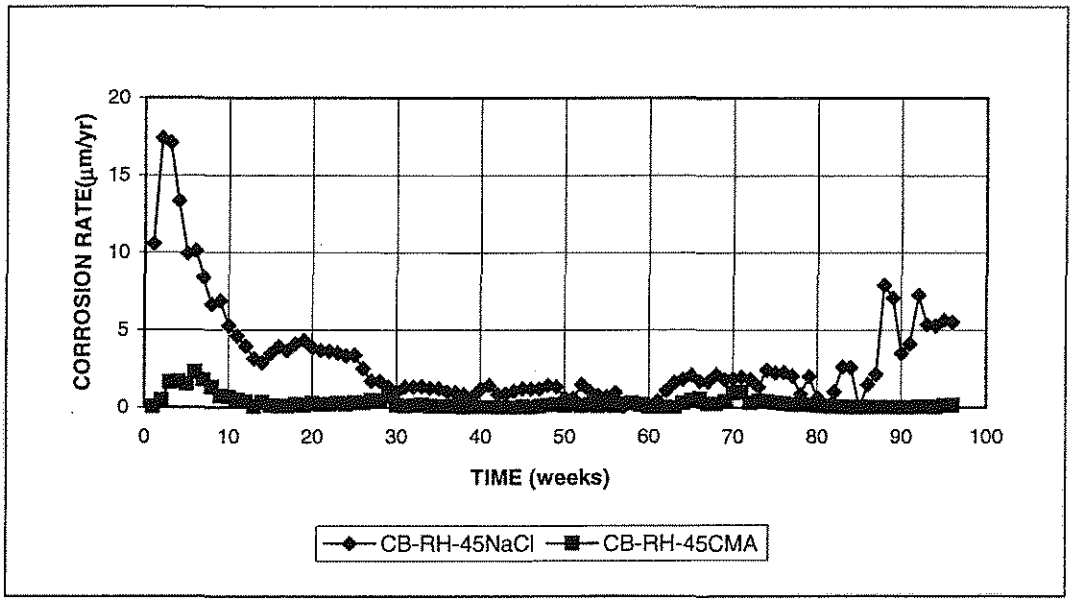

Figure 3.92 Cracked Beam test: Average corrosion rate for different deicer solution, coventional steel, normalized, Rheocrete, w/c=0.45, 6.04 m ion NaCl or CMA

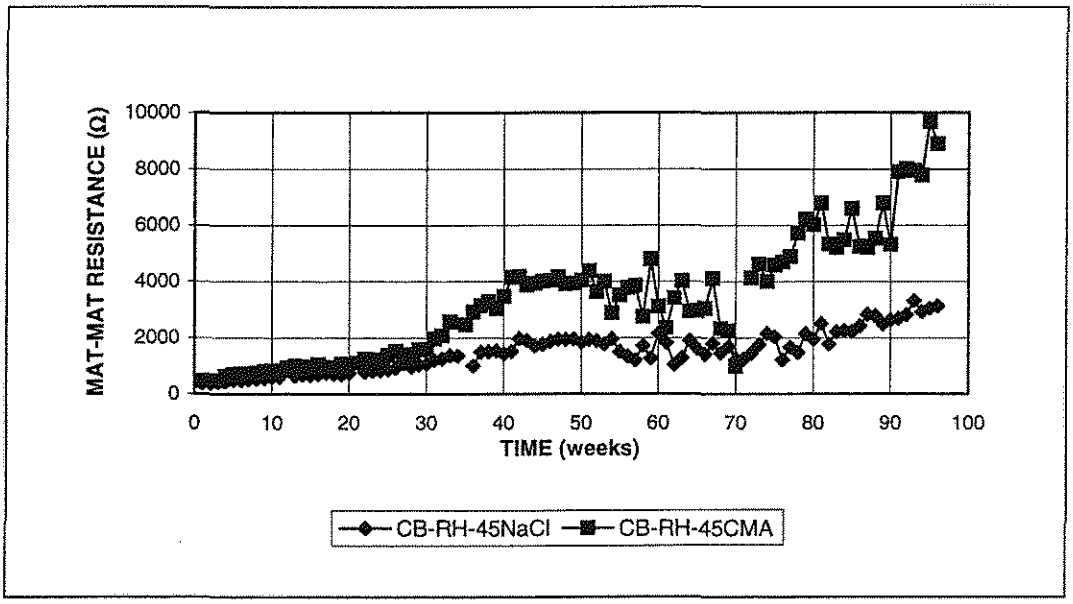

Figure 3.93 Cracked Beam test: Average mat-to-mat resistance for different deicer solution, coventional steel, normalized, Rheocrete, w/c=0.45, 6.04 m ion NaCl or CMA

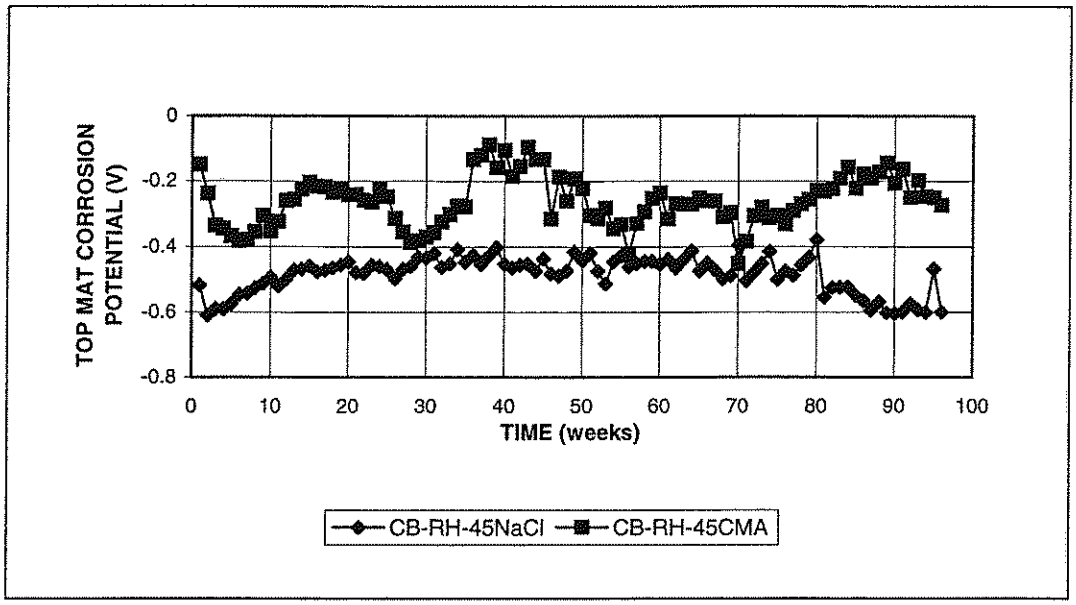

Figure 3.94 Cracked Beam test: Average corrosion potential with respect to copper-copper sulfate electrode. Top mat, different deicer solution, coventional steel, normalized, Rheocrete, w/c=0.45, 6.04 m ion NaCl or CMA

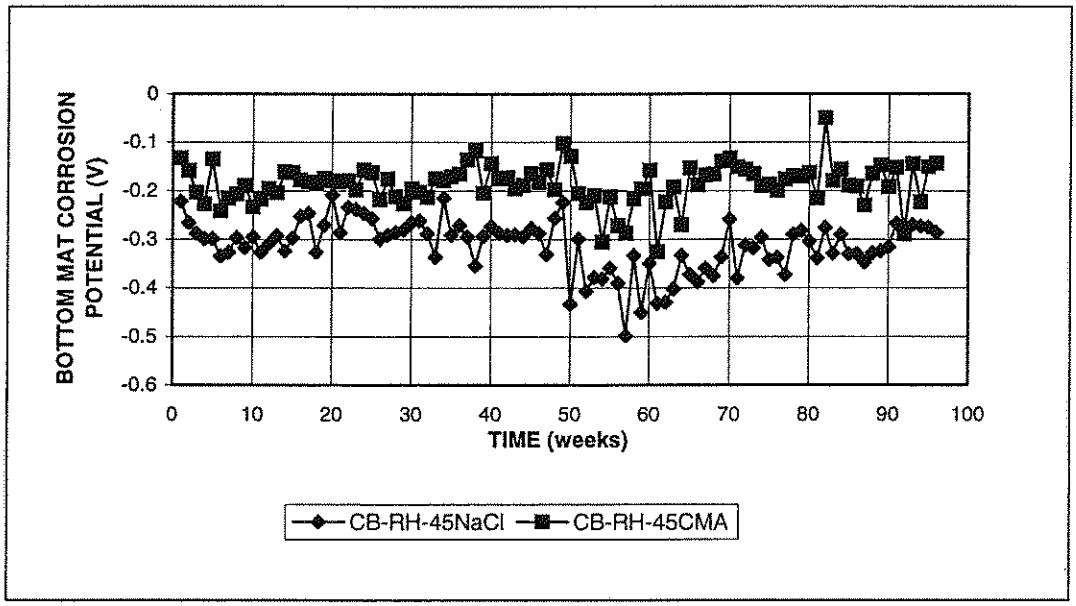

Figure 3.95 Cracked Beam test: Average corrosion potential with respect to copper-copper sulfate electrode. Bottom mat, different deicer solution, coventional steel, normalized, Rheocrete, w/c=0.45, 6.04 m ion NaCl or CMA

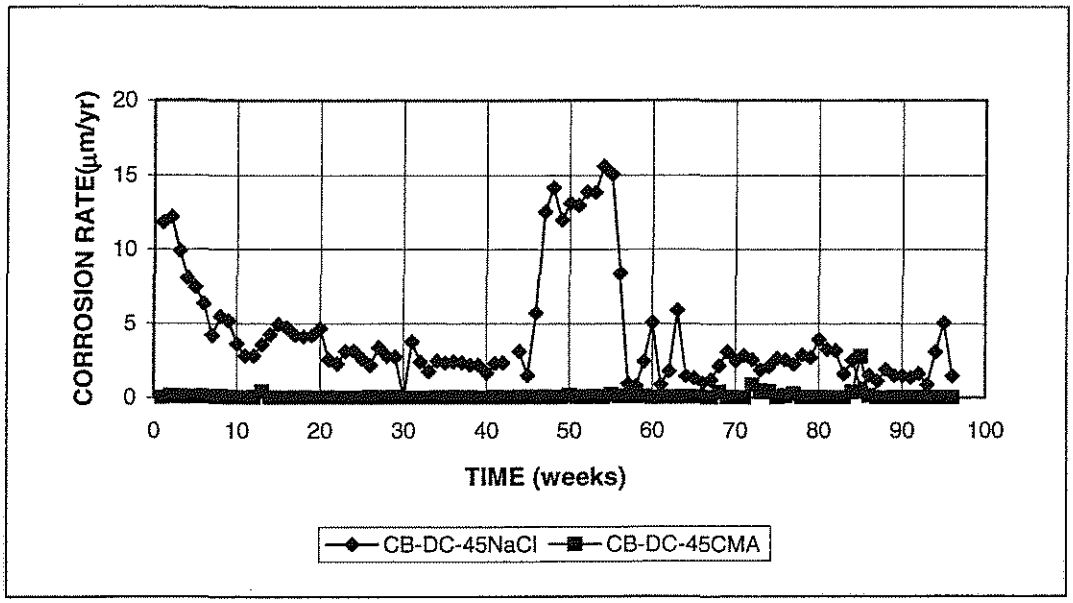

Figure 3.96 Cracked Beam test: Average corrosion rate for different deicer solution, coventional steel, normalized, DCI, w/c=0.45, 6.04 m ion NaCl or CMA

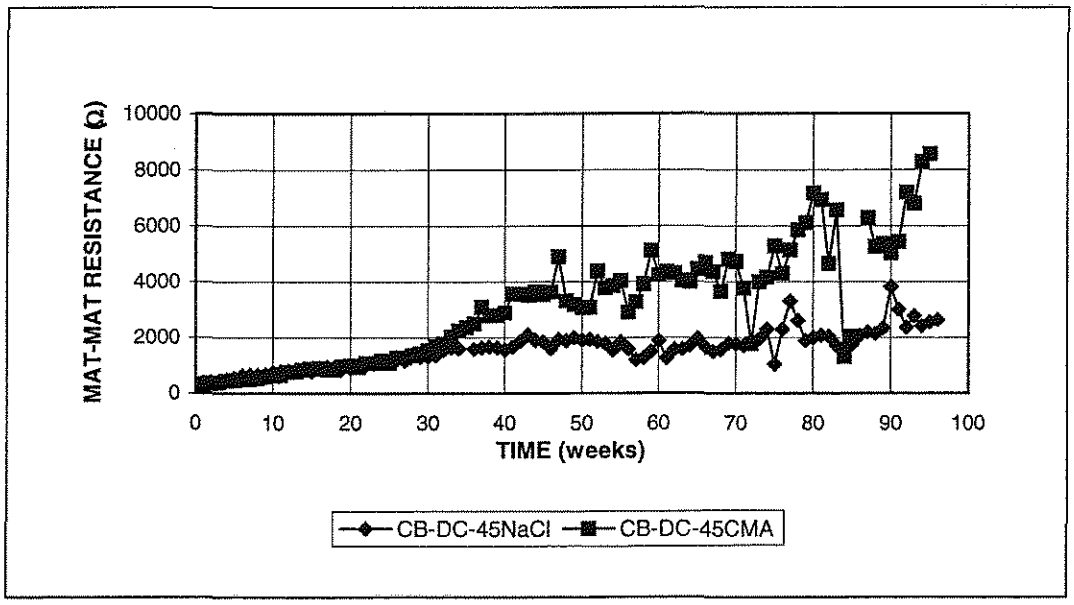

Figure 3.97 Cracked Beam test: Average mat-to-mat resistance for different deicer solution, coventional steel, normalized, DCI, w/c=0.45, 6.04 m ion NaCl or CMA

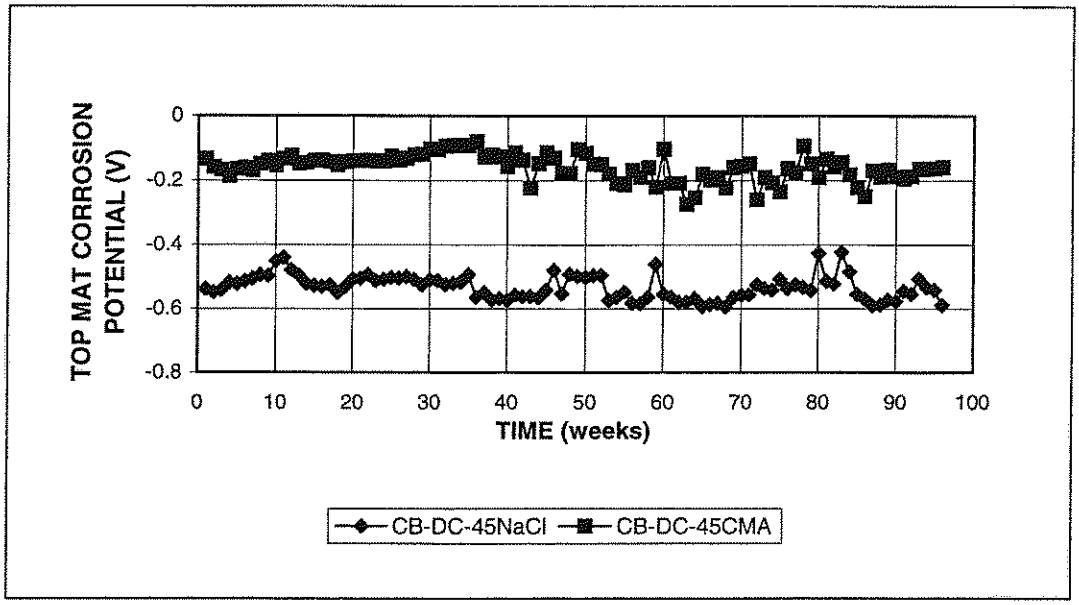

Figure 3.98 Cracked Beam test: Average corrosion potential with respect to copper-copper sulfate electrode. Top mat, different deicer solution, coventional steel, normalized, DCI, w/c=0.45, 6.04 m ion NaCl or CMA

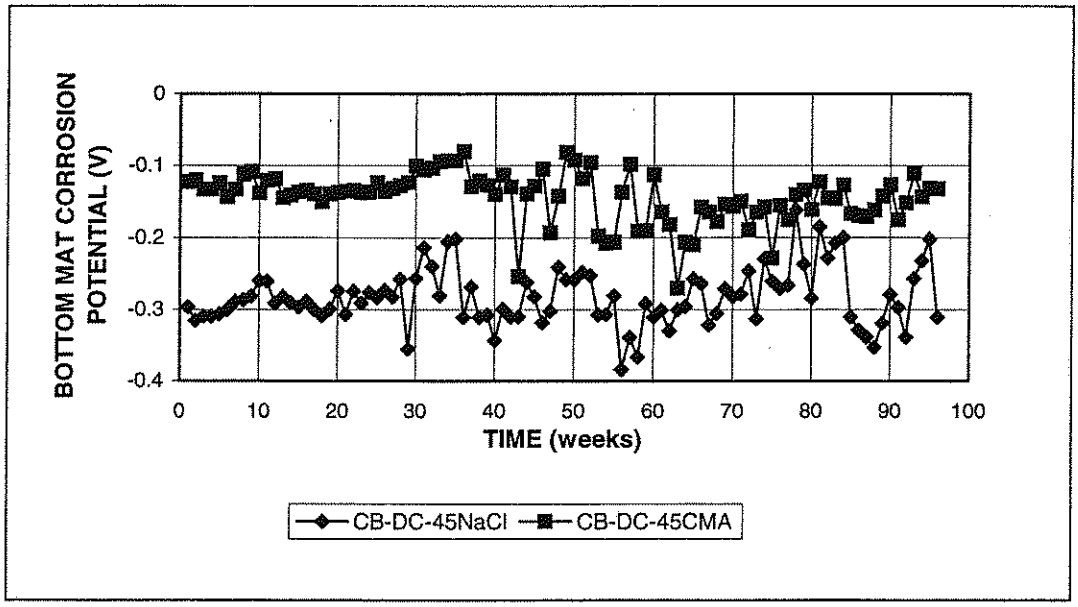

Figure 3.99 Cracked Beam test: Average corrosion potential with respect to copper-copper sulfate electrode. Bottom mat, different deicer solution, coventional steel, normalized, DCI, w/c=0.45, 6.04 m ion NaCl or CMA

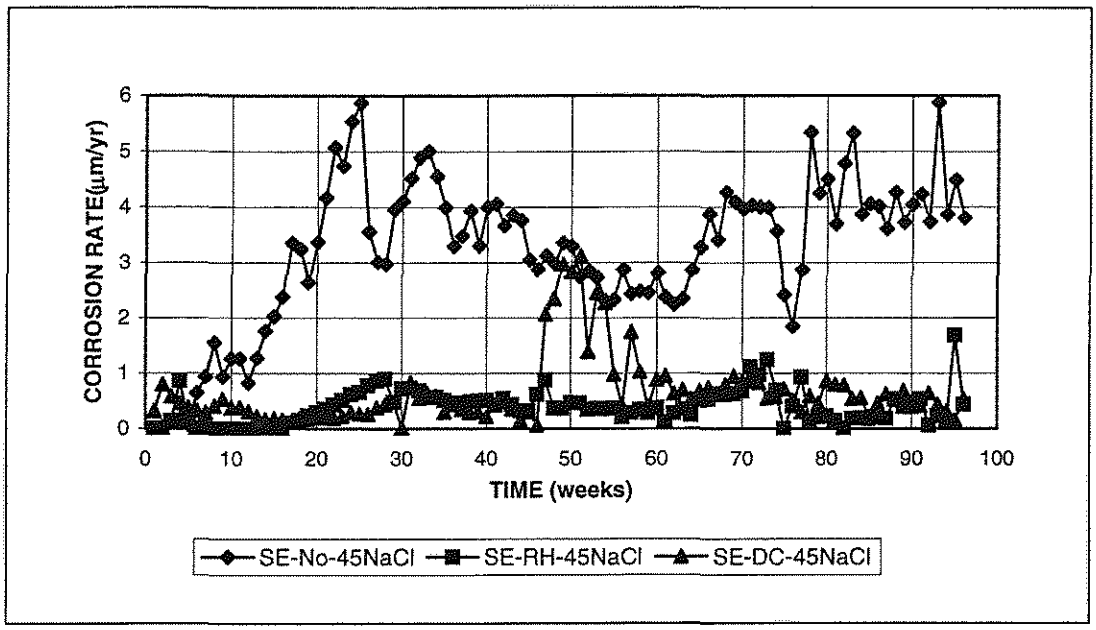

Figure 3.100 Southern Exposure test: Average corrosion rate for different inhibitors, coventional steel, normalized, w/c=0.45, 6.04 m ion NaCl

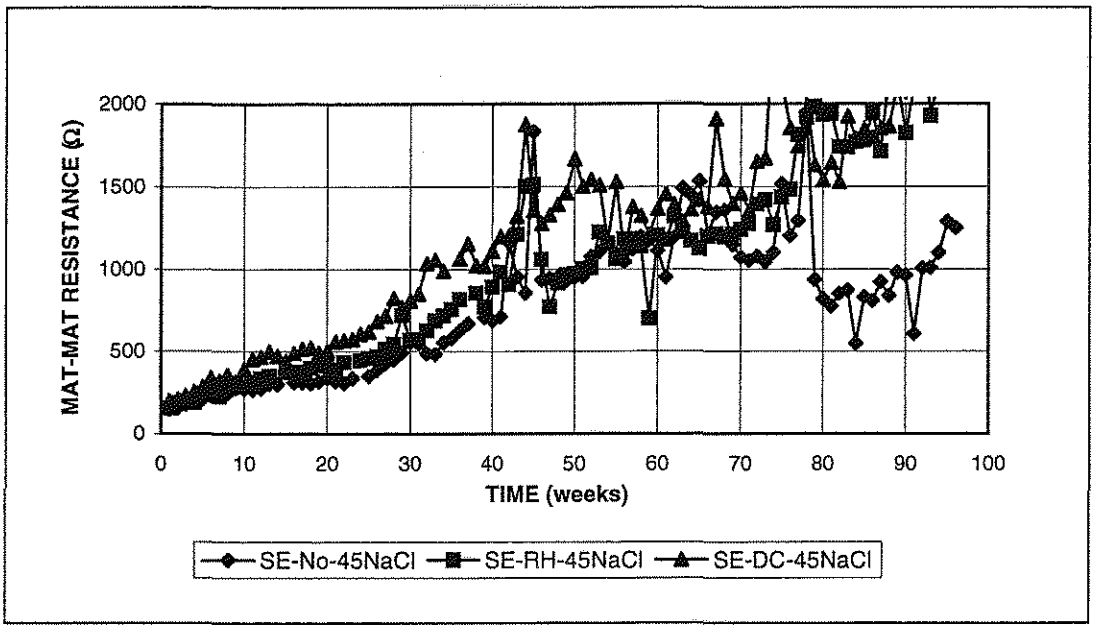

Figure 3.101 Southern Exposure test: Average mat-to-mat resistance for different inhibitors, coventional steel, normalized, w/c=0.45, 6.04 m ion NaCl

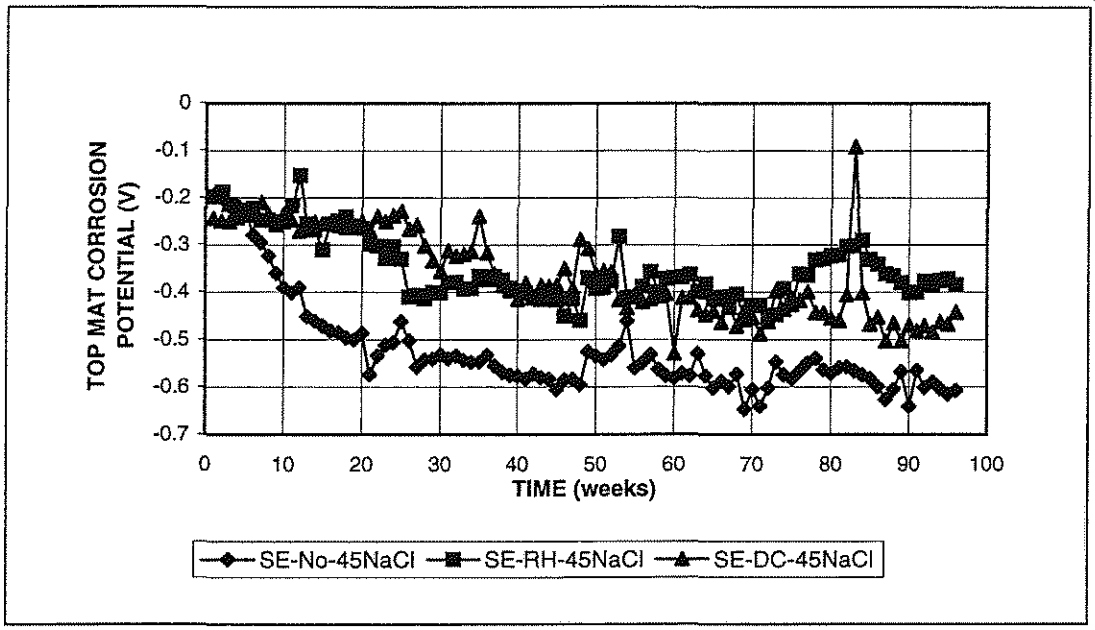

Figure 3.102 Southern Exposure test: Average corrosion potential with respect to copper-copper sulfate electrode. Top mat, different inhibitors, coventional steel, normalized, w/c=0.45, 6.04 m ion NaCl

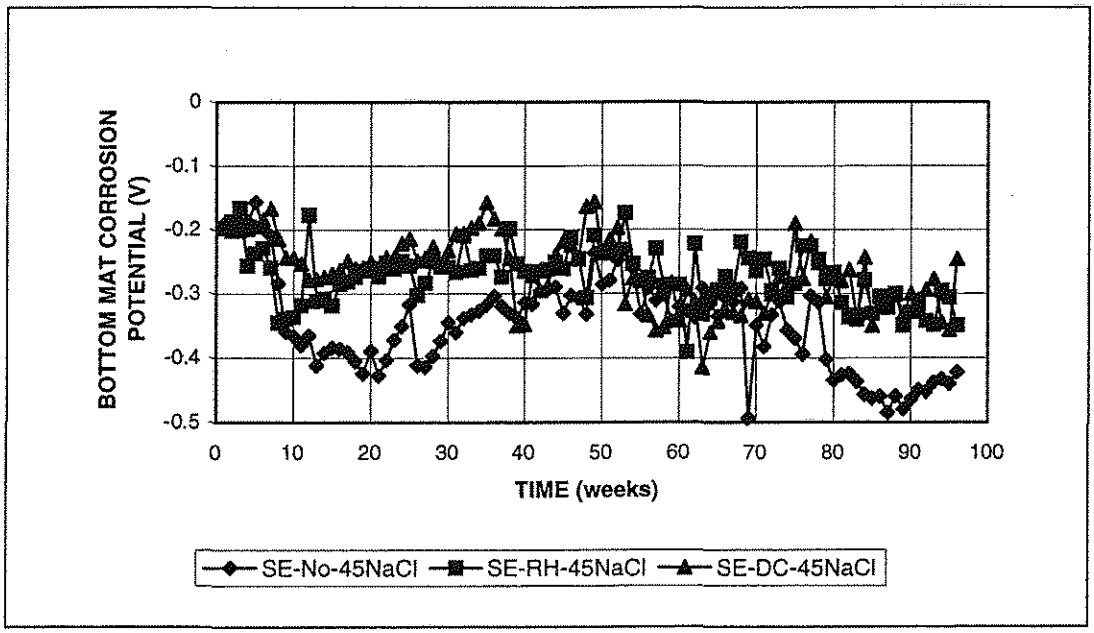

Figure 3.103 Southern Exposure test: Average corrosion potential with respect to copper-copper sulfate electrode. Bottom mat, different inhibitors, coventional steel, normalized, w/c=0.45, 6.04 m ion NaCl

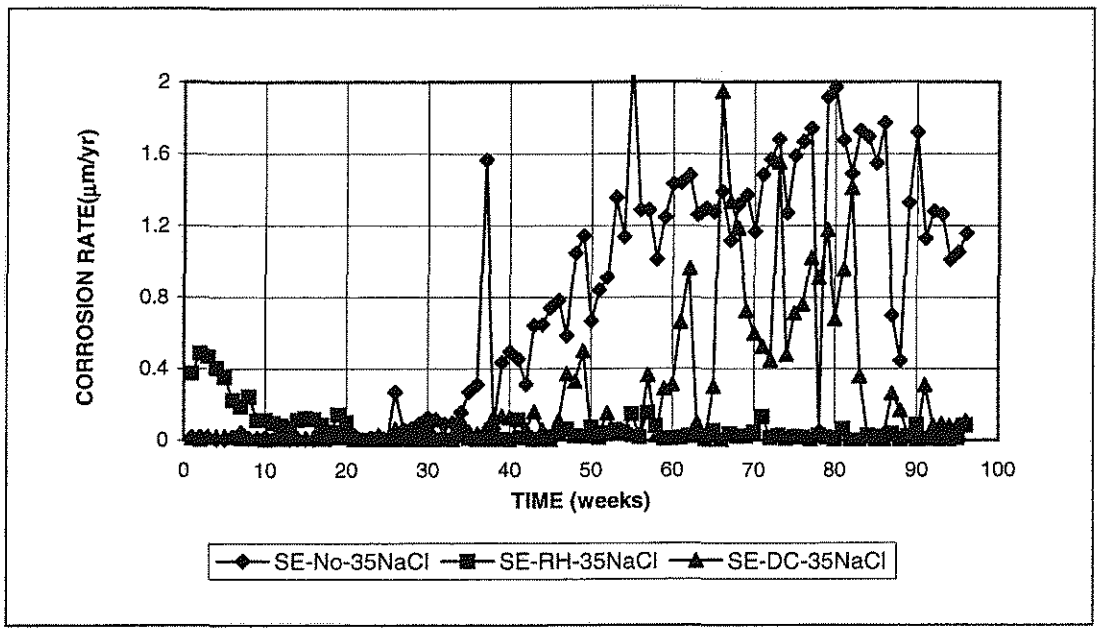

Figure 3.104 Southern Exposure test: Average corrosion rate for different inhibitors, coventional steel, normalized, w/c=0.35, 6.04 m ion NaCl

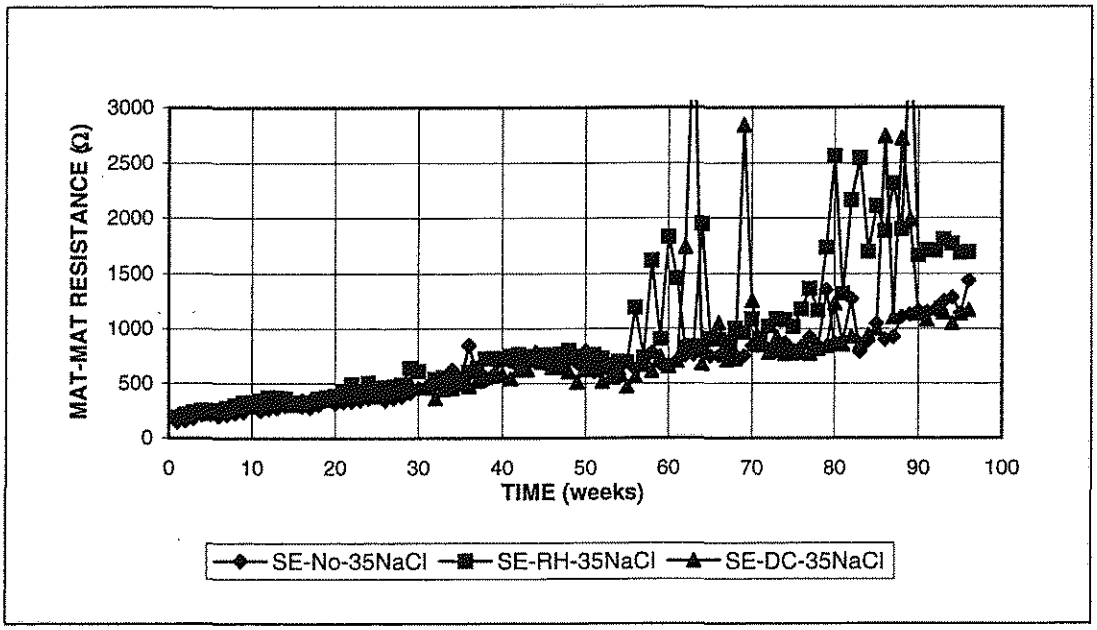

Figure 3.105 Southern Exposure test: Average mat-to-mat resistance for different inhibitors, coventional steel, normalized, w/c=0.35, 6.04 m ion NaCl

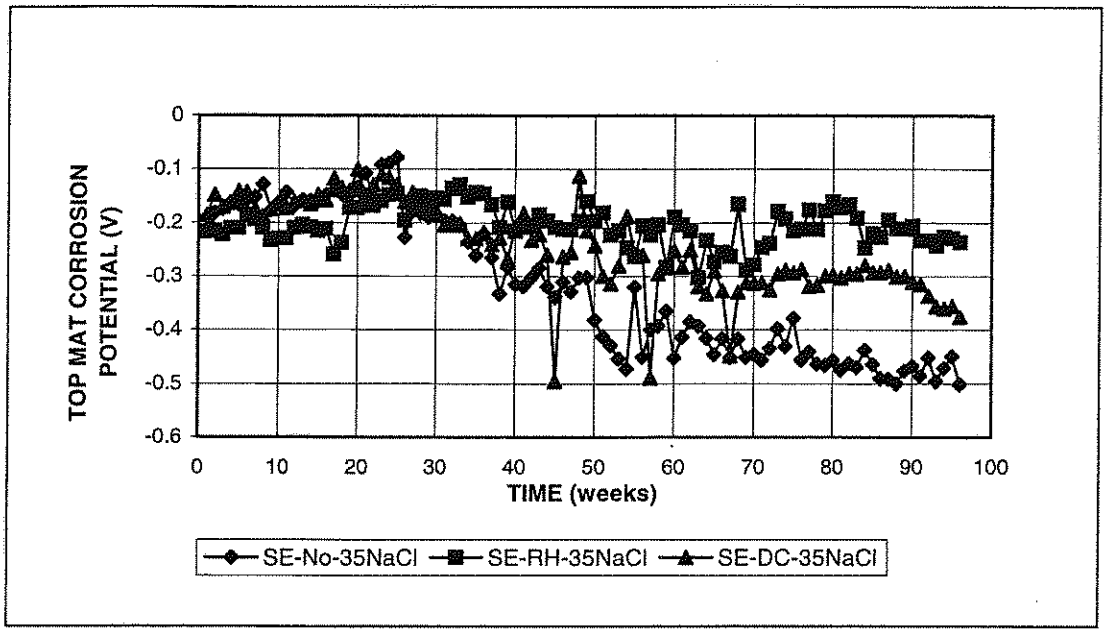

Figure 3.106 Southern Exposure test: Average corrosion potential with respect to copper-copper sulfate electrode. Top mat, different inhibitors, coventional steel, normalized, w/c=0.35, 6.04 m ion NaCl

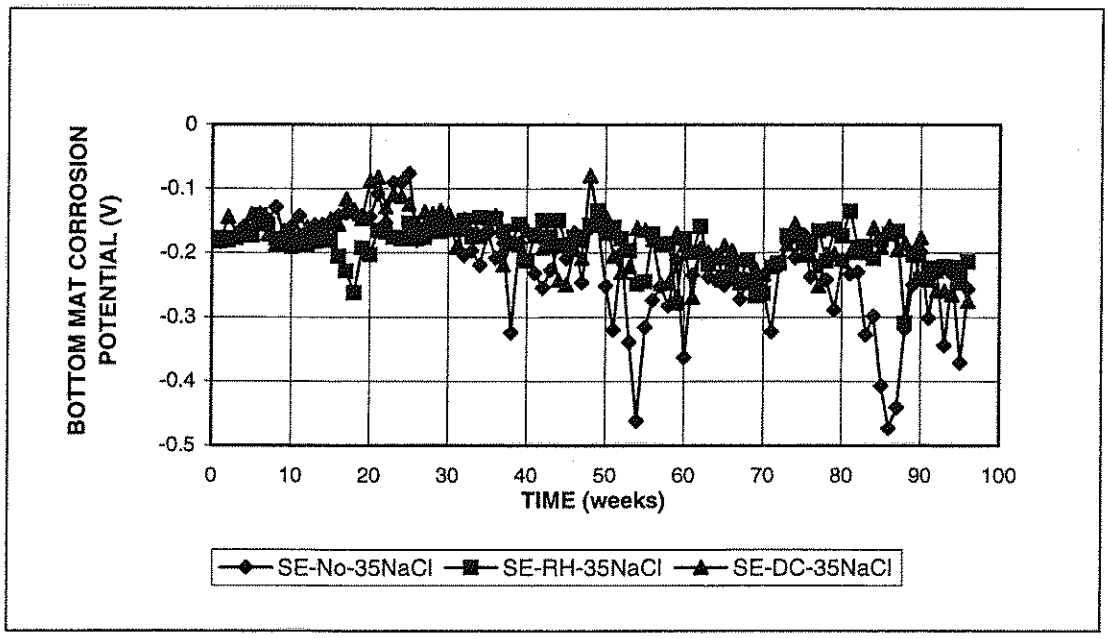

Figure 3.107 Southern Exposure test: Average corrosion potential with respect to copper-copper sulfate electrode. Bottom mat, different inhibitors, coventional steel, normalized, w/c=0.35, 6.04 m ion NaCl

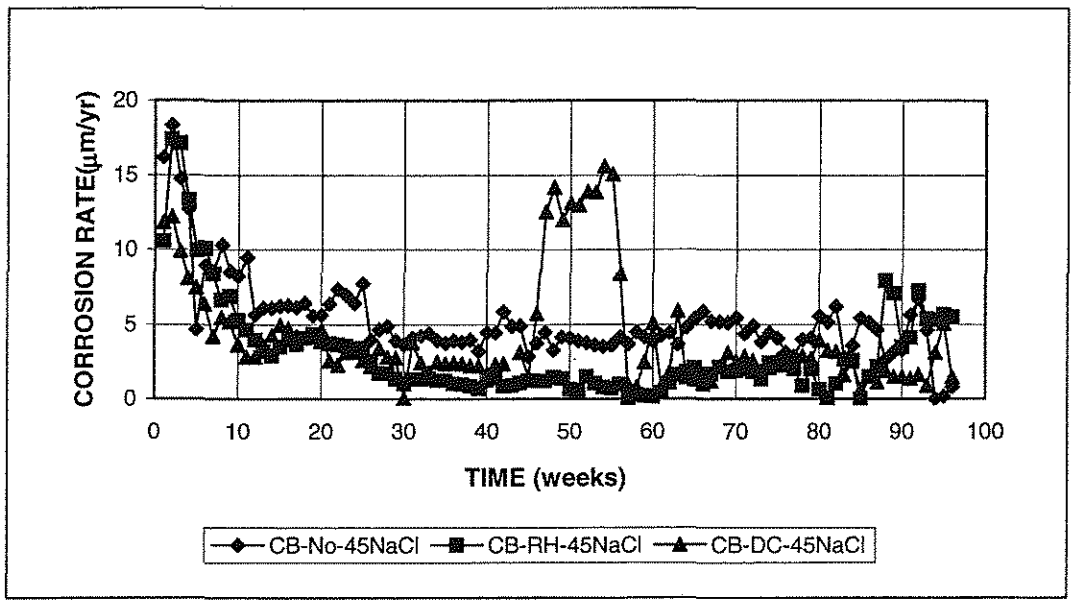

Figure 3.108 Cracked Beam test: Average corrosion rate for different inhibitors, coventional steel, normalized, w/c=0.45, 6.04 m ion NaCl

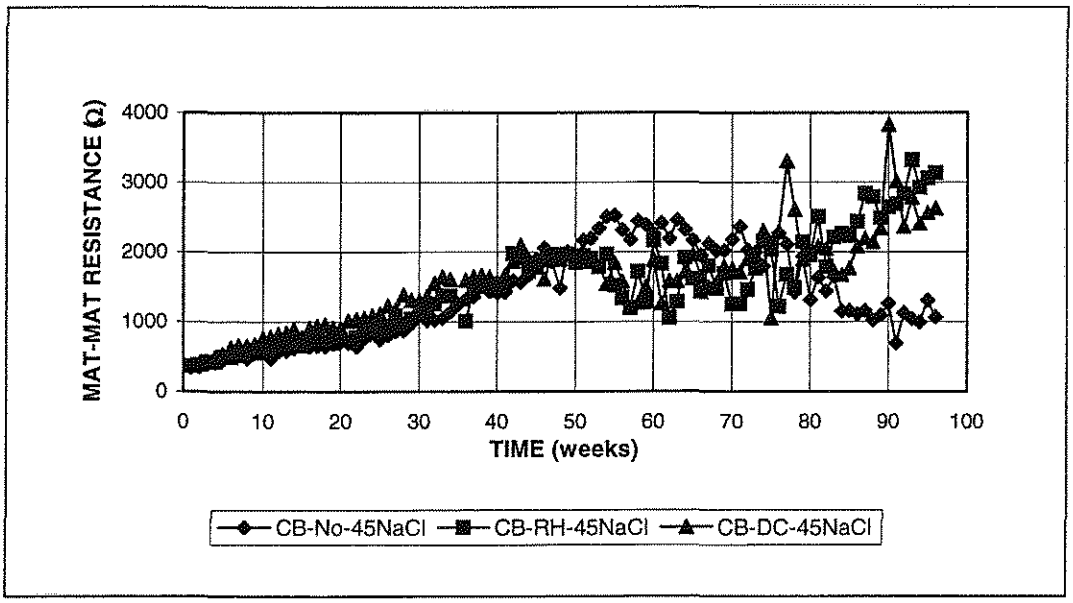

Figure 3.109 Cracked Beam test: Average mat-to-mat resistance for different inhibitors, coventional steel, normalized, w/c=0.45, 6.04 m ion NaCl

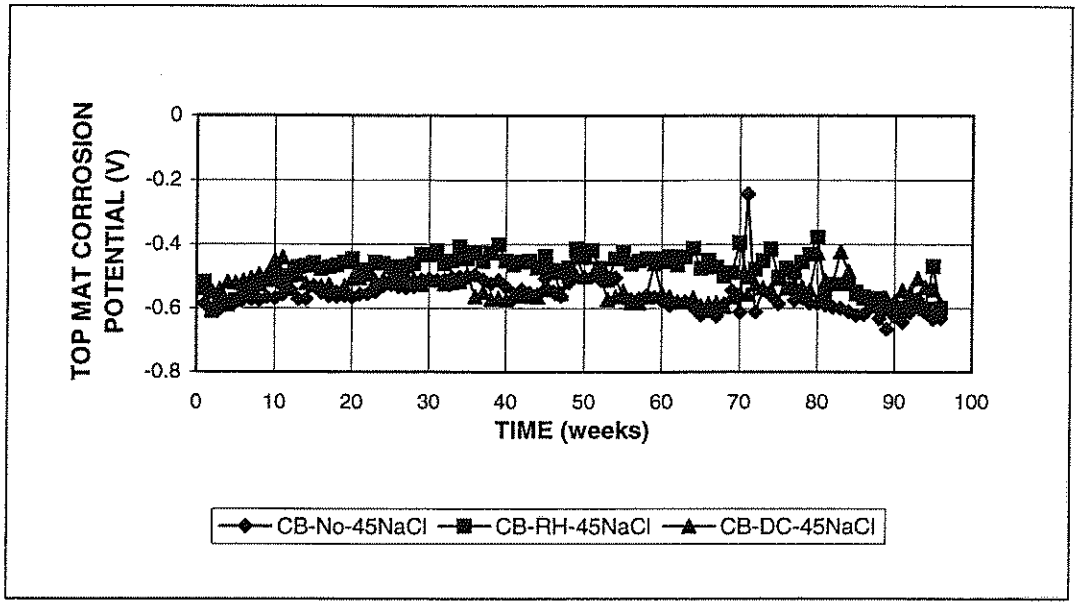

Figure 3.110 Cracked Beam test: Average corrosion potential with respect to copper-copper sulfate electrode. Top mat, different inhibitors, coventional steel, normalized, w/c=0.45, 6.04 m ion NaCl

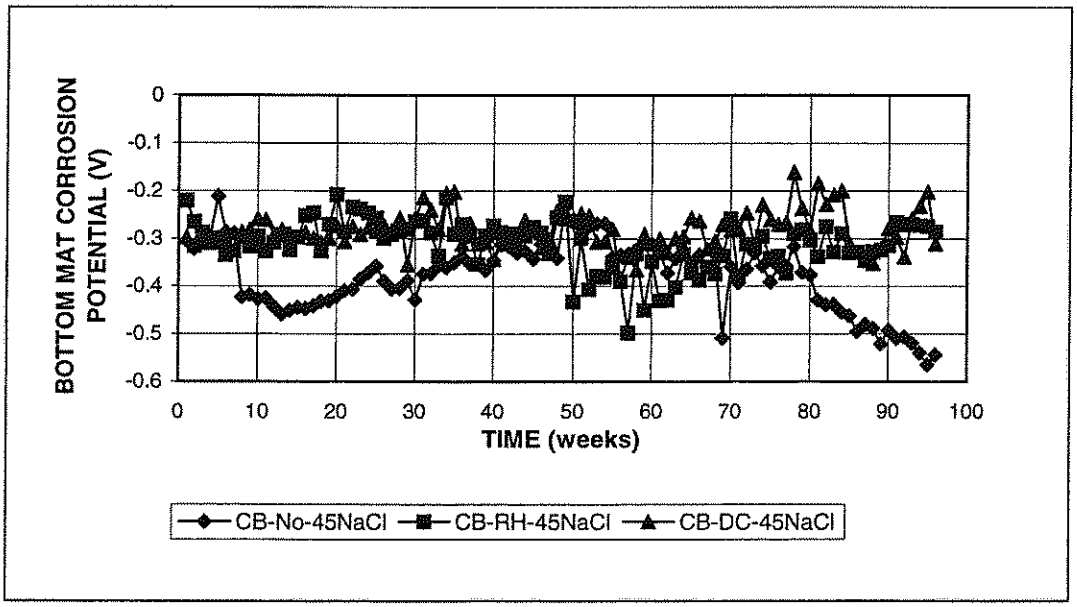

Figure 3.111 Cracked Beam test: Average corrosion potential with respect to copper-copper sulfate electrode. Bottom mat, different inhibitors, coventional steel, normalized, w/c=0.45, 6.04 m ion NaCl

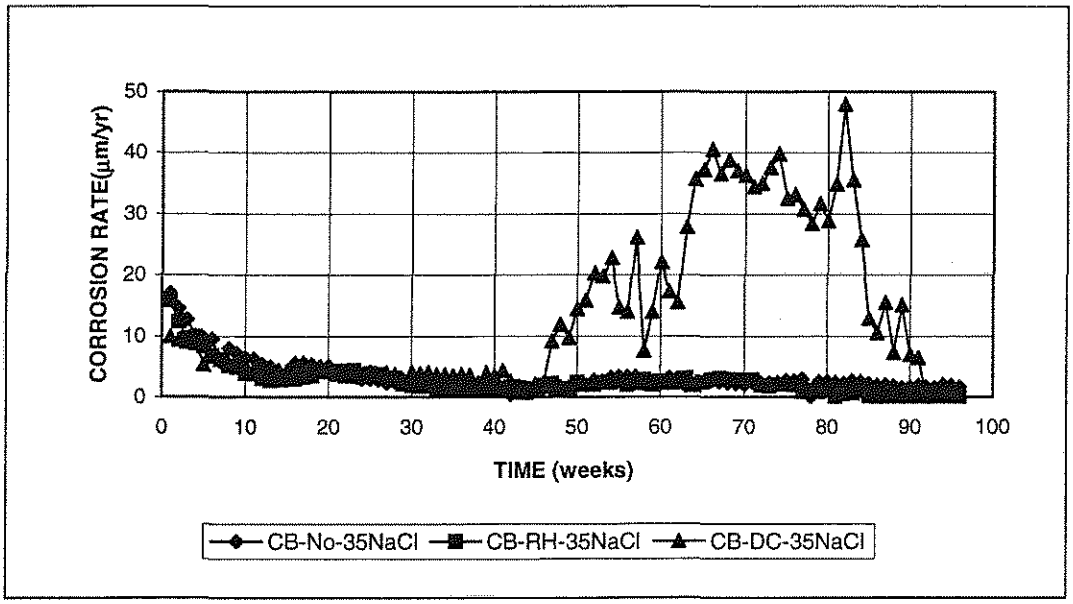

Figure 3.112 Cracked Beam test: Average corrosion rate for different inhibitors, coventional steel, normalized, w/c=0.35, 6.04 m ion NaCl

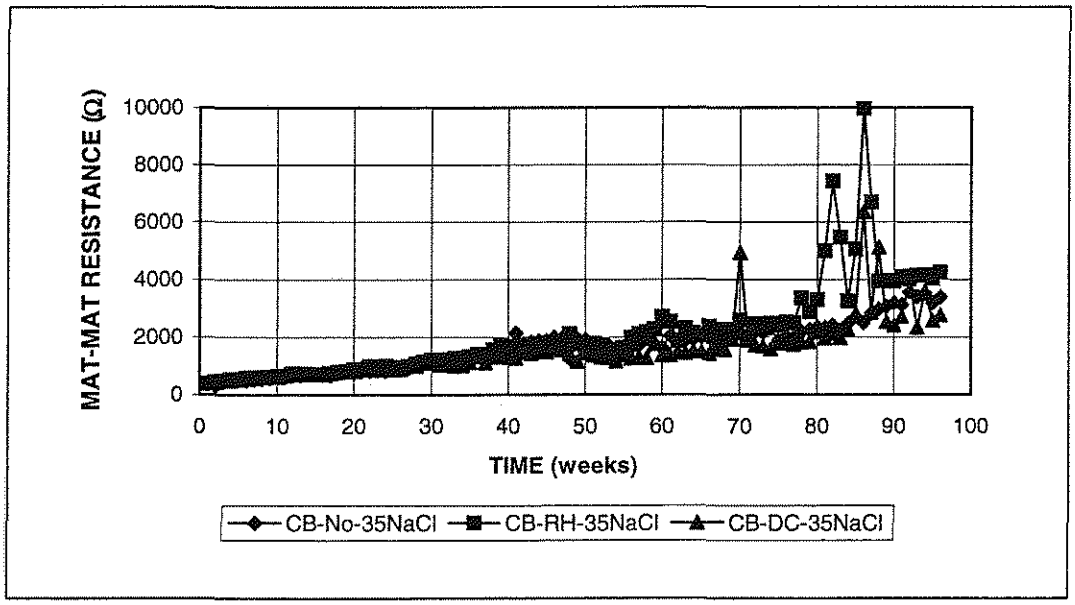

Figure 3.113 Cracked Beam test: Average mat-to-mat resistance for different inhibitors, coventional steel, normalized, w/c=0.35, 6.04 m ion NaCl

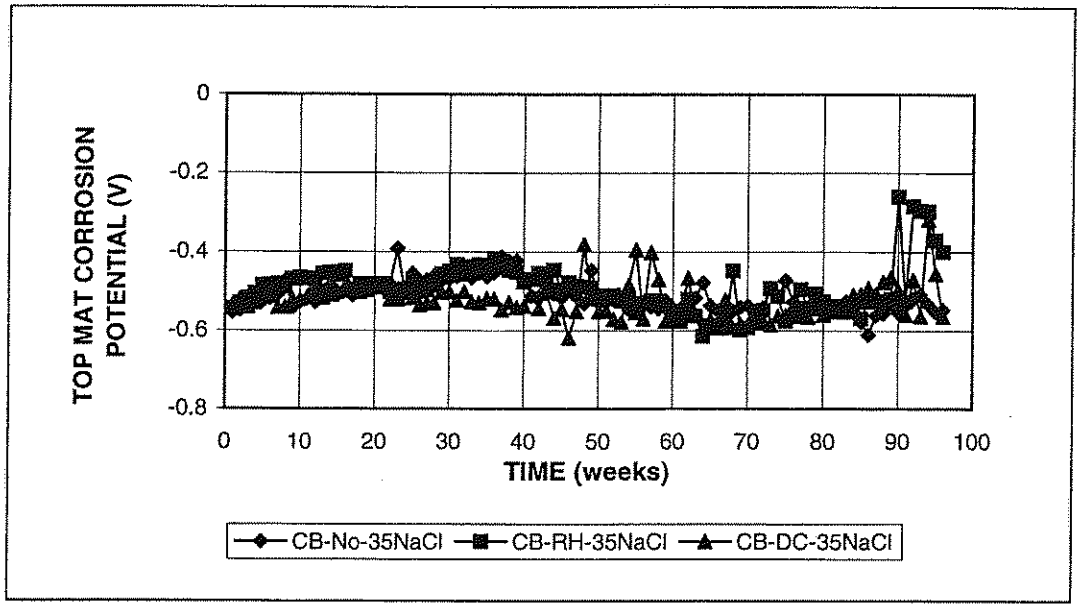

Figure 3.114 Cracked Beam test: Average corrosion potential with respect to copper-copper sulfate electrode. Top mat, different inhibitors, coventional steel, normalized, w/c=0.35, 6.04 m ion NaCl

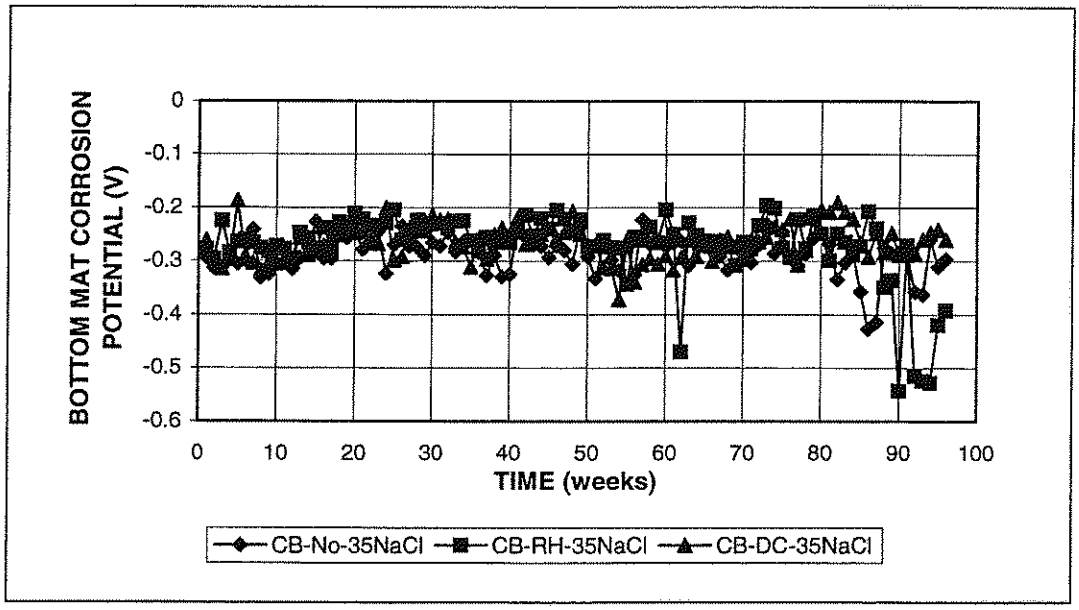

Figure 3.115 Cracked Beam test: Average corrosion potential with respect to copper-copper sulfate electrode. Bottom mat, different inhibitors, coventional steel, normalized, w/c=0.35, 6.04 m ion NaCl

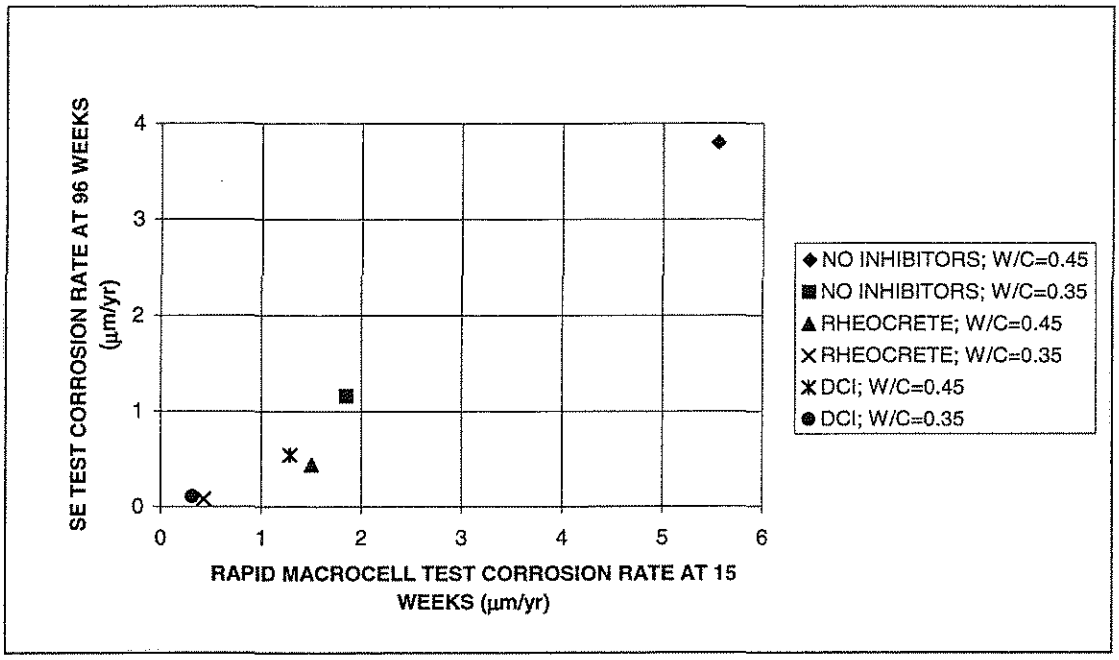

Fig 3.116 Corrosion rate comparison between SE tests (at 96 weeks) and rapid macrocell tests (at 15 weeks)

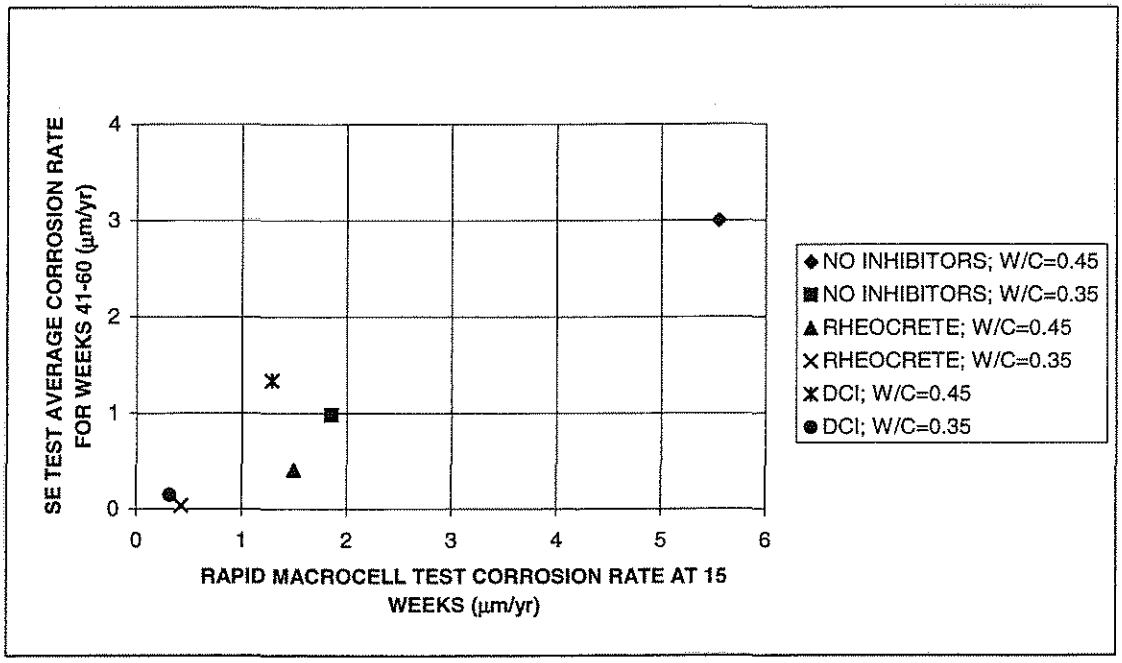

Fig 3.117 Corrosion rate comparison between SE tests (average for weeks 41-60) and rapid macrocell tests (at 15 weeks)

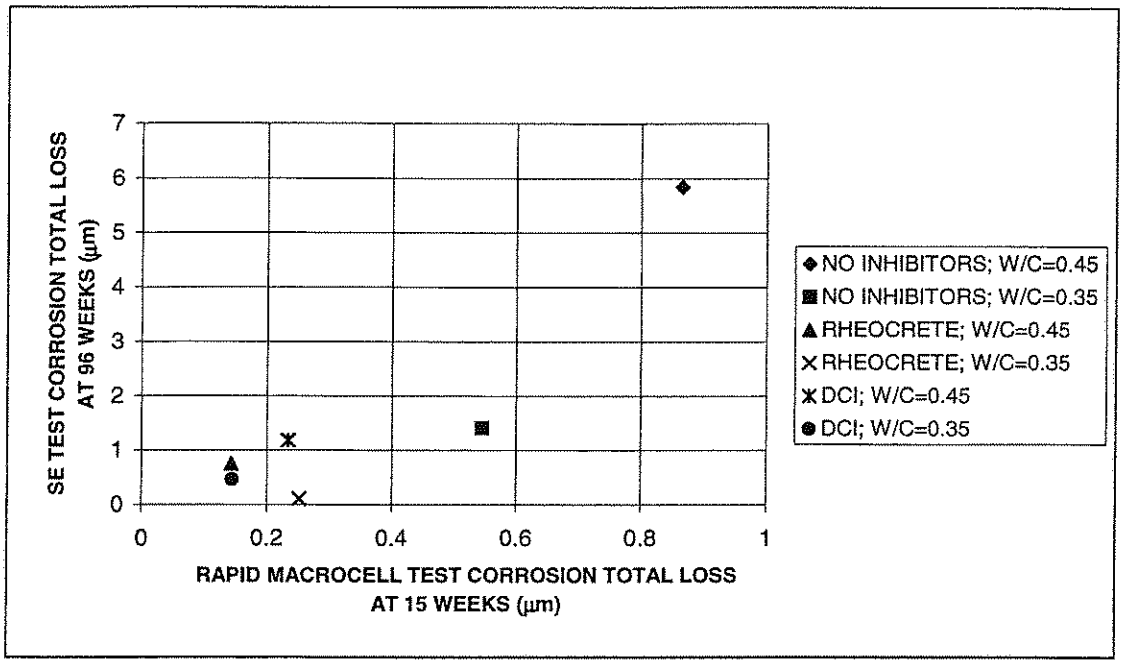

Fig 3.118 Total loss comparison between SE tests (at 96 weeks) and rapid macrocell tests (at 15 weeks)

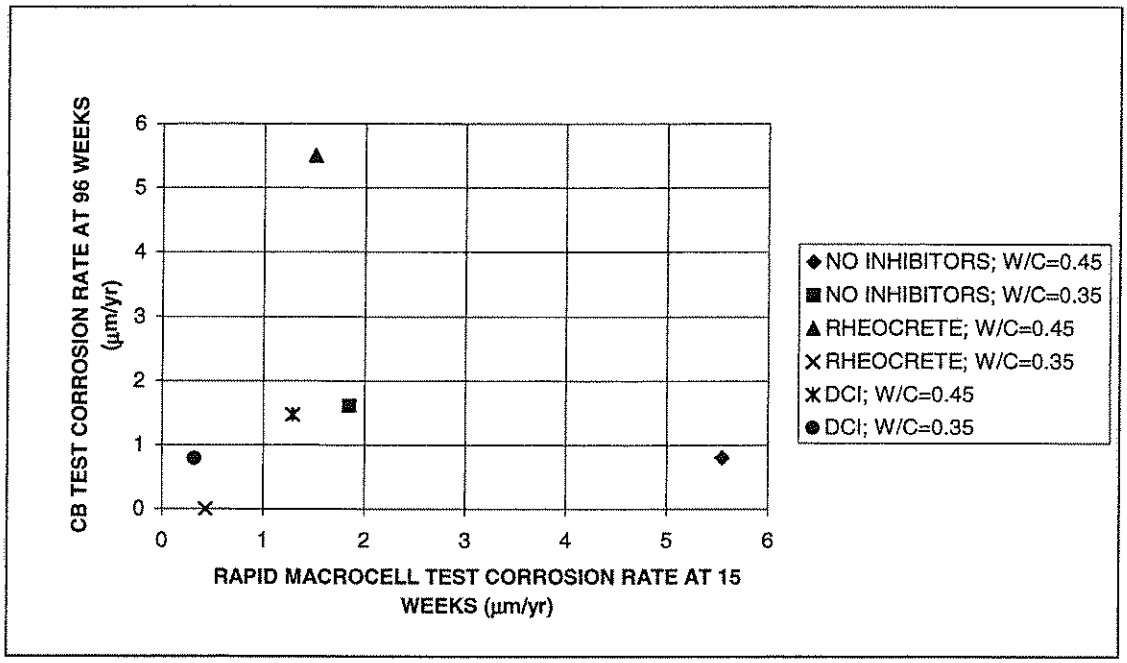

Fig 3.119 Corrosion rate comparison between CB tests (at 96 weeks) and rapid macrocell tests (at 15 weeks)

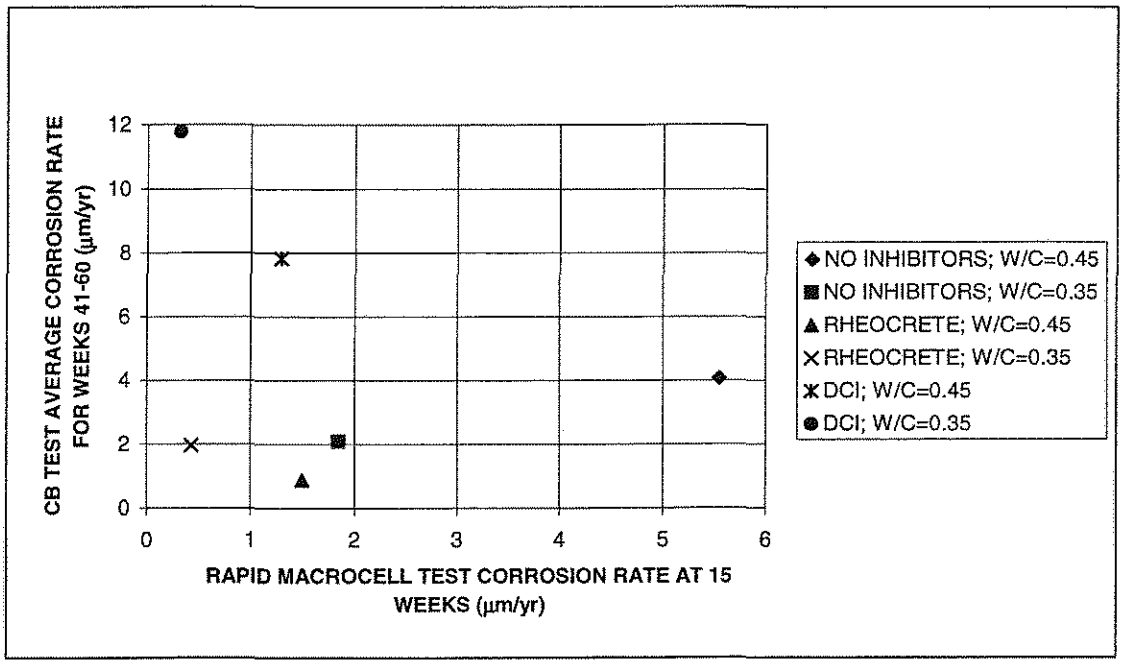

Fig 3.120 Corrosion rate comparison between CB tests (average for weeks 41-60) and rapid macrocell tests (at 15 weeks)

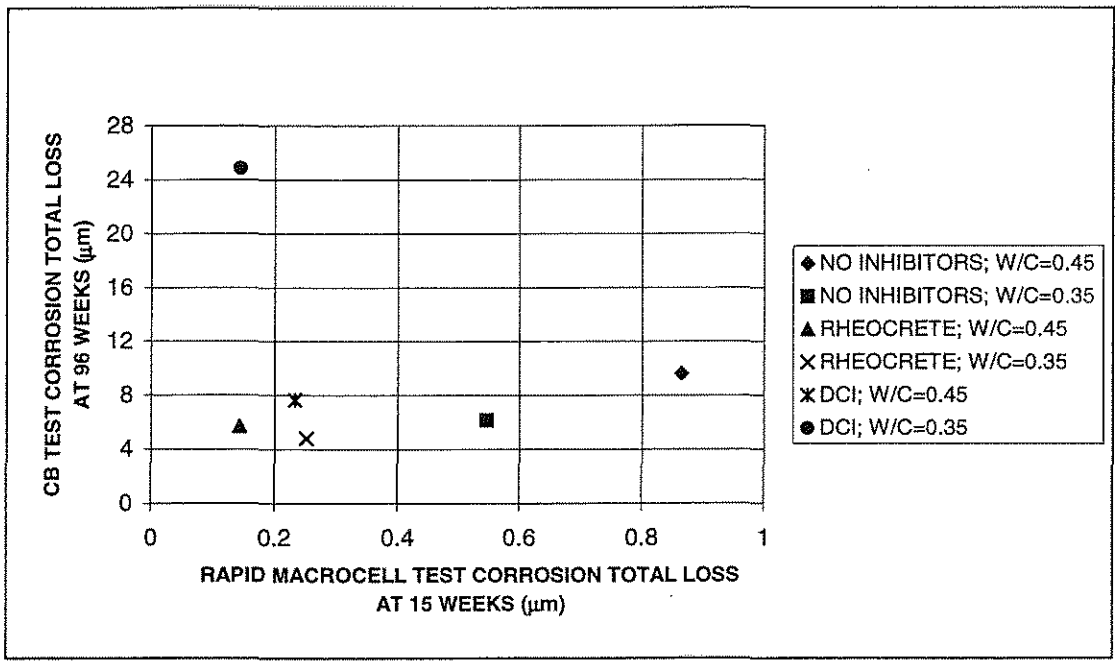

Fig 3.121 Total loss comparison between CB tests (at 96 weeks) and rapid macrocell tests (at 15 weeks)

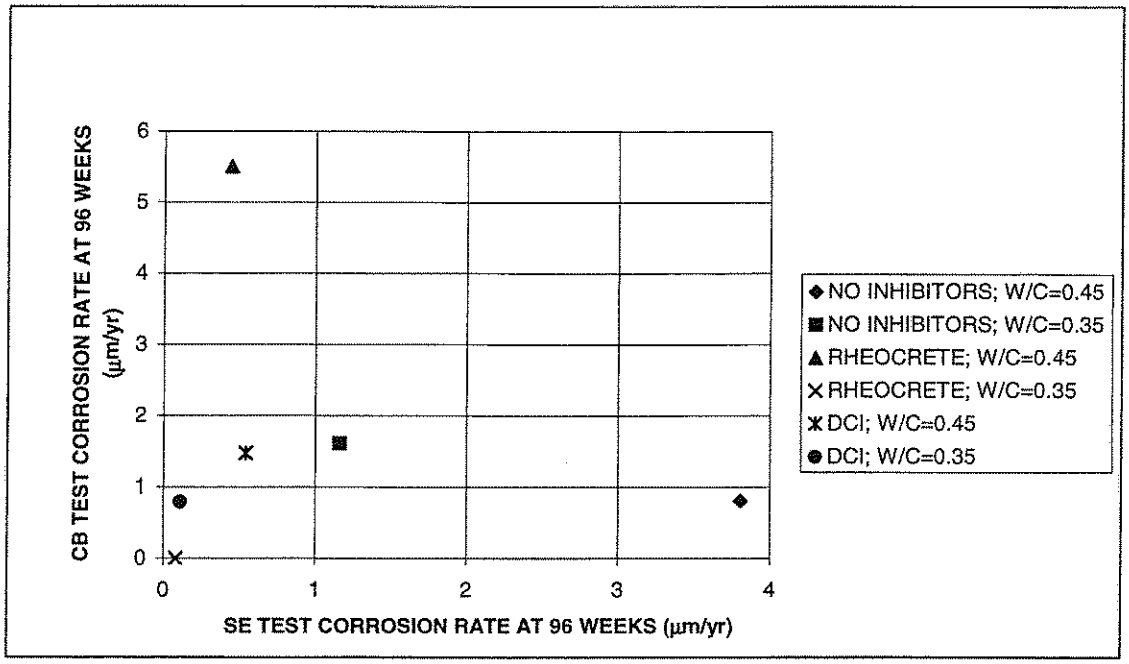

Fig 3.122 Corrosion rate comparison between CB tests (at 96 weeks) and SE tests (at 96 weeks)

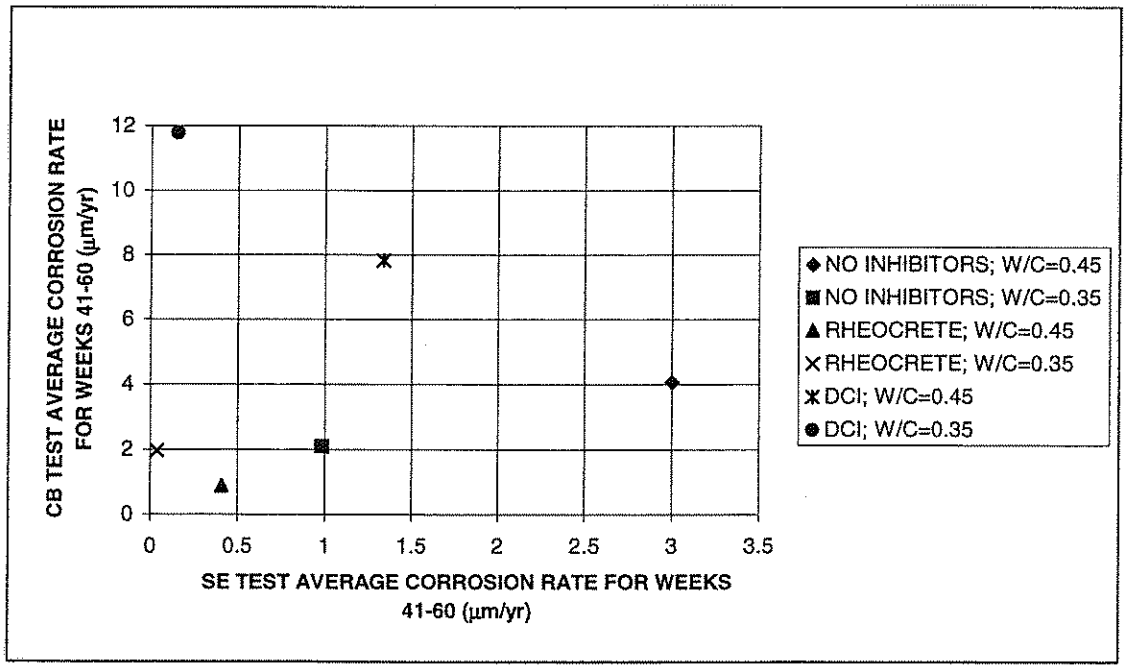

Fig 3.123 Corrosion rate comparison between CB tests (average for weeks 41-60) and SE tests (average for weeks 41-60)

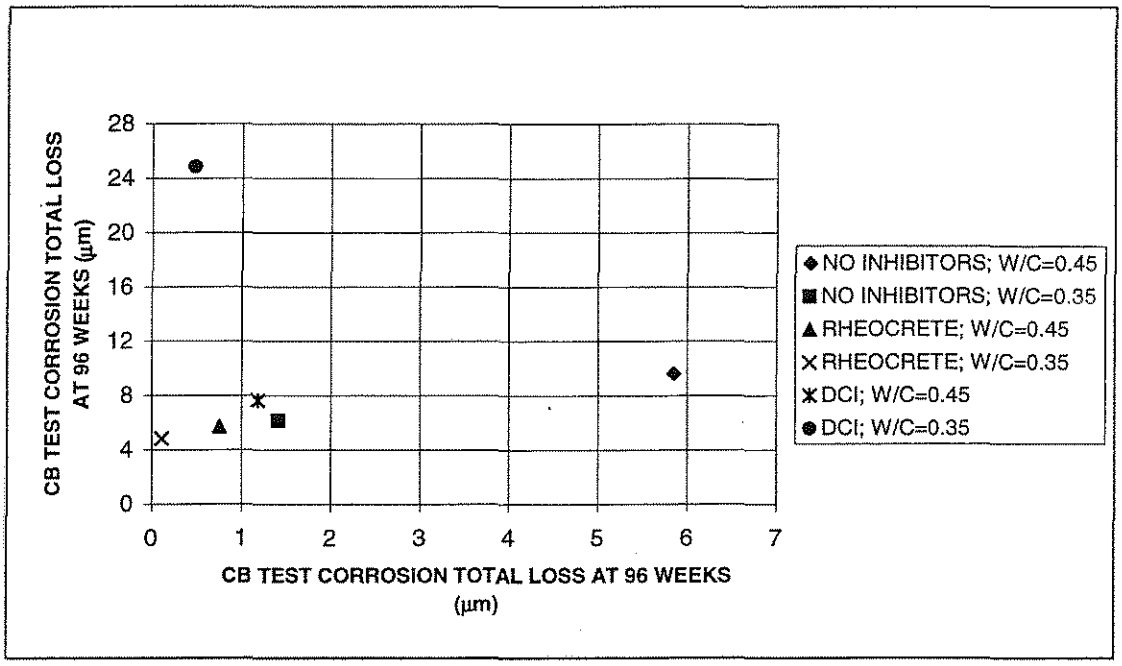

Fig 3.124 Corrosion rate comparison between CB tests (at 96 weeks) and SE tests (at 96 weeks)

Appendix A

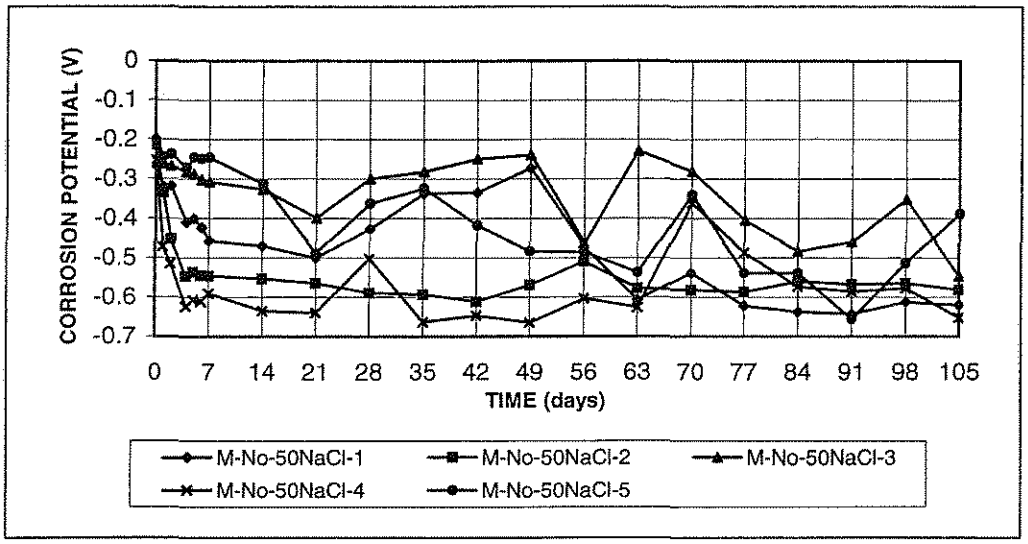

Figure A1.a Anode Potential with respect to standard calomel electrode; w/c=0.50; no inhibitor; 1.6 m ion NaCl in simulated pore solution

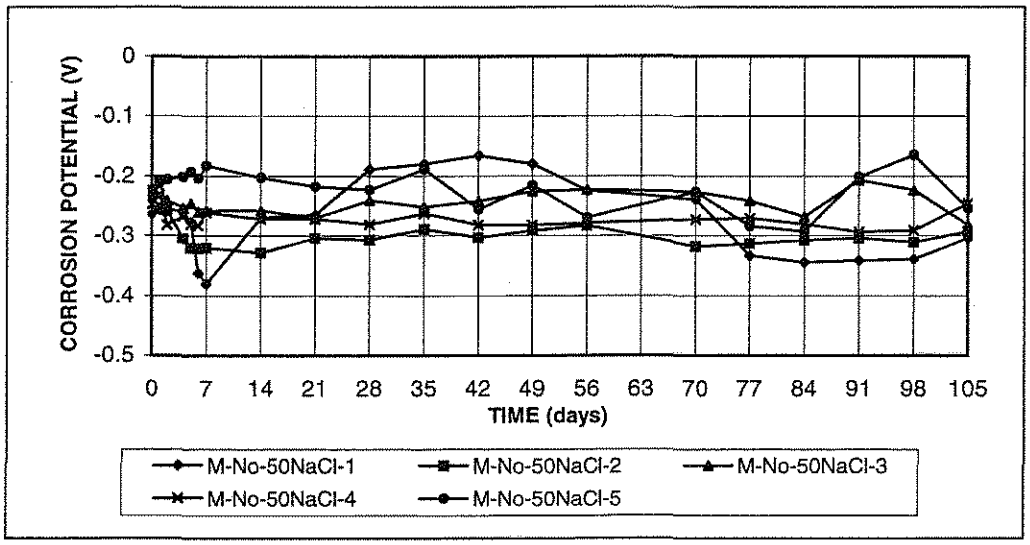

Figure A1.b Cathode Potential with respect to standard calomel electrode; w/c=0.50; no inhibitor; 1.6 m ion NaCl in simulated pore solution

Note: 1. Rust on M-No-50-NaCl-1,2,3,4,5 were cleaned on the 21 day after taking readings.
2. Rust on M-No-50-NaCl-1,2,3,4,5 were cleaned on the 48 day.
3. Rust on M-No-50-NaCl-1,2,3,4,5 were cleaned on the 88 day.

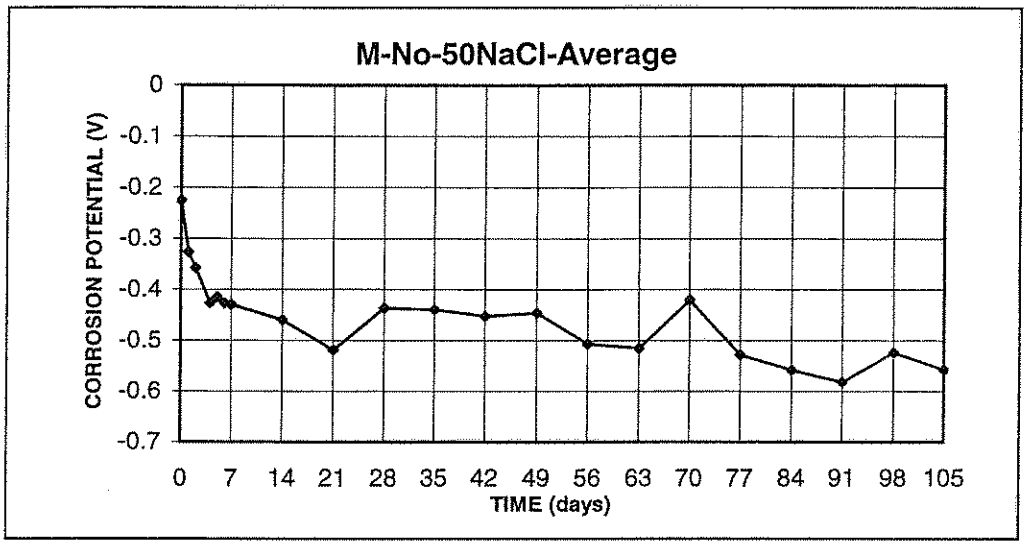

Figure A1.c Anode Potential with respect to standard calomel electrode; w/c=0.50; no inhibitor; 1.6 m ion NaCl in simulated pore solution

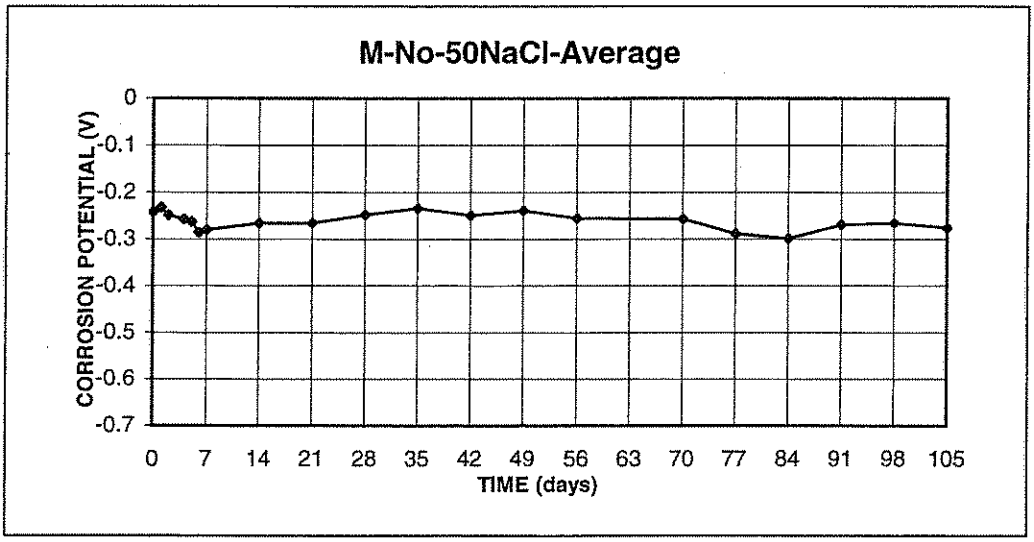

Figure A1.d Cathode Potential with respect to standard calomel electrode; w/c=0.50; no inhibitor; 1.6 m ion NaCl in simulated pore solution

Note: 1. Rust on M-No-50-NaCl-1,2,3,4,5 were cleaned on the 21 day after taking readings.
2. Rust on M-No-50-NaCl-1,2,3,4,5 were cleaned on the 48 day.
3. Rust on M-No-50-NaCl-1,2,3,4,5 were cleaned on the 88 day.

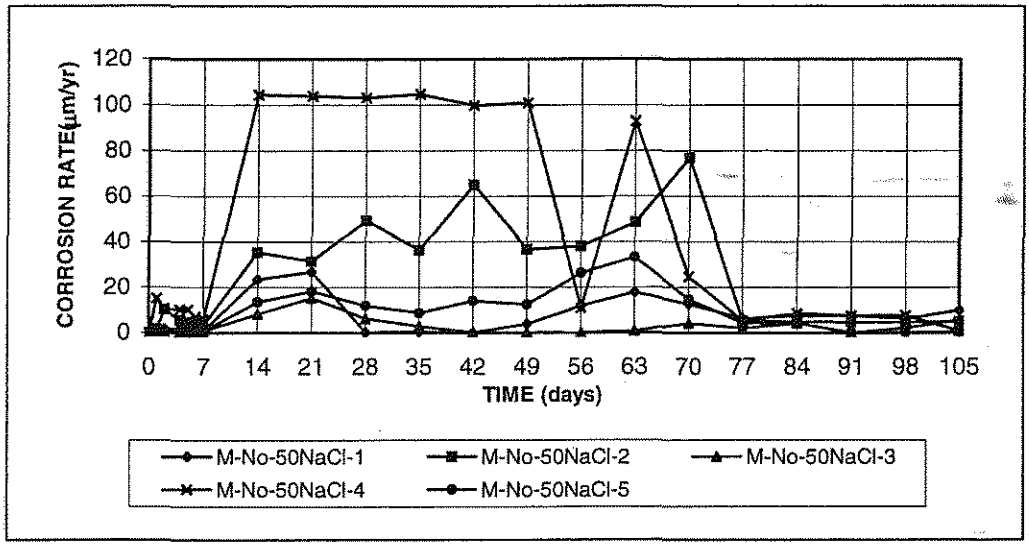

Figure A1.e Corrosion Rate;
w/c=0.50; no inhibitor; 1.6 m ion NaCl in simulated pore solution

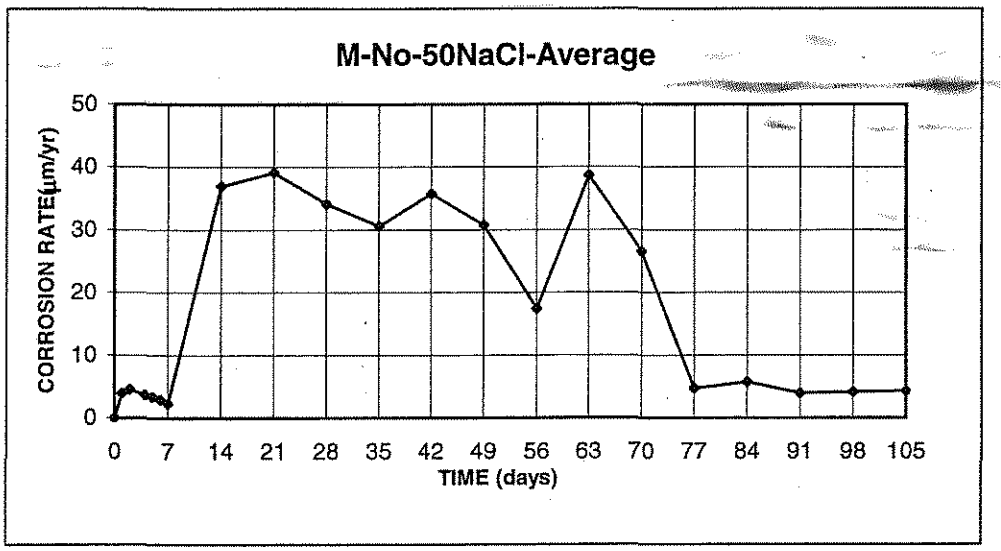

Figure A1.f Corrosion Rate;
w/c=0.50; no inhibitor; 1.6 m ion NaCl in simulated pore solution

Note: 1. Rust on M-No-50-NaCl-1,2,3,4,5 were cleaned on the 21 day after taking readings.
2. Rust on M-No-50-NaCl-1,2,3,4,5 were cleaned on the 48 day.
3. Rust on M-No-50-NaCl-1,2,3,4,5 were cleaned on the 88 day.

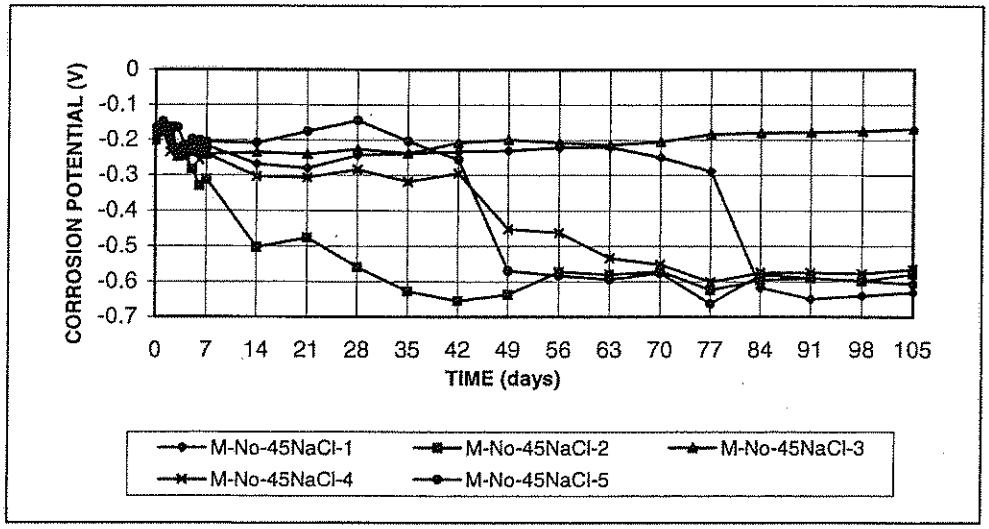

Figure A2.a Anode Potential with respect to standard calomel electrode; w/c=0.45; no inhibitor; 1.6 m ion NaCl in simulated pore solution

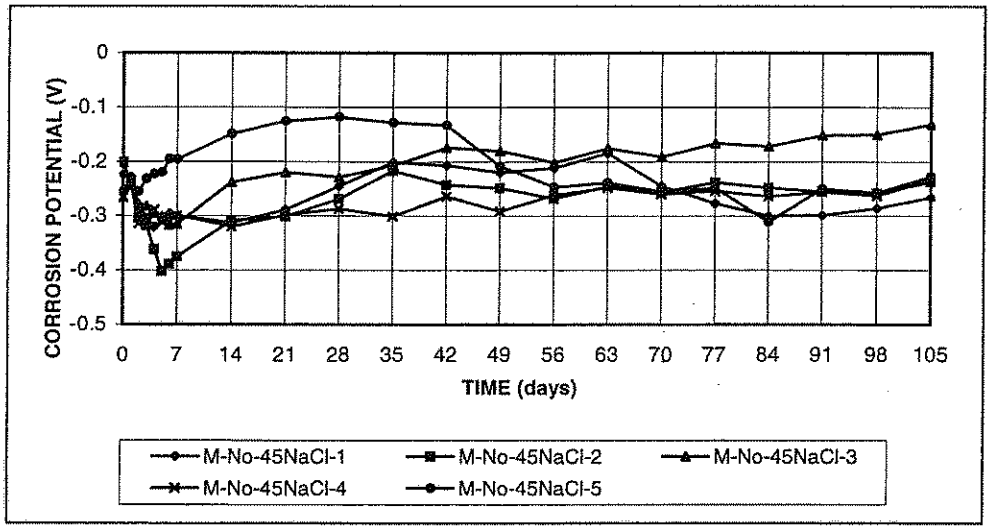

Figure A2.b Cathode Potential with respect to standard calomel electrode; w/c=0.45; no inhibitor; 1.6 m ion NaCl in simulated pore solution

Note: 1. Rust on M-No-45-NaCl-2 was cleaned on the 91 day after taking readings.

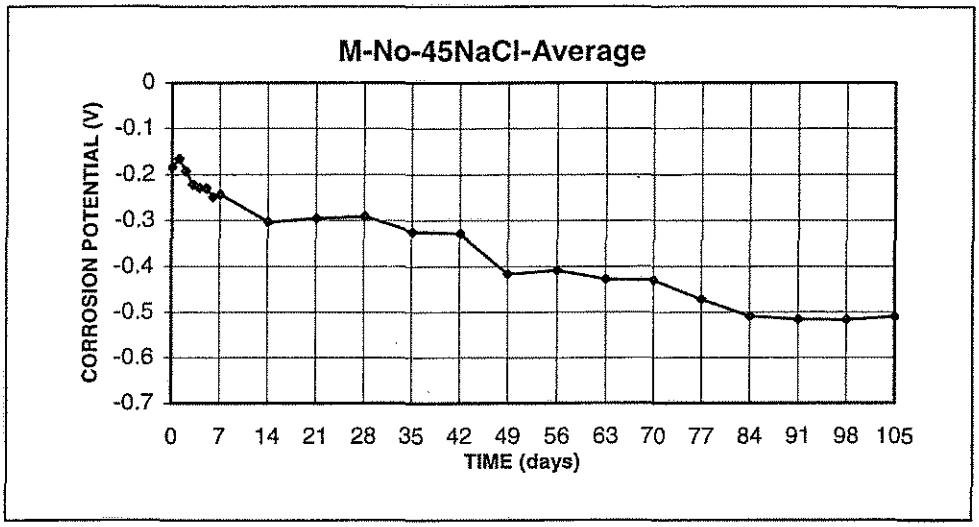

Figure A2.c Anode Potential with respect to standard calomel electrode; w/c=0.45; no inhibitor; 1.6 m ion NaCl in simulated pore solution

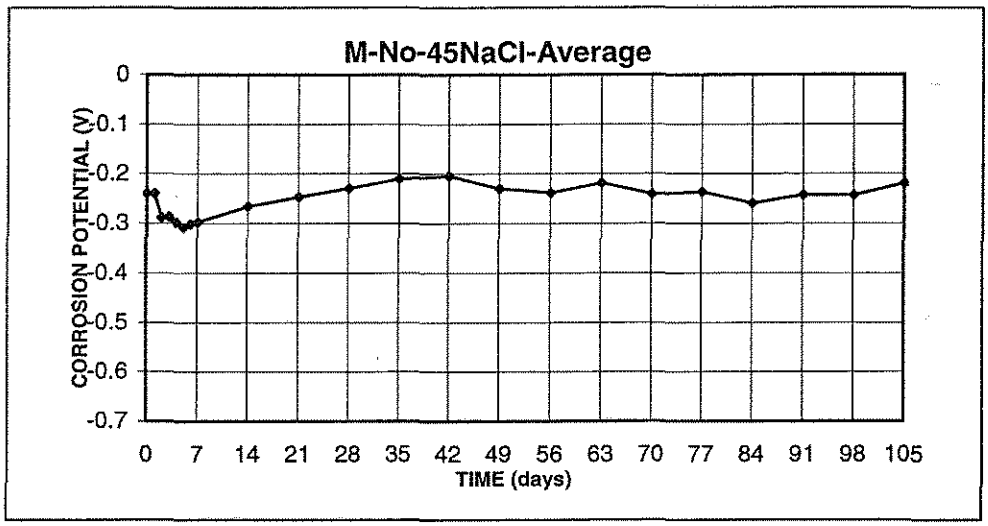

Figure A2.d Cathode Potential with respect to standard calomel electrode; w/c=0.45; no inhibitor; 1.6 m ion NaCl in simulated pore solution

Note: 1. Rust on M-No-45-NaCl-2 was cleaned on the 91 day after taking readings.

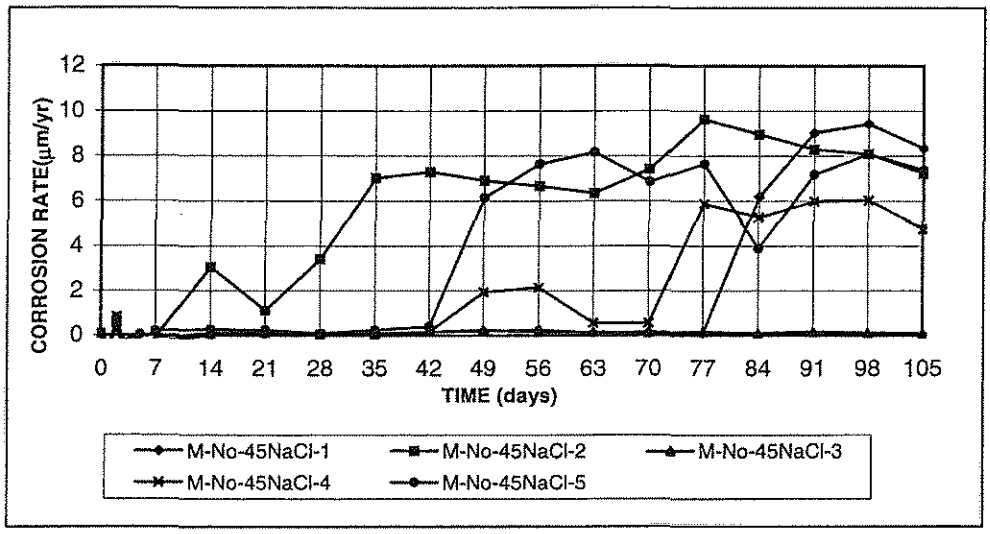

Figure A2.e Corrosion Rate;
w/c=0.45; no inhibitor; 1.6 m ion NaCl in simulated pore solution

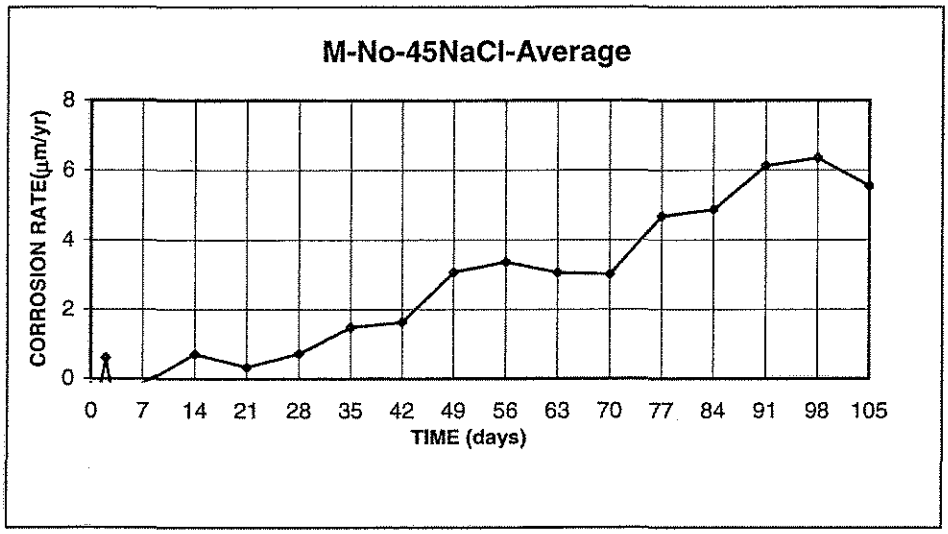

Figure A2.f Corrosion Rate;
w/c=0.45; no inhibitor; 1.6 m ion NaCl in simulated pore solution

Note: 1. Rust on M-No-45-NaCl-2 was cleaned on the 91 day after taking readings.

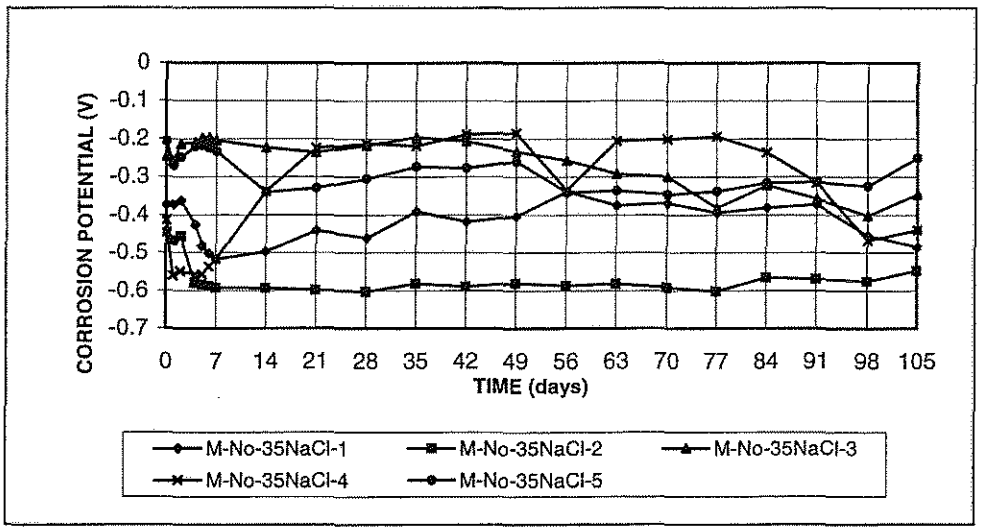

Figure A3.a Anode Potential with respect to standard calomel electrode; w/c=0.35; no inhibitor; 1.6 m ion NaCl in simulated pore solution

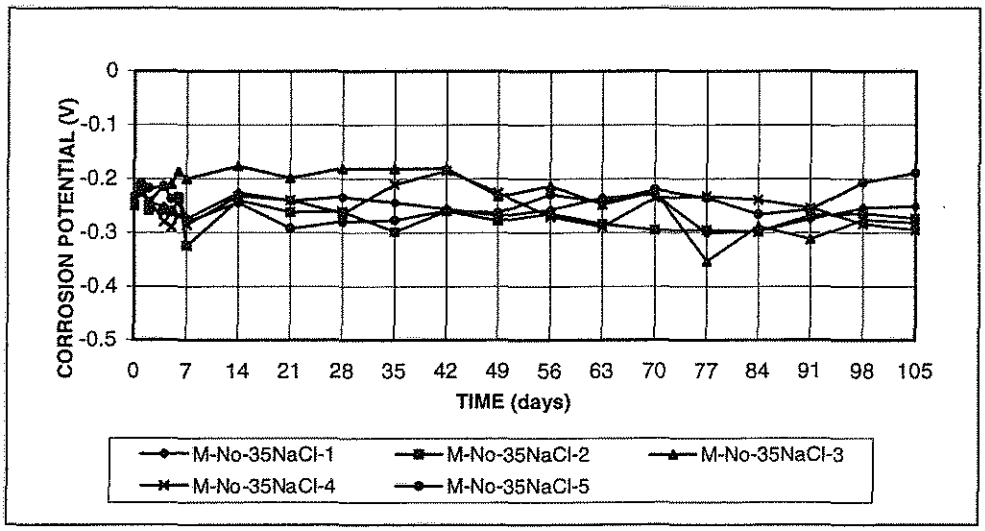

Figure A3.b Cathode Potential with respect to standard calomel electrode; w/c=0.35; no inhibitor; 1.6 m ion NaCl in simulated pore solution

Note: 1. Rust on M-No-35-NaCl-1,2,3,4,5 were cleaned on the 97 day.

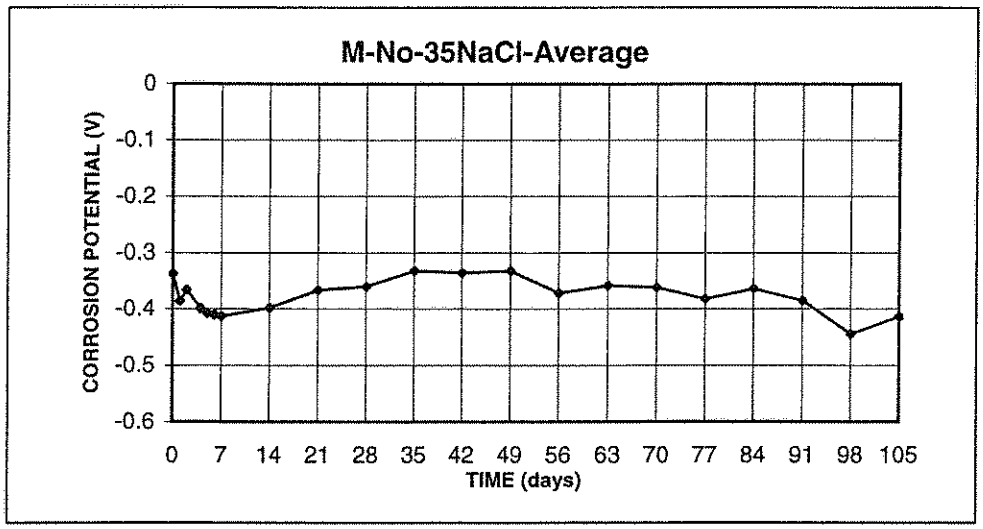

Figure A3.c Anode Potential with respect to standard calomel electrode; w/c=0.35; no inhibitor; 1.6 m ion NaCl in simulated pore solution

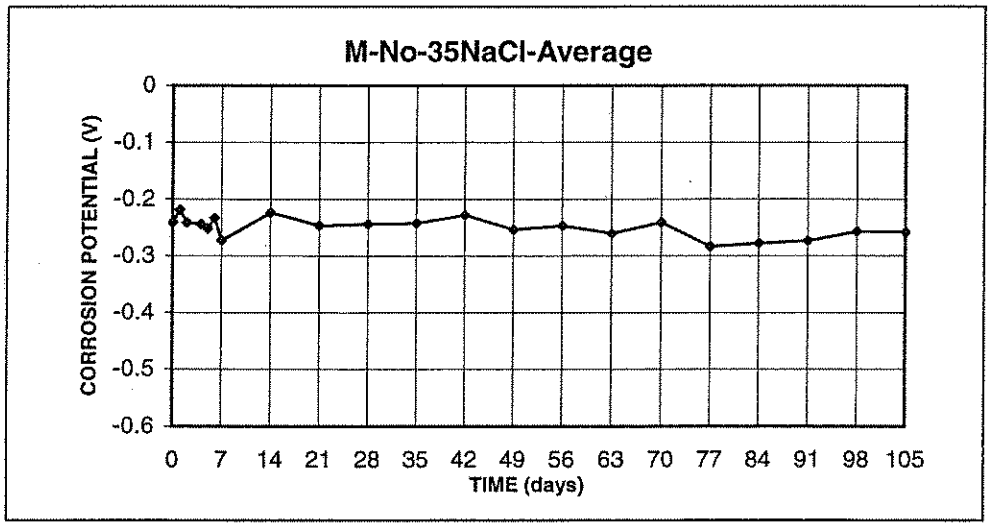

Figure A3.d Cathode Potential with respect to standard calomel electrode; w/c=0.35; no inhibitor; 1.6 m ion NaCl in simulated pore solution

Note: 1. Rust on M-No-35-NaCl-1,2,3,4,5 were cleaned on the 97 day.

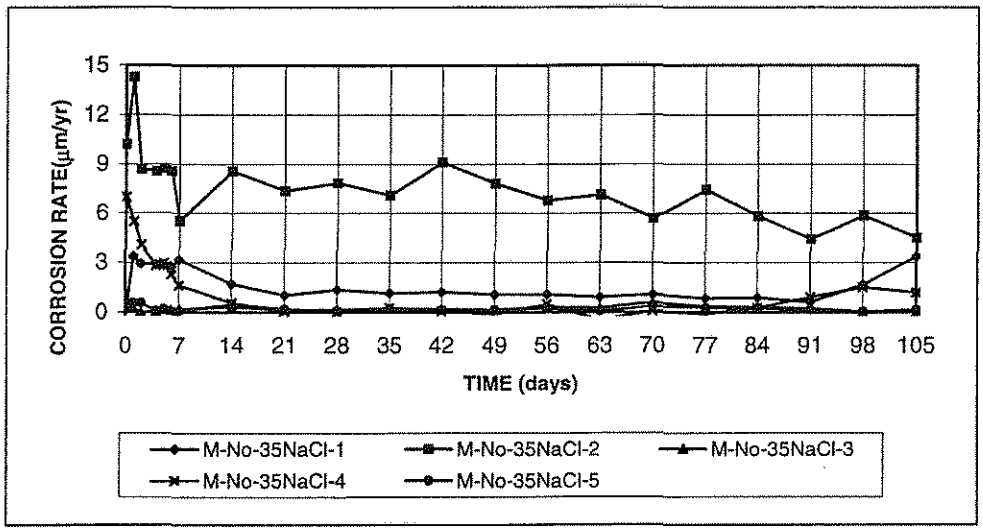

Figure A3.e Corrosion Rate;
w/c=0.35; no inhibitor; 1.6 m ion NaCl in simulated pore solution

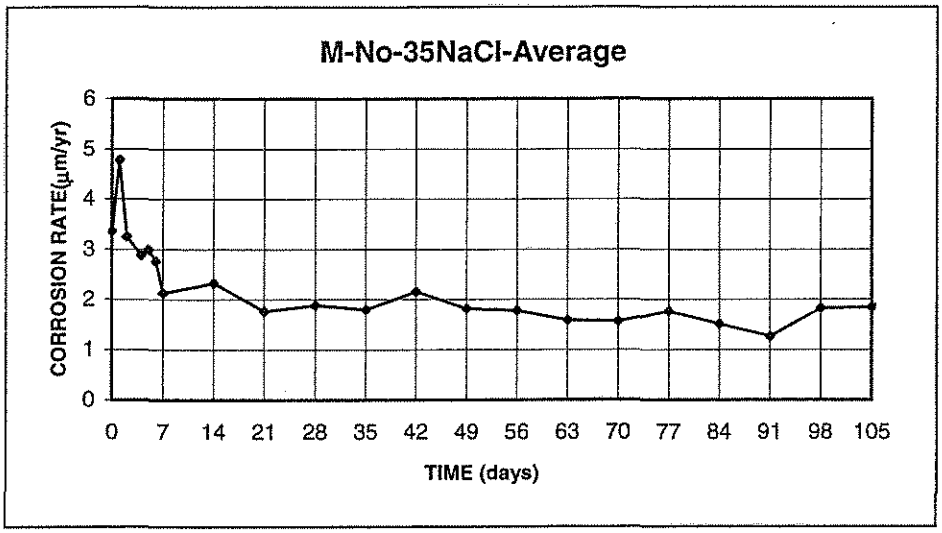

Figure A3.f Corrosion Rate;
w/c=0.35; no inhibitor; 1.6 m ion NaCl in simulated pore solution

Note: 1. Rust on M-No-35-NaCl-1,2,3,4,5 were cleaned on the 97 day.

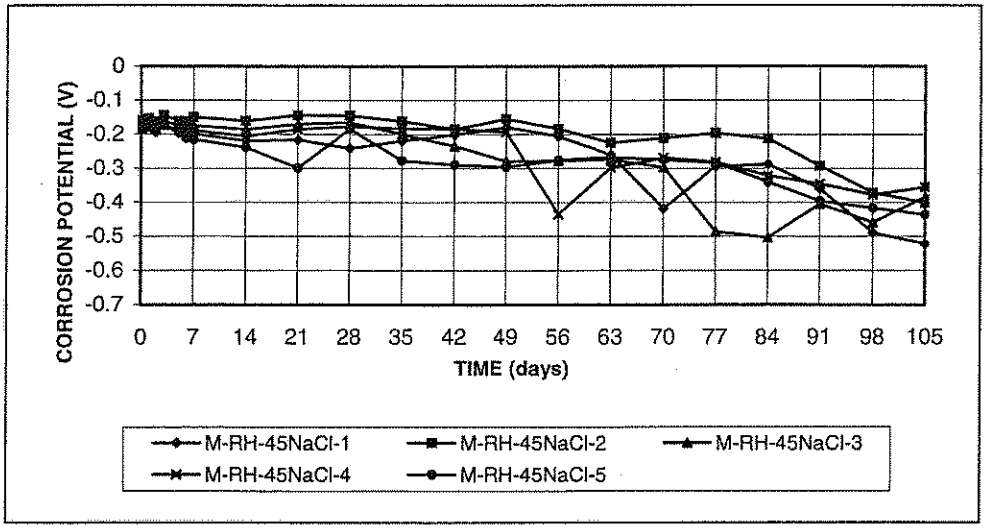

Figure A4.a Anode Potential with respect to standard calomel electrode; w/c=0.45; Rheocrete; 1.6 m ion NaCl in simulated pore solution

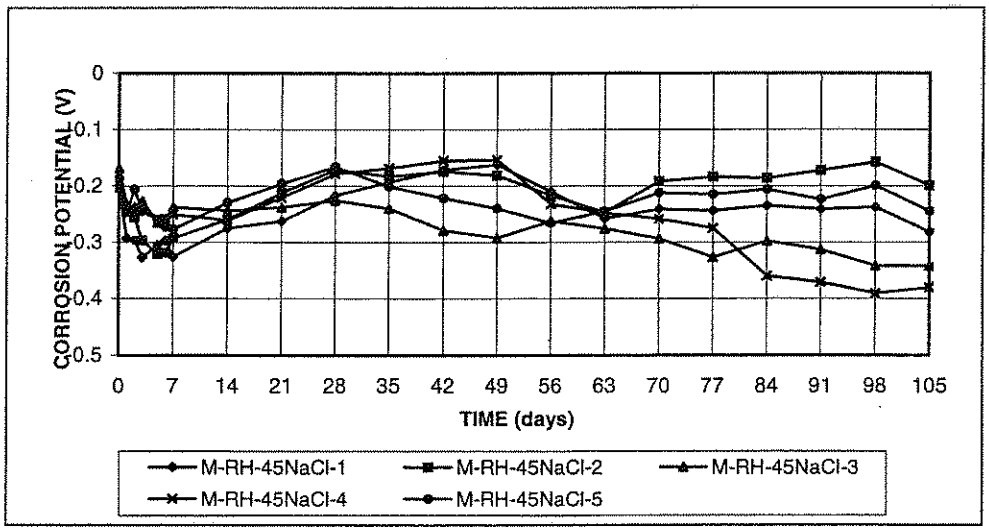

Figure A4.b Cathode Potential with respect to standard calomel electrode; w/c=0.45; Rheocrete; 1.6 m ion NaCl in simulated pore solution

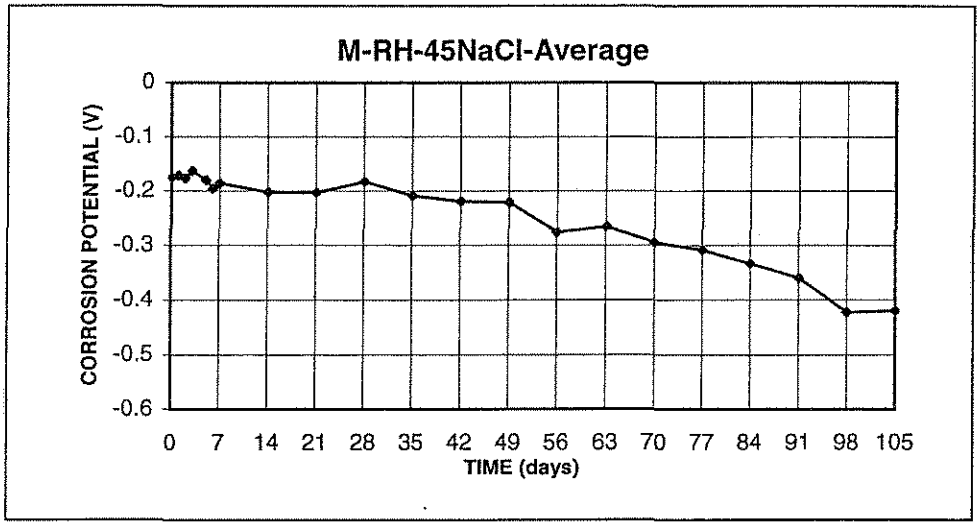

Figure A4.c Anode Potential with respect to standard calomel electrode; w/c=0.45; Rheocrete; 1.6 m ion NaCl in simulated pore solution

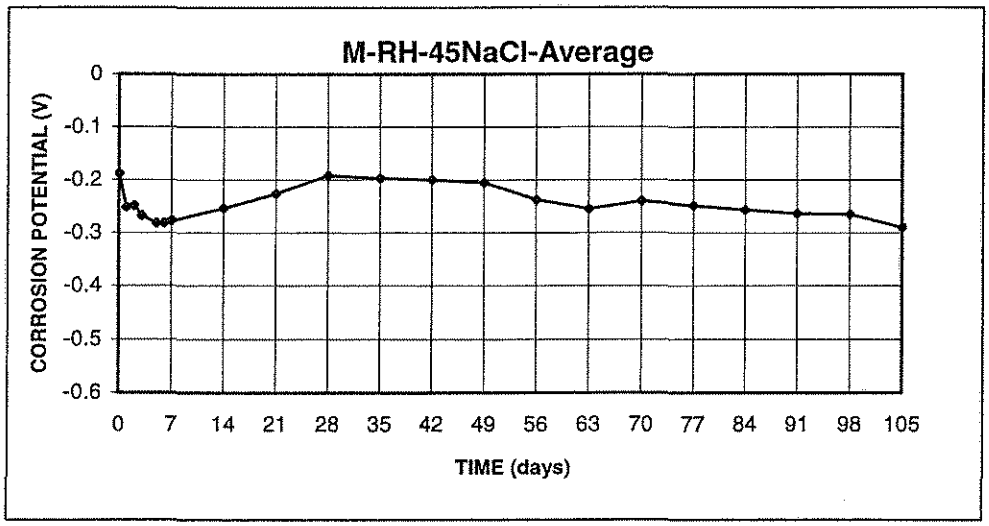

Figure A4.d Cathode Potential with respect to standard calomel electrode; w/c=0.45; Rheocrete; 1.6 m ion NaCl in simulated pore solution

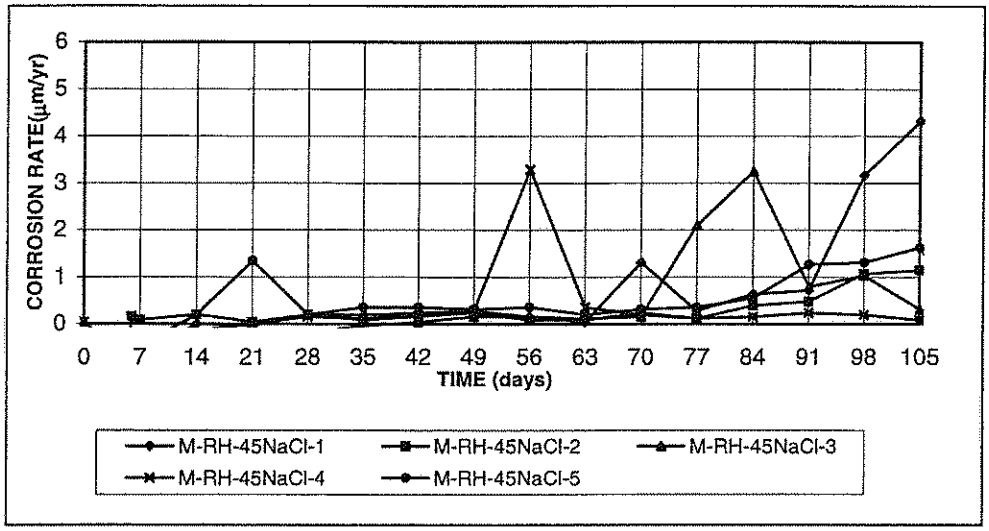

Figure A4.e Corrosion Rate;
w/c=0.45; Rheocrete; 1.6 m ion NaCl in simulated pore solution

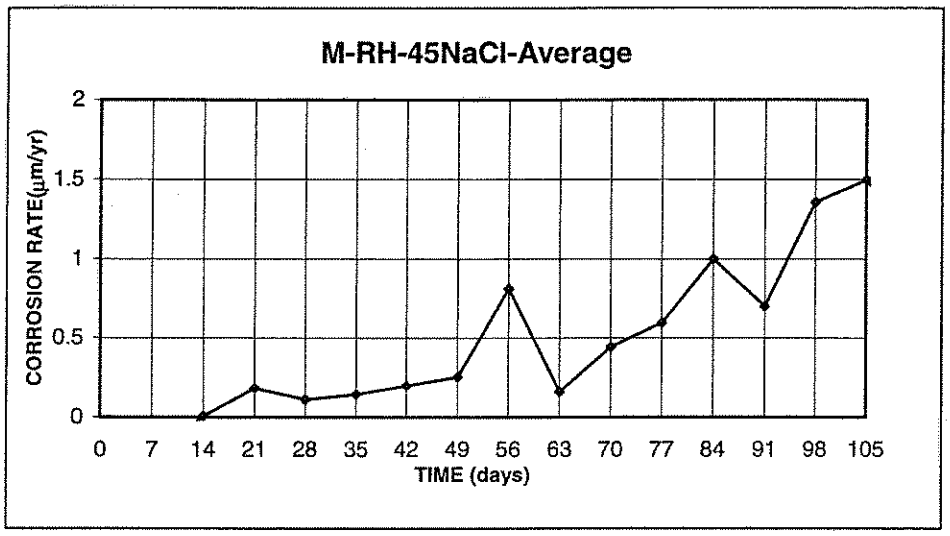

Figure A4.f Corrosion Rate;
w/c=0.45; Rheocrete; 1.6 m ion NaCl in simulated pore solution

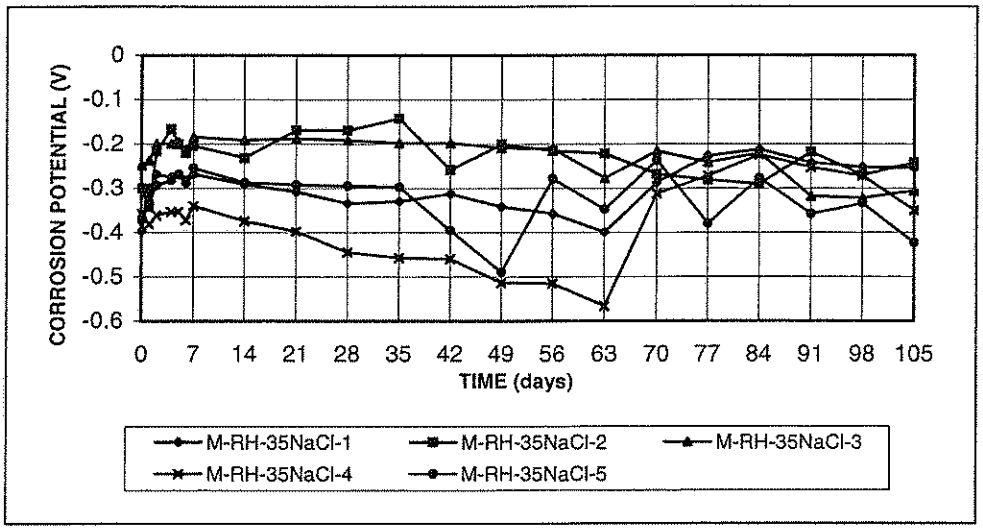

Figure A5.a Anode Potential with respect to standard calomel electrode; w/c=0.35; Rheocrete; 1.6 m ion NaCl in simulated pore solution

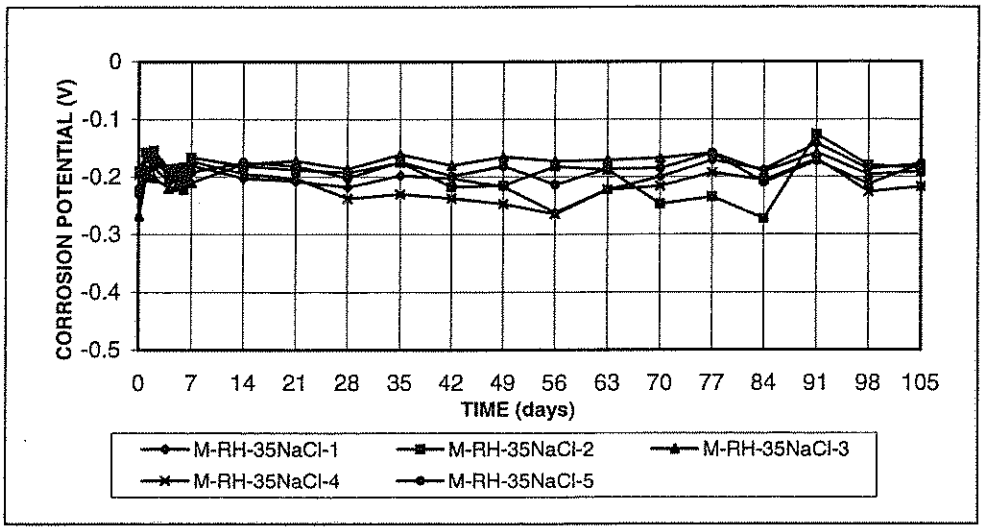

Figure A5.b Cathode Potential with respect to standard calomel electrode; w/c=0.35; Rheocrete; 1.6 m ion NaCl in simulated pore solution

Note: 1. Rust on M-Rh-35-NaCl-4 was cleaned on the 63 day after taking readings.
2. Rust on M-Rh-35-NaCl-1,2,3,4,5 were cleaned on the 90 day.

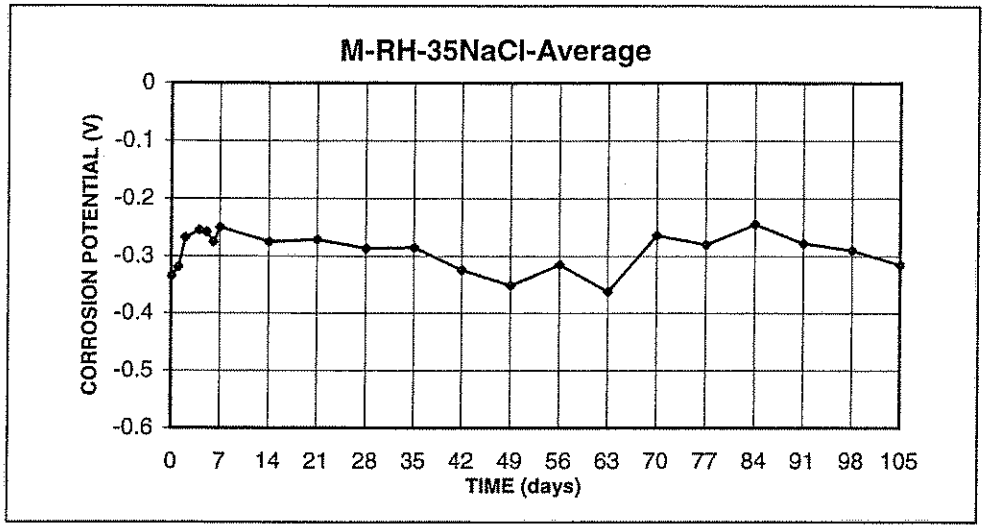

Figure A5.c Anode Potential with respect to standard calomel electrode; w/c=0.35; Rheocrete; 1.6 m ion NaCl in simulated pore solution

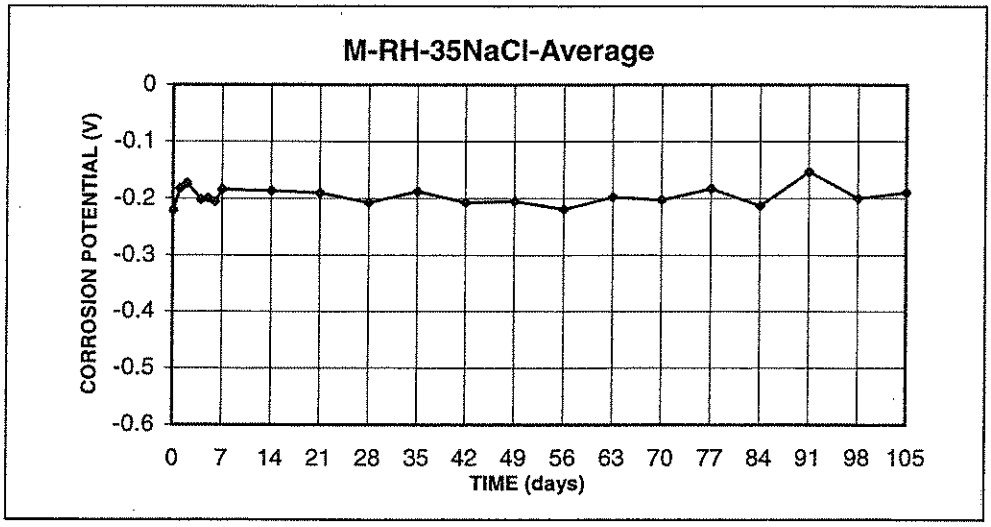

Figure A5.d Cathode Potential with respect to standard calomel electrode; w/c=0.35 Rheocrete, 1.6m NaCl

Note: 1. Rust on M-Rh-35-NaCl-4 was cleaned on the 63 day after taking readings.
2. Rust on M-Rh-35-NaCl-1,2,3,4,5 were cleaned on the 90 day.

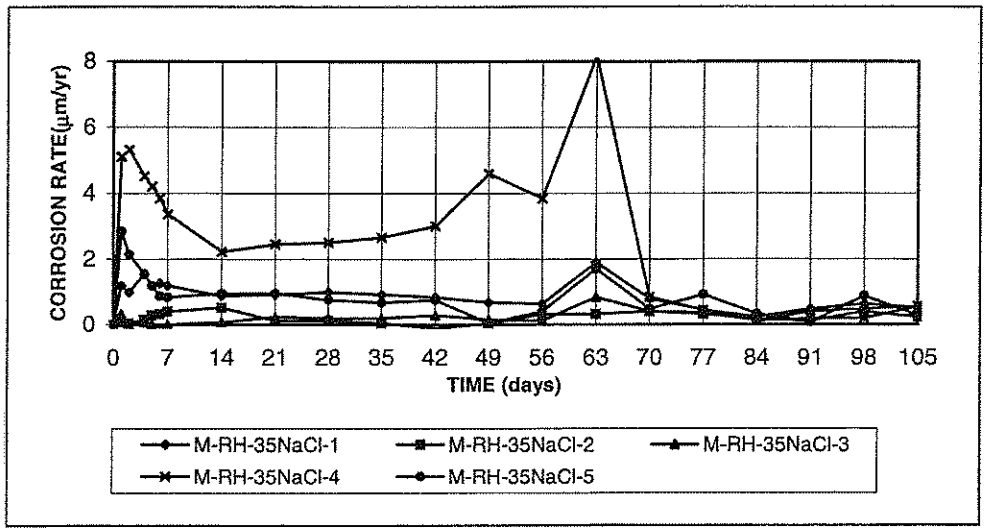

Figure A5.e Corrosion Rate;
w/c=0.35; Rheocrete; 1.6 m ion NaCl in simulated pore solution

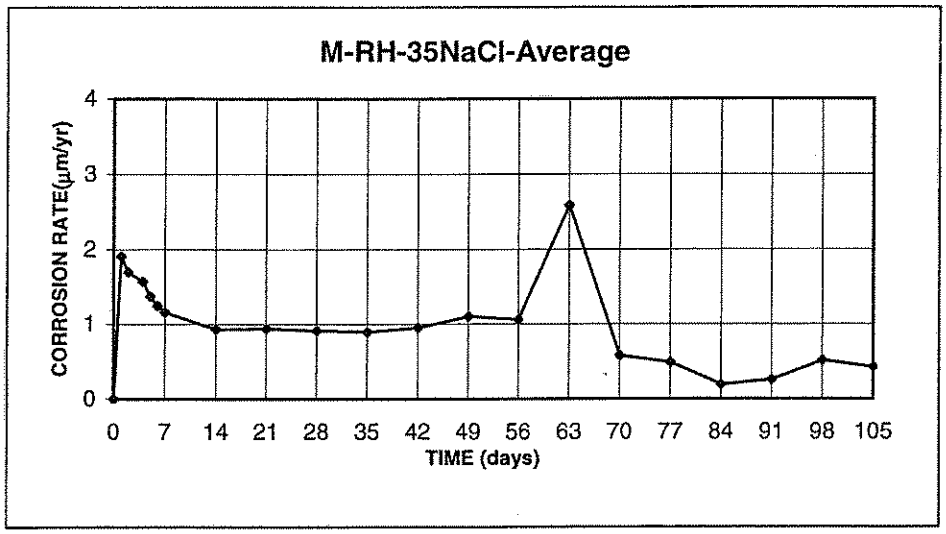

Figure A5.f Corrosion Rate;
w/c=0.35; Rheocrete; 1.6 m ion NaCl in simulated pore solution

Note: 1. Rust on M-Rh-35-NaCl-4 was cleaned on the 63 day after taking readings.
2. Rust on M-Rh-35-NaCl-1,2,3,4,5 were cleaned on the 90 day.

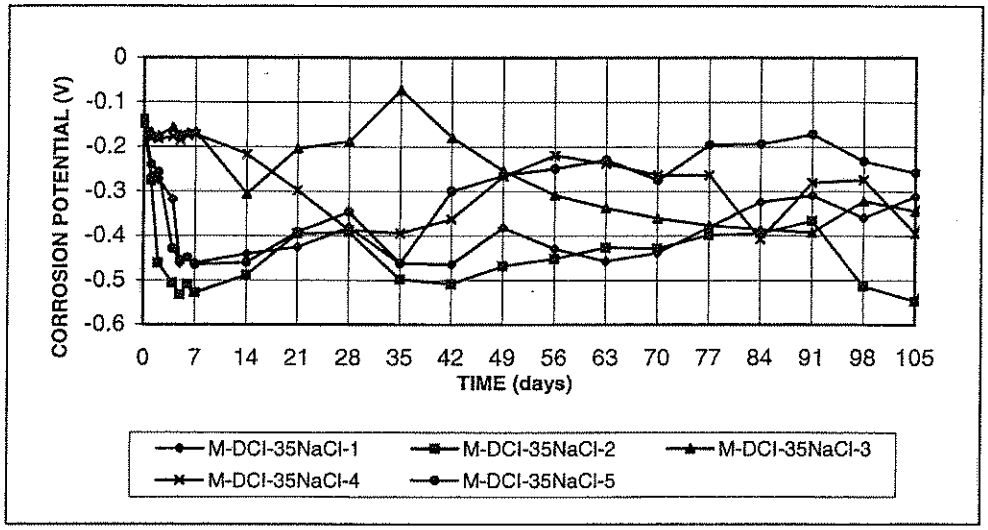

Figure A7.a Anode Potential with respect to standard calomel electrode; w/c=0.35; DCI; 1.6 m ion NaCl in simulated pore solution

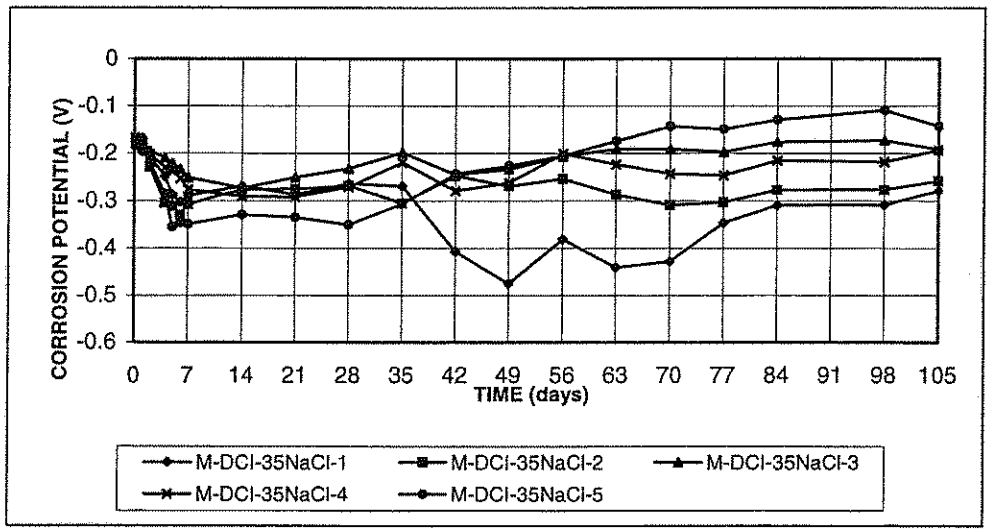

Figure A7.b Cathode Potential with respect to standard calomel electrode; w/c=0.35; DCI; 1.6 m ion NaCl in simulated pore solution

Note: 1. Rust on M-DCI-35-NaCl-1,2,3,4,5 were cleaned on the 83 day.

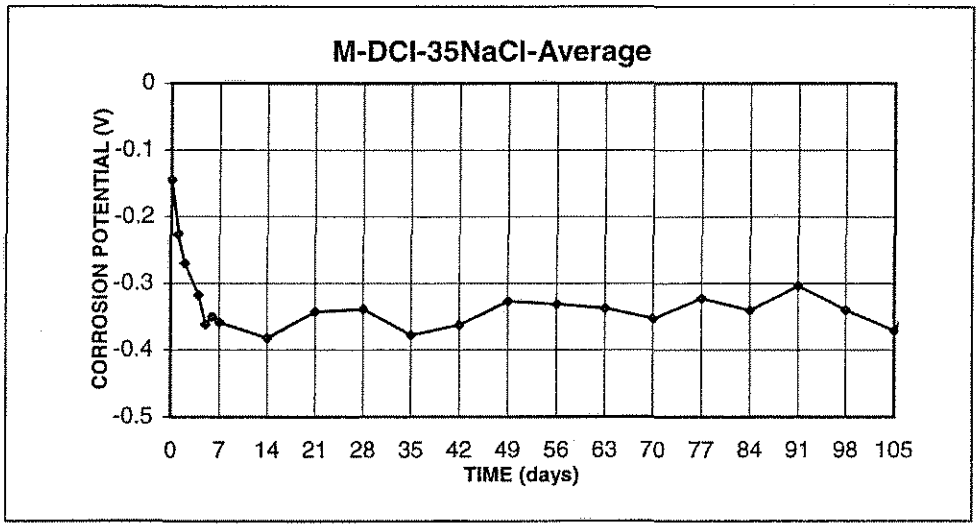

Figure A7.c Anode Potential with respect to standard calomel electrode; w/c=0.35; DCI; 1.6 m ion NaCl in simulated pore solution

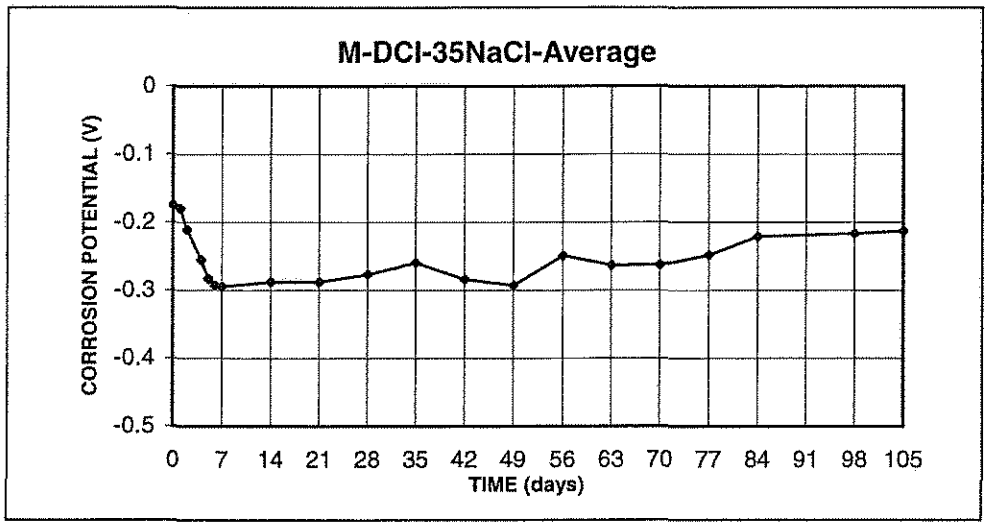

Figure A7.d Cathode Potential with respect to standard calomel electrode; w/c=0.35; DCI; 1.6 m ion NaCl in simulated pore solution

Note: 1. Rust on M-DCI-35-NaCl-1,2,3,4,5 were cleaned on the 83 day.

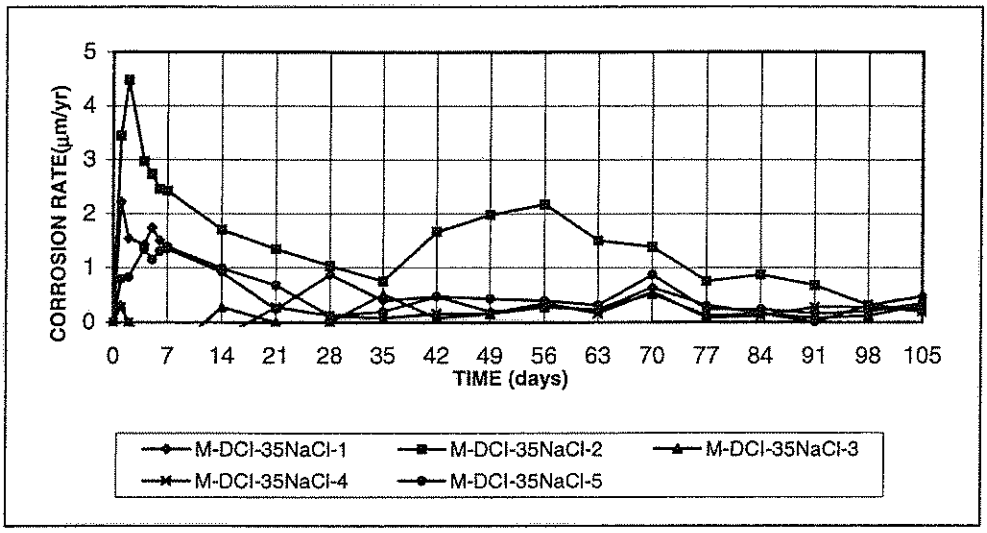

Figure A7.e Corrosion Rate;
w/c=0.35; DCI; 1.6 m ion NaCl in simulated pore solution

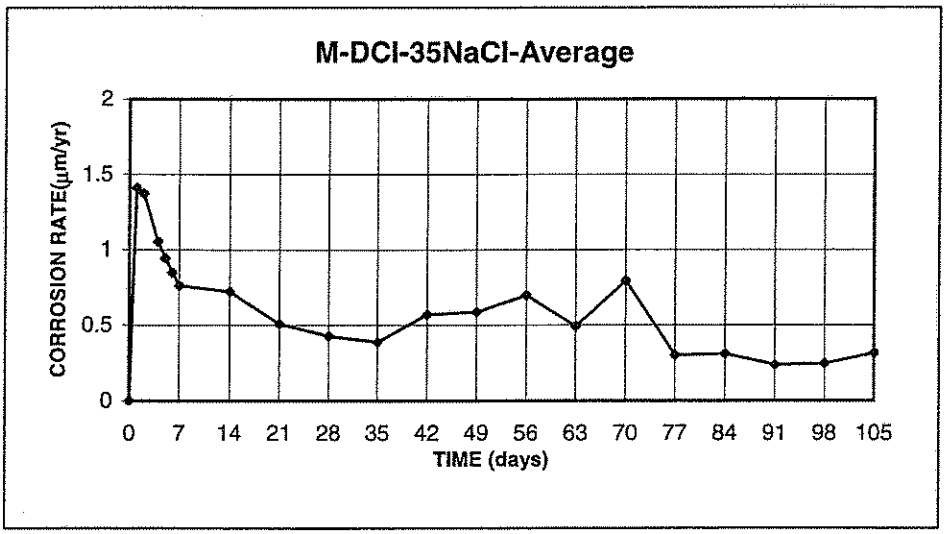

Figure A7.f Corrosion Rate;
w/c=0.35; DCI; 1.6 m ion NaCl in simulated pore solution

Note: 1. Rust on M-DCI-35-NaCl-1,2,3,4,5 were cleaned on the 83 day.

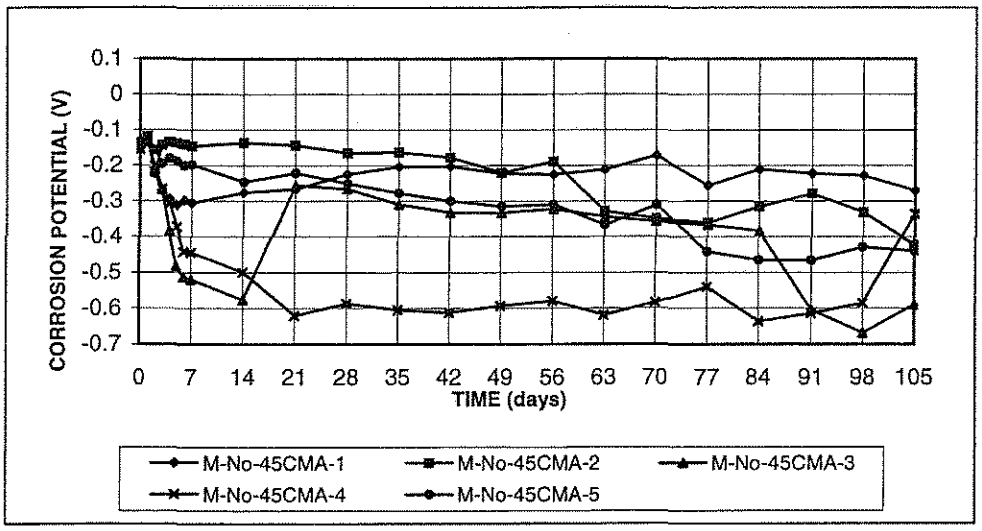

Figure A8.a Anode Potential with respect to standard calomel electrode; w/c=0.45; no inhibitor; 1.6 m ion CMA in simulated pore solution

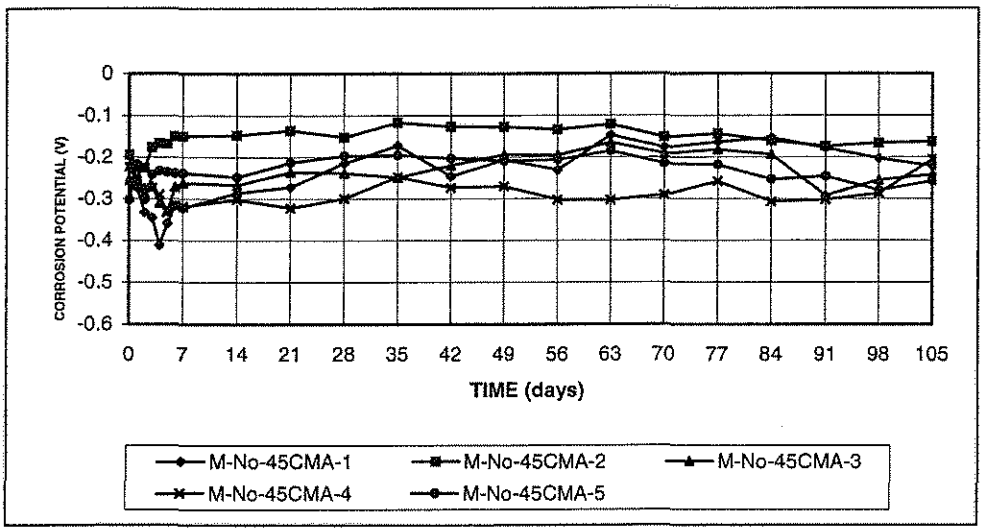

Figure A8.b Cathode Potential with respect to standard calomel electrode; w/c=0.45; no inhibitor; 1.6 m ion CMA in simulated pore solution

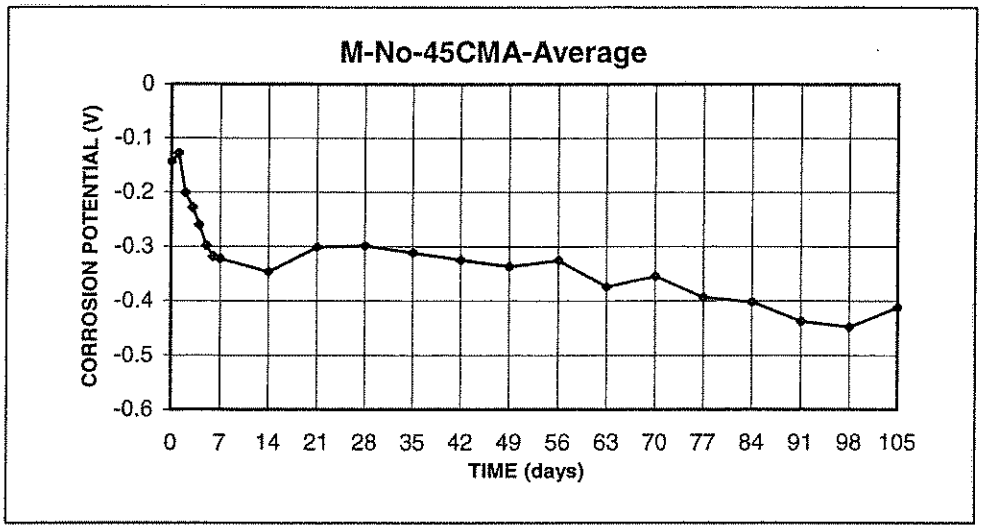

Figure A8.c Anode Potential with respect to standard calomel electrode; w/c=0.45; no inhibitor; 1.6 m ion CMA in simulated pore solution

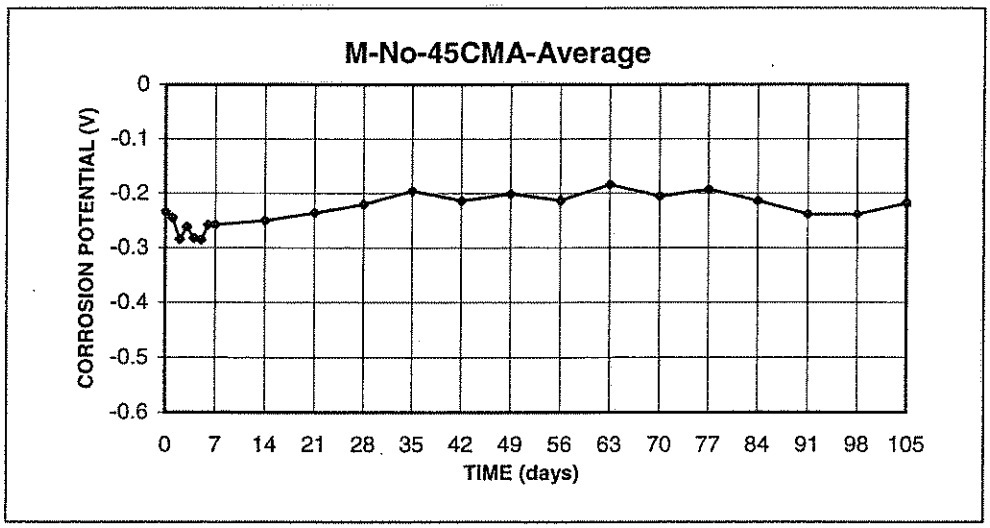

Figure A8.d Cathode Potential with respect to standard calomel electrode; w/c=0.45; no inhibitor; 1.6 m ion CMA in simulated pore solution

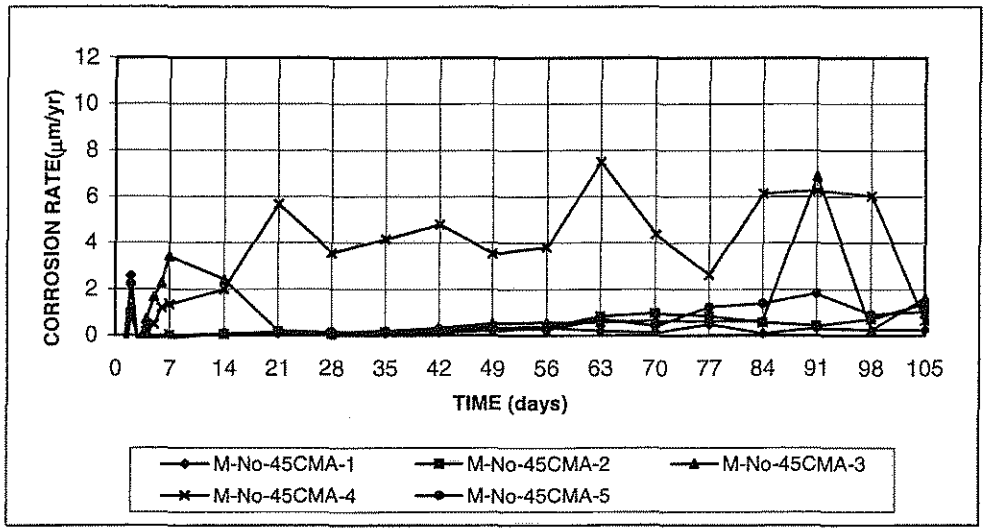

Figure A8.e Corrosion Rate;
w/c=0.45; no inhibitor; 1.6 m ion CMA in simulated pore solution

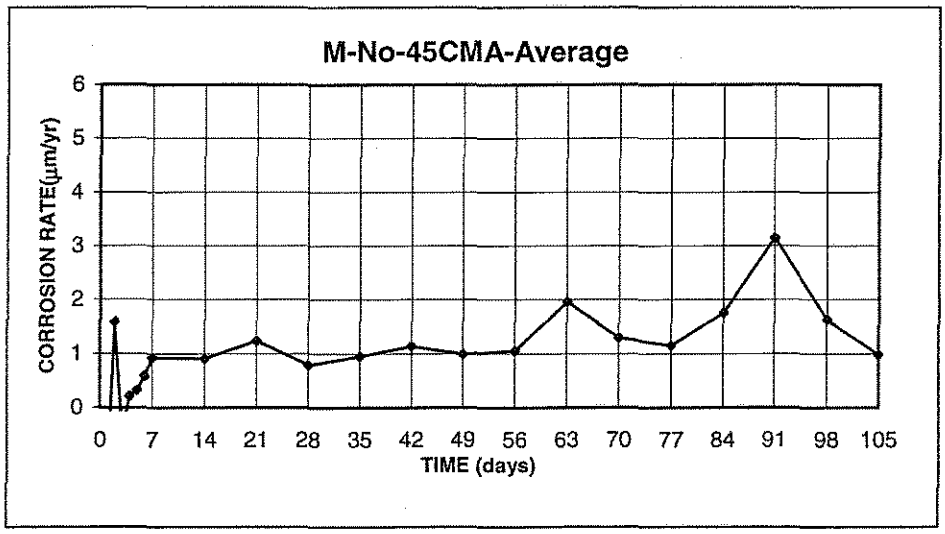

Figure A8.f Corrosion Rate;
w/c=0.45; no inhibitor; 1.6 m ion CMA in simulated pore solution

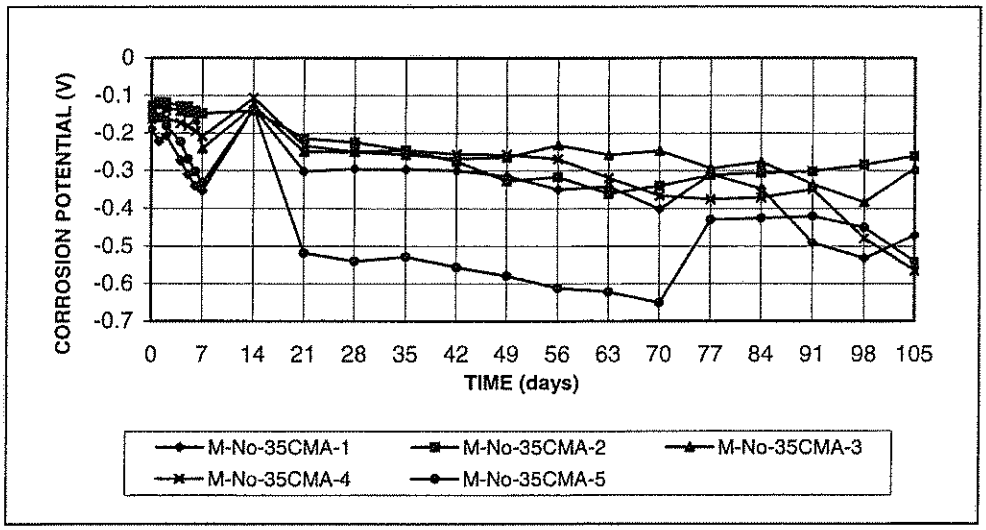

Figure A9.a Anode Potential with respect to standard calomel electrode; w/c=0.35; no inhibitor; 1.6 m ion CMA in simulated pore solution

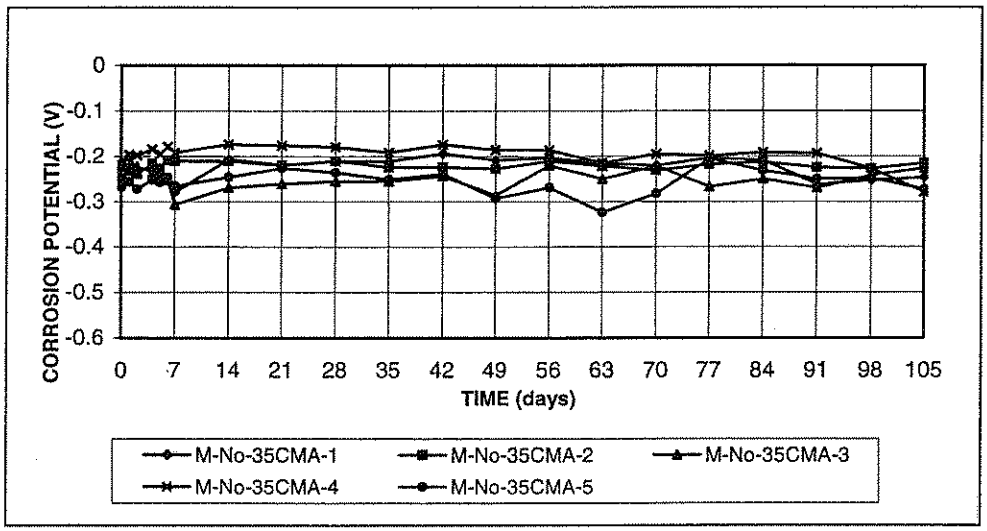

Figure A9.b Cathode Potential with respect to standard calomel electrode; w/c=0.35; no inhibitor; 1.6 m ion CMA in simulated pore solution

Note: 1. Rust on M-No-35-CMA-5 was cleaned on the 70 day after taking readings.
2. Rust on M-No-35-CMA-1,2,3,4,5 were cleaned on the 97 day.

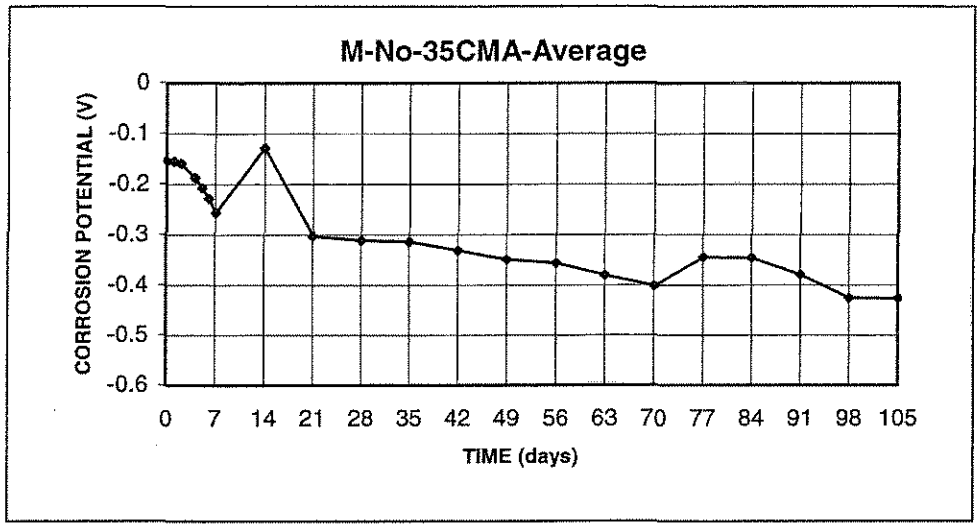

Figure A9.c Anode Potential with respect to standard calomel electrode; w/c=0.35; no inhibitor; 1.6 m ion CMA in simulated pore solution

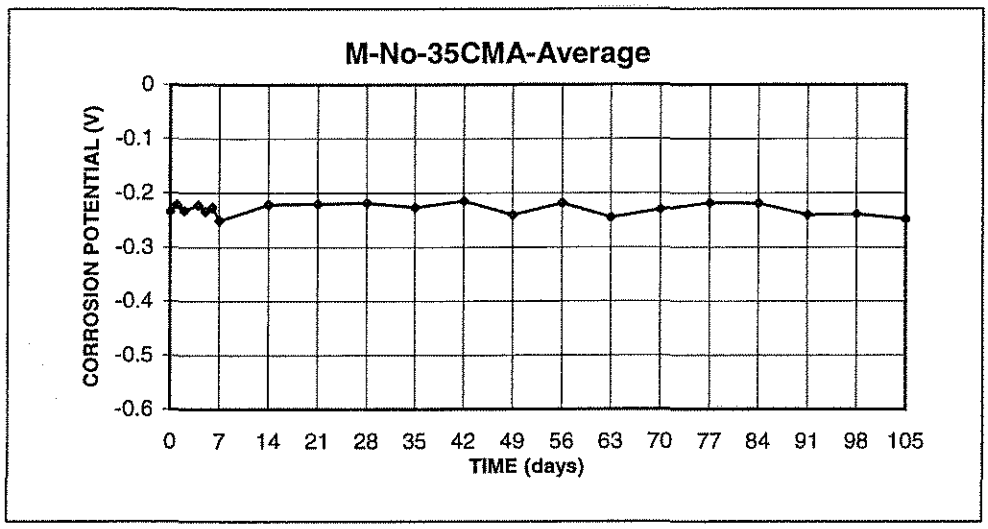

Figure A9.d Cathode Potential with respect to standard calomel electrode; w/c=0.35; no inhibitor; 1.6 m ion CMA in simulated pore solution

Note: 1. Rust on M-No-35-CMA-5 was cleaned on the 70 day after taking readings.
2. Rust on M-No-35-CMA-1,2,3,4,5 were cleaned on the 97 day.

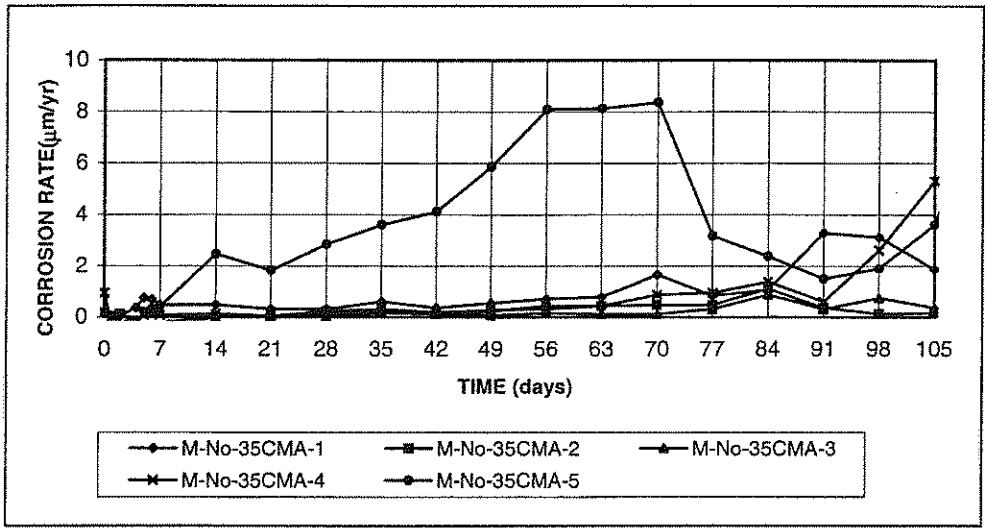

Figure A9.e Corrosion Rate;
w/c=0.35; no inhibitor; 1.6 m ion CMA in simulated pore solution

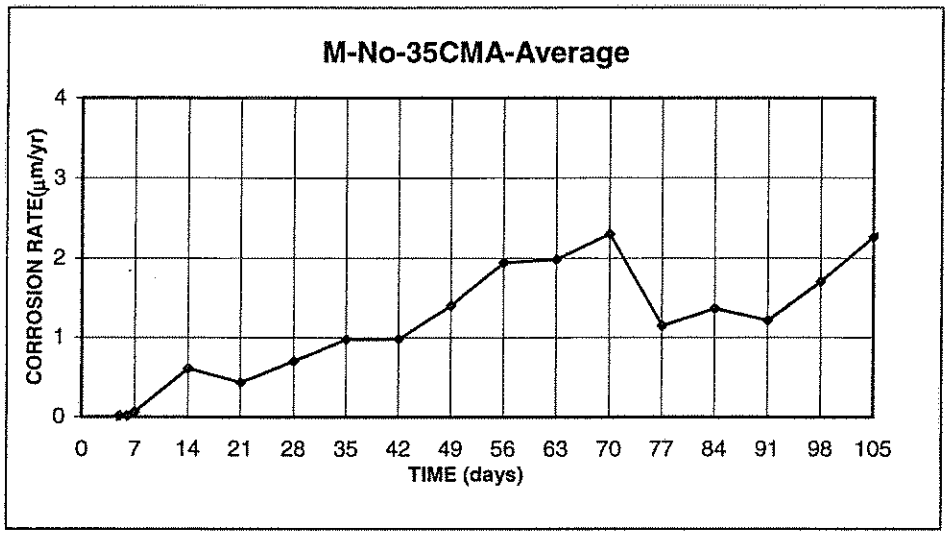

Figure A9.f Corrosion Rate;
w/c=0.35; no inhibitor; 1.6 m ion CMA in simulated pore solution

Note: 1. Rust on M-No-35-CMA-5 was cleaned on the 70 day after taking readings.
2. Rust on M-No-35-CMA-1,2,3,4,5 were cleaned on the 97 day.

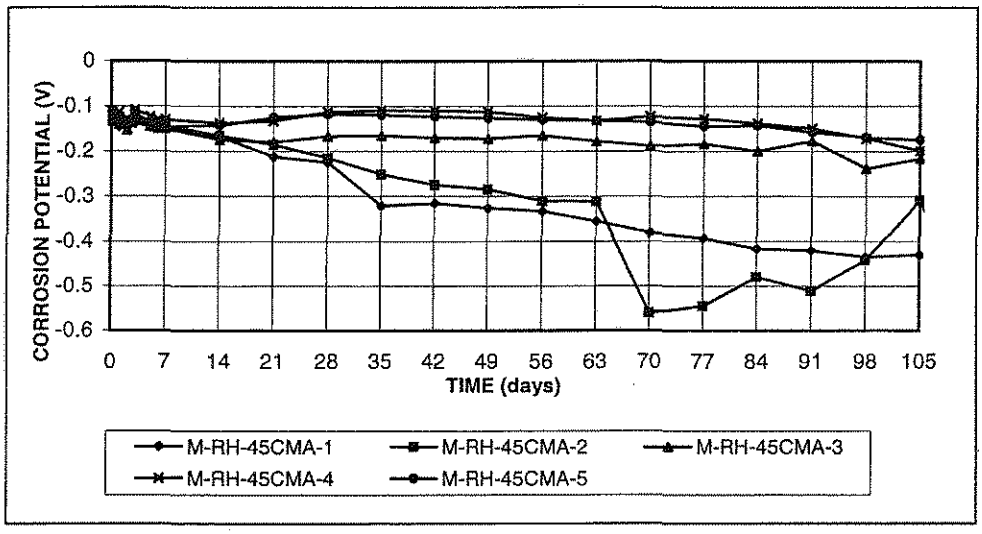

Figure A10.a Anode Potential with respect to standard calomel electrode; w/c=0.45; Rheocrete; 1.6 m ion CMA in simulated pore solution

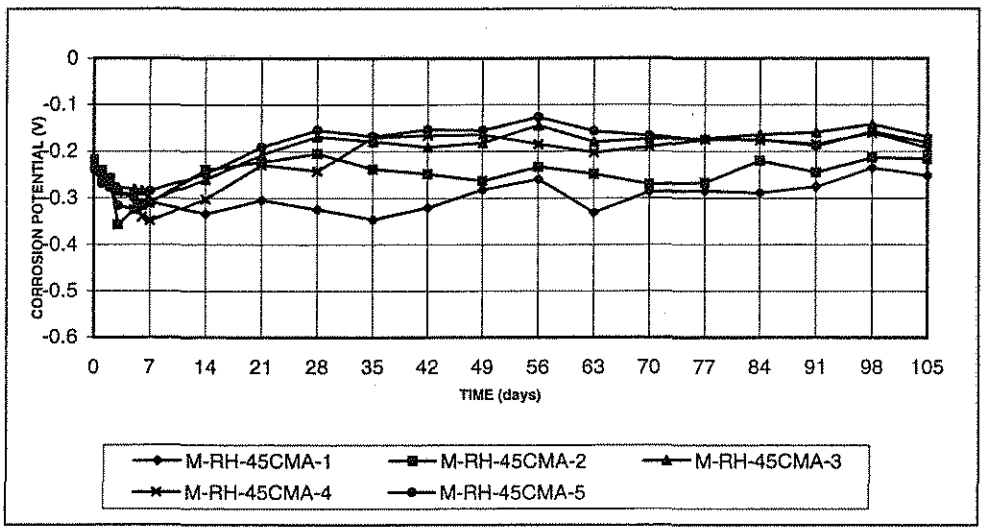

Figure A10.b Cathode Potential with respect to standard calomel electrode; w/c=0.45; Rheocrete; 1.6 m ion CMA in simulated pore solution

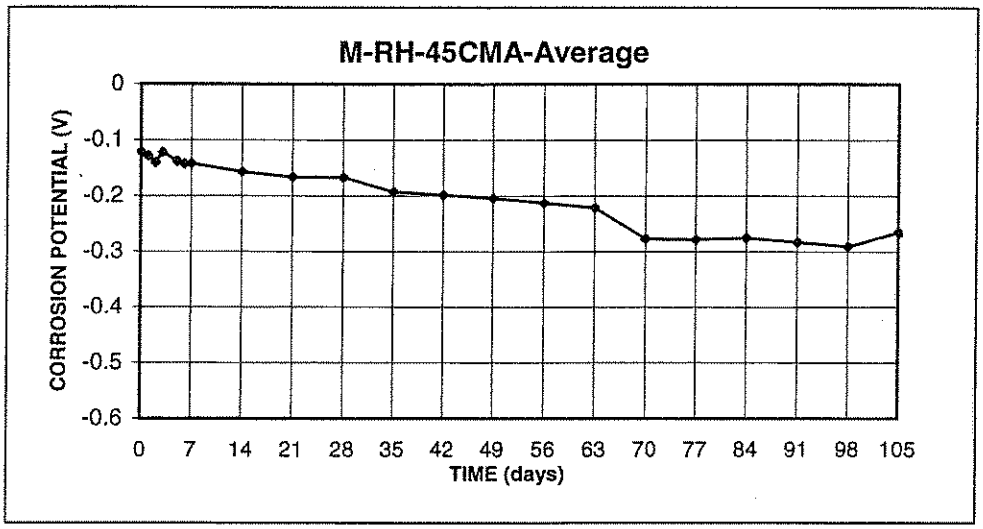

Figure A10.c Anode Potential with respect to standard calomel electrode; w/c=0.45; Rheocrete; 1.6 m ion CMA in simulated pore solution

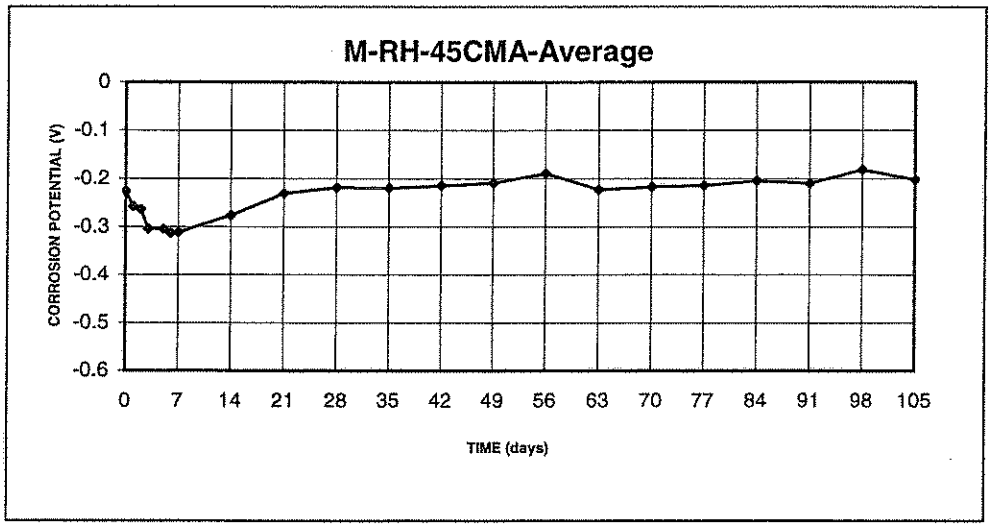

Figure A10.d Cathode Potential with respect to standard calomel electrode; w/c=0.45; Rheocrete; 1.6 m ion CMA in simulated pore solution

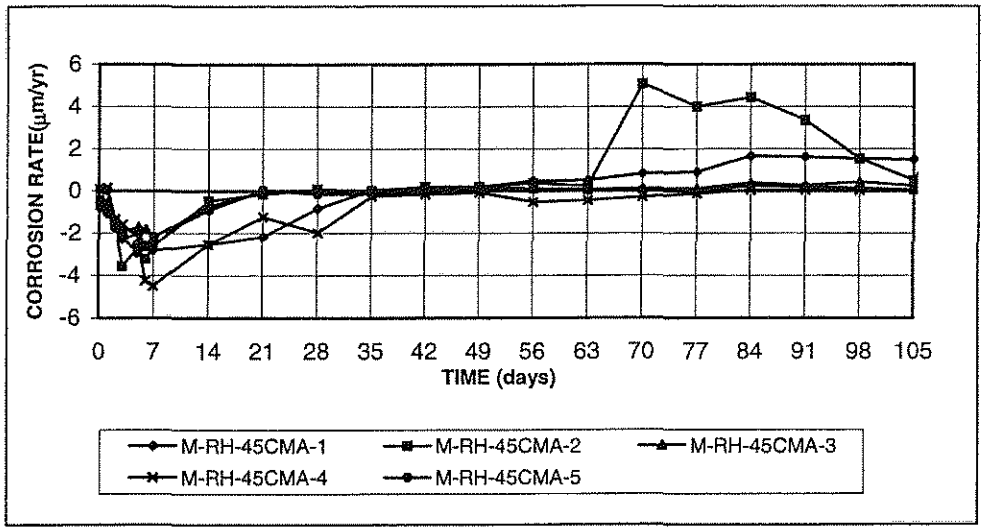

Figure A10.e Corrosion Rate;
w/c=0.45; Rheocrete; 1.6 m ion CMA in simulated pore solution

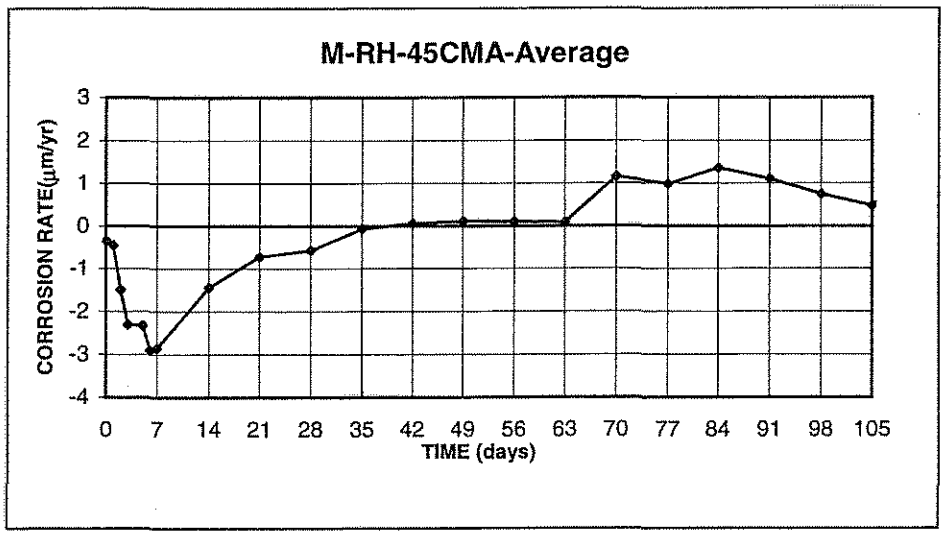

Figure A10.f Corrosion Rate;
w/c=0.45; Rheocrete; 1.6 m ion CMA in simulated pore solution

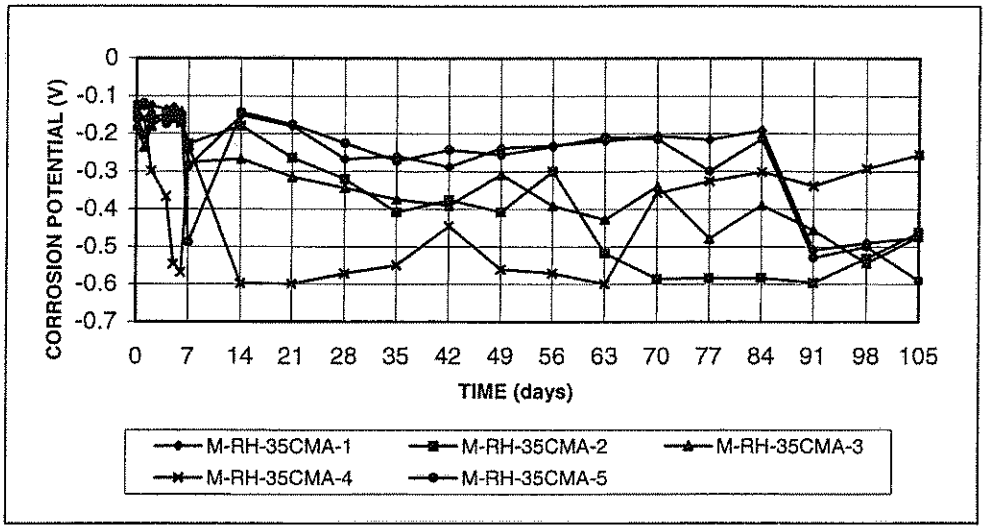

Figure A11.a Anode Potential with respect to standard calomel electrode; w/c=0.35; Rheocrete; 1.6 m ion CMA in simulated pore solution

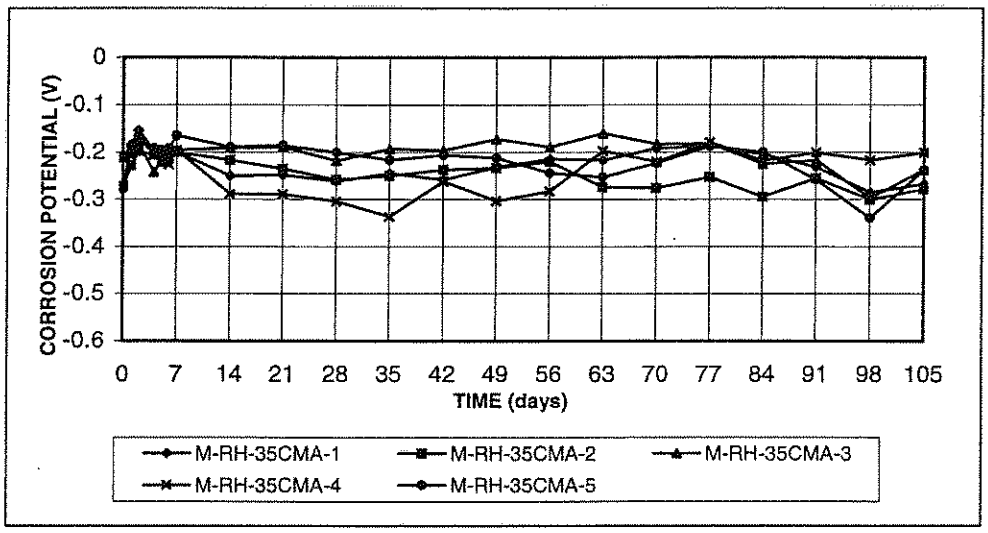

Figure A11.b Cathode Potential with respect to standard calomel electrode; w/c=0.35; Rheocrete; 1.6 m ion CMA in simulated pore solution

Note: 1. Rust on M-Rh-35-CMA-4 was cleaned on the 63 day after taking readings.
2. Rust on M-Rh-35-CMA-1,2,3,4,5 were cleaned on the 90 day.

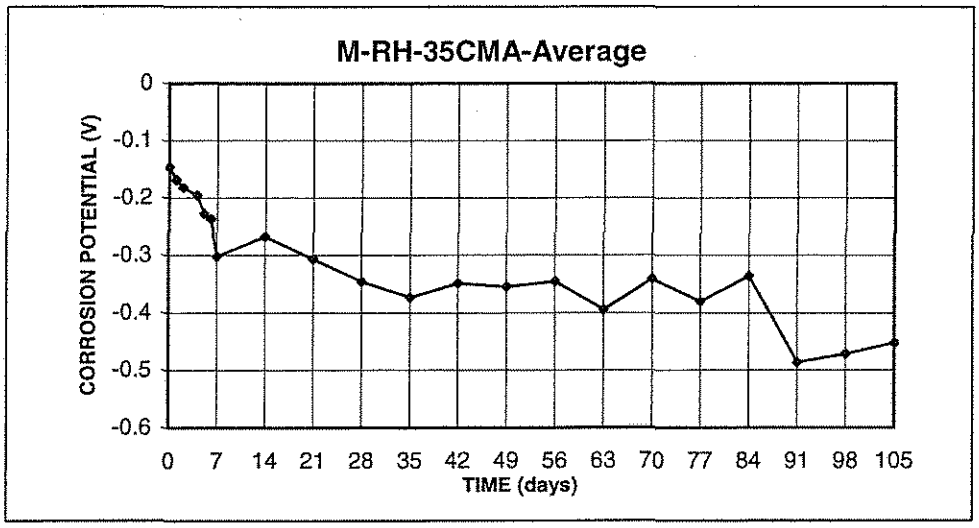

Figure A11.c Anode Potential with respect to standard calomel electrode; w/c=0.35; Rheocrete; 1.6 m ion CMA in simulated pore solution

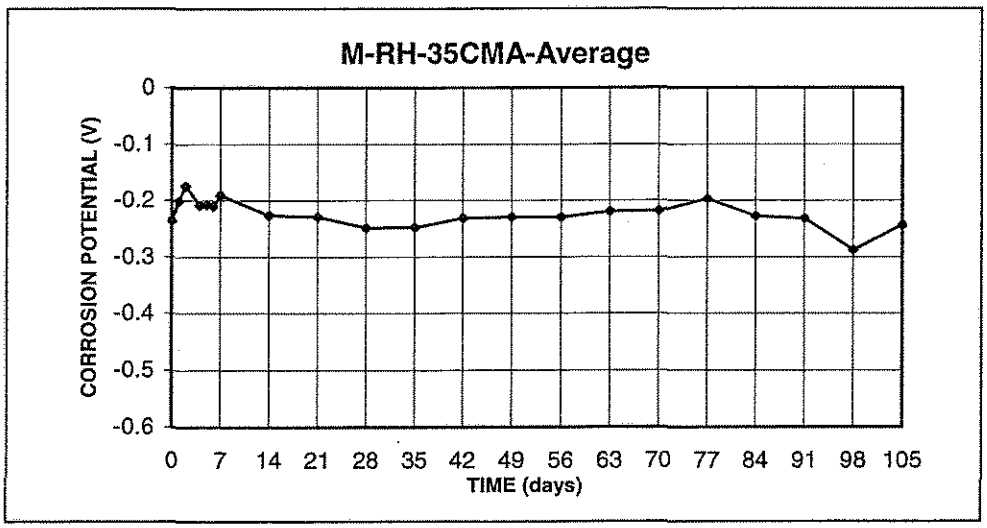

Figure A11.d Cathode Potential with respect to standard calomel electrode; w/c=0.35; Rheocrete; 1.6 m ion CMA in simulated pore solution

Note: 1. Rust on M-Rh-35-CMA-4 was cleaned on the 63 day after taking readings.
2. Rust on M-Rh-35-CMA-1,2,3,4,5 were cleaned on the 90 day.

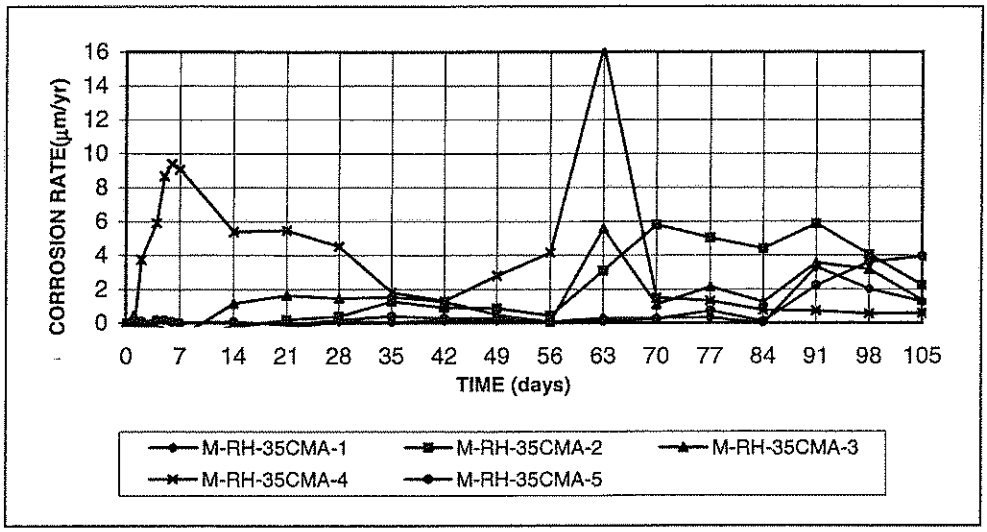

Figure A11.e Corrosion Rate;
w/c=0.35; Rheocrete; 1.6 m ion CMA in simulated pore solution

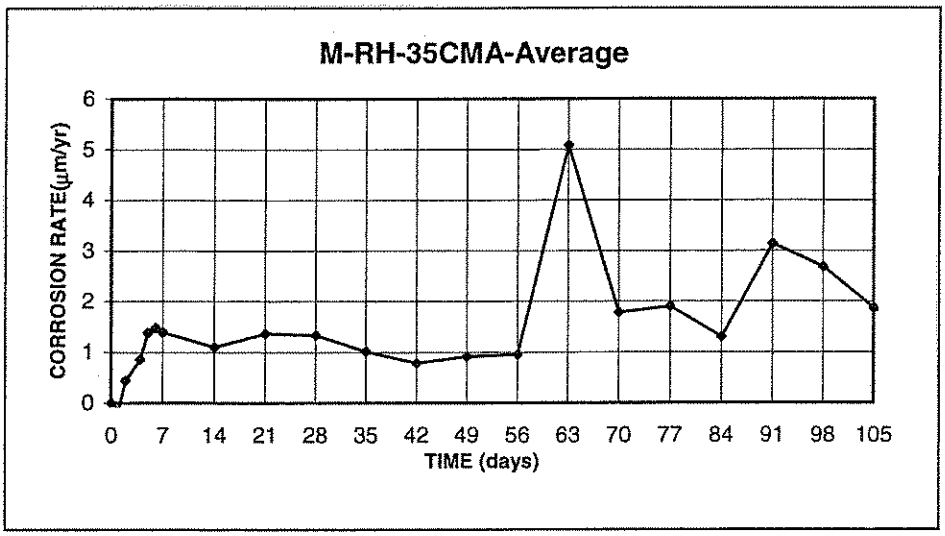

Figure A11.f Corrosion Rate;
w/c=0.35; Rheocrete; 1.6 m ion CMA in simulated pore solution

Note: 1. Rust on M-Rh-35-CMA-4 was cleaned on the 63 day after taking readings.
2. Rust on M-Rh-35-CMA-1,2,3,4,5 were cleaned on the 90 day.

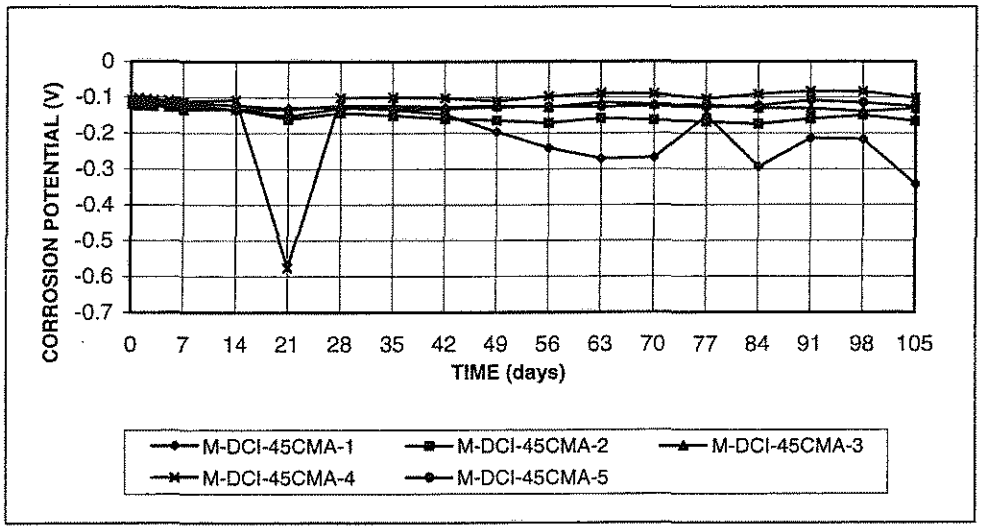

Figure A12.a Anode Potential with respect to standard calomel electrode; w/c=0.45; DCI; 1.6 m ion CMA in simulated pore solution

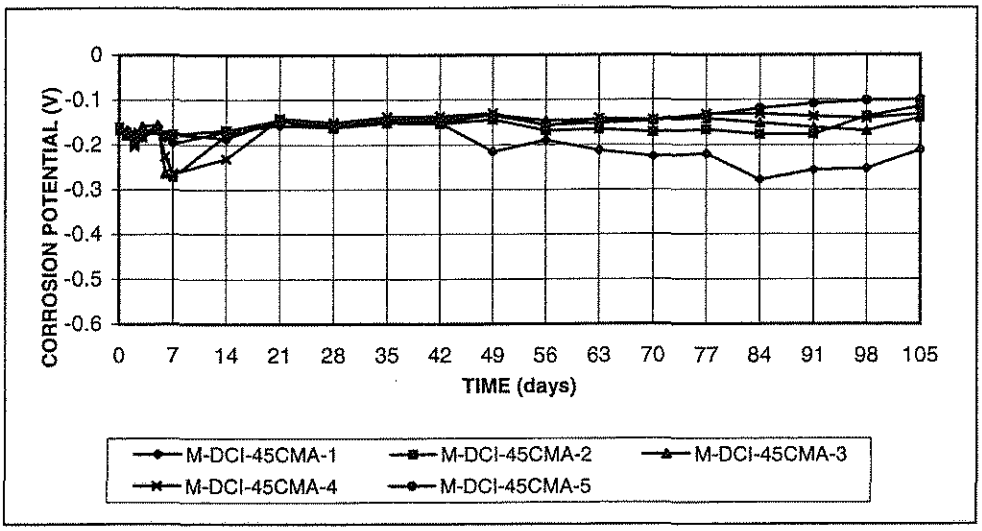

Figure A12.b Cathode Potential with respect to standard calomel electrode; w/c=0.45; DCI; 1.6 m ion CMA in simulated pore solution

Note: 1. Rust on M-DCI-45-CMA-1,2,3,4,5 were cleaned on the 97 day.

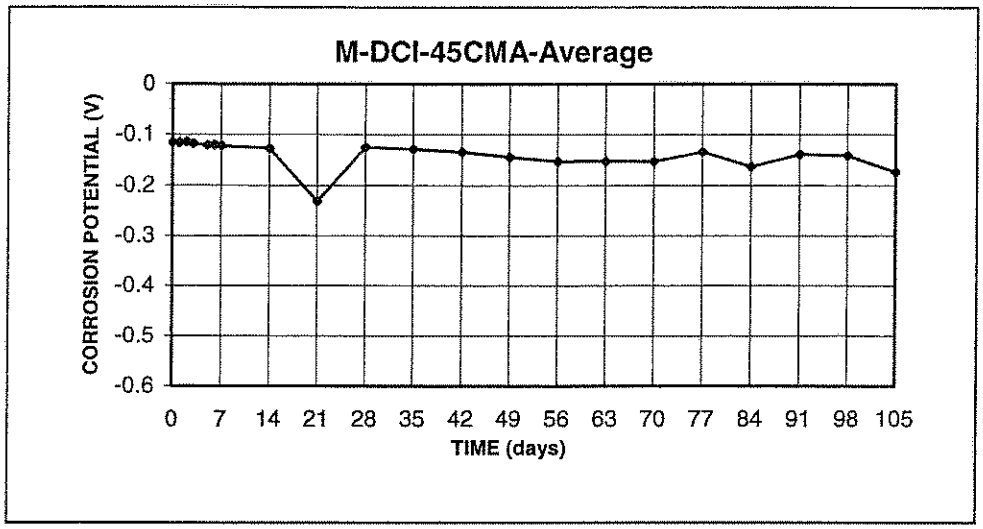

Figure A12.c Anode Potential with respect to standard calomel electrode; w/c=0.45; DCI; 1.6 m ion CMA in simulated pore solution

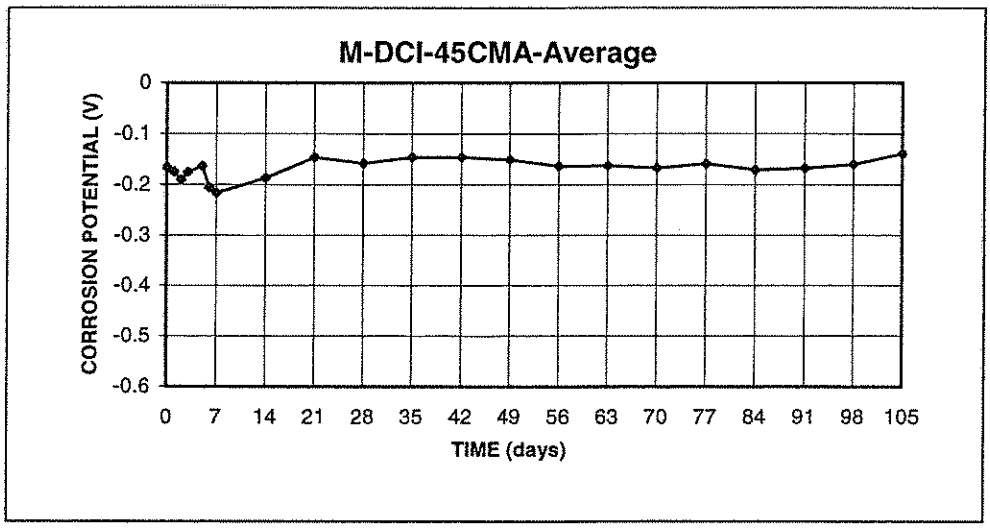

Figure A12.d Cathode Potential with respect to standard calomel electrode; w/c=0.45; DCI; 1.6 m ion CMA in simulated pore solution

Note: 1. Rust on M-DCI-45-CMA-1,2,3,4,5 were cleaned on the 97 day.

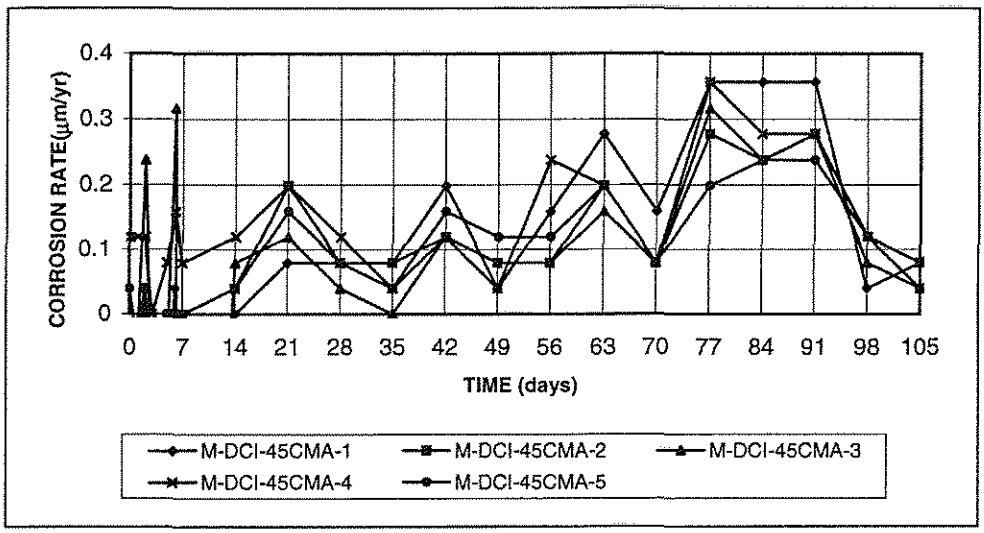

Figure A12.e Corrosion Rate;
w/c=0.45; DCI; 1.6 m ion CMA in simulated pore solution

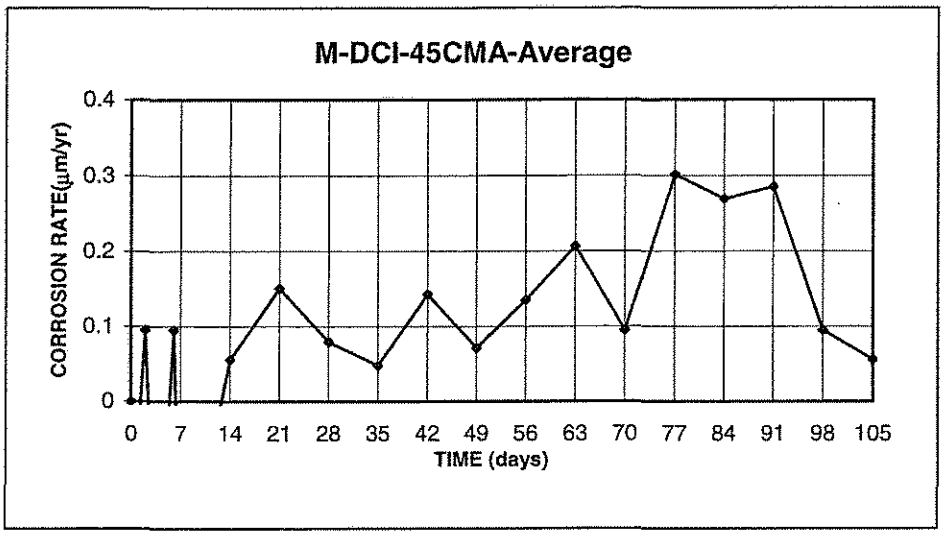

Figure A12.f Corrosion Rate;
w/c=0.45; DCI; 1.6 m ion CMA in simulated pore solution

Note: 1. Rust on M-DCI-45-CMA-1,2,3,4,5 were cleaned on the 97 day.

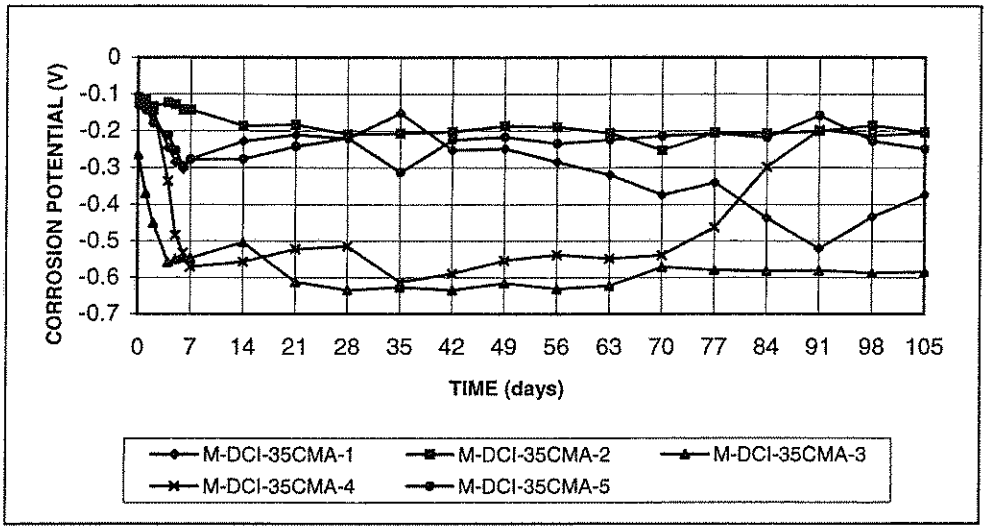

Figure A13.a Anode Potential with respect to standard calomel electrode; w/c=0.35; DCI; 1.6 m ion CMA in simulated pore solution

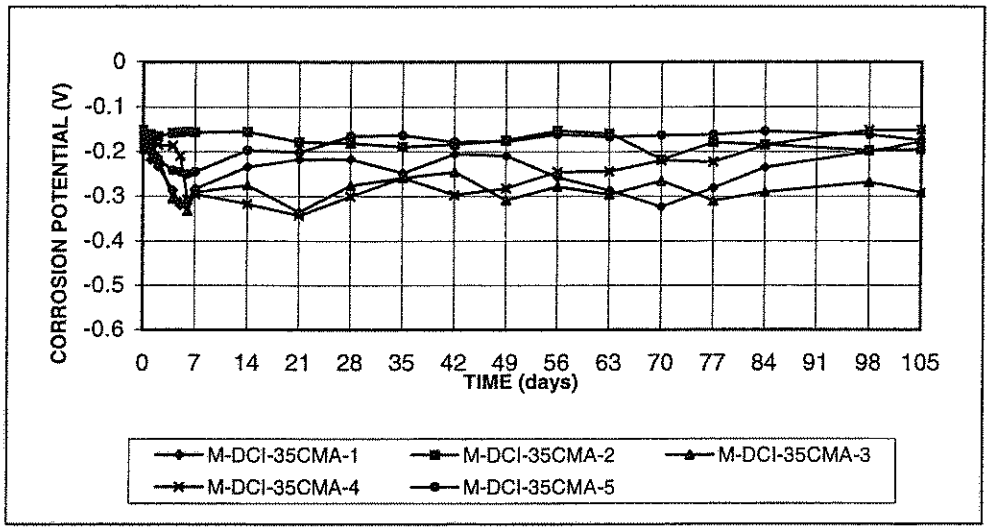

Figure A13.b Cathode Potential with respect to standard calomel electrode; w/c=0.35; DCI; 1.6 m ion CMA in simulated pore solution

Note: 1. Rust on M-DCI-35-CMA-1,2,3,4,5 were cleaned on the 83 day.

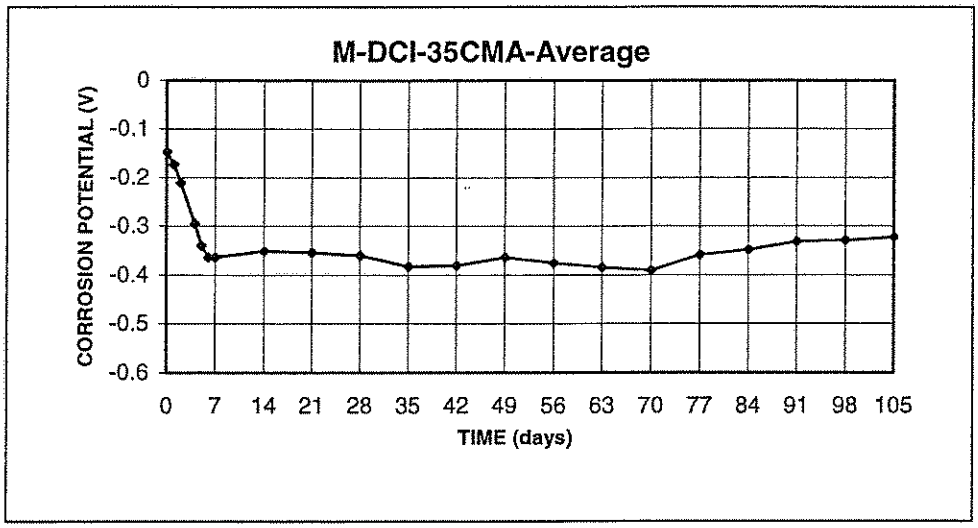

Figure A13.c Anode Potential with respect to standard calomel electrode; w/c=0.35; DCI; 1.6 m ion CMA in simulated pore solution

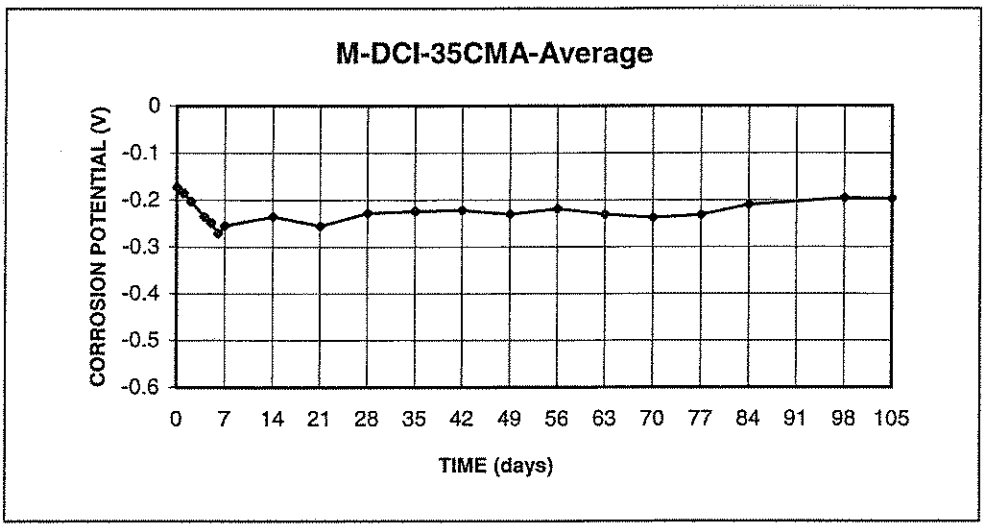

Figure A13.d Cathode Potential with respect to standard calomel electrode; w/c=0.35; DCI; 1.6 m ion CMA in simulated pore solution

Note: 1. Rust on M-DCI-35-CMA-1,2,3,4,5 were cleaned on the 83 day.

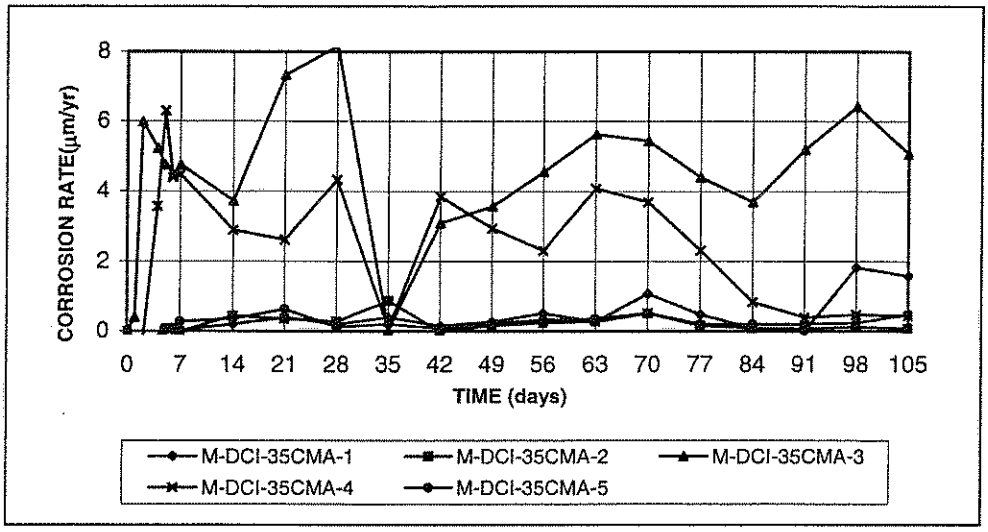

Figure A13.e Corrosion Rate;
w/c=0.35; DCI; 1.6 m ion CMA in simulated pore solution

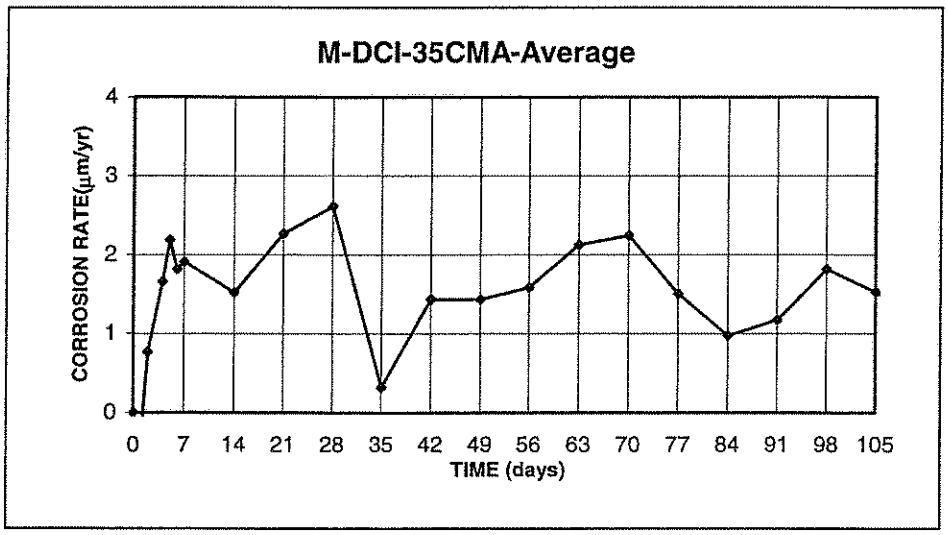

Figure A13.f Corrosion Rate;
w/c=0.35; DCI; 1.6 m ion CMA in simulated pore solution

Note: 1. Rust on M-DCI-35-CMA-1,2,3,4,5 were cleaned on the 83 day.

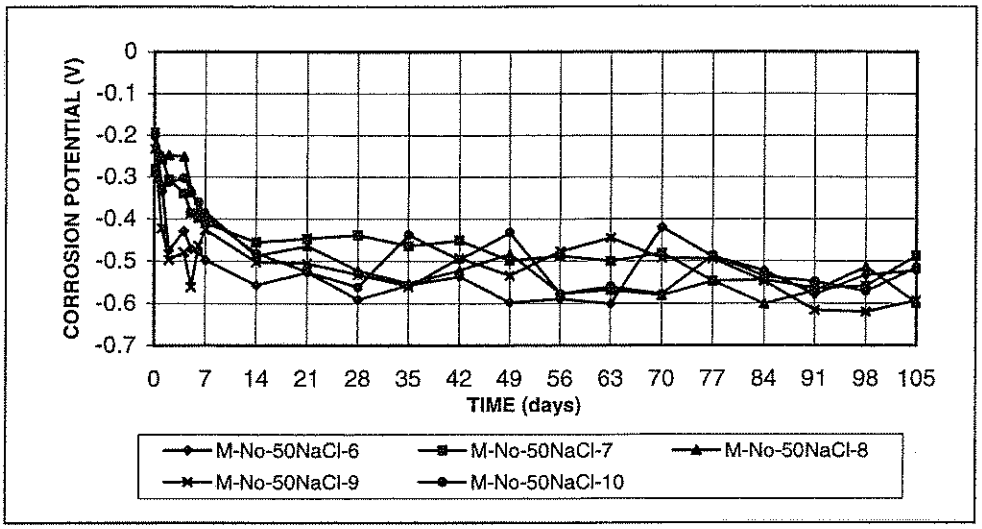

Figure A14.a Anode Potential with respect to standard calomel electrode; w/c=0.50; no inhibitor; 1.6 m ion NaCl in simulated pore solution

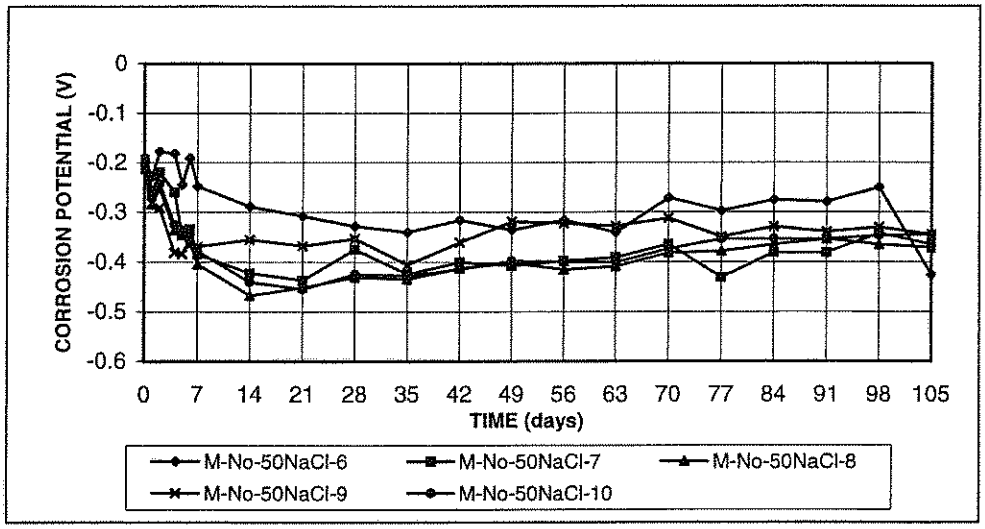

Figure A14.b Cathode Potential with respect to standard calomel electrode; w/c=0.50; no inhibitor; 1.6 m ion NaCl in simulated pore solution

Note: 1. Rust on M-No-50-NaCl-6,7,8,9,10 were cleaned on the 13 day.

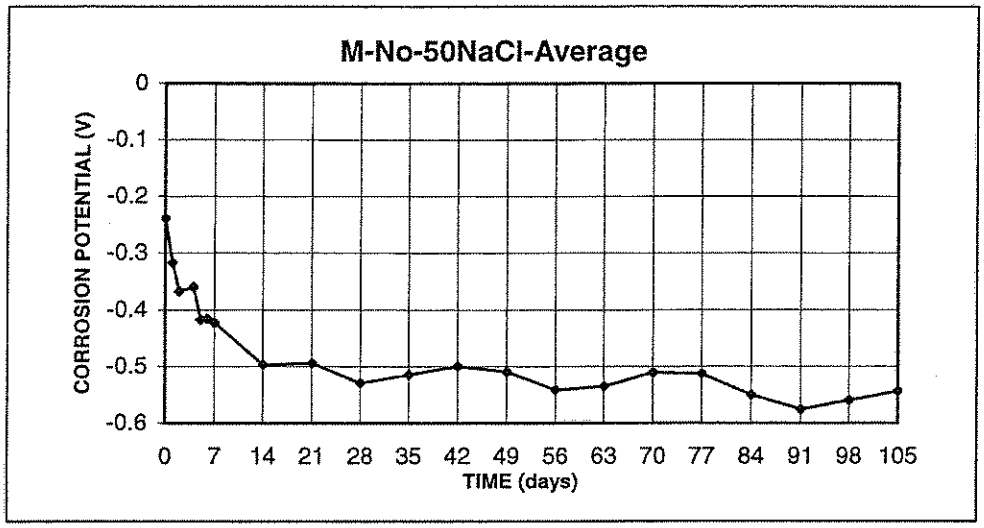

Figure A14.c Anode Potential with respect to standard calomel electrode; w/c=0.50; no inhibitor; 1.6 m ion NaCl in simulated pore solution

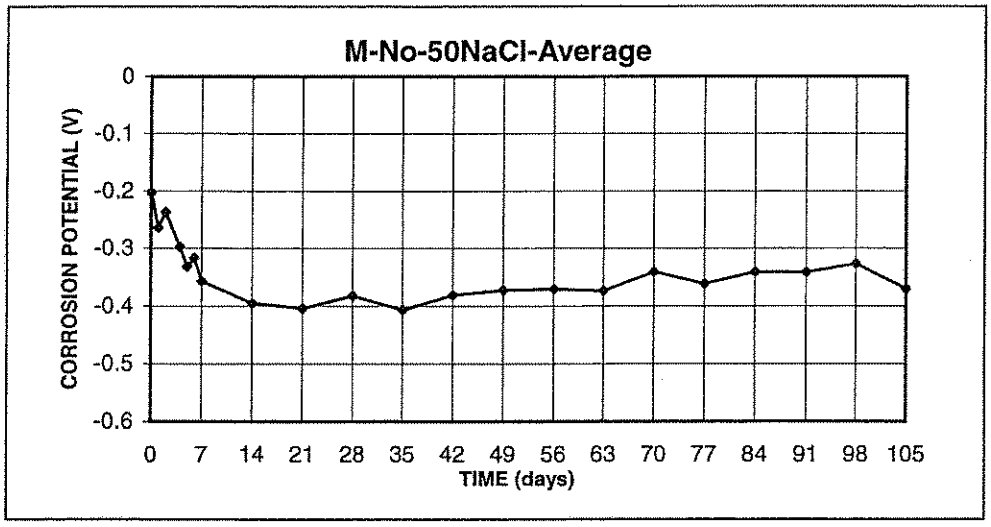

Figure A14.d Cathode Potential with respect to standard calomel electrode; w/c=0.50; no inhibitor; 1.6 m ion NaCl in simulated pore solution

Note: 1. Rust on M-No-50-NaCl-6,7,8,9,10 were cleaned on the 13 day.

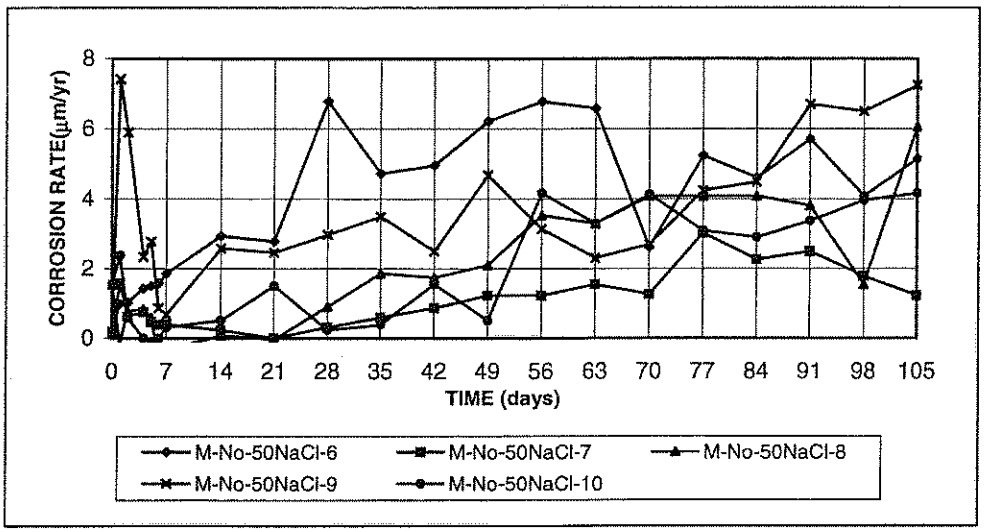

Figure A14.e Corrosion Rate;
w/c=0.50; no inhibitor; 1.6 m ion NaCl in simulated pore solution

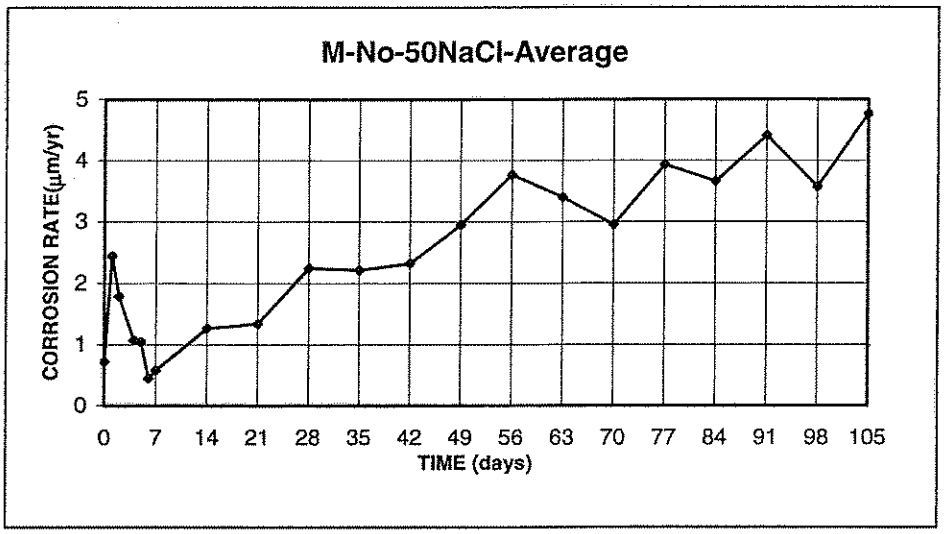

Figure A14.f Corrosion Rate;
w/c=0.50; no inhibitor; 1.6 m ion NaCl in simulated pore solution

Note: 1. Rust on M-No-50-NaCl-6,7,8,9,10 were cleaned on the 13 day.

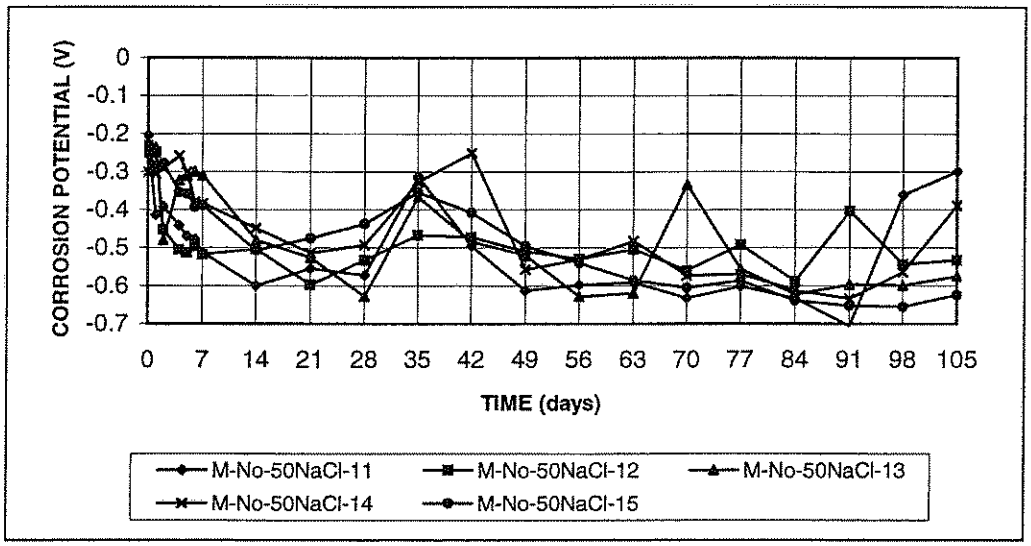

Figure A15.a Anode Potential with respect to standard calomel electrode; w/c=0.50; no inhibitor; 1.6 m ion NaCl in simulated pore solution

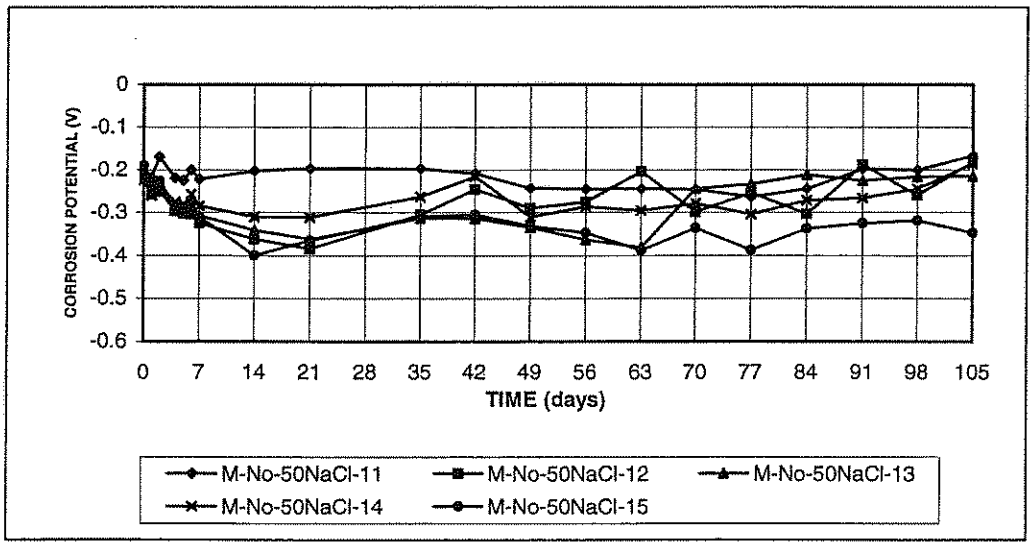

Figure A15.b Cathode Potential with respect to standard calomel electrode; w/c=0.50; no inhibitor; 1.6 m ion NaCl in simulated pore solution

Note: 1. Rust on M-No-50-NaCl-11,12,13,14,15 were cleaned on the 13 day.

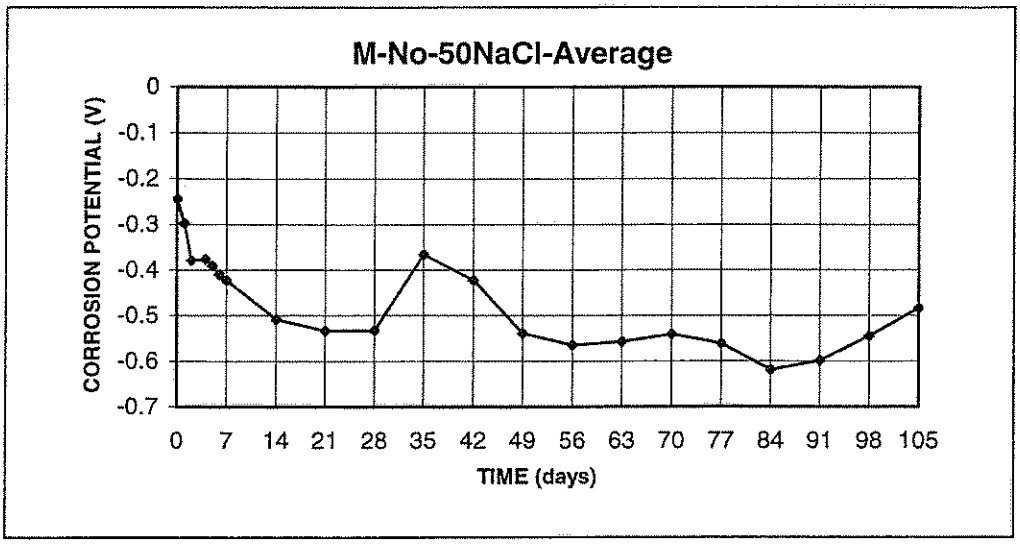

Figure A15.c Anode Potential with respect to standard calomel electrode; w/c=0.50; no inhibitor; 1.6 m ion NaCl in simulated pore solution

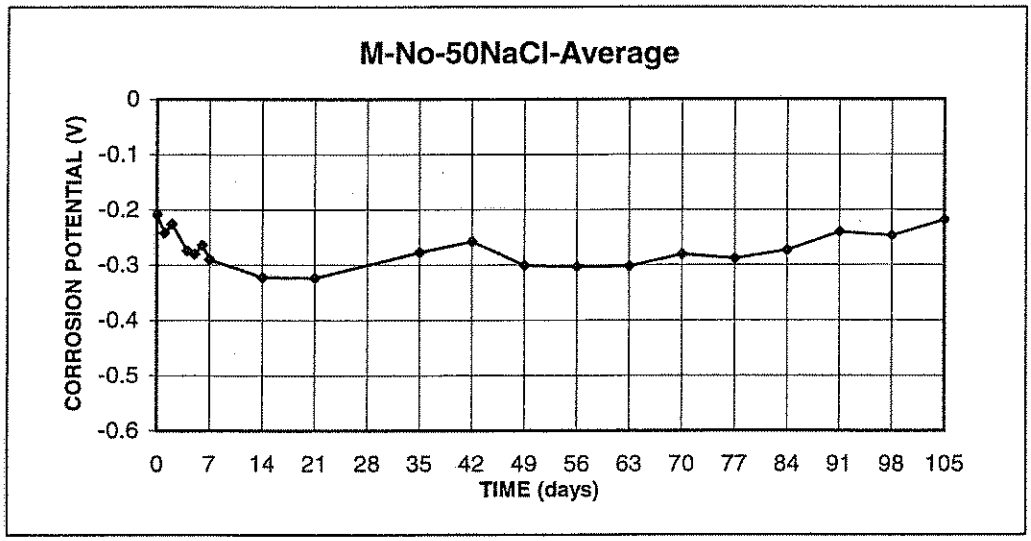

Figure A15.d Cathode Potential with respect to standard calomel electrode; w/c=0.50; no inhibitor; 1.6 m ion NaCl in simulated pore solution

Note: 1. Rust on M-No-50-NaCl-11,12,13,14,15 were cleaned on the 13 day.

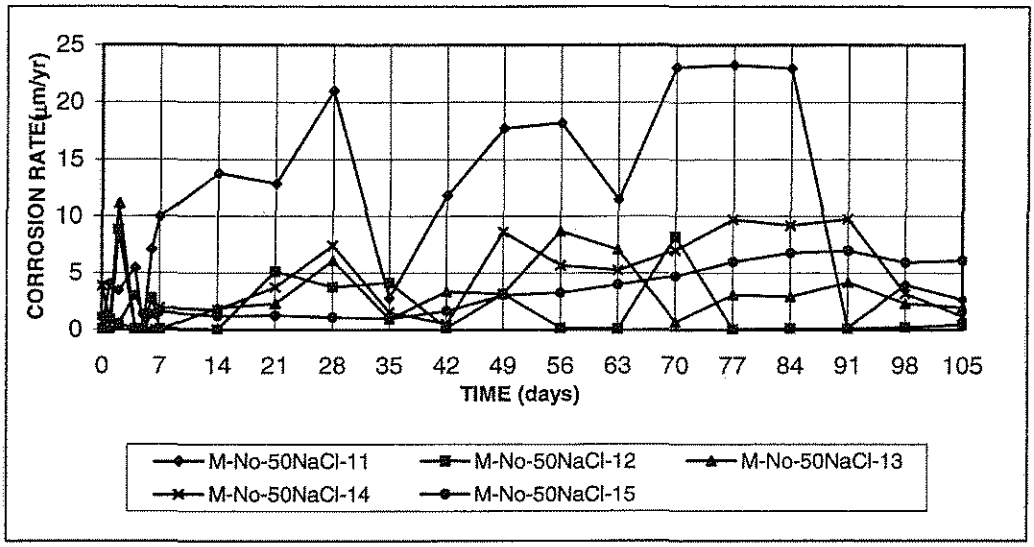

Figure A15.e Corrosion Rate;
w/c=0.50; no inhibitor; 1.6 m ion NaCl in simulated pore solution

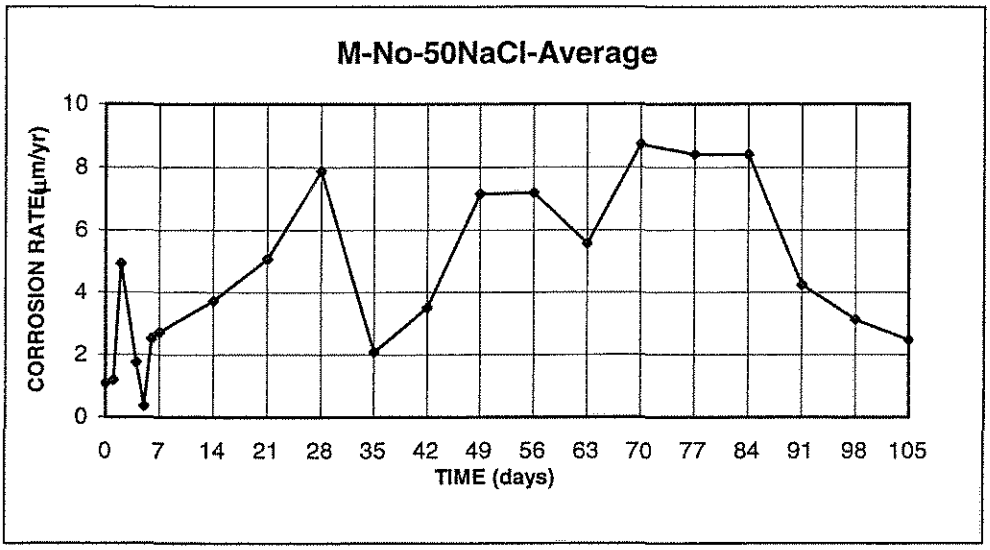

Figure A15.f Corrosion Rate;
w/c=0.50; no inhibitor; 1.6 m ion NaCl in simulated pore solution

Note: 1. Rust on M-No-50-NaCl-11,12,13,14,15 were cleaned on the 13 day.

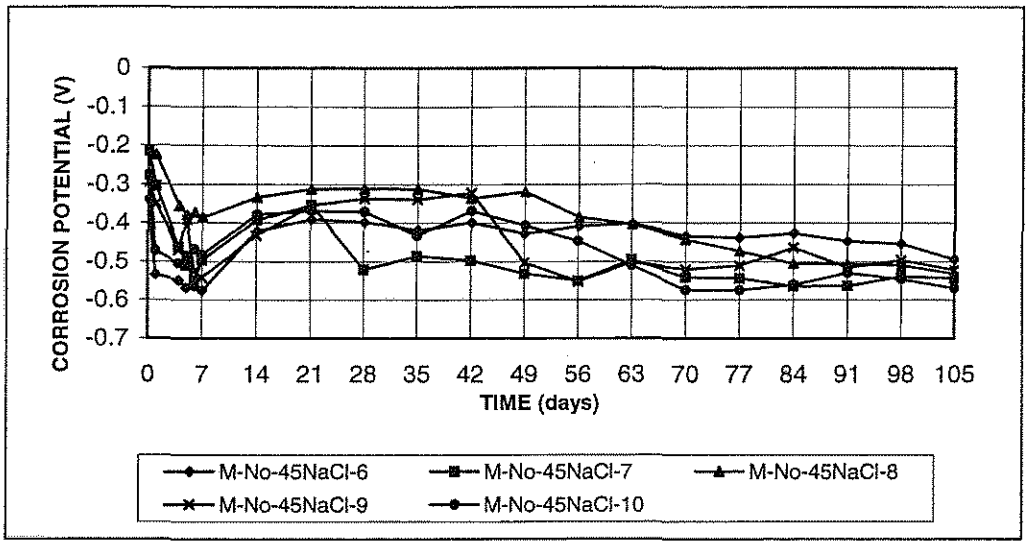

Figure A16.a Anode Potential with respect to standard calomel electrode; w/c=0.45; no inhibitor; 1.6 m ion NaCl in simulated pore solution

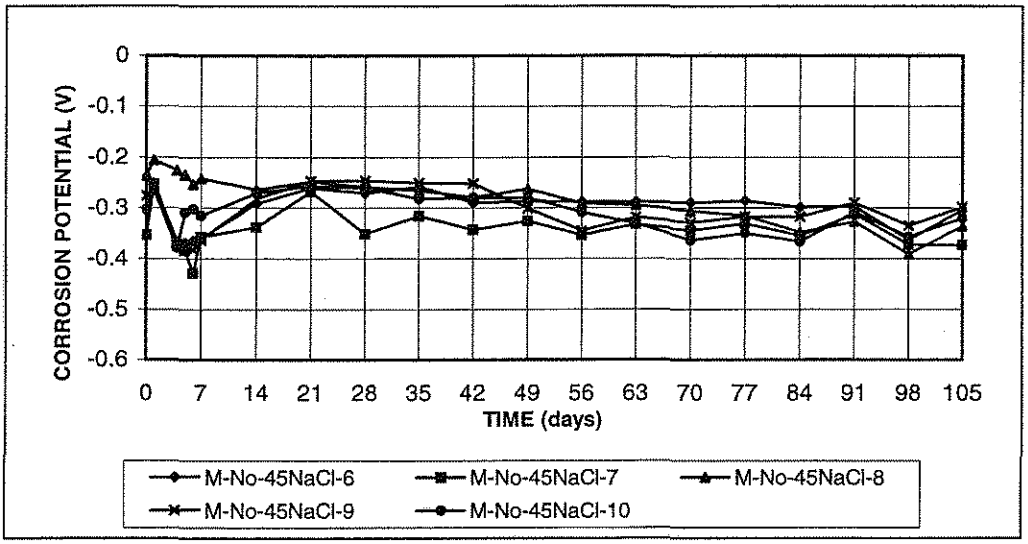

Figure A16.b Cathode Potential with respect to standard calomel electrode; w/c=0.45; no inhibitor; 1.6 m ion NaCl in simulated pore solution

Note: 1. Rust on M-No-45-NaCl-6,7,8,9,10 were cleaned on the 7 day after taking readings.
2. Rust on M-No-45-NaCl-6,7,8,9,10 were cleaned on the 34 day.
3. Rust on M-No-45-NaCl-6,7,8,9,10 were cleaned on the 74 day.

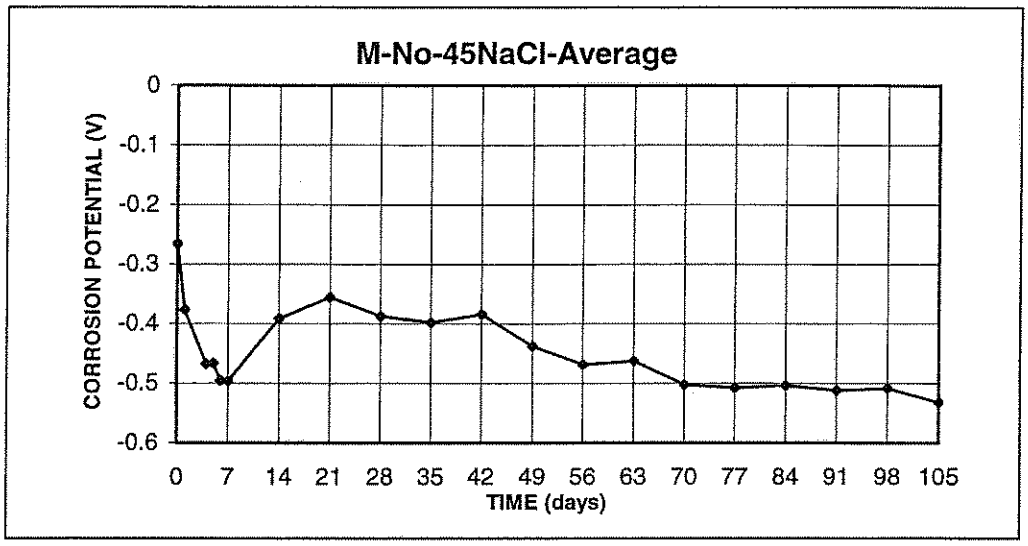

Figure A16.c Anode Potential with respect to standard calomel electrode; w/c=0.45; no inhibitor; 1.6 m ion NaCl in simulated pore solution

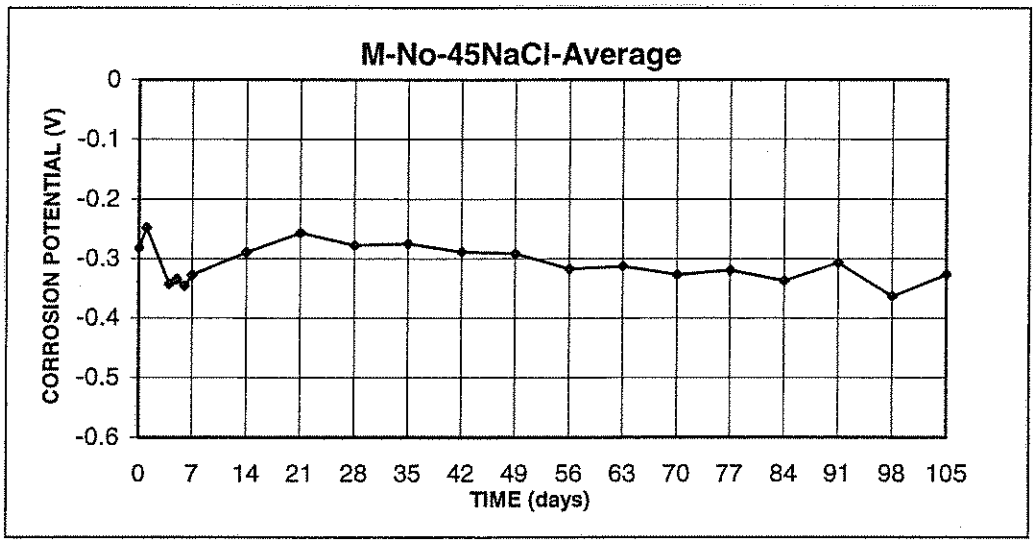

Figure A16.d Cathode Potential with respect to standard calomel electrode; w/c=0.45; no inhibitor; 1.6 m ion NaCl in simulated pore solution

Note: 1. Rust on M-No-45-NaCl-6,7,8,9,10 were cleaned on the 7 day after taking readings.
2. Rust on M-No-45-NaCl-6,7,8,9,10 were cleaned on the 34 day.
3. Rust on M-No-45-NaCl-6,7,8,9,10 were cleaned on the 74 day.

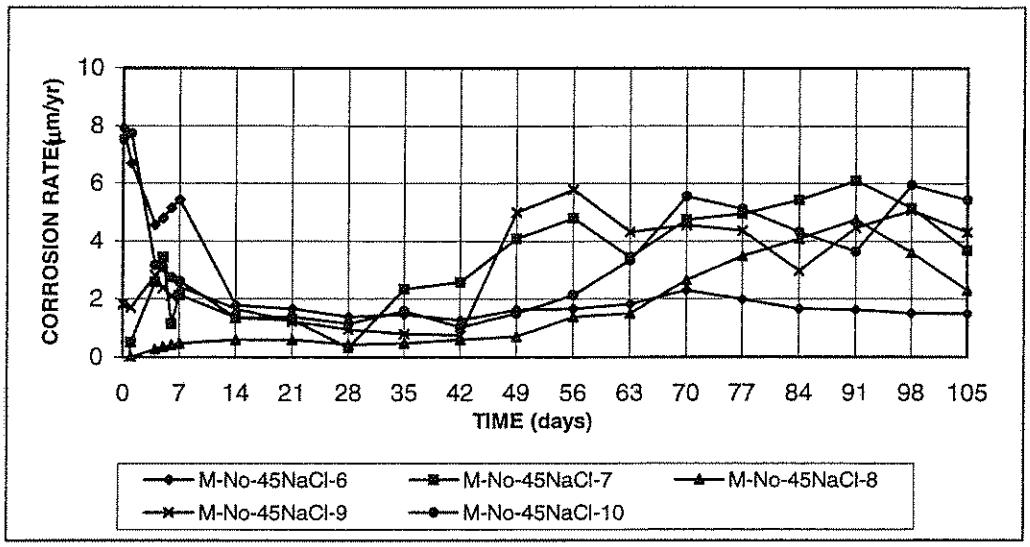

Figure A16.e Corrosion Rate;
w/c=0.45; no inhibitor; 1.6 m ion NaCl in simulated pore solution

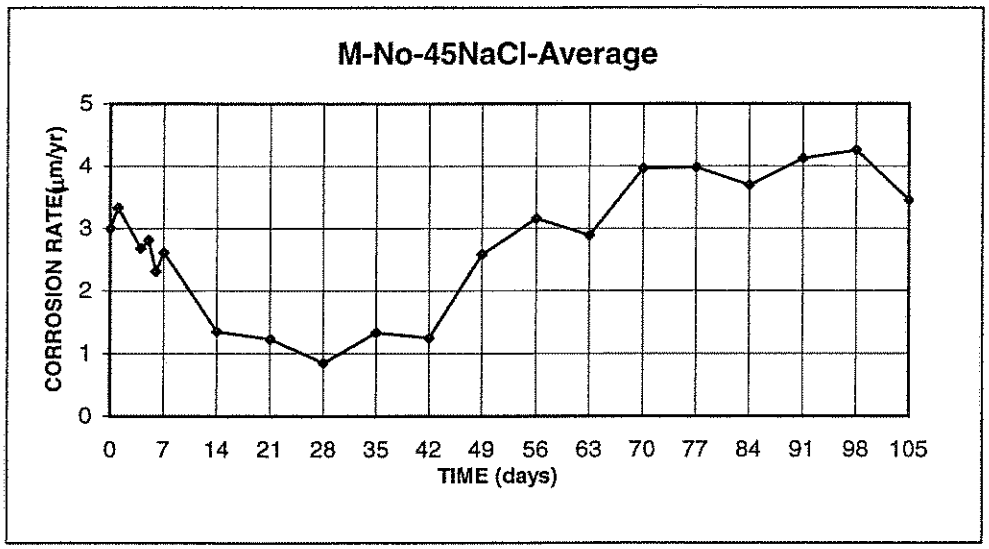

Figure A16.f Corrosion Rate;
w/c=0.45; no inhibitor; 1.6 m ion NaCl in simulated pore solution

Note: 1. Rust on M-No-45-NaCl-6,7,8,9,10 were cleaned on the 7 day after taking readings.
2. Rust on M-No-45-NaCl-6,7,8,9,10 were cleaned on the 34 day.
3. Rust on M-No-45-NaCl-6,7,8,9,10 were cleaned on the 74 day.

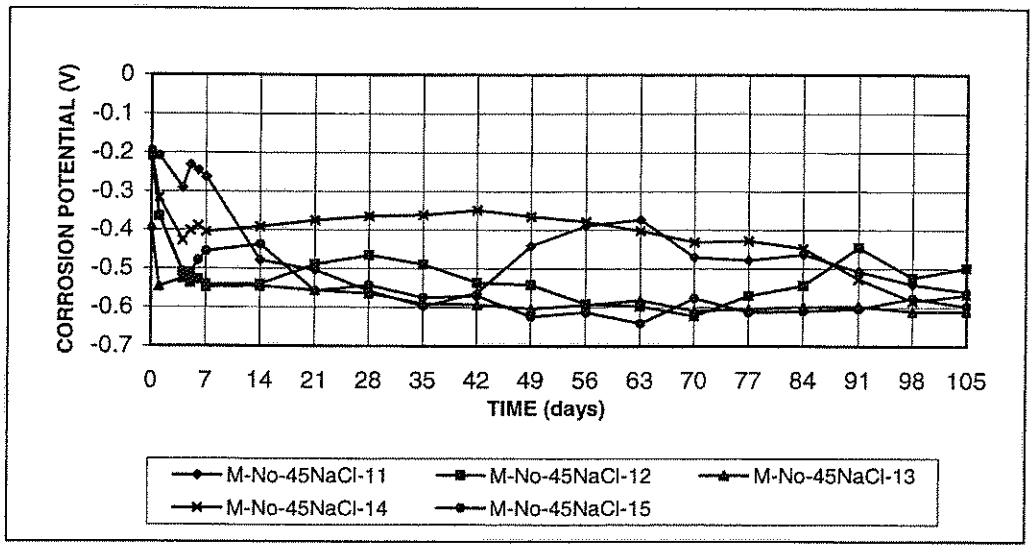

Figure A17.a Anode Potential with respect to standard calomel electrode; w/c=0.45; no inhibitor; 1.6 m ion NaCl in simulated pore solution

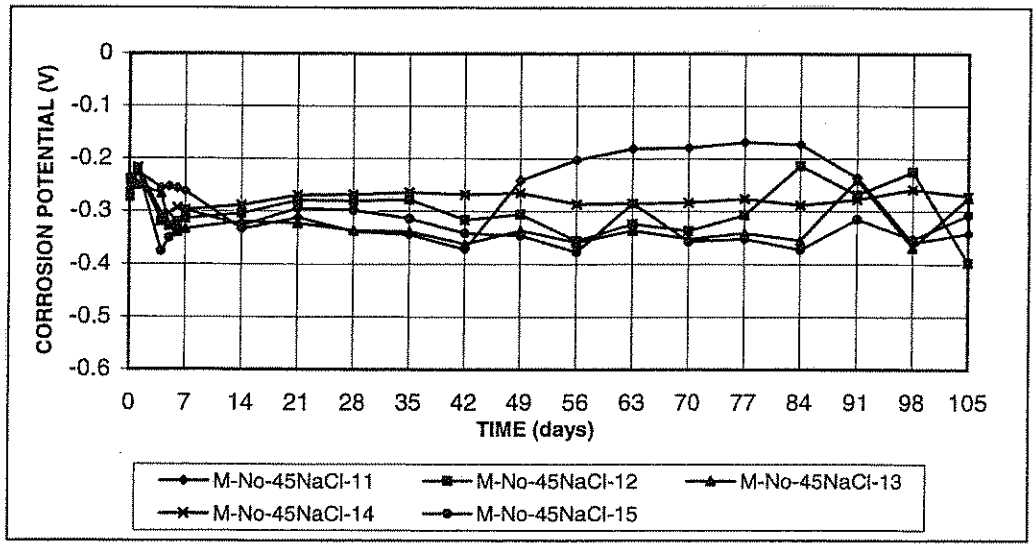

Figure A17.b Cathode Potential with respect to standard calomel electrode; w/c=0.45; no inhibitor; 1.6 m ion NaCl in simulated pore solution

Note: 1. Rust on M-No-45-NaCl-11,12,13,15 were cleaned on the 7 day after taking readings.
2. Rust on M-No-45-NaCl-11,12,13,14,15 were cleaned on the 34 day.
3. Rust on M-No-45-NaCl-11,12,13,14,15 were cleaned on the 74 day.

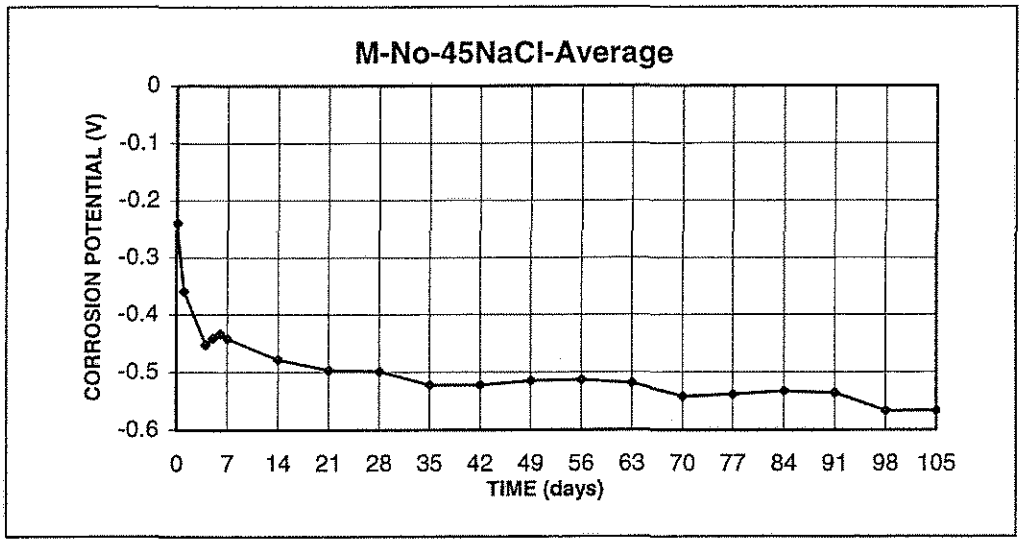

Figure A17.c Anode Potential with respect to standard calomel electrode; w/c=0.45; no inhibitor; 1.6 m ion NaCl in simulated pore solution

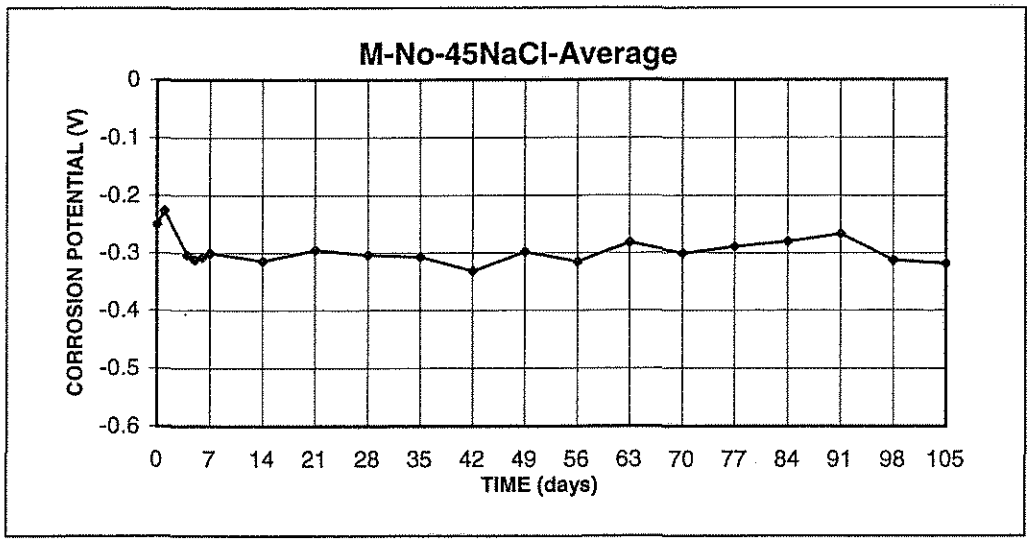

Figure A17.d Cathode Potential with respect to standard calomel electrode; w/c=0.45; no inhibitor; 1.6 m ion NaCl in simulated pore solution

Note: 1. Rust on M-No-45-NaCl-11,12,13,15 were cleaned on the 7 day after taking readings.
2. Rust on M-No-45-NaCl-11,12,13,14,15 were cleaned on the 34 day.
3. Rust on M-No-45-NaCl-11,12,13,14,15 were cleaned on the 74 day.

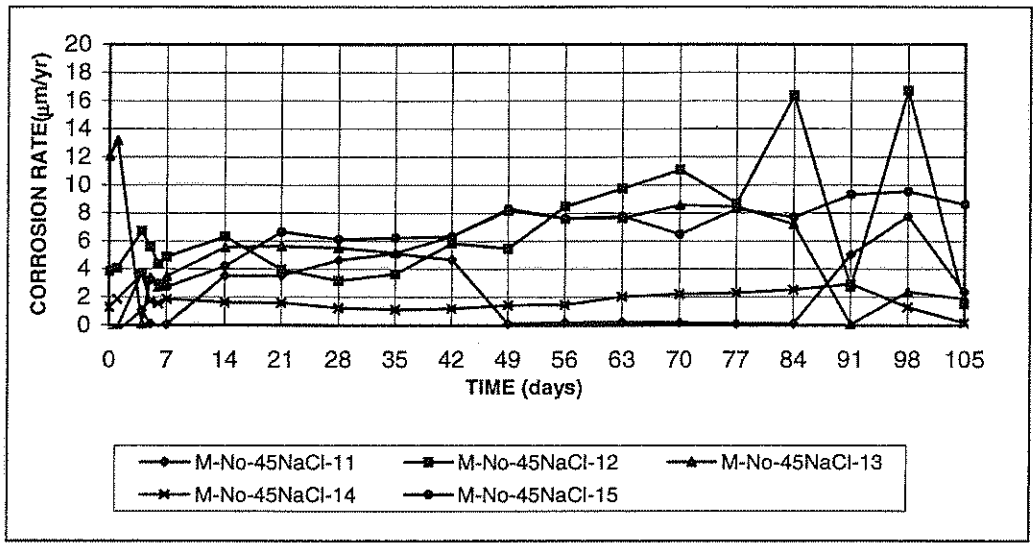

Figure A17.e Corrosion Rate;
w/c=0.45; no inhibitor; 1.6 m ion NaCl in simulated pore solution

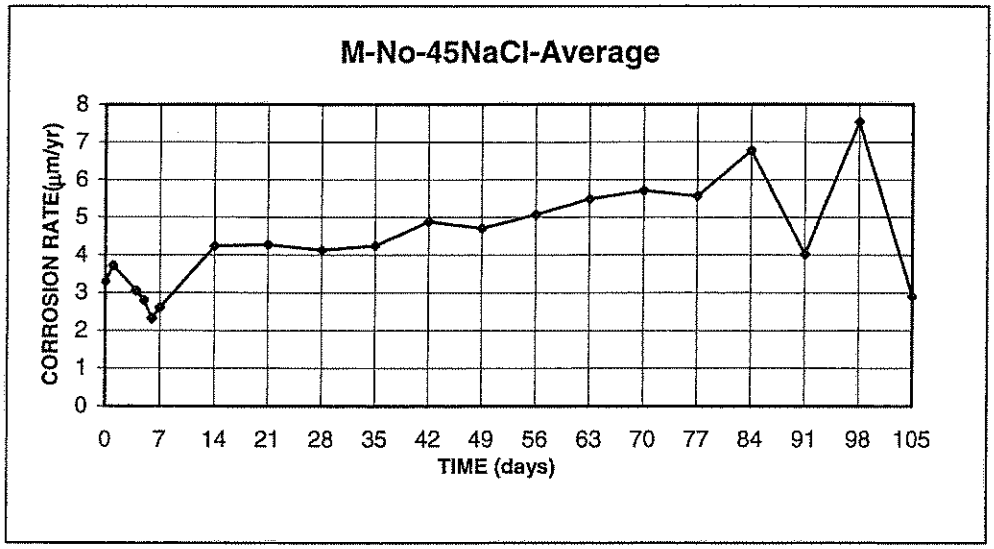

Figure A17.f Corrosion Rate;
w/c=0.45; no inhibitor; 1.6 m ion NaCl in simulated pore solution

Note: 1. Rust on M-No-45-NaCl-11,12,13,15 were cleaned on the 7 day after taking readings.
2. Rust on M-No-45-NaCl-11,12,13,14,15 were cleaned on the 34 day.
3. Rust on M-No-45-NaCl-11,12,13,14,15 were cleaned on the 74 day.

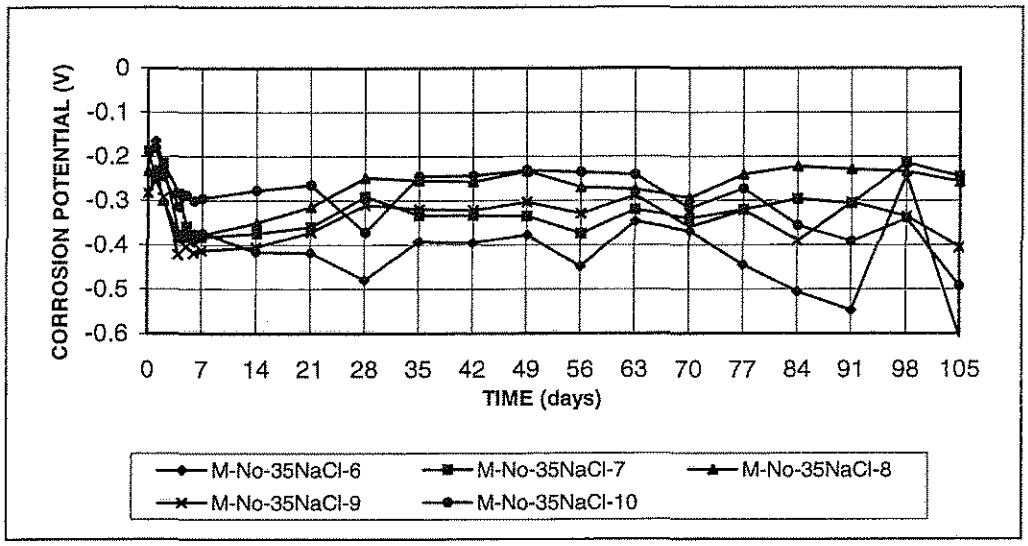

Figure A18.a Anode Potential with respect to standard calomel electrode; w/c=0.35; no inhibitor; 1.6 m ion NaCl in simulated pore solution

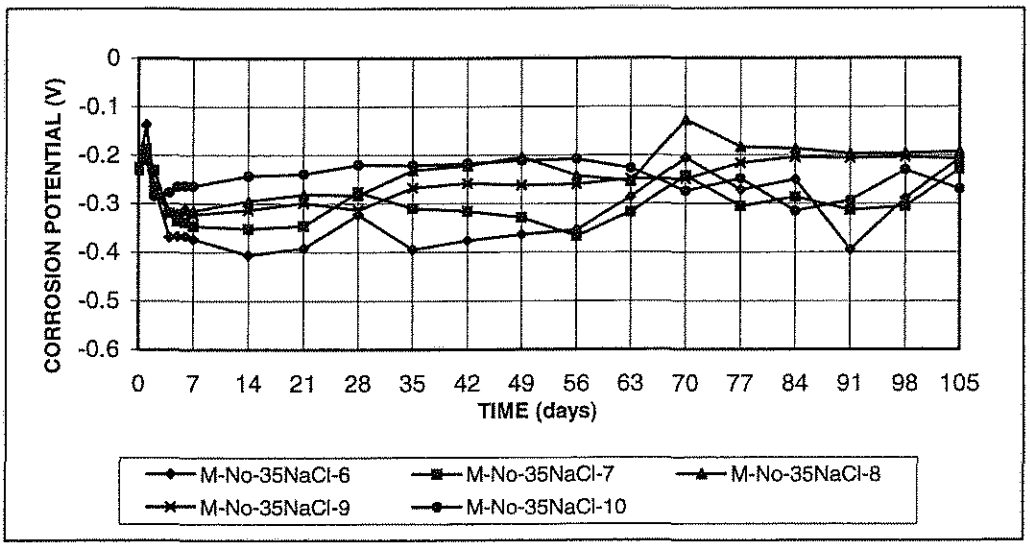

Figure A18.b Cathode Potential with respect to standard calomel electrode; w/c=0.35; no inhibitor; 1.6 m ion NaCl in simulated pore solution

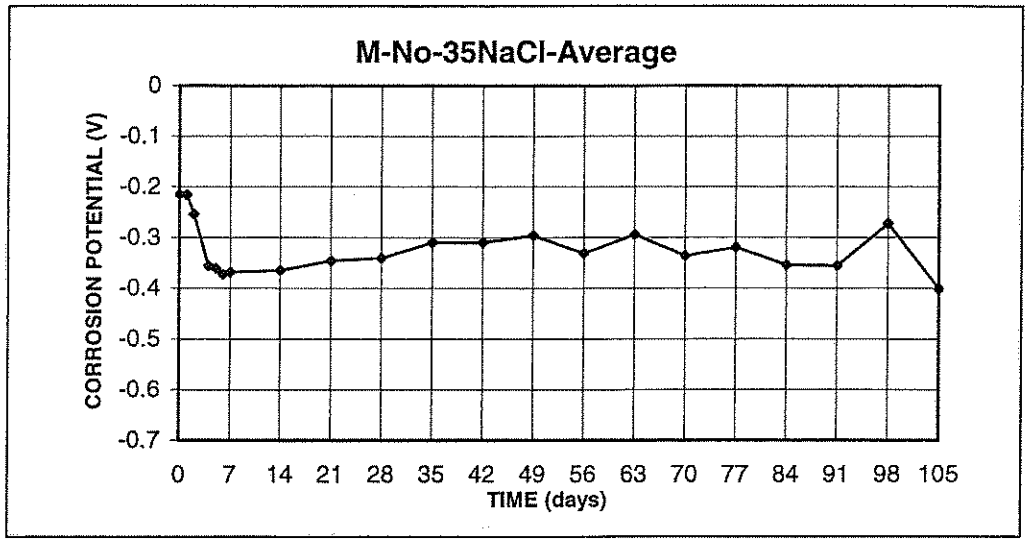

Figure A18.c Anode Potential with respect to standard calomel electrode; w/c=0.35; no inhibitor; 1.6 m ion NaCl in simulated pore solution

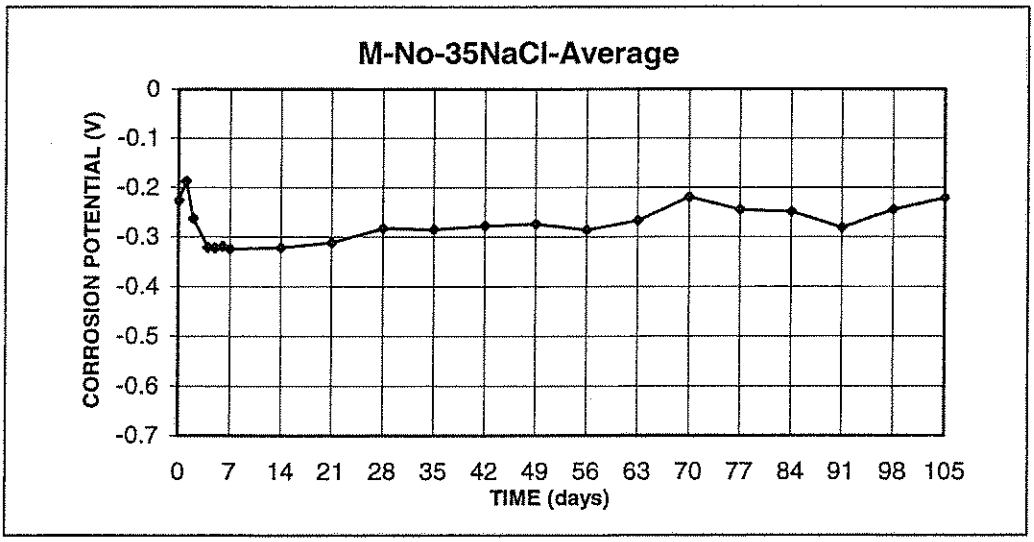

Figure A18.d Cathode Potential with respect to standard calomel electrode; w/c=0.35; no inhibitor; 1.6 m ion NaCl in simulated pore solution

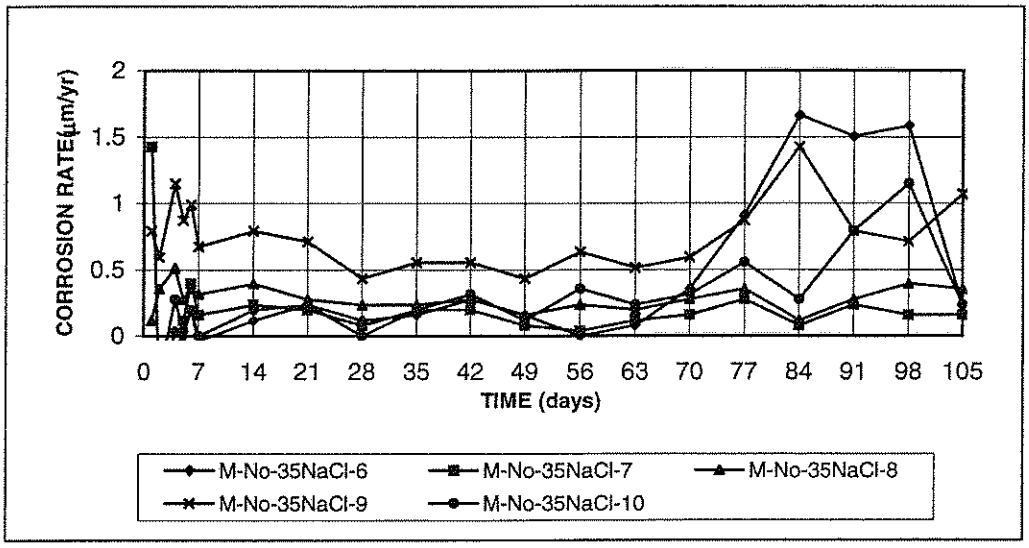

Figure A18.e Corrosion Rate;
w/c=0.35; no inhibitor; 1.6 m ion NaCl in simulated pore solution

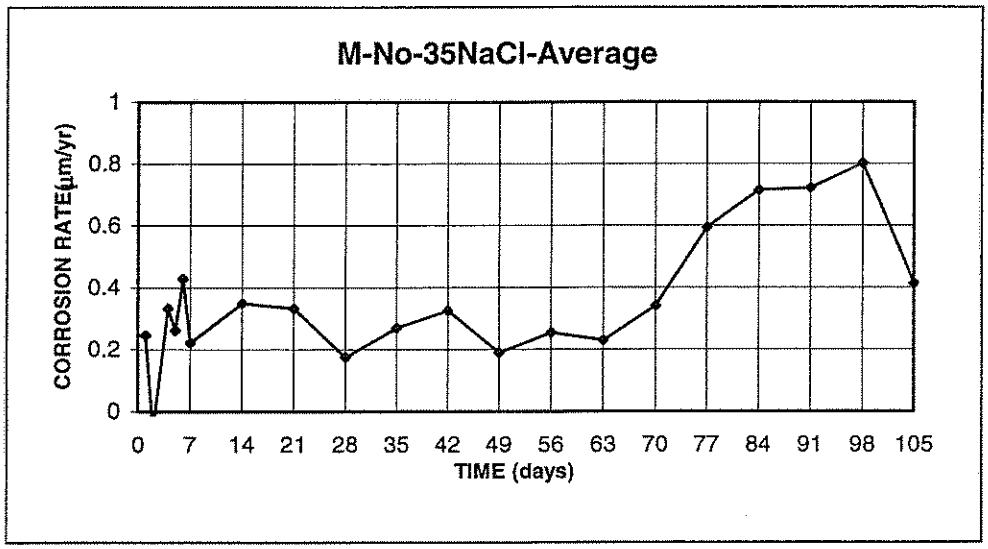

Figure A18.f Corrosion Rate;
w/c=0.35; no inhibitor; 1.6 m ion NaCl in simulated pore solution

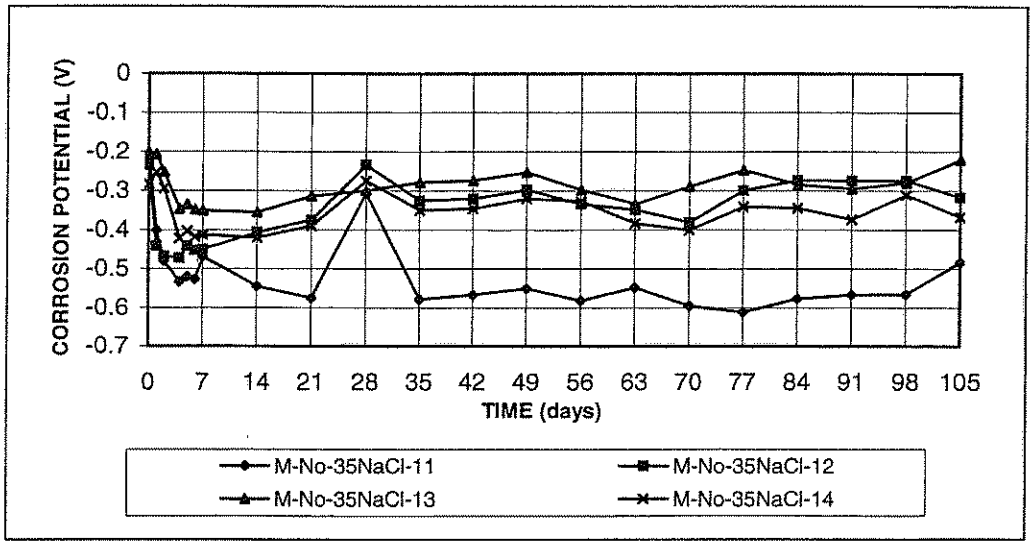

Figure A19.a Anode Potential with respect to standard calomel electrode; w/c=0.35; no inhibitor; 1.6 m ion NaCl in simulated pore solution

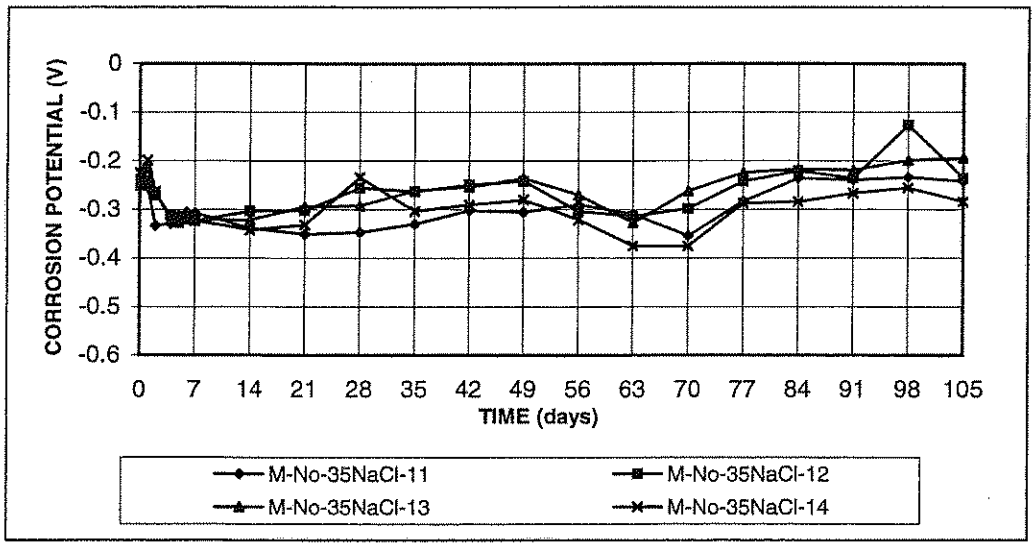

Figure A19.b Cathode Potential with respect to standard calomel electrode; w/c=0.35; no inhibitor; 1.6 m ion NaCl in simulated pore solution

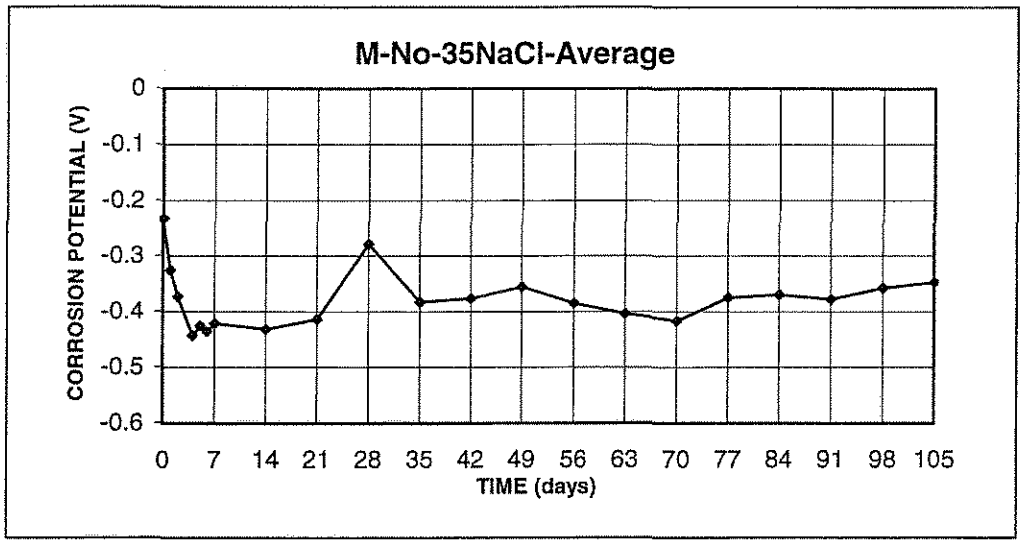

Figure A19.c Anode Potential with respect to standard calomel electrode; w/c=0.35; no inhibitor; 1.6 m ion NaCl in simulated pore solution

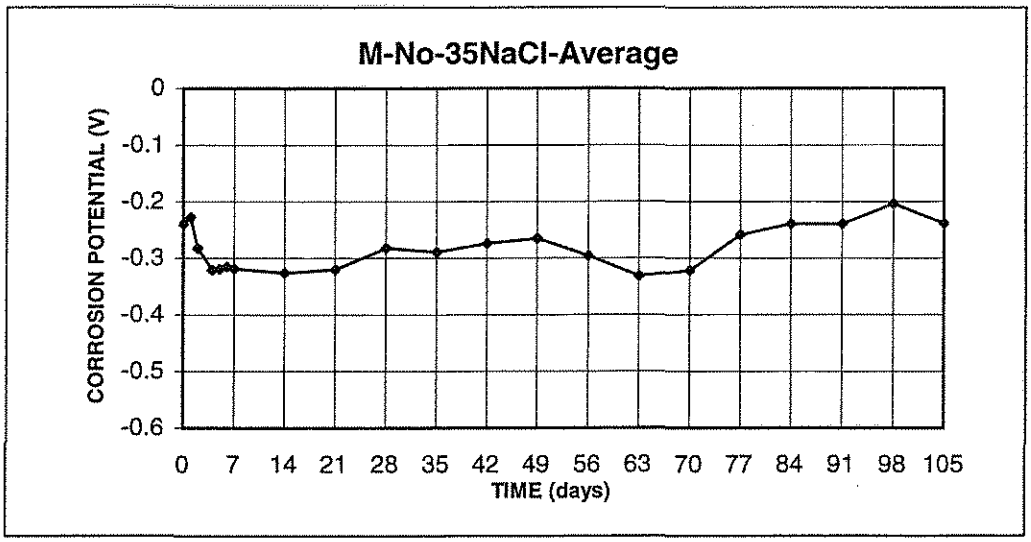

Figure A19.d Cathode Potential with respect to standard calomel electrode; w/c=0.35; no inhibitor; 1.6 m ion NaCl in simulated pore solution

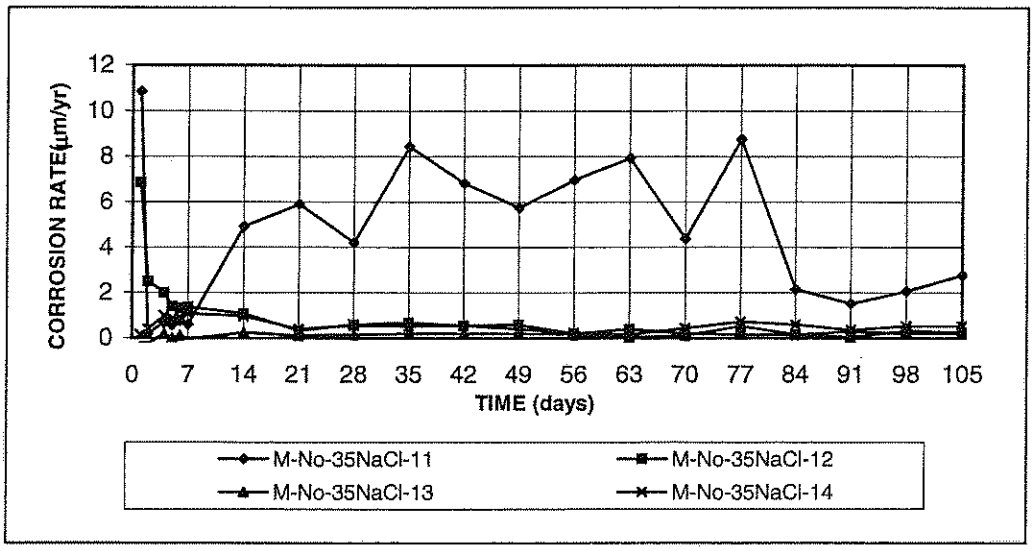

Figure A19.e Corrosion Rate;
w/c=0.35; no inhibitor; 1.6 m ion NaCl in simulated pore solution

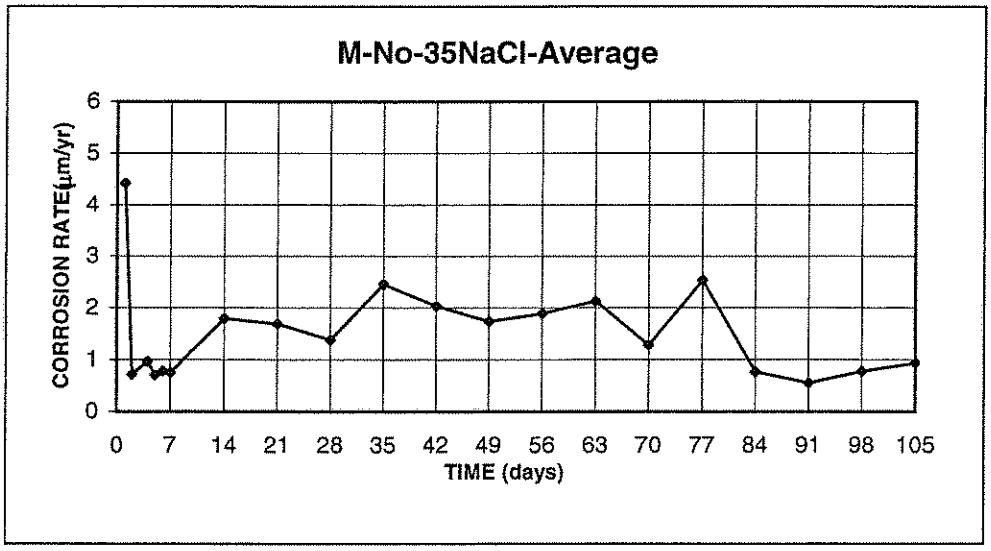

Figure A19.f Corrosion Rate;
w/c=0.35; no inhibitor; 1.6 m ion NaCl in simulated pore solution

Appendix B

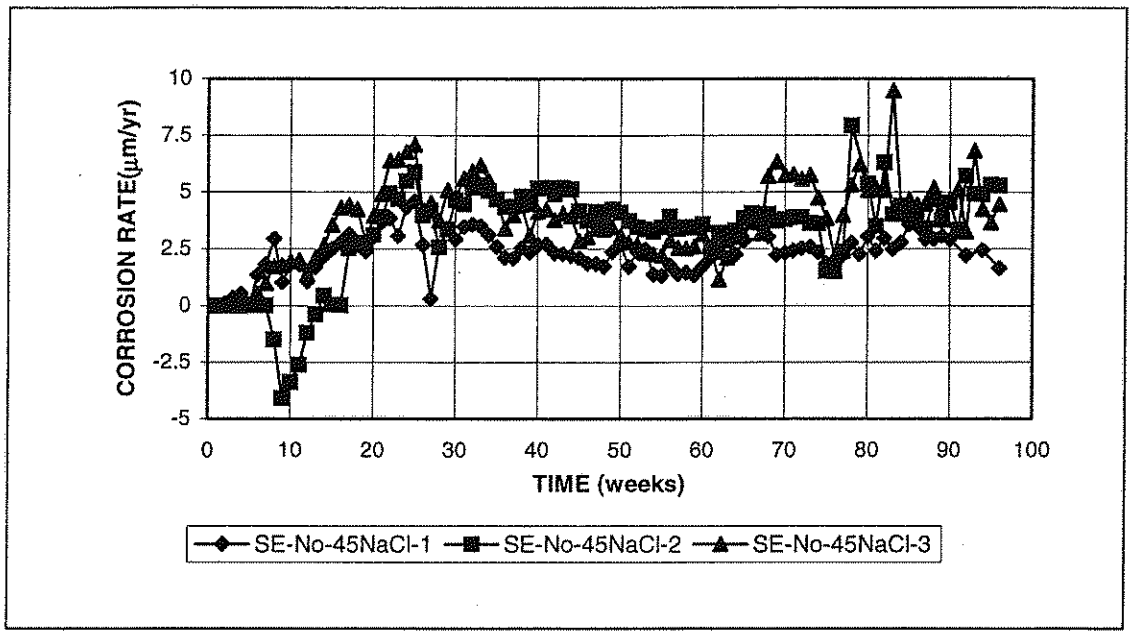

Figure B1.a Southern Exposure Test. Corrosion rate for conventional steel, normalized, no inhibitors, w/c=0.45, 6.04 m ion NaCl.

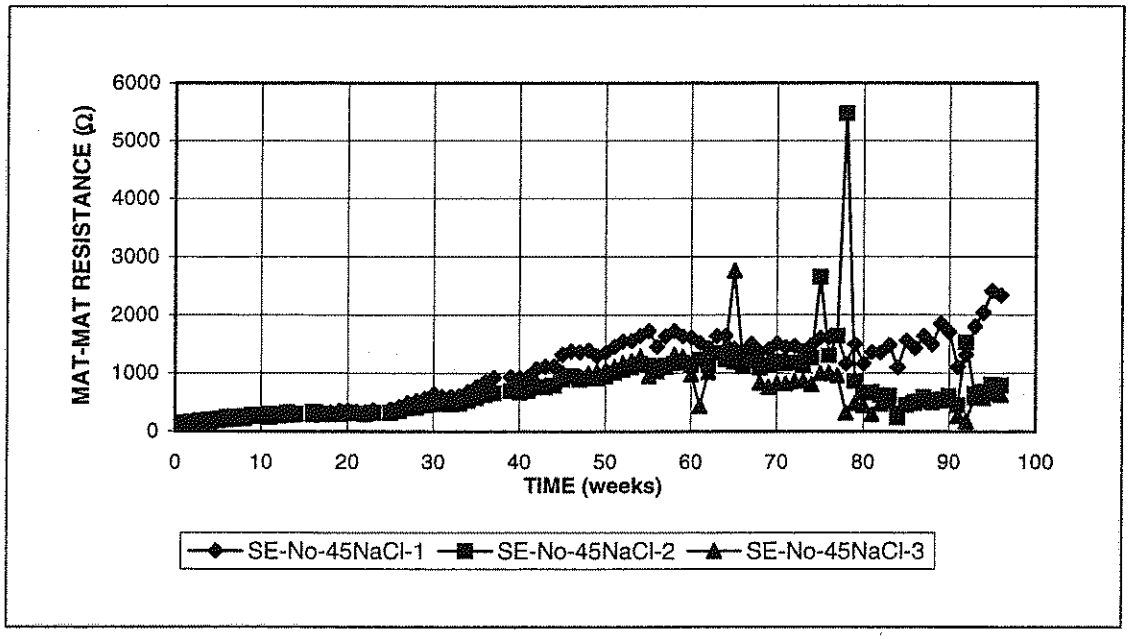

Figure B1.b Southern Exposure Test. Mat-to-mat resistance, conventional steel, normalized, no inhibitors, w/c=0.45, 6.04 m ion NaCl.

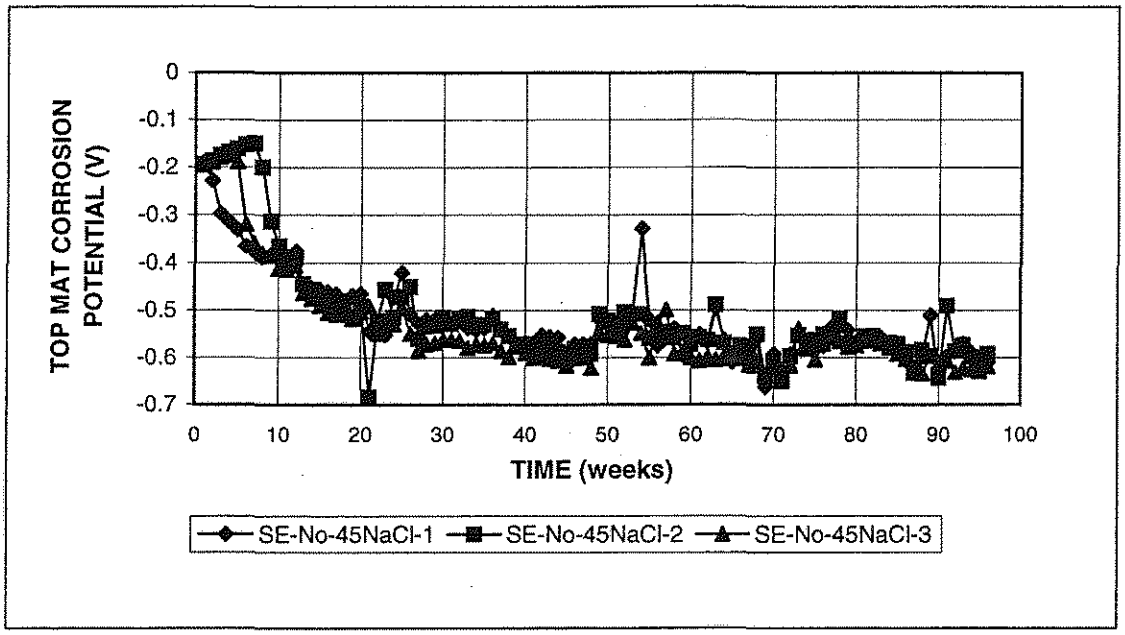

Figure B1.c Southern Exposure Test. Corrosion potential, top mat, conventional steel, normalized, no inhibitors, w/c=0.45, 6.04 m ion NaCl.

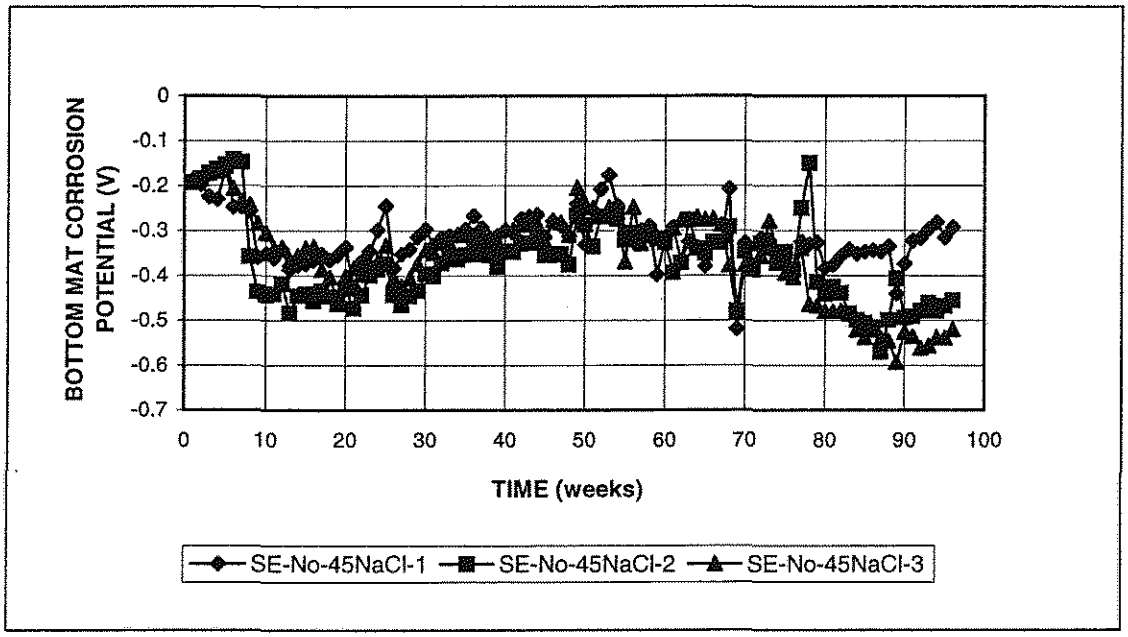

Figure B1.d Southern Exposure Test. Corrosion potential, bottom mat, conventional steel, normalized, no inhibitors, w/c=0.45, 6.04 m ion NaCl.

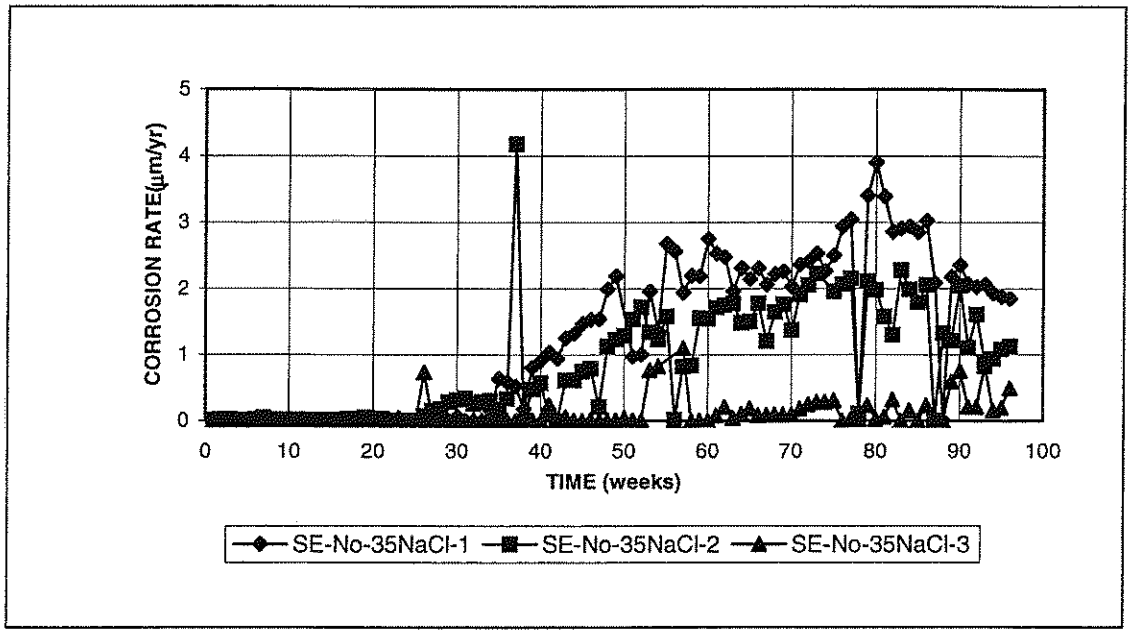

Figure B2.a Southern Exposure Test. Corrosion rate for conventional steel, normalized, no inhibitors, w/c=0.35, 6.04 m ion NaCl.

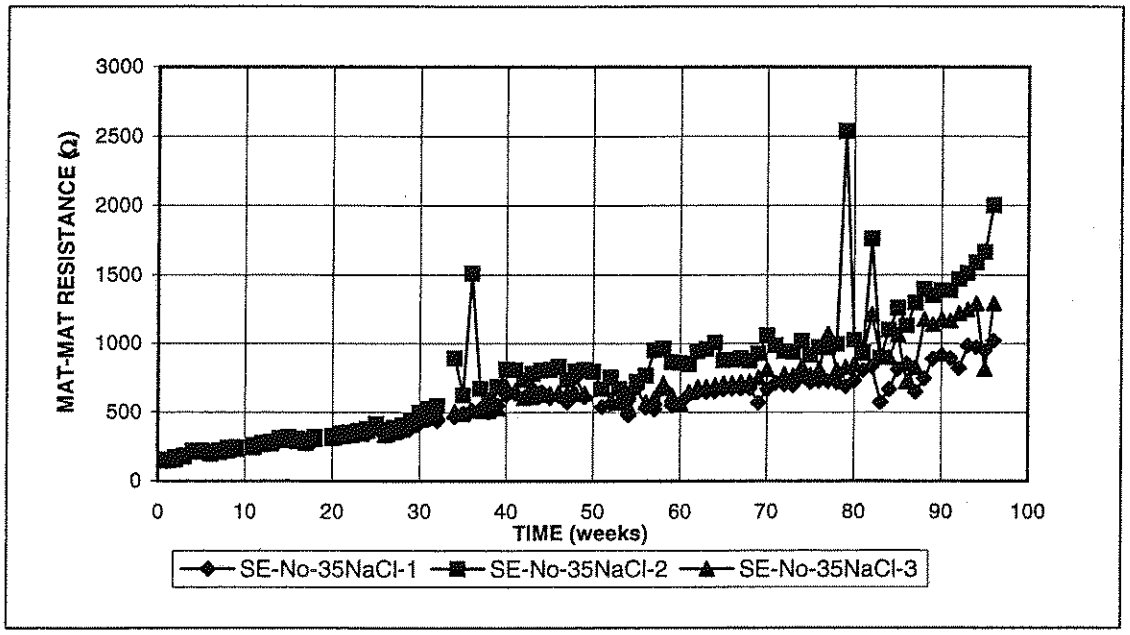

Figure B2.b Southern Exposure Test. Mat-to-mat resistance, conventional steel, normalized, no inhibitors, w/c=0.35, 6.04 m ion NaCl.

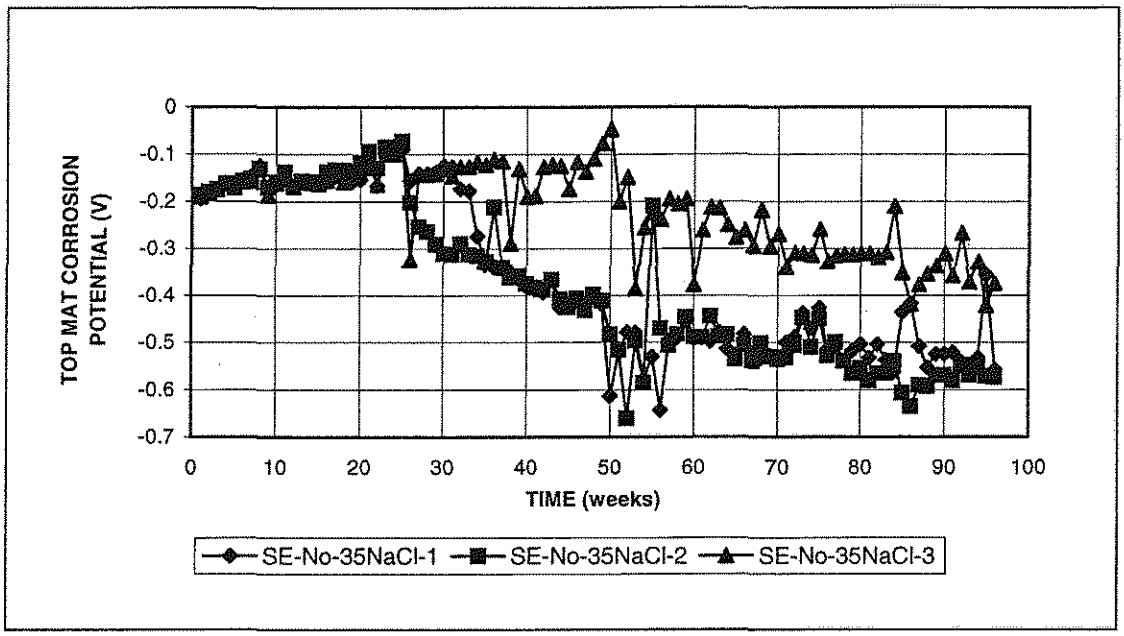

Figure B2.c Southern Exposure Test. Corrosion potential, top mat, conventional steel, normalized, no inhibitors, w/c=0.35, 6.04 m ion NaCl.

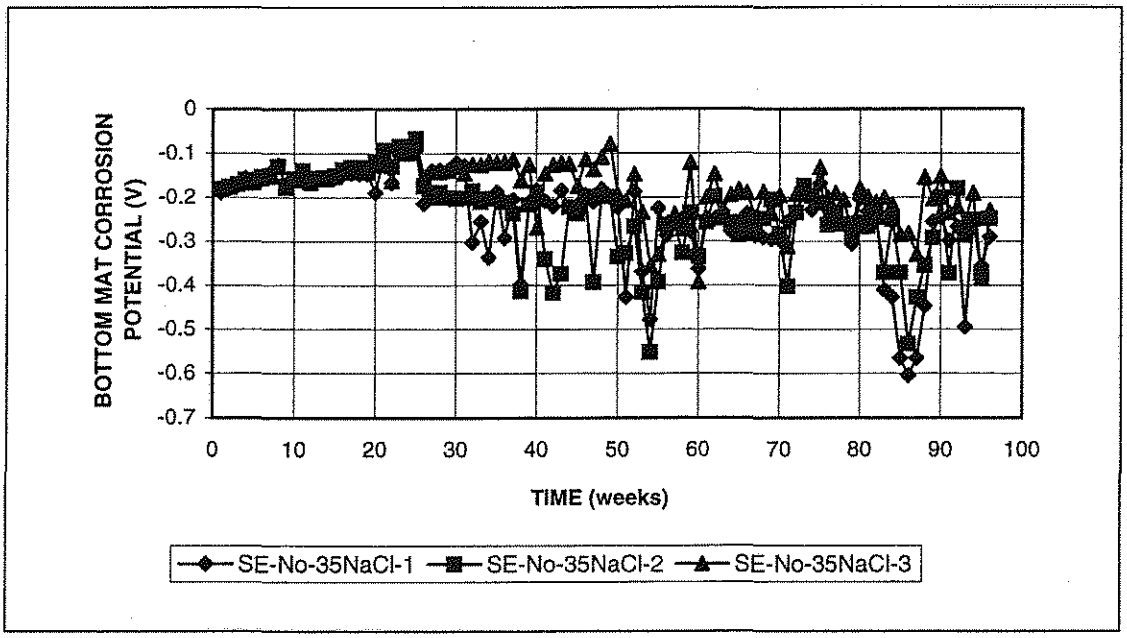

Figure B2.d Southern Exposure Test. Corrosion potential, bottom mat, conventional steel, normalized, no inhibitors, w/c=0.35, 6.04 m ion NaCl.

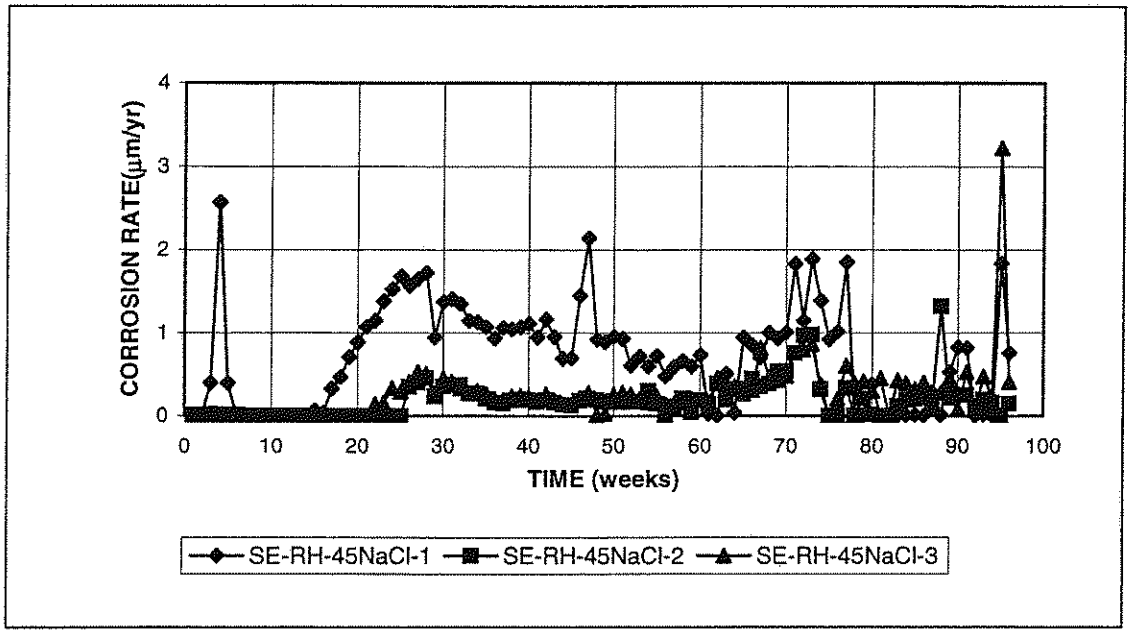

Figure B3.a Southern Exposure Test. Corrosion rate for conventional steel, normalized, Rheocrete, w/c=0.45, 6.04 m ion NaCl.

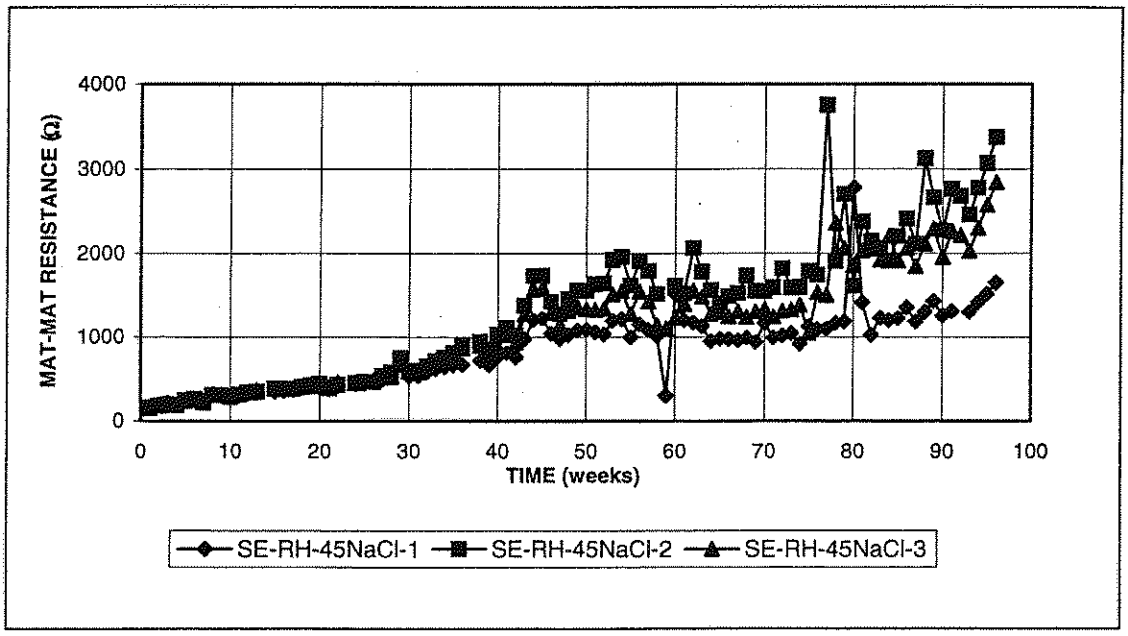

Figure B3.b Southern Exposure Test. Mat-to-mat resistance, conventional steel, normalized, Rheocrete, w/c=0.45, 6.04 m ion NaCl.

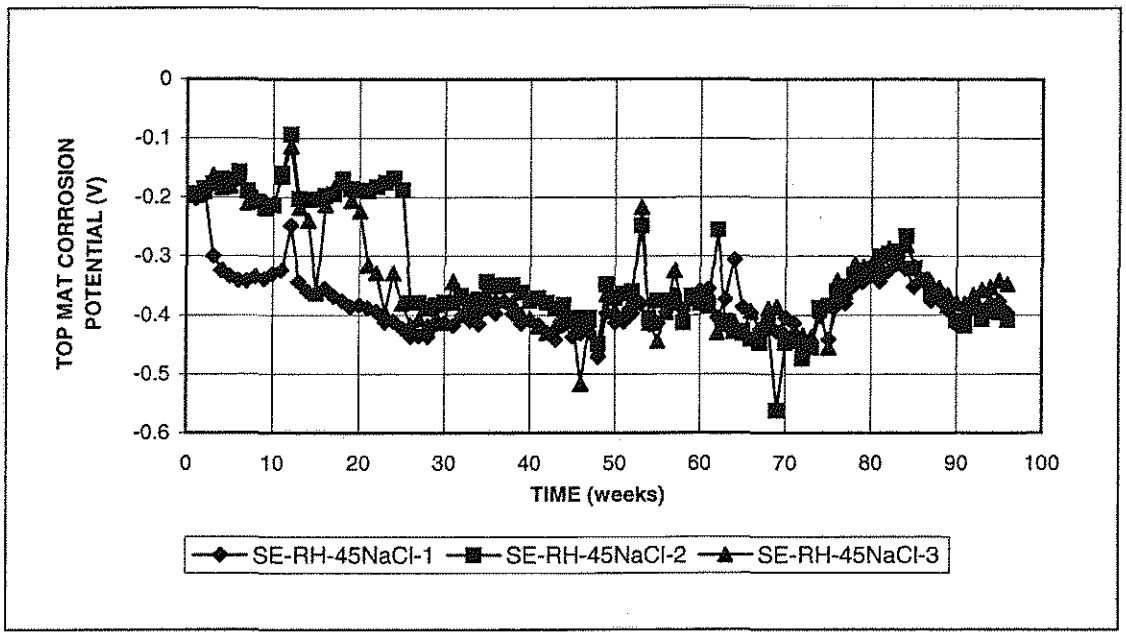

Figure B3.c Southern Exposure Test. Corrosion potential, top mat, conventional steel, normalized, Rheocrete, w/c=0.45, 6.04 m ion NaCl.

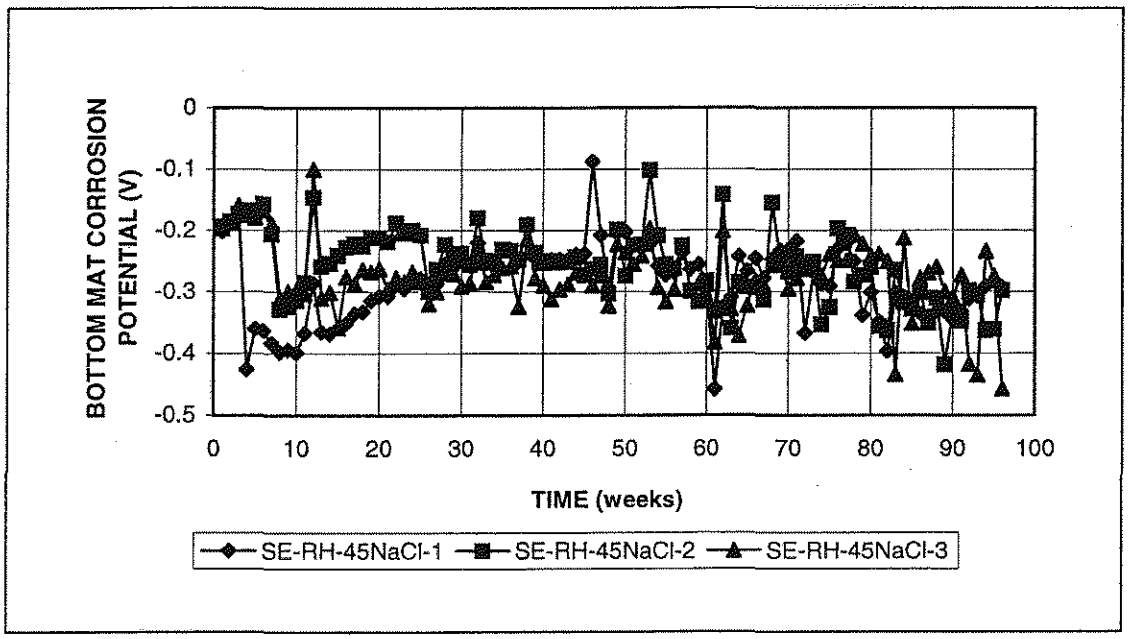

Figure B3.d Southern Exposure Test. Corrosion potential, bottom mat, conventional steel, normalized, Rheocrete, w/c=0.45, 6.04 m ion NaCl.

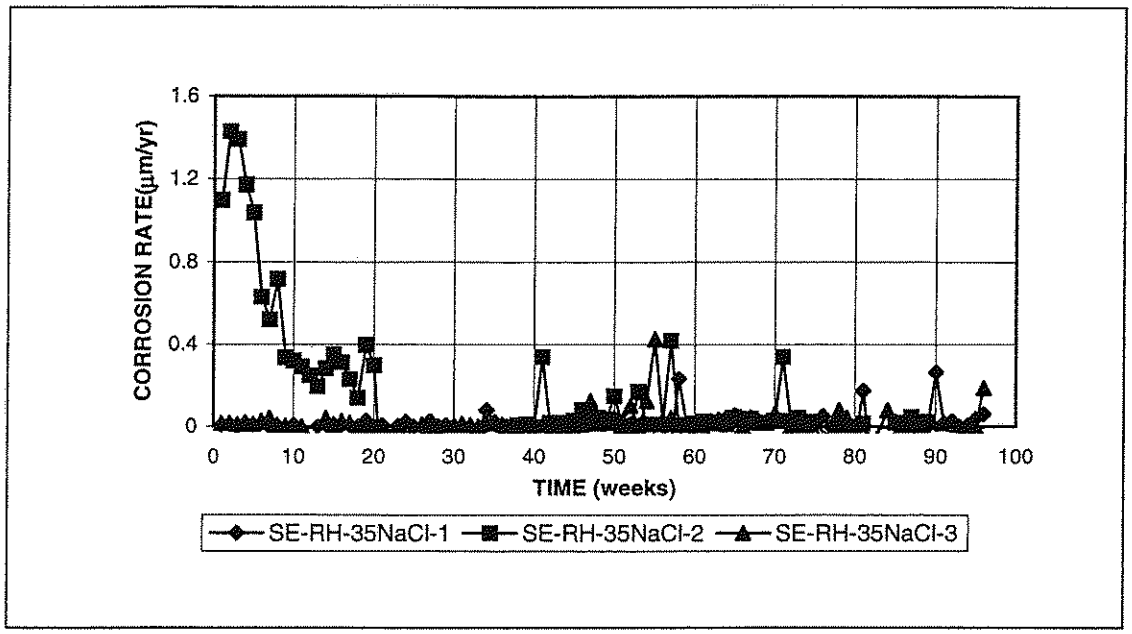

Figure B4.a Southern Exposure Test. Corrosion rate for conventional steel, normalized, Rheocrete, w/c=0.35, 6.04 m ion NaCl.

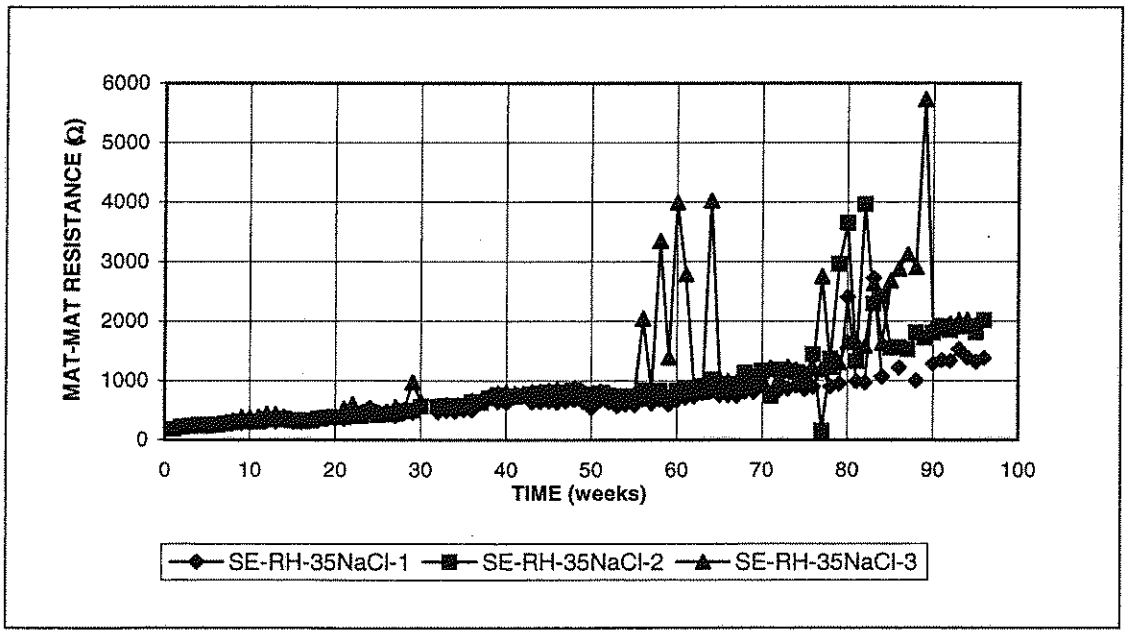

Figure B4.b Southern Exposure Test. Mat-to-mat resistance, conventional steel, normalized, Rheocrete, w/c=0.35, 6.04 m ion NaCl.

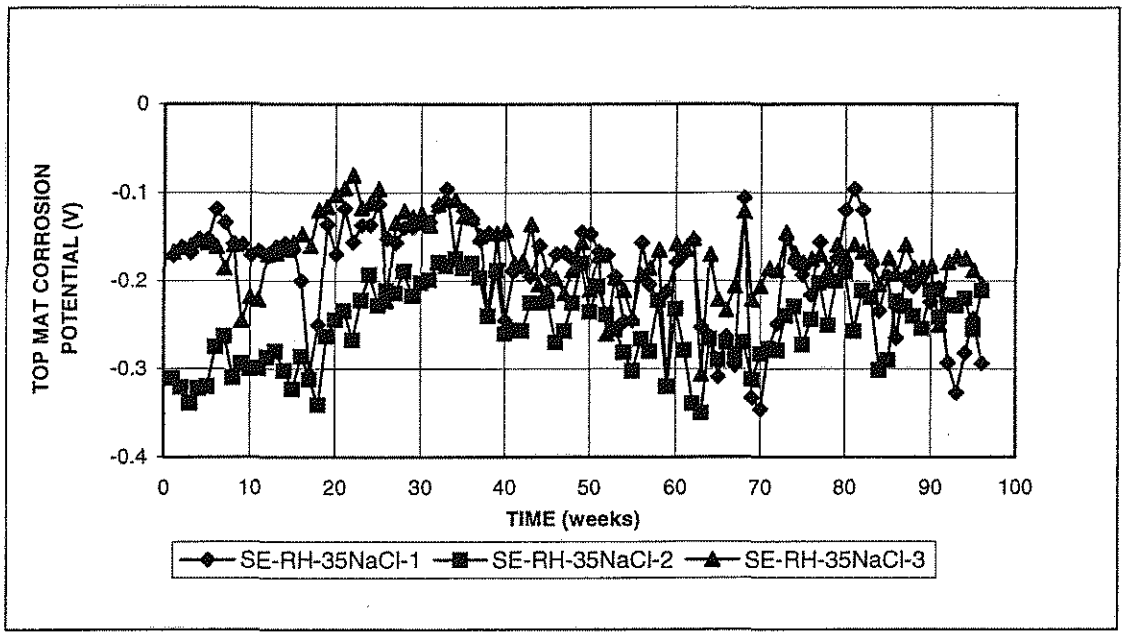

Figure B4.c Southern Exposure Test. Corrosion potential, top mat, conventional steel, normalized, Rheocrete, w/c=0.35, 6.04 m ion NaCl.

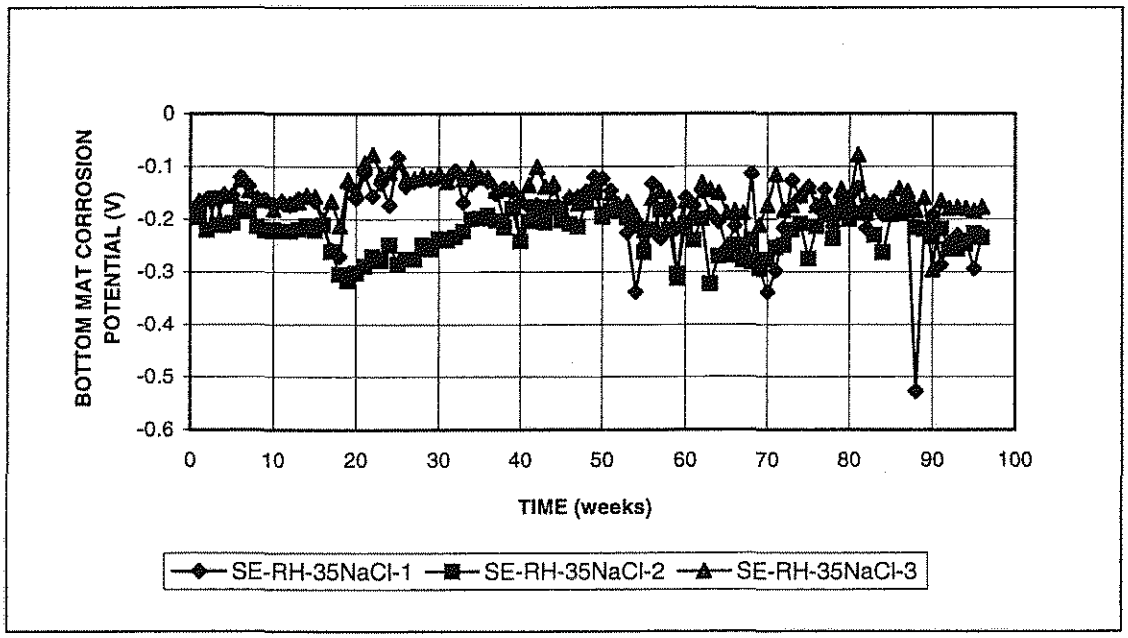

Figure B4.d Southern Exposure Test. Corrosion potential, bottom mat, conventional steel, normalized, Rheocrete, w/c=0.35, 6.04 m ion NaCl.

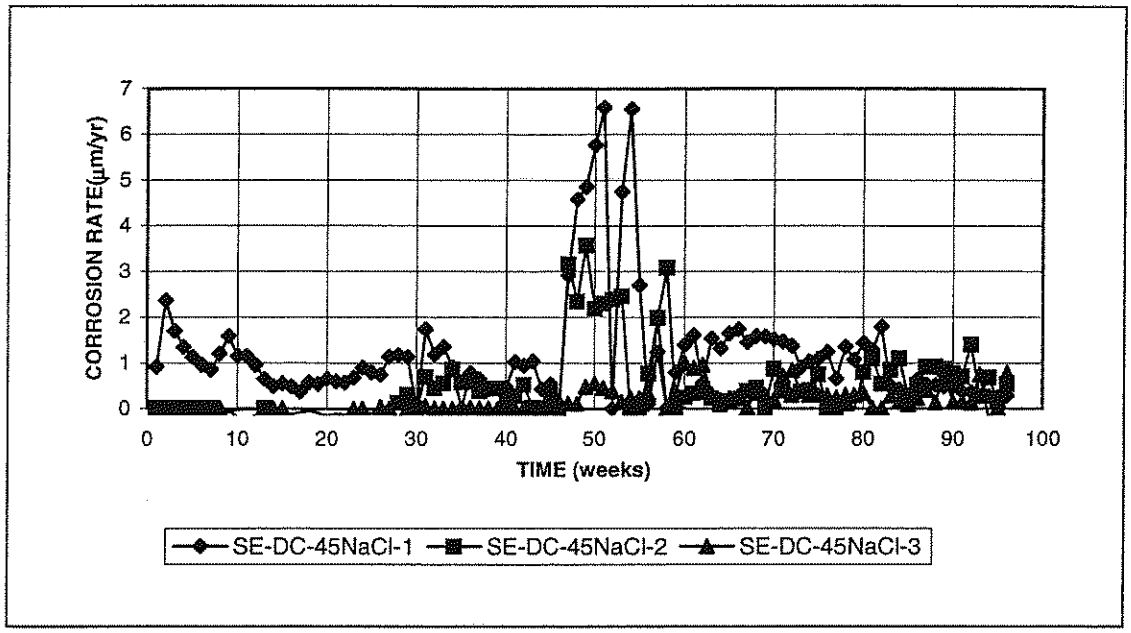

Figure B5.a Southern Exposure Test. Corrosion rate for conventional steel, normalized, DCI-S, w/c=0.45, 6.04 m ion NaCl.

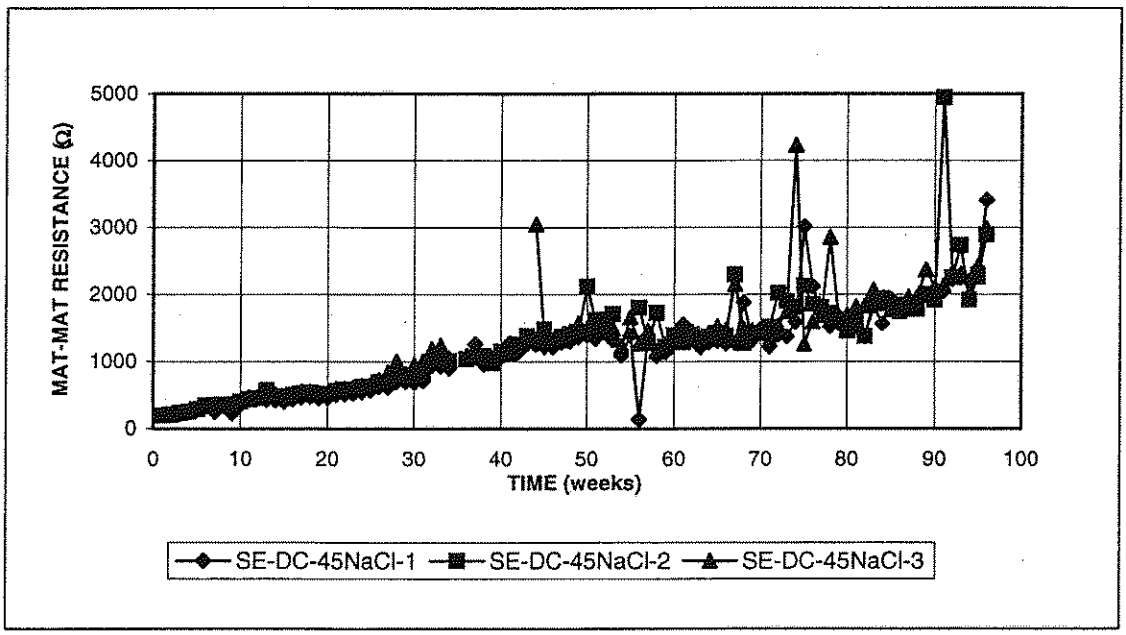

Figure B5.b Southern Exposure Test. Mat-to-mat resistance, conventional steel, normalized, DCI-S, w/c=0.45, 6.04 m ion NaCl.

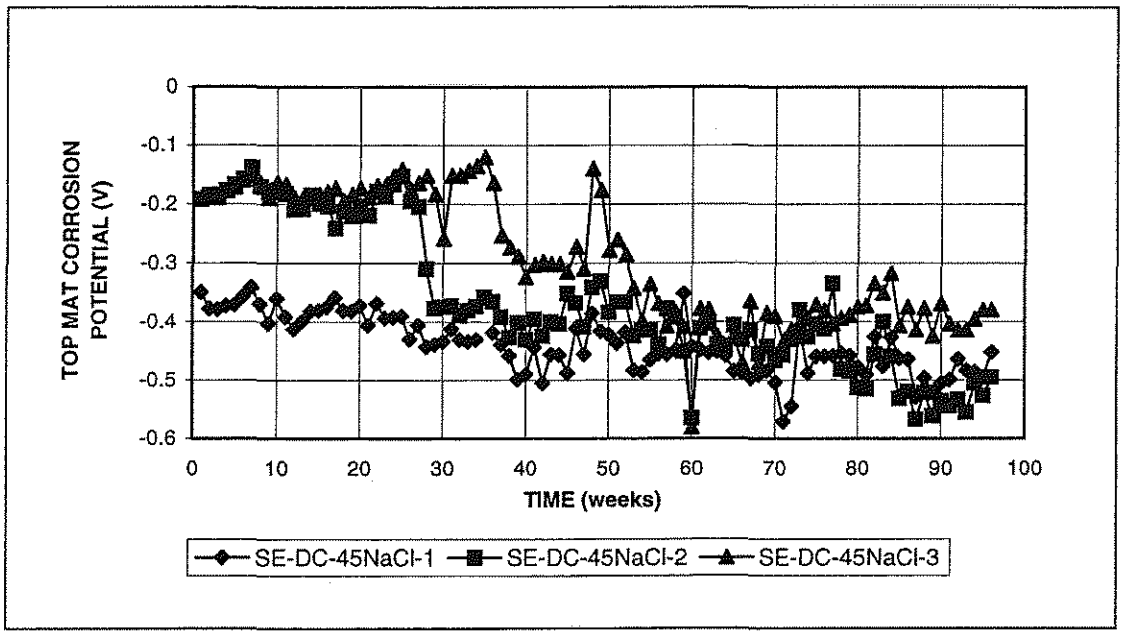

Figure B5.c Southern Exposure Test. Corrosion potential, top mat, conventional steel, normalized, DCI-S, w/c=0.45, 6.04 m ion NaCl.

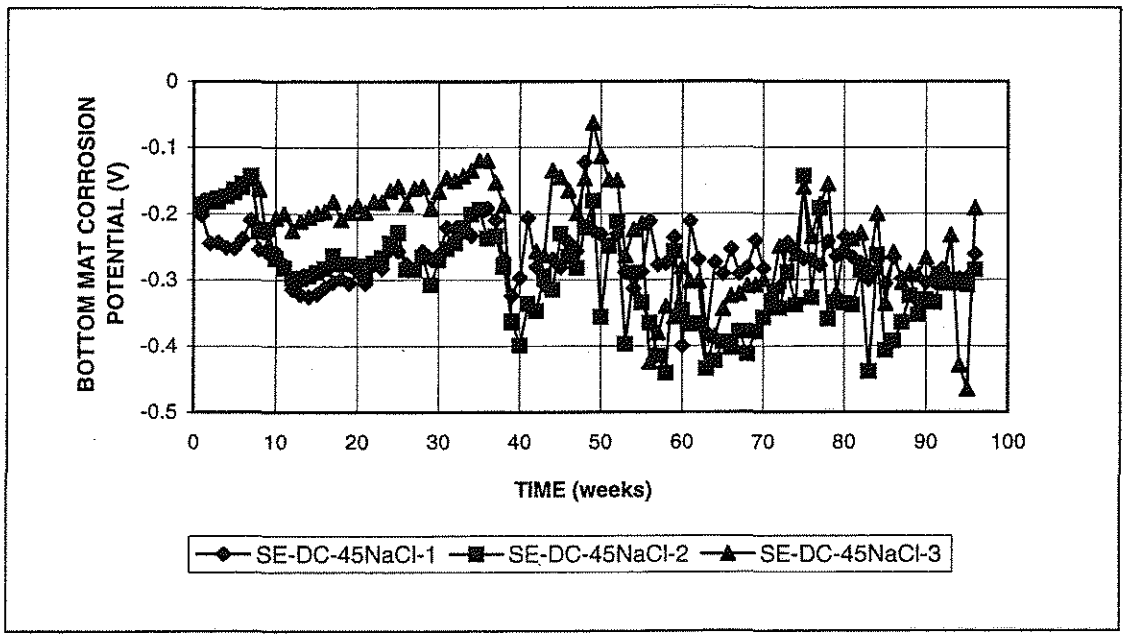

Figure B5.d Southern Exposure Test. Corrosion potential, bottom mat, conventional steel, normalized, DCI-S, w/c=0.45, 6.04 m ion NaCl.

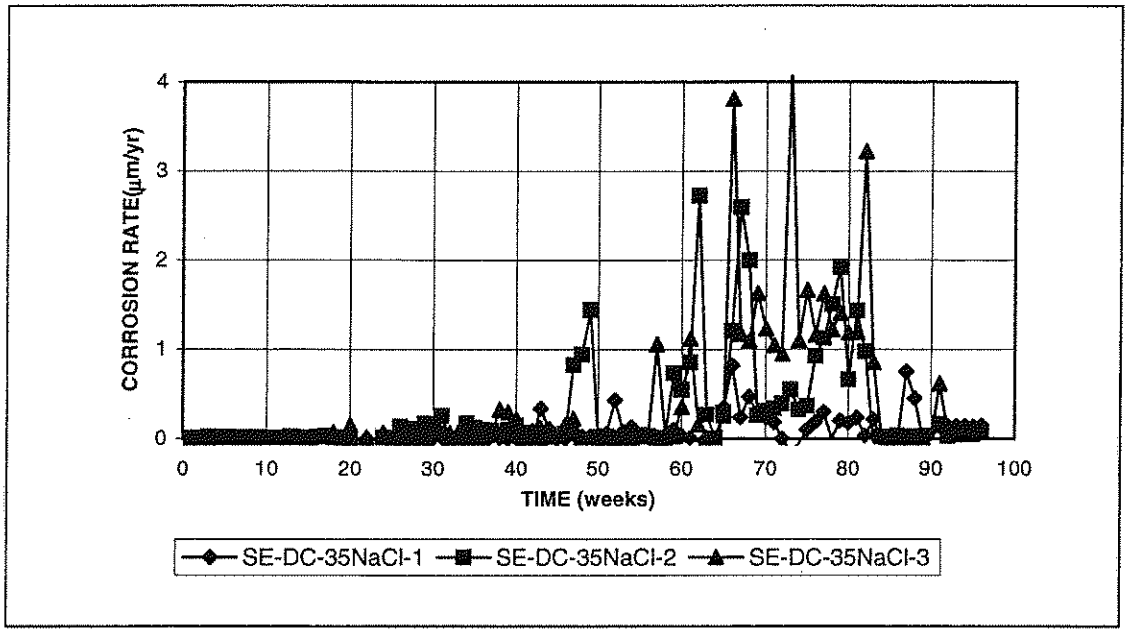

Figure B6.a Southern Exposure Test. Corrosion rate for conventional steel, normalized, DCI-S, w/c=0.35, 6.04 m ion NaCl.

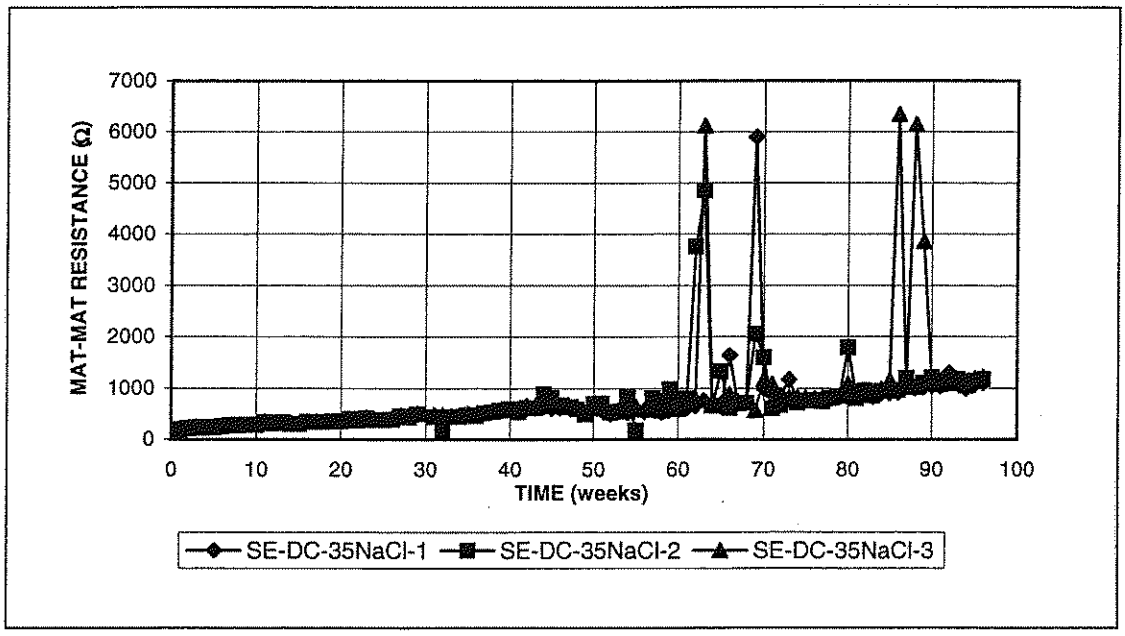

Figure B6.b Southern Exposure Test. Mat-to-mat resistance, conventional steel, normalized, DCI-S, w/c=0.35, 6.04 m ion NaCl.

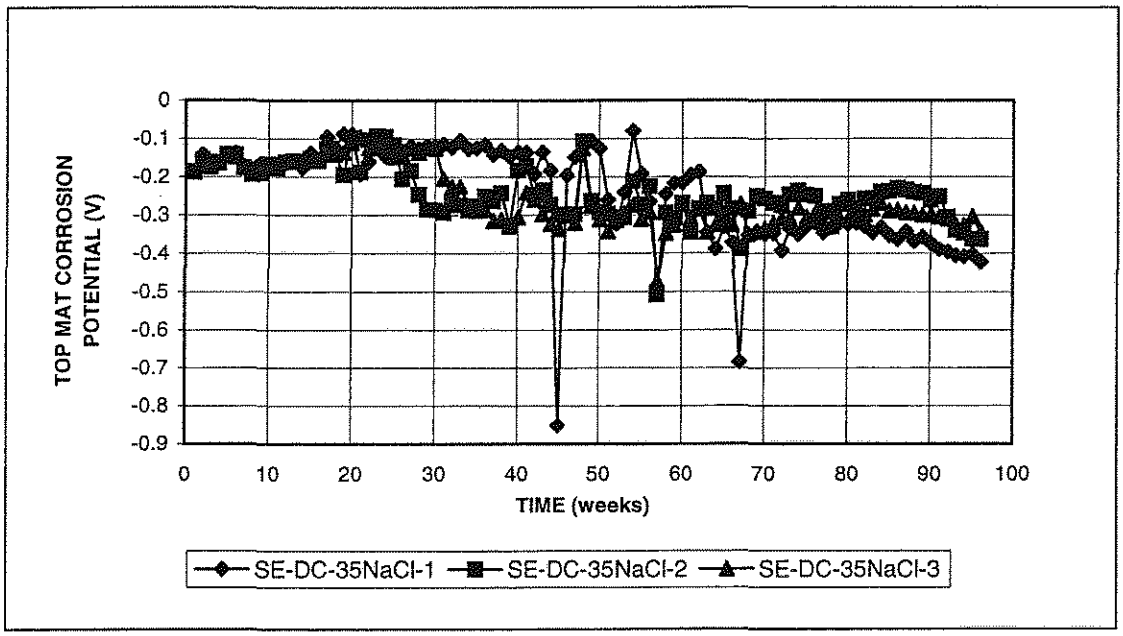

Figure B6.c Southern Exposure Test. Corrosion potential, top mat, conventional steel, normalized, DCI-S, w/c=0.35, 6.04 m ion NaCl.

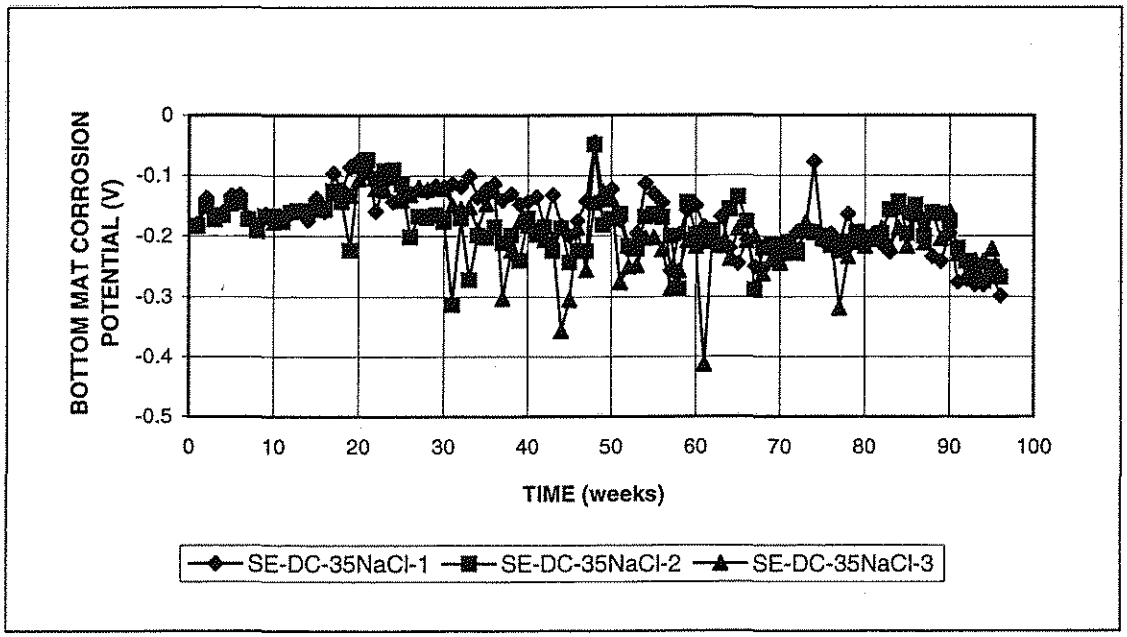

Figure B6.d Southern Exposure Test. Corrosion potential, bottom mat, conventional steel, normalized, DCI-S, w/c=0.35, 6.04 m ion NaCl.

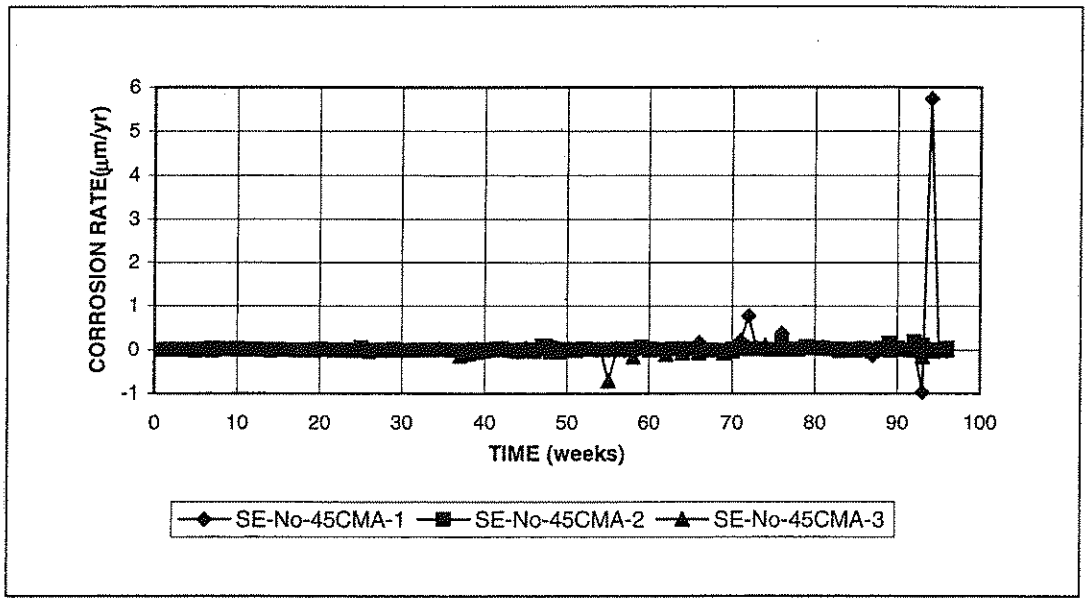

Figure B7.a Southern Exposure Test. Corrosion rate for conventional steel, normalized, no inhibitors, w/c=0.45, 6.04 m ion CMA.

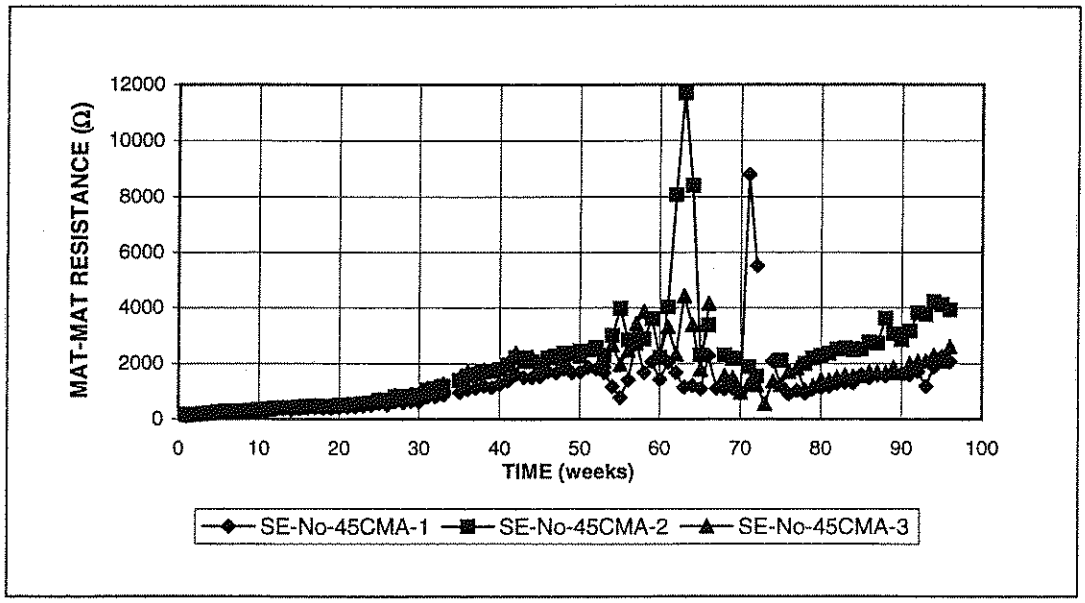

Figure B7.b Southern Exposure Test. Mat-to-mat resistance, conventional steel, normalized, no inhibitors, w/c=0.45, 6.04 m ion CMA.

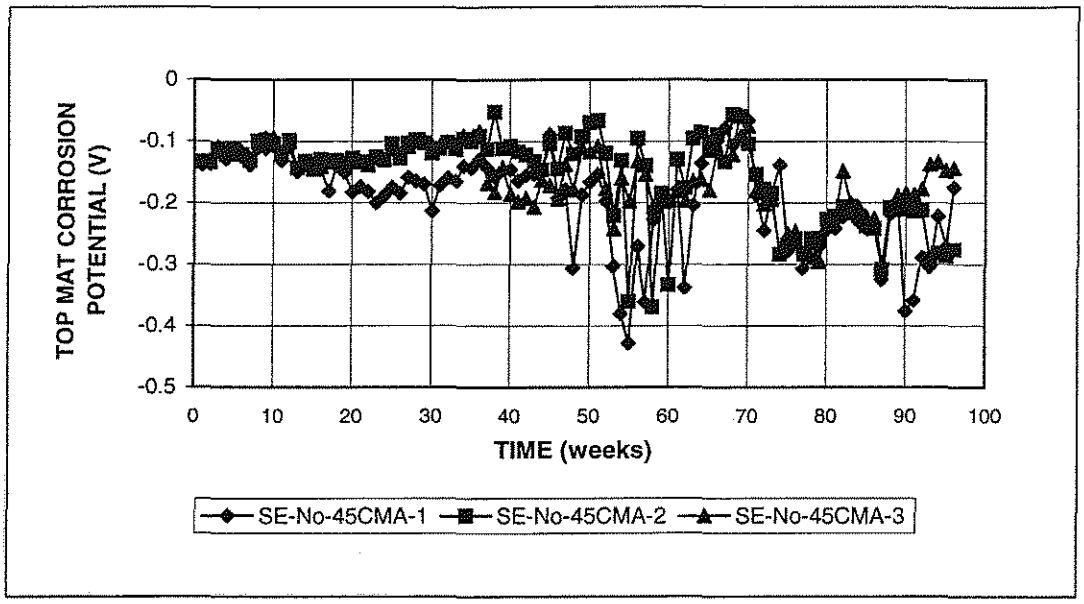

Figure B7.c Southern Exposure Test. Corrosion potential, top mat, conventional steel, normalized, no inhibitors, w/c=0.45, 6.04 m ion CMA.

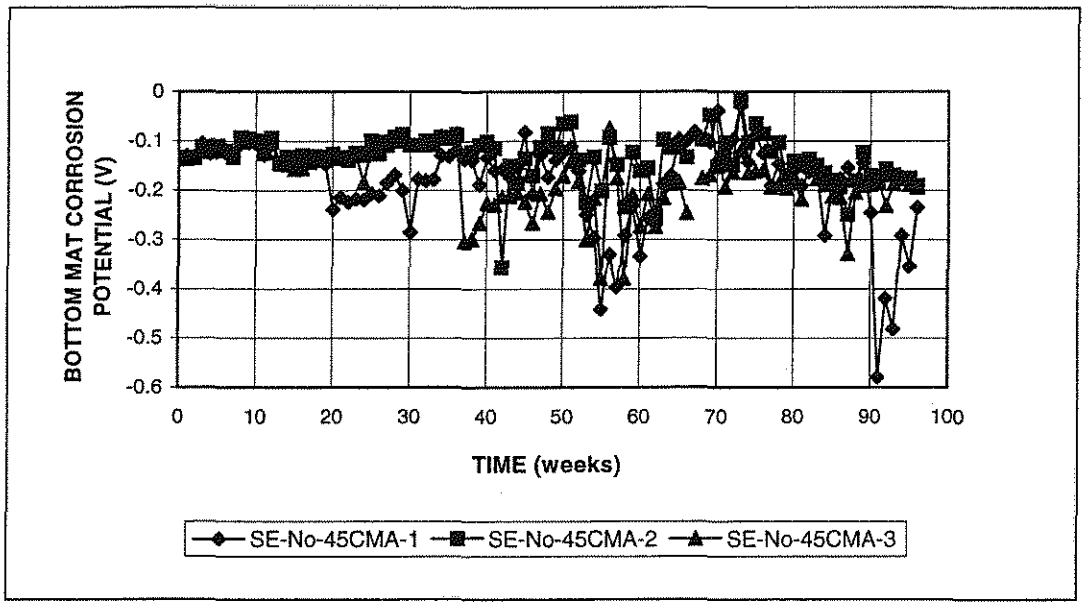

Figure B7.d Southern Exposure Test. Corrosion potential, bottom mat, conventional steel, normalized, no inhibitors, w/c=0.45, 6.04 m ion CMA.

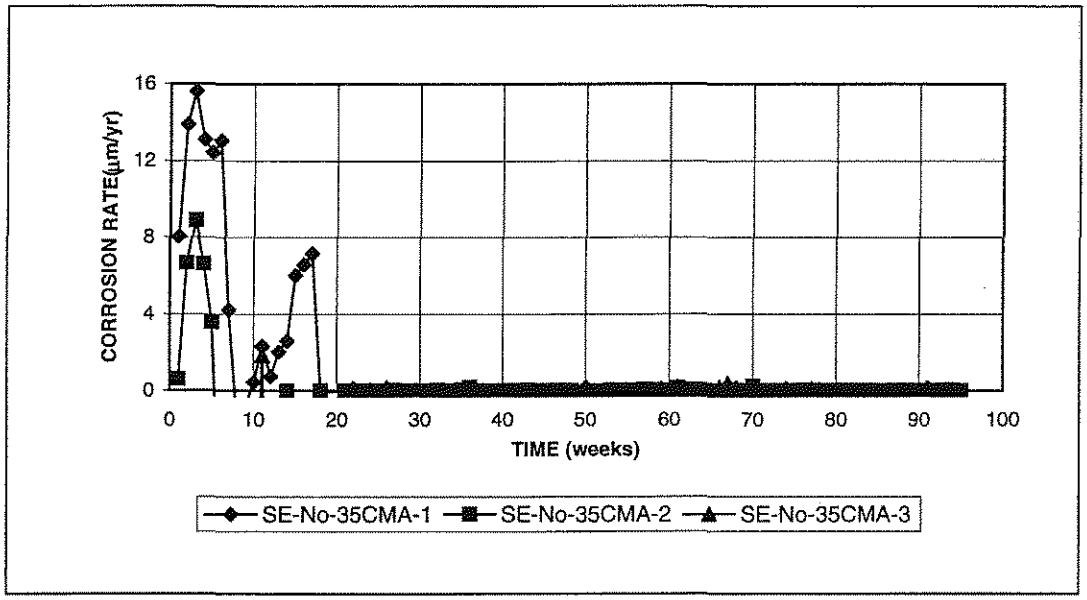

Figure B8.a Southern Exposure Test. Corrosion rate for conventional steel, normalized, no inhibitors, w/c=0.35, 6.04 m ion CMA.

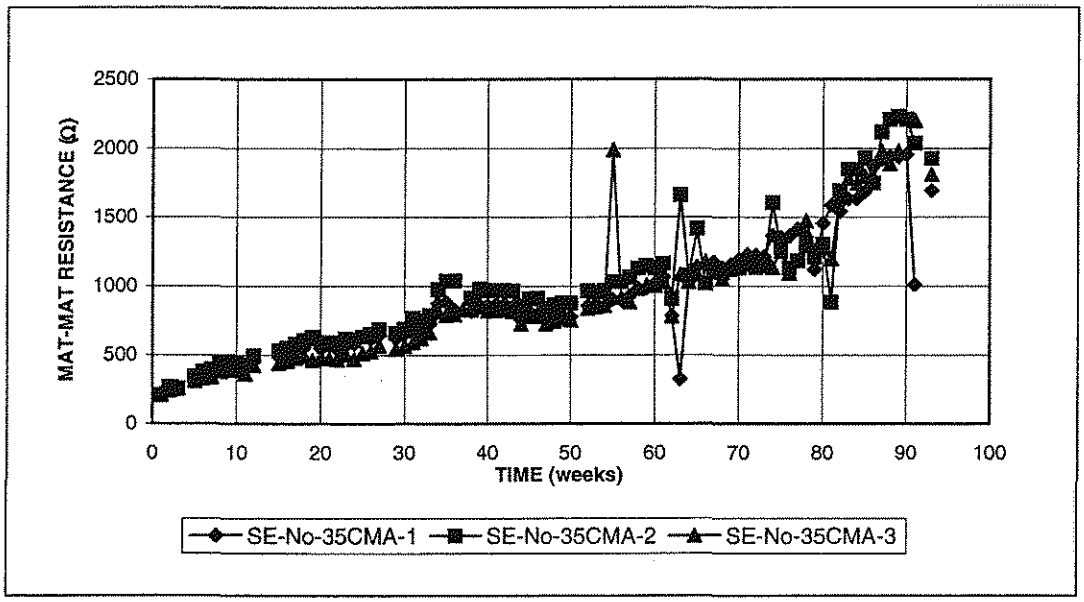

Figure B8.b Southern Exposure Test. Mat-to-mat resistance, conventional steel, normalized, no inhibitors, w/c=0.35, 6.04 m ion CMA.

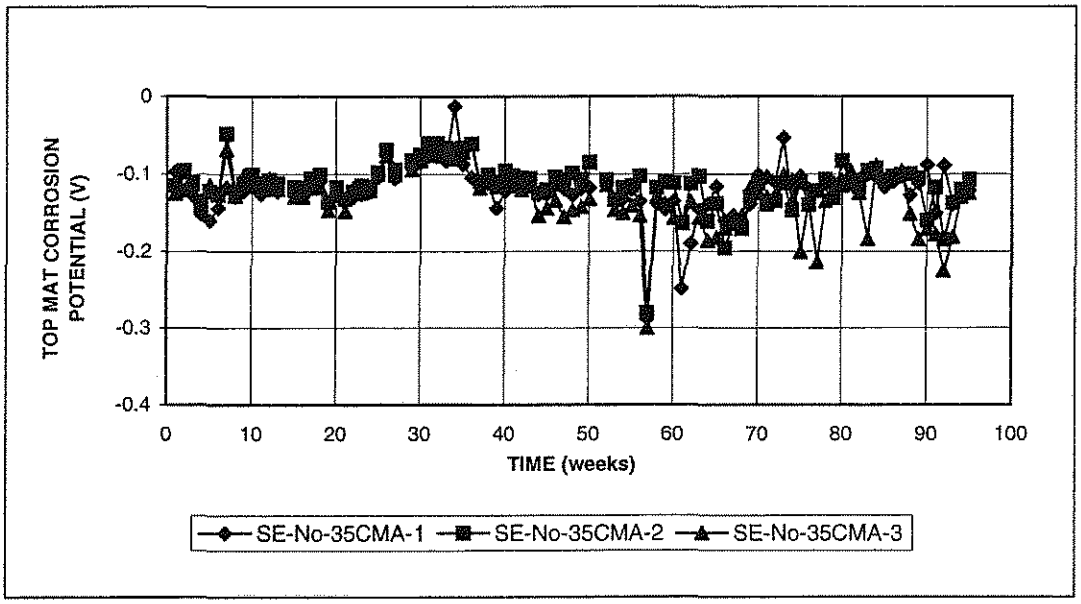

Figure B8.c Southern Exposure Test. Corrosion potential, top mat, conventional steel, normalized, no inhibitors, w/c=0.35, 6.04 m ion CMA.

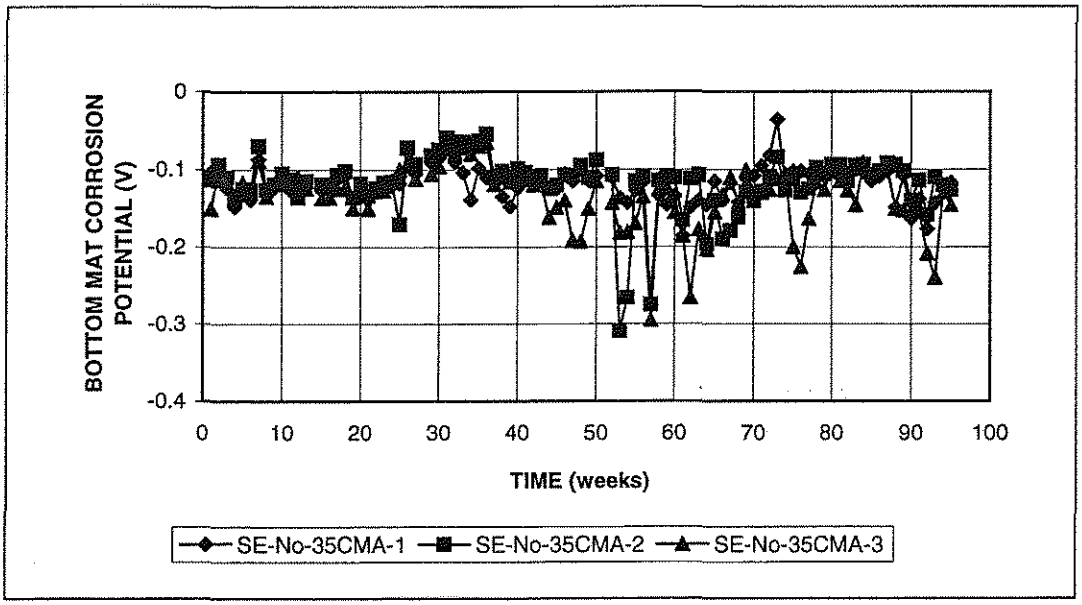

Figure B8.d Southern Exposure Test. Corrosion potential, bottom mat, conventional steel, normalized, no inhibitors, w/c=0.35, 6.04 m ion CMA.

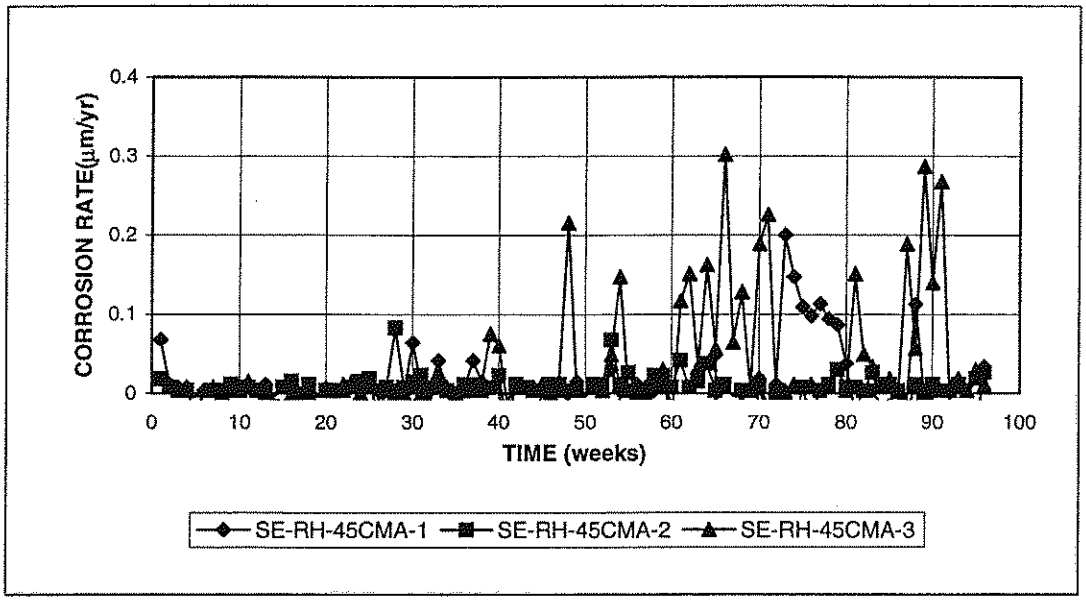

Figure B9.a Southern Exposure Test. Corrosion rate for conventional steel, normalized, Rheocrete, w/c=0.45, 6.04 m ion CMA.

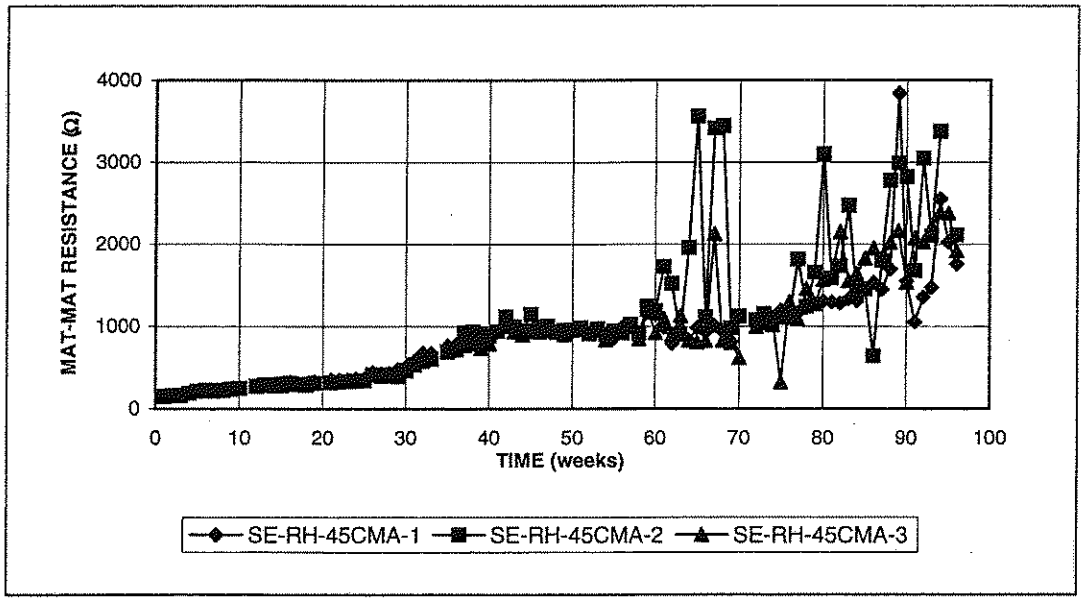

Figure B9.b Southern Exposure Test. Mat-to-mat resistance, conventional steel, normalized, Rheocrete, w/c=0.45, 6.04 m ion CMA.

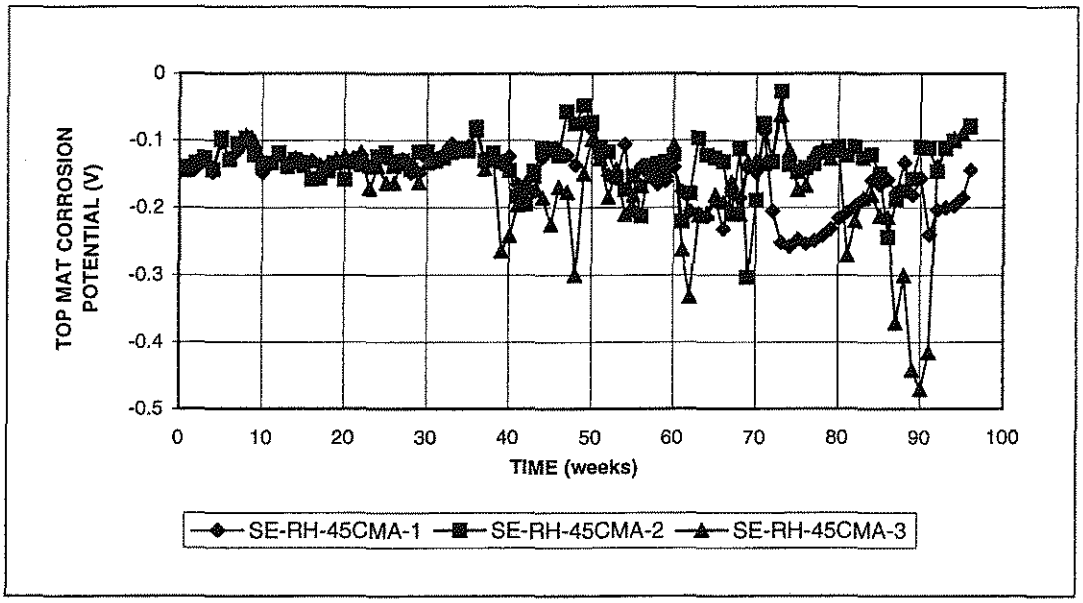

Figure B9.c Southern Exposure Test. Corrosion potential, top mat, conventional steel, normalized, Rheocrete, w/c=0.45, 6.04 m ion CMA.

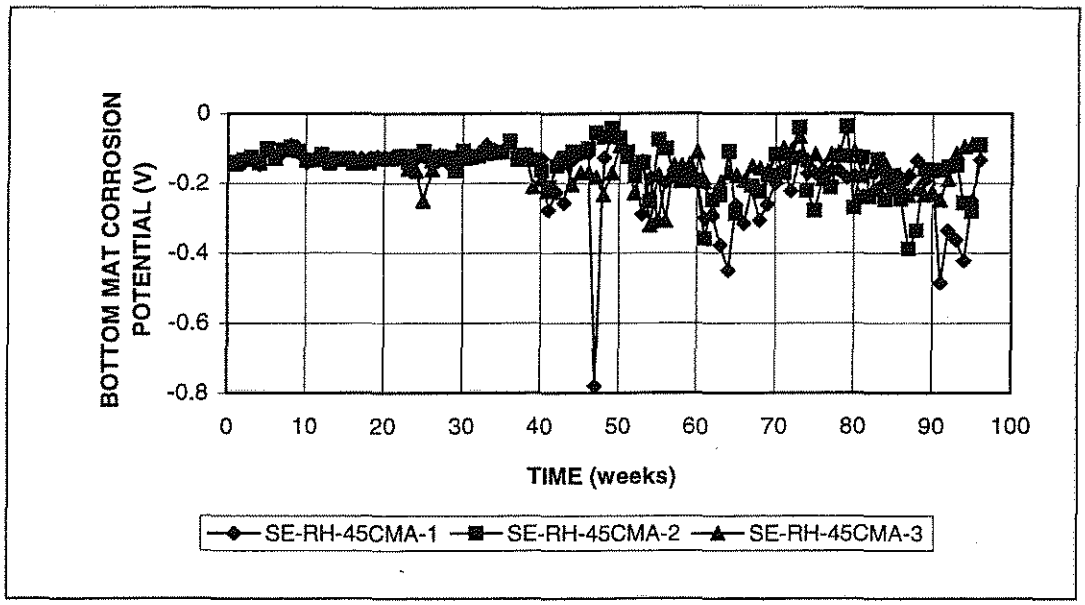

Figure B9.d Southern Exposure Test. Corrosion potential, bottom mat, conventional steel, normalized, Rheocrete, w/c=0.45, 6.04 m ion CMA.

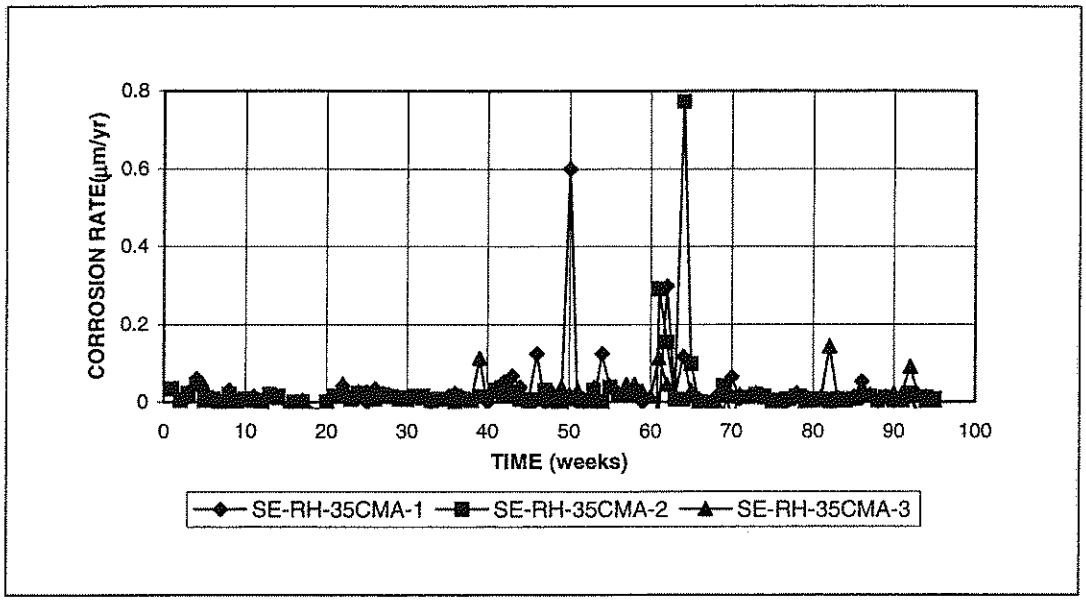

Figure B10.a Southern Exposure Test. Corrosion rate for conventional steel, normalized, Rheocrete, w/c=0.35, 6.04 m ion CMA.

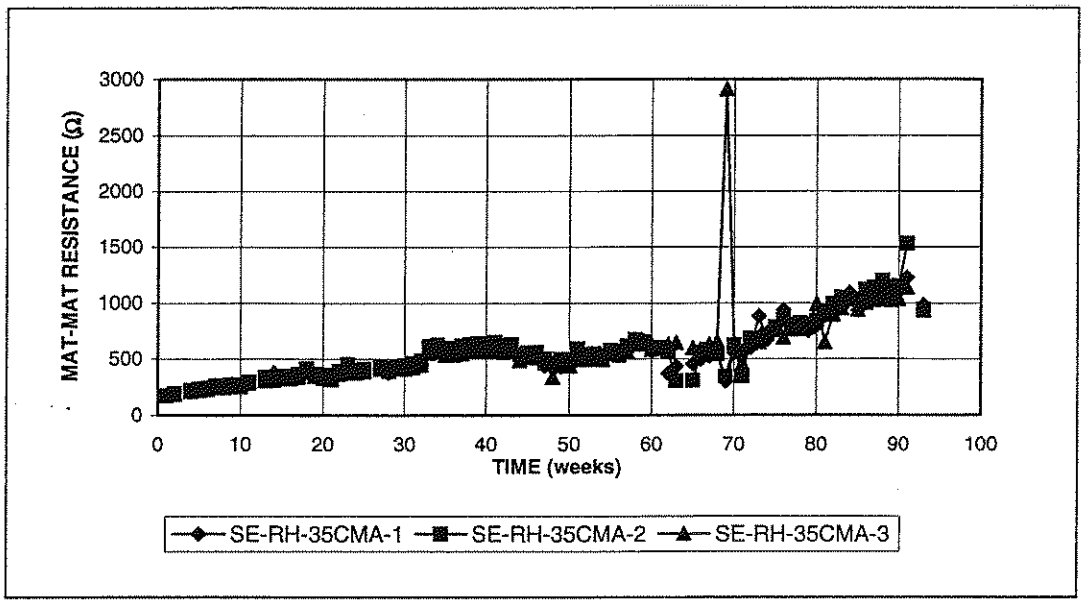

Figure B10.b Southern Exposure Test. Mat-to-mat resistance, conventional steel, normalized, Rheocrete, w/c=0.35, 6.04 m ion CMA.

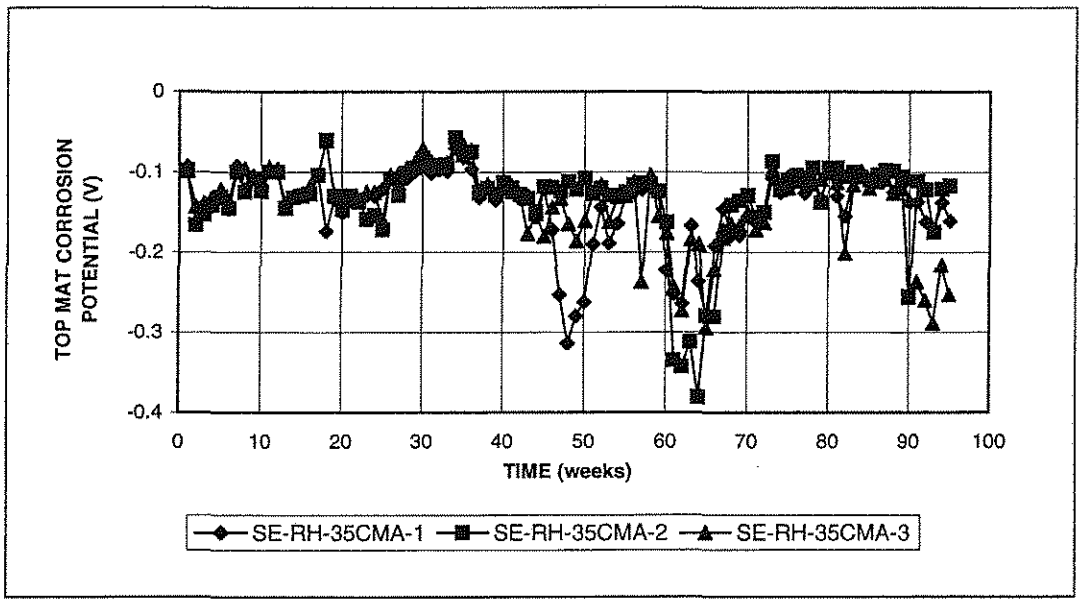

Figure B10.c Southern Exposure Test. Corrosion potential, top mat, conventional steel, normalized, Rheocrete, w/c=0.35, 6.04 m ion CMA.

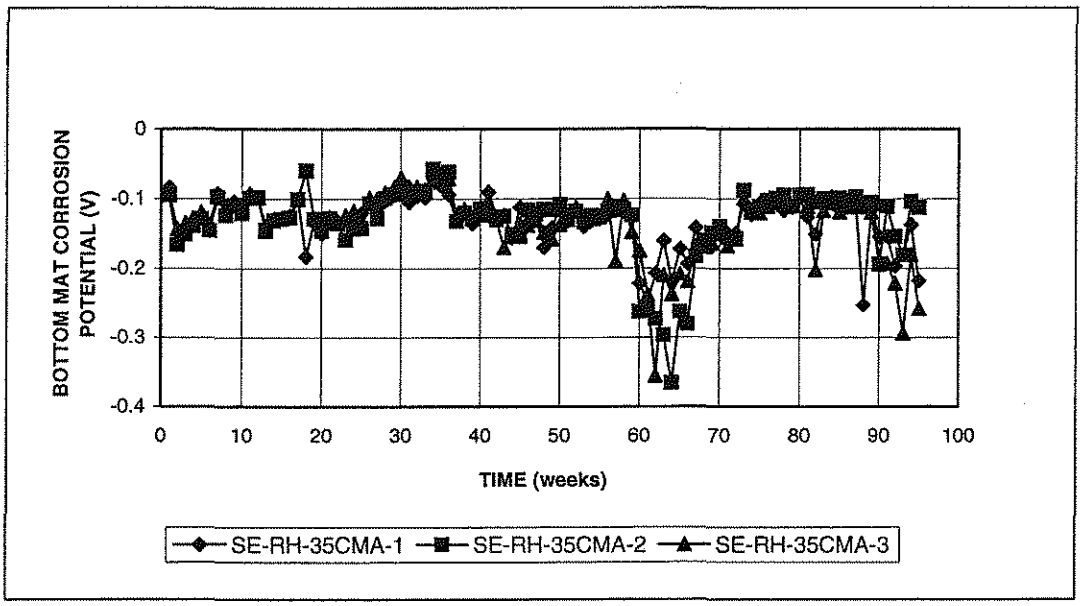

Figure B10.d Southern Exposure Test. Corrosion potential, bottom mat, conventional steel, normalized, Rheocrete, w/c=0.35, 6.04 m ion CMA.

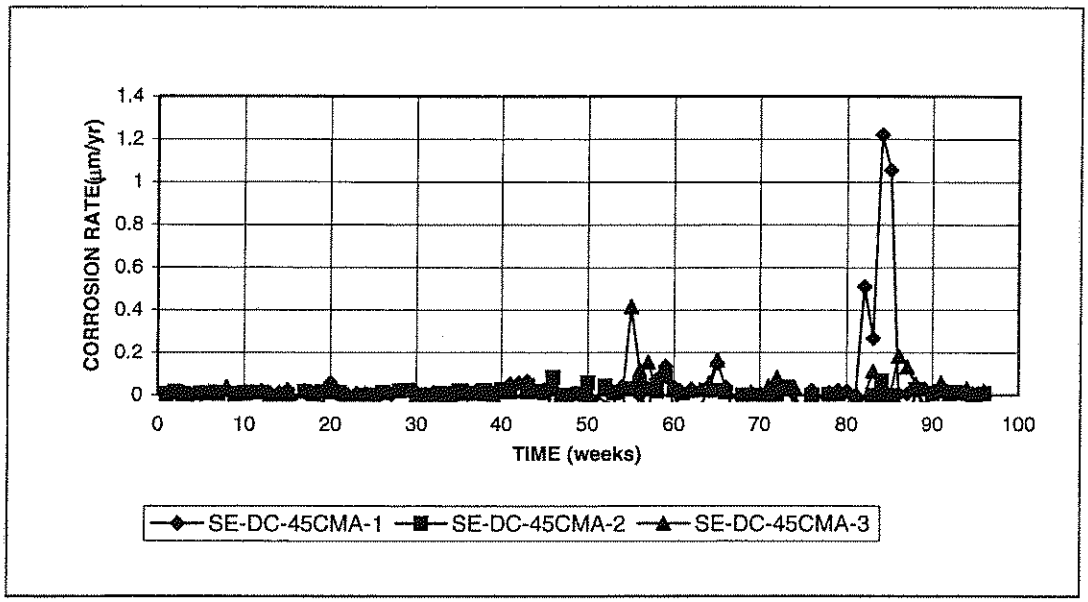

Figure B11.a Southern Exposure Test. Corrosion rate for conventional steel, normalized, DCI-S, w/c=0.45, 6.04 m ion CMA.

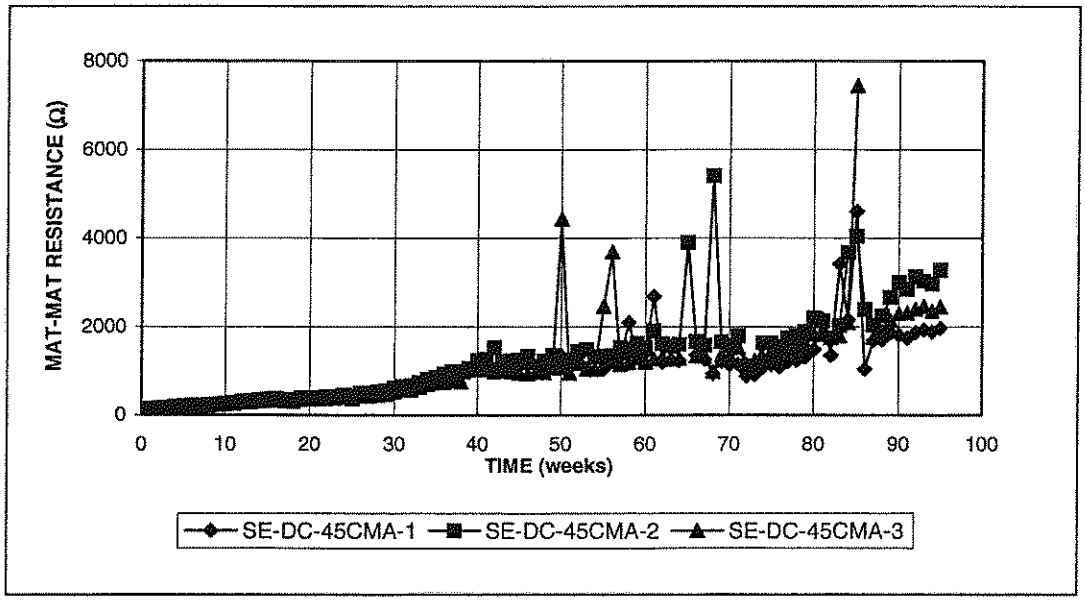

Figure B11.b Southern Exposure Test. Mat-to-mat resistance, conventional steel, normalized, DCI-S, w/c=0.45, 6.04 m ion CMA.

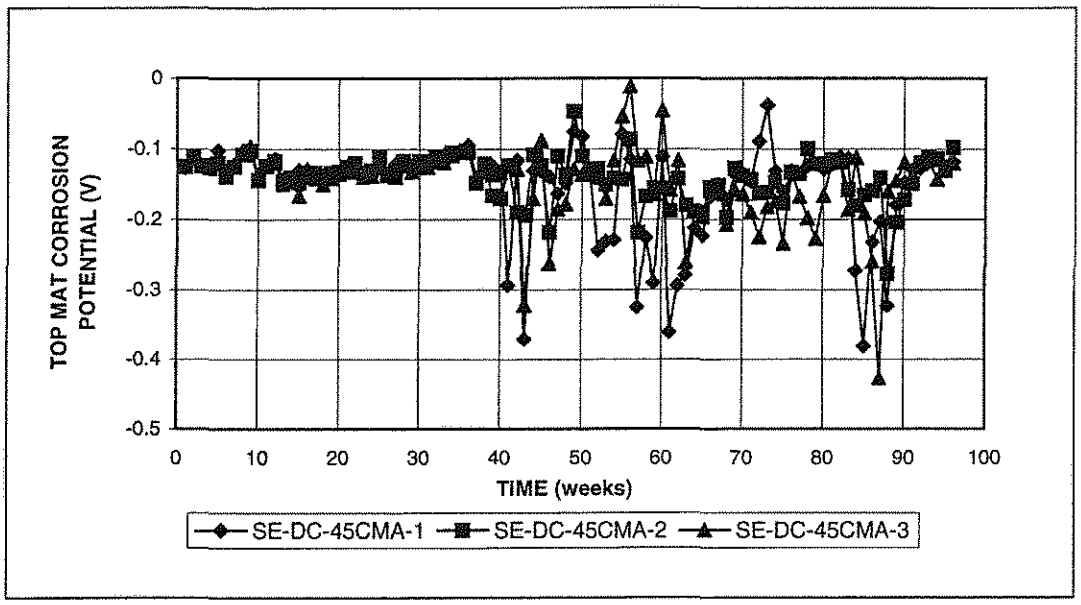

Figure B11.c Southern Exposure Test. Corrosion potential, top mat, conventional steel, normalized, DCI-S, w/c=0.45, 6.04 m ion CMA.

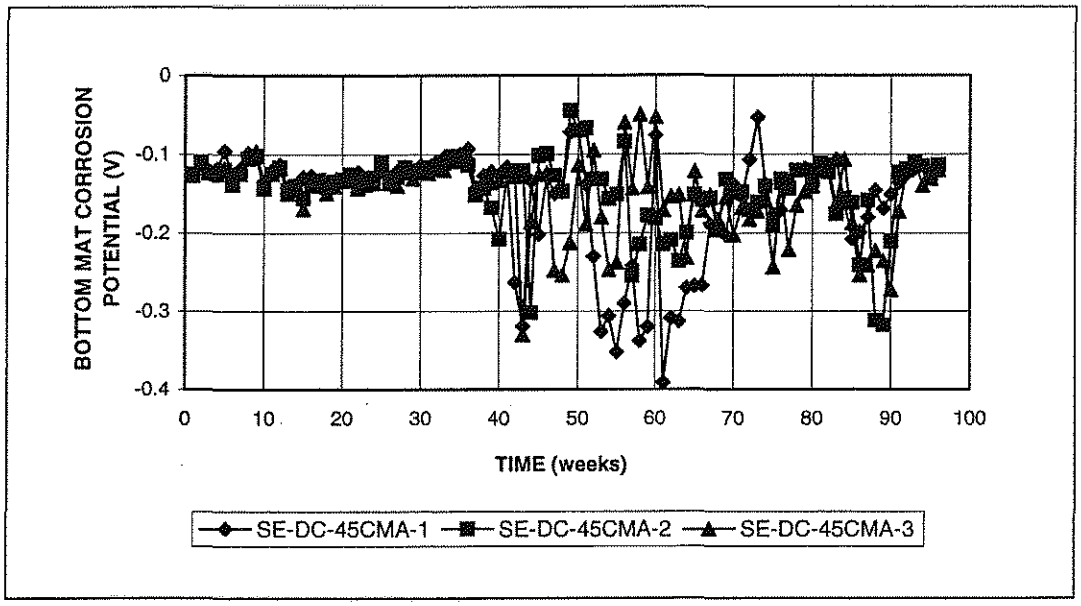

Figure B11.d Southern Exposure Test. Corrosion potential, bottom mat, conventional steel, normalized, DCI-S, w/c=0.45, 6.04 m ion CMA.

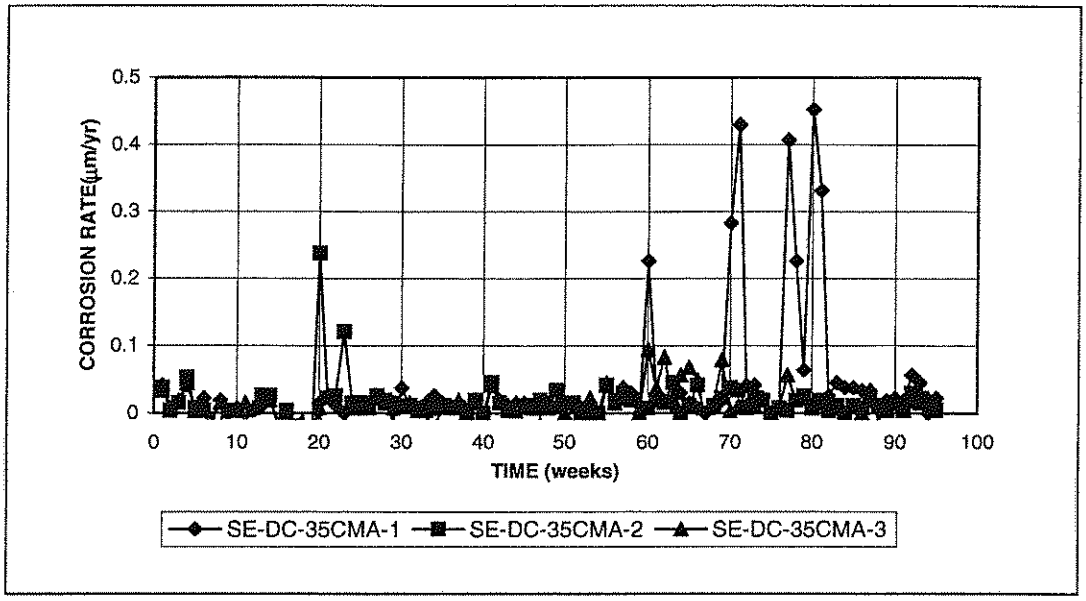

Figure B12.a Southern Exposure Test. Corrosion rate for conventional steel, normalized, DCI-S, w/c=0.35, 6.04 m ion CMA.

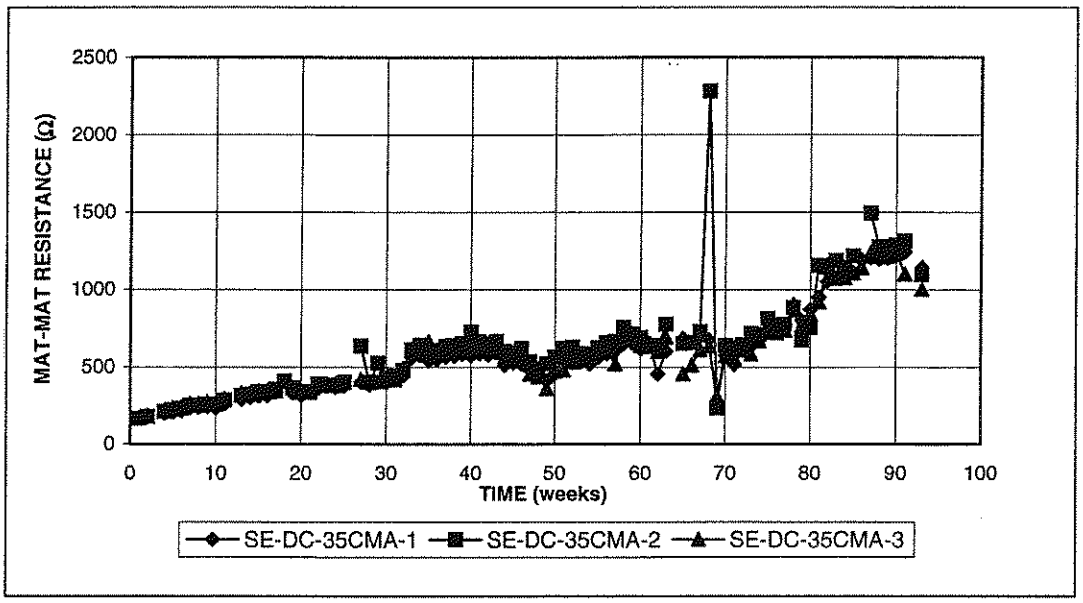

Figure B12.b Southern Exposure Test. Mat-to-mat resistance, conventional steel, normalized, DCI-S, w/c=0.35, 6.04 m ion CMA.

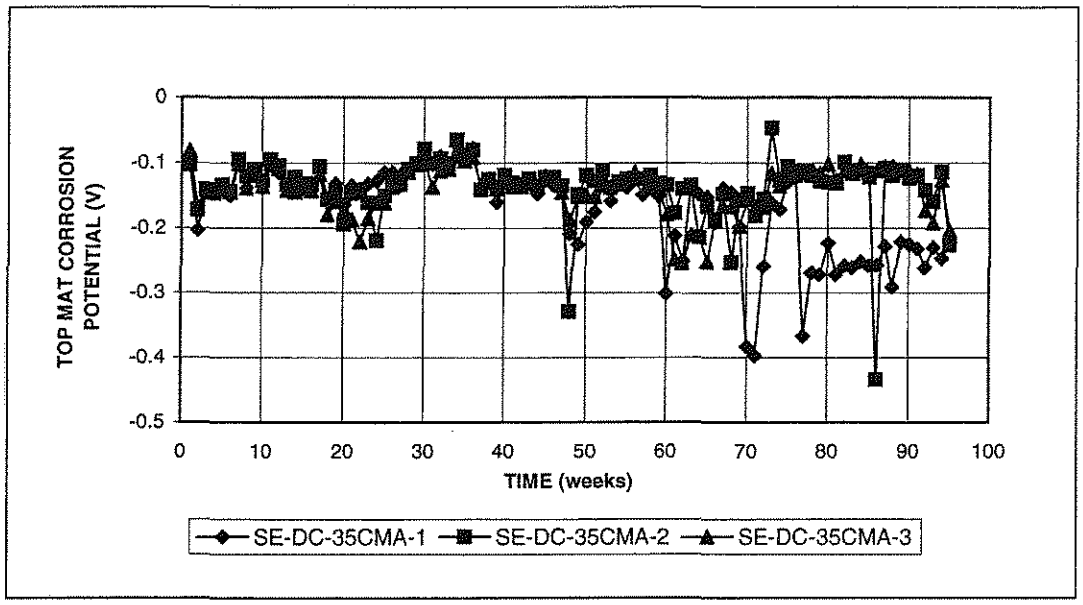

Figure B12.c Southern Exposure Test. Corrosion potential, top mat, conventional steel, normalized, DCI-S, w/c=0.35, 6.04 m ion CMA.

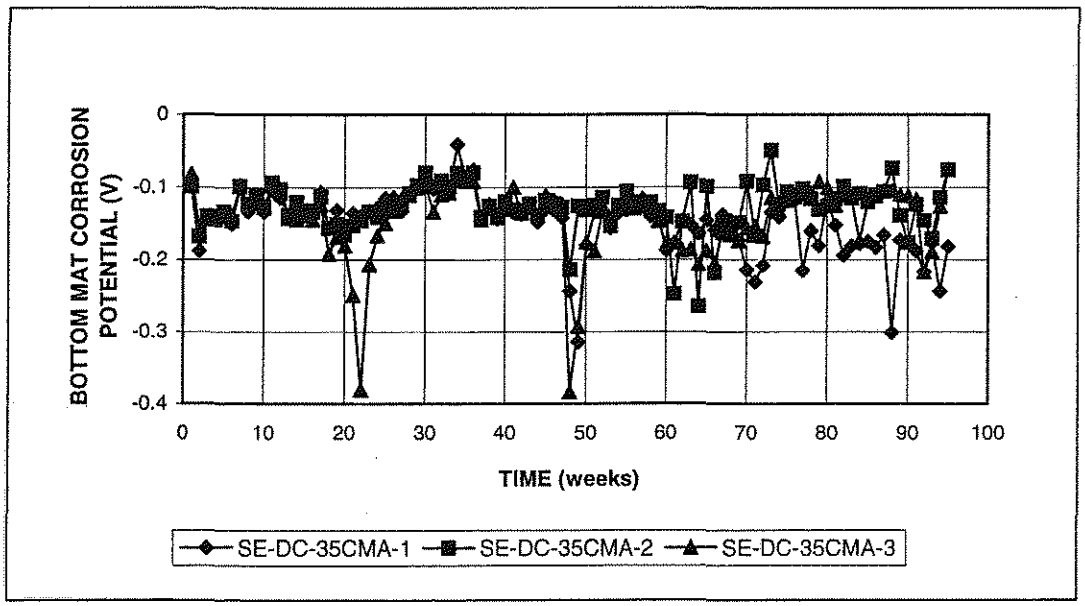

Figure B12.d Southern Exposure Test. Corrosion potential, bottom mat, conventional steel, normalized, DCI-S, w/c=0.35, 6.04 m ion CMA.

Appendix C

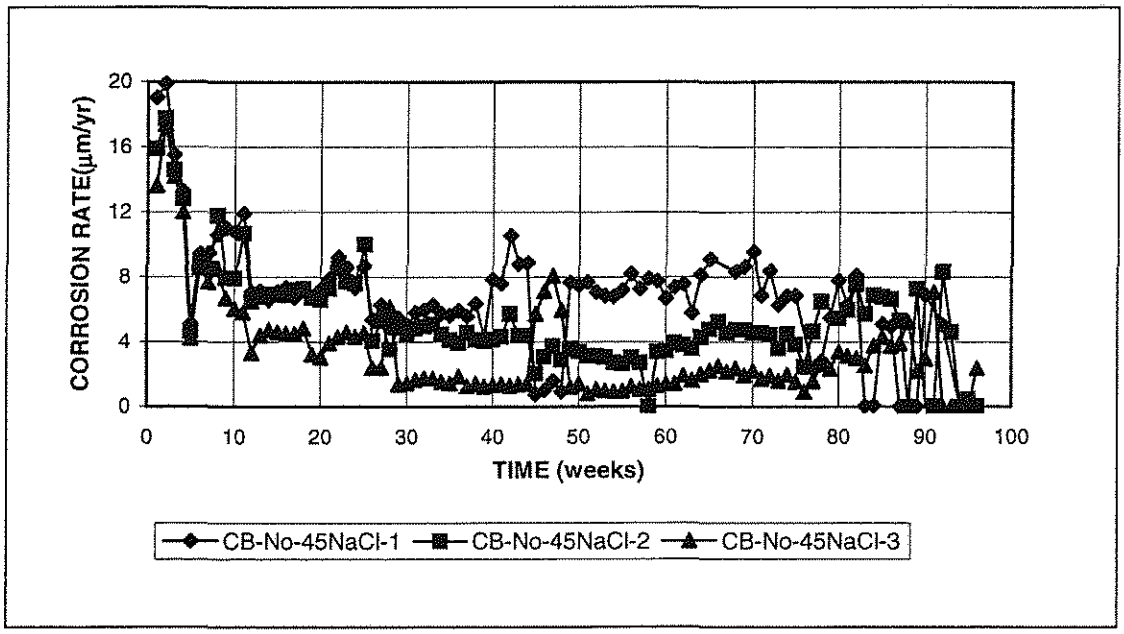

Figure C1.a Cracked Beam Test. Corrosion rate for conventional steel, normalized, no inhibitors, w/c=0.45, 6.04 m ion NaCl.

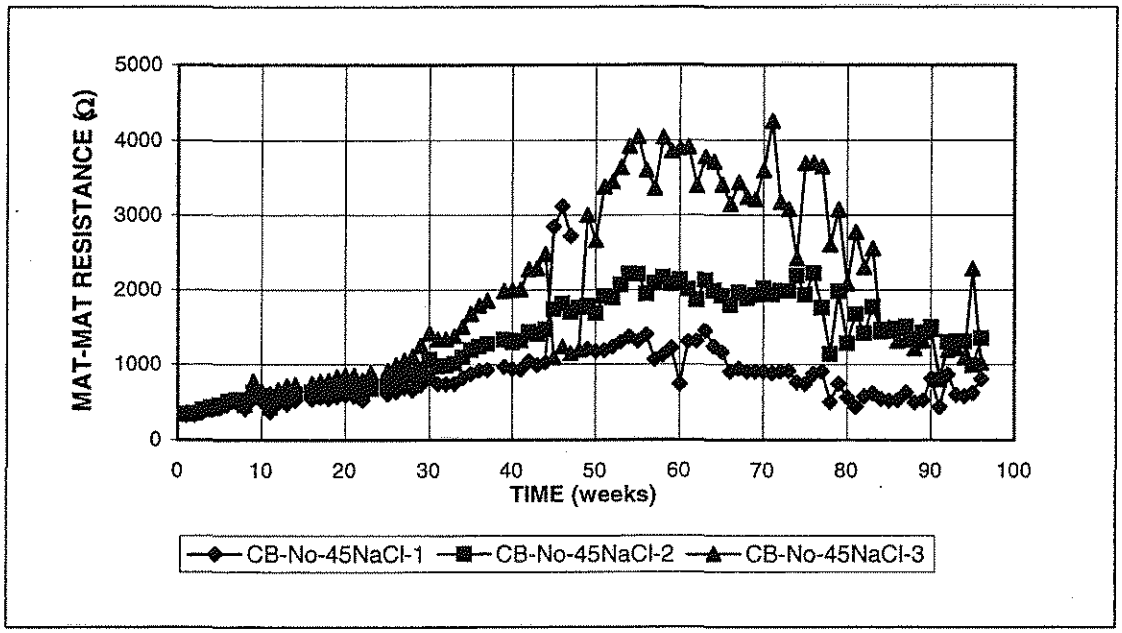

Figure C1.b Cracked Beam Test. Mat-to-mat resistance, conventional steel, normalized, no inhibitors, w/c=0.45, 6.04 m ion NaCl.

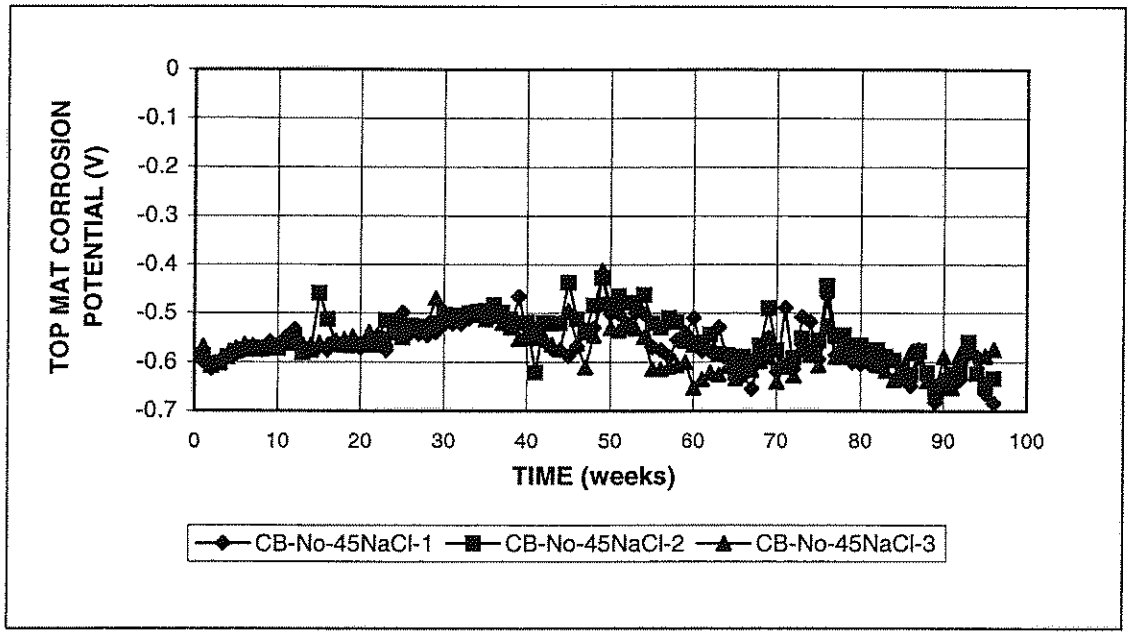

Figure C1.c Cracked Beam Test. Corrosion potential, top mat, conventional steel, normalized, no inhibitors, w/c=0.45, 6.04 m ion NaCl.

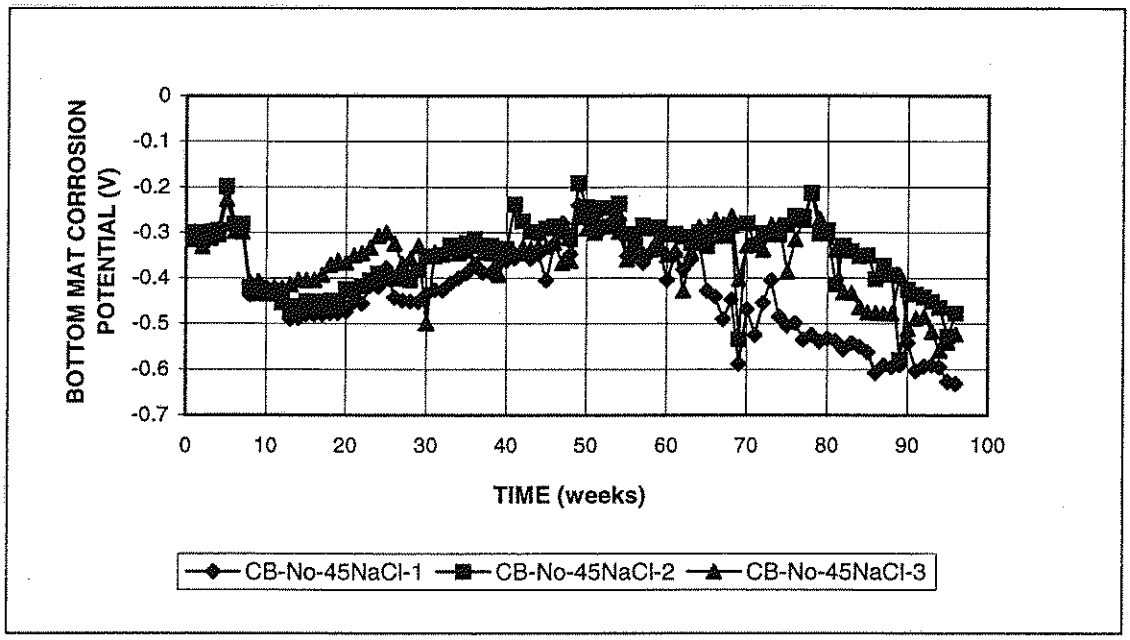

Figure C1.d Cracked Beam Test. Corrosion potential, bottom mat, conventional steel, normalized, no inhibitors, w/c=0.45, 6.04 m ion NaCl.

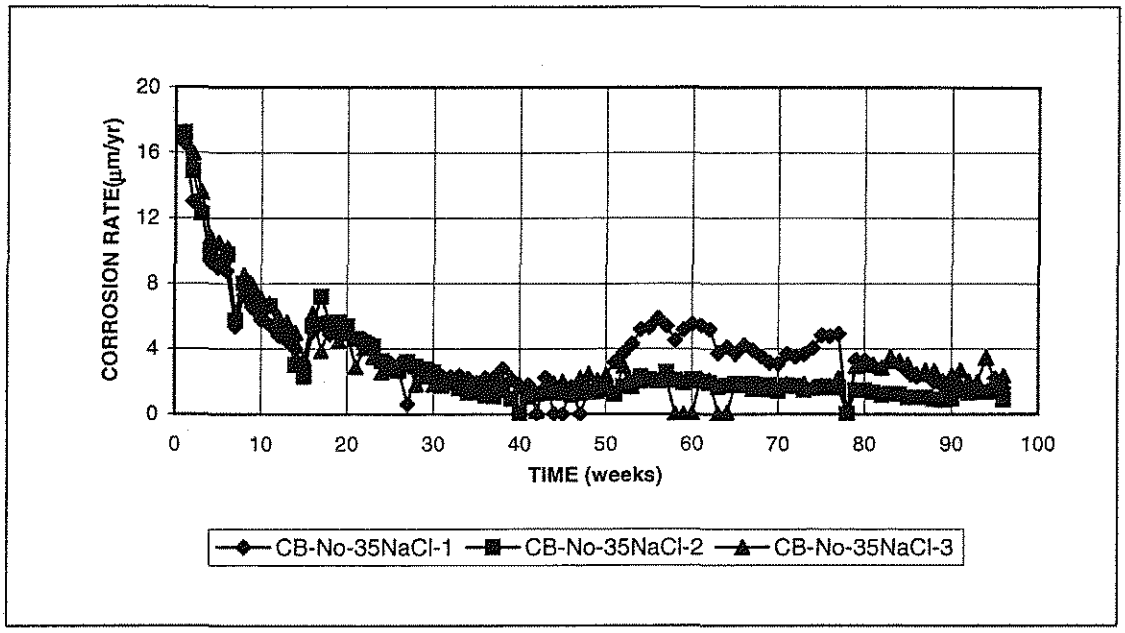

Figure C2.a Cracked Beam Test. Corrosion rate for conventional steel, normalized, no inhibitors, w/c=0.35, 6.04 m ion NaCl.

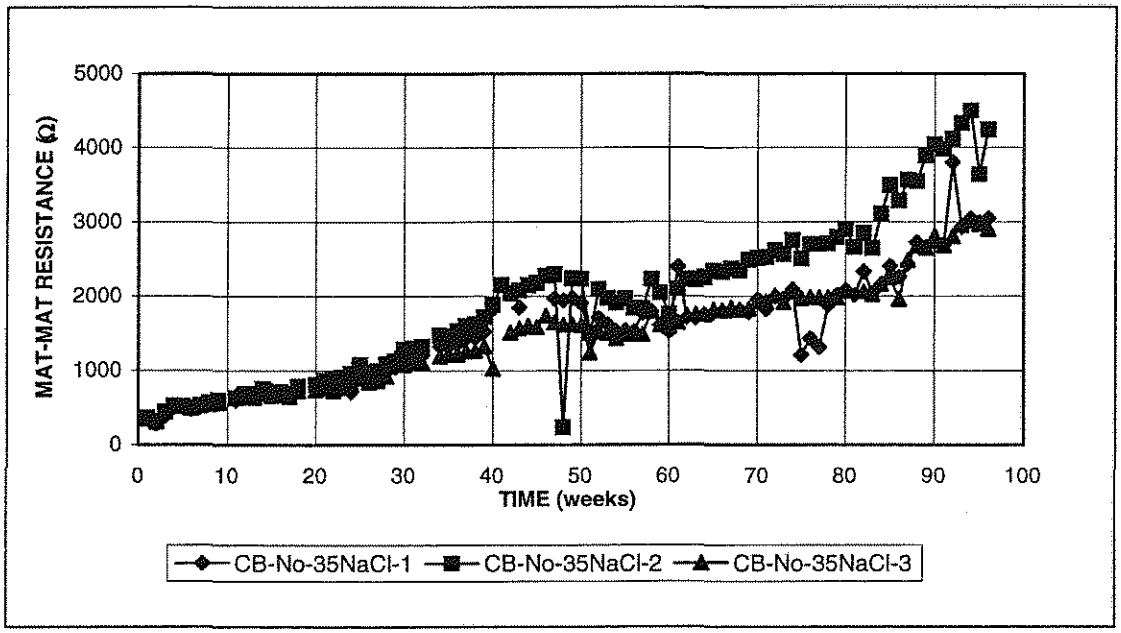

Figure C2.b Cracked Beam Test. Mat-to-mat resistance, conventional steel, normalized, no inhibitors, w/c=0.35, 6.04 m ion NaCl.

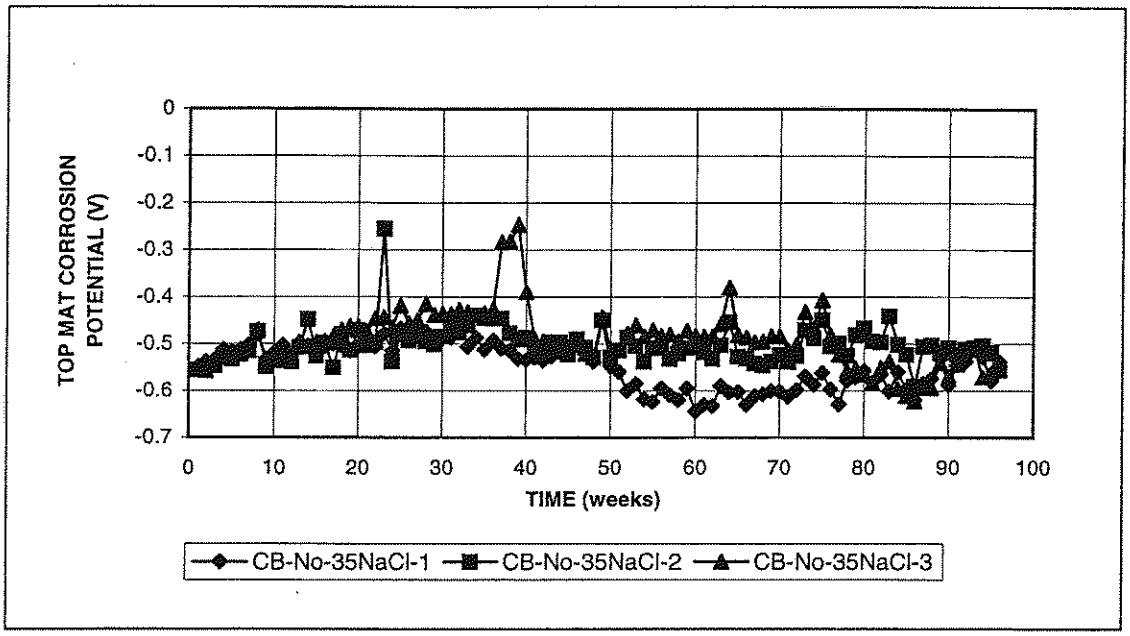

Figure C2.c Cracked Beam Test. Corrosion potential, top mat, conventional steel, normalized, no inhibitors, w/c=0.35, 6.04 m ion NaCl.

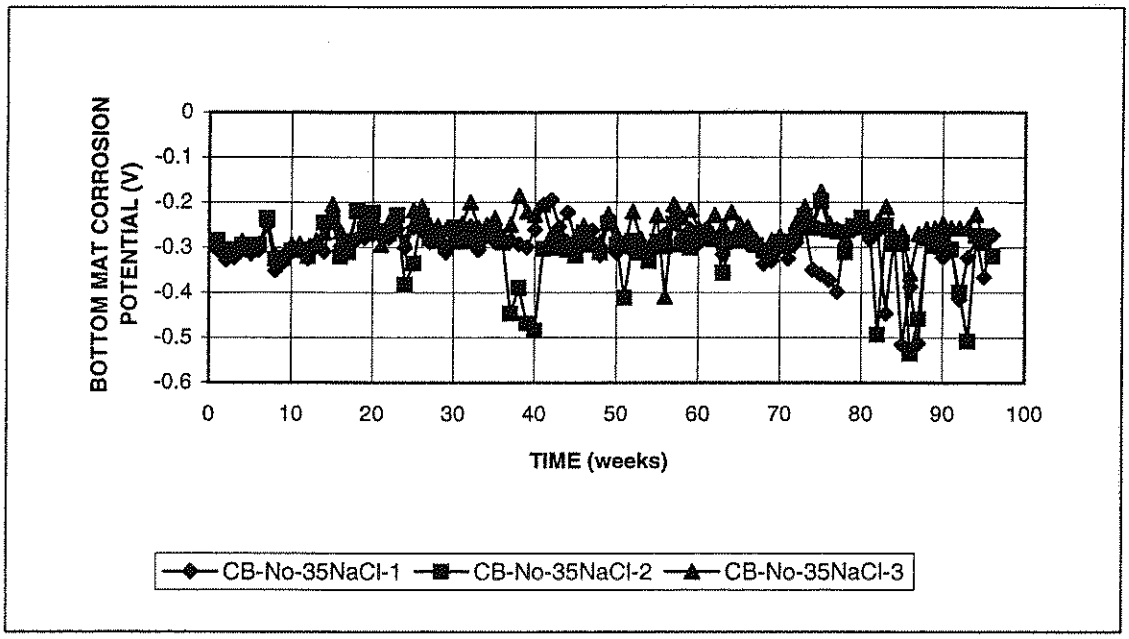

Figure C2.d Cracked Beam Test. Corrosion potential, bottom mat, conventional steel, normalized, no inhibitors, w/c=0.35, 6.04 m ion NaCl.

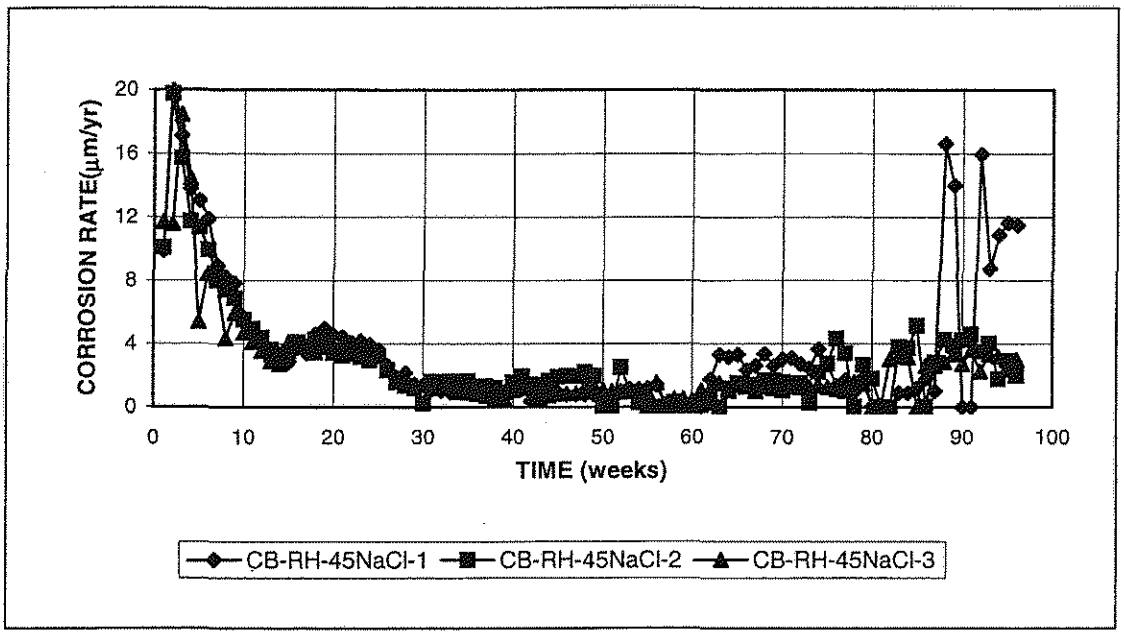

Figure C3.a Cracked Beam Test. Corrosion rate for conventional steel, normalized, Rheocrete, w/c=0.45, 6.04 m ion NaCl.

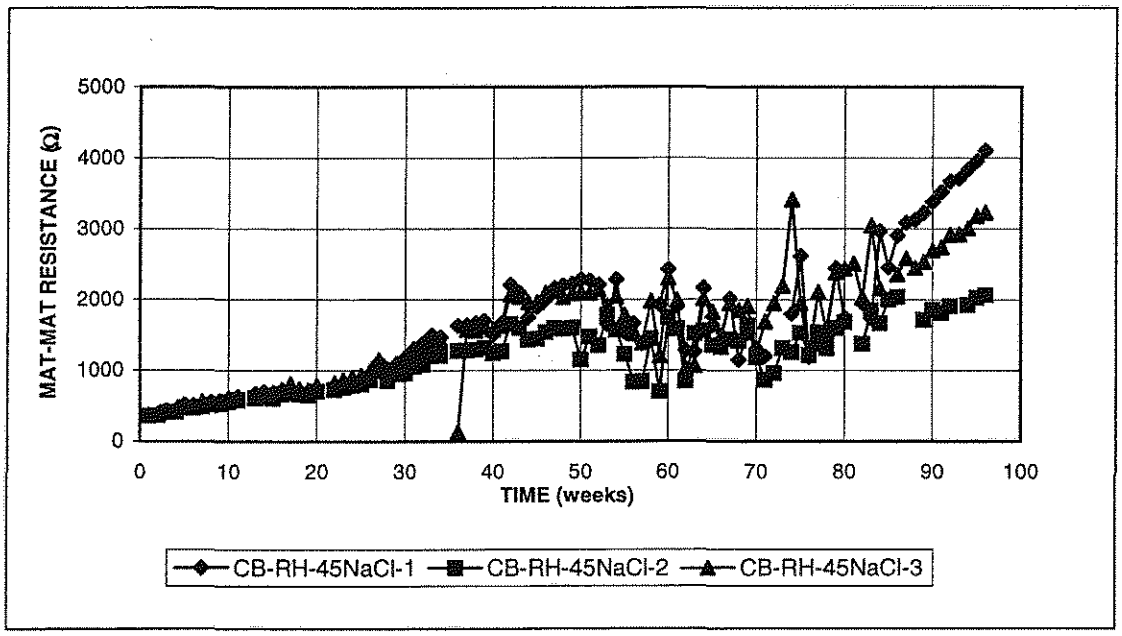

Figure C3.b Cracked Beam Test. Mat-to-mat resistance, conventional steel, normalized, Rheocrete, w/c=0.45, 6.04 m ion NaCl.

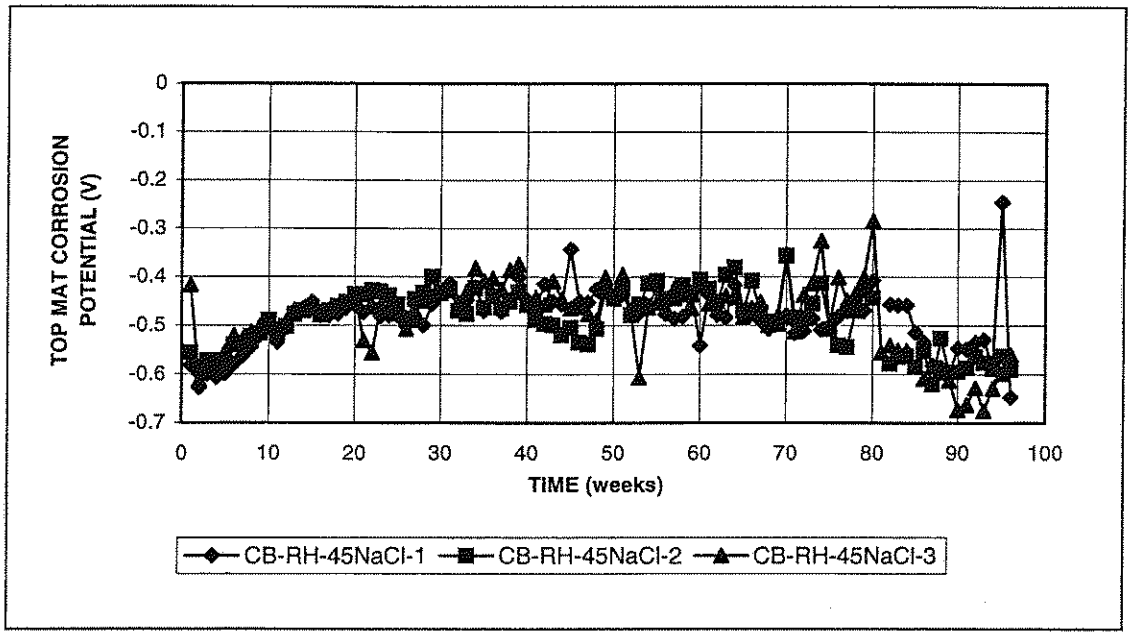

Figure C3.c Cracked Beam Test. Corrosion potential, top mat, conventional steel, normalized, Rheocrete, w/c=0.45, 6.04 m ion NaCl.

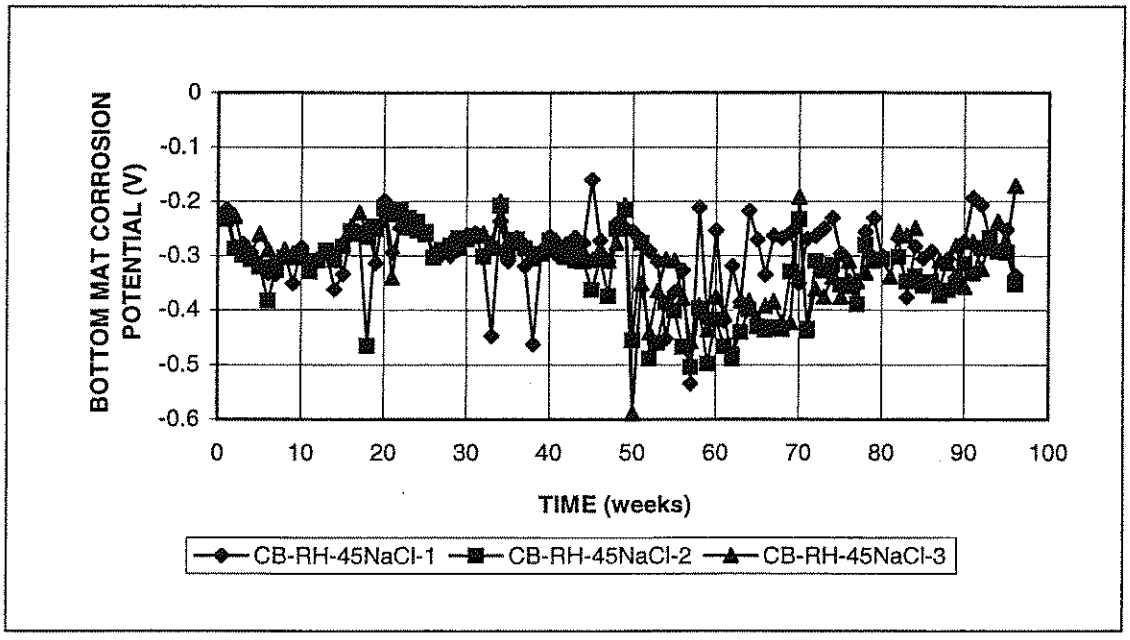

Figure C3.d Cracked Beam Test. Corrosion potential, bottom mat, conventional steel, normalized, Rheocrete, w/c=0.45, 6.04 m ion NaCl.

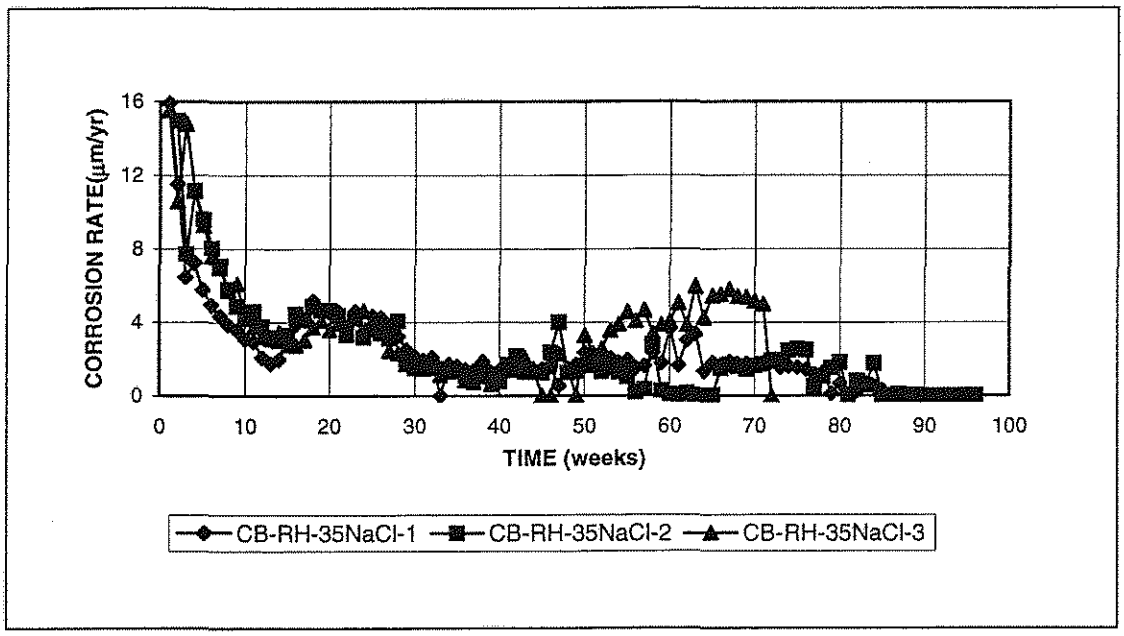

Figure C4.a Cracked Beam Test. Corrosion rate for conventional steel, normalized, Rheocrete, w/c=0.35, 6.04 m ion NaCl.

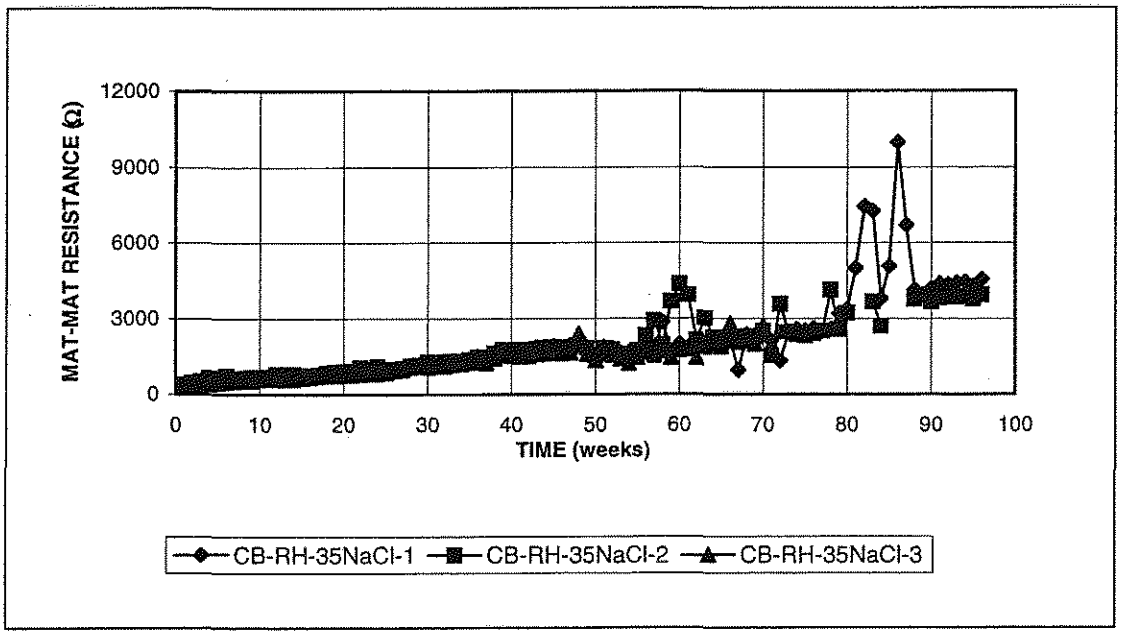

Figure C4.b Cracked Beam Test. Mat-to-mat resistance, conventional steel, normalized, Rheocrete, w/c=0.35, 6.04 m ion NaCl.

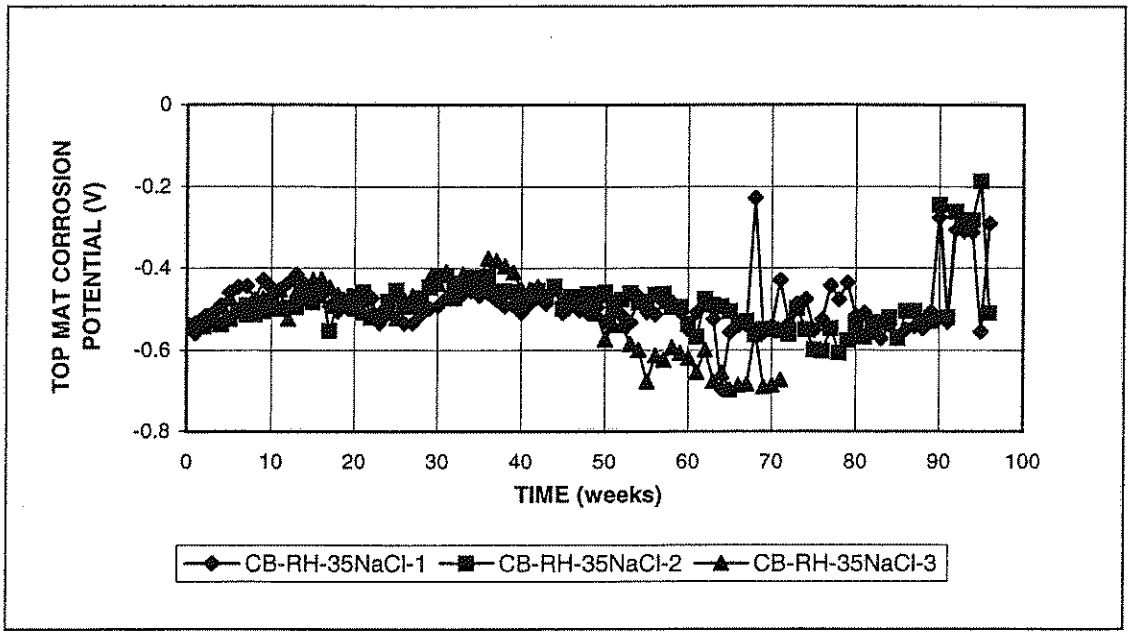

Figure C4.c Cracked Beam Test. Corrosion potential, top mat, conventional steel, normalized, Rheocrete, w/c=0.35, 6.04 m ion NaCl.

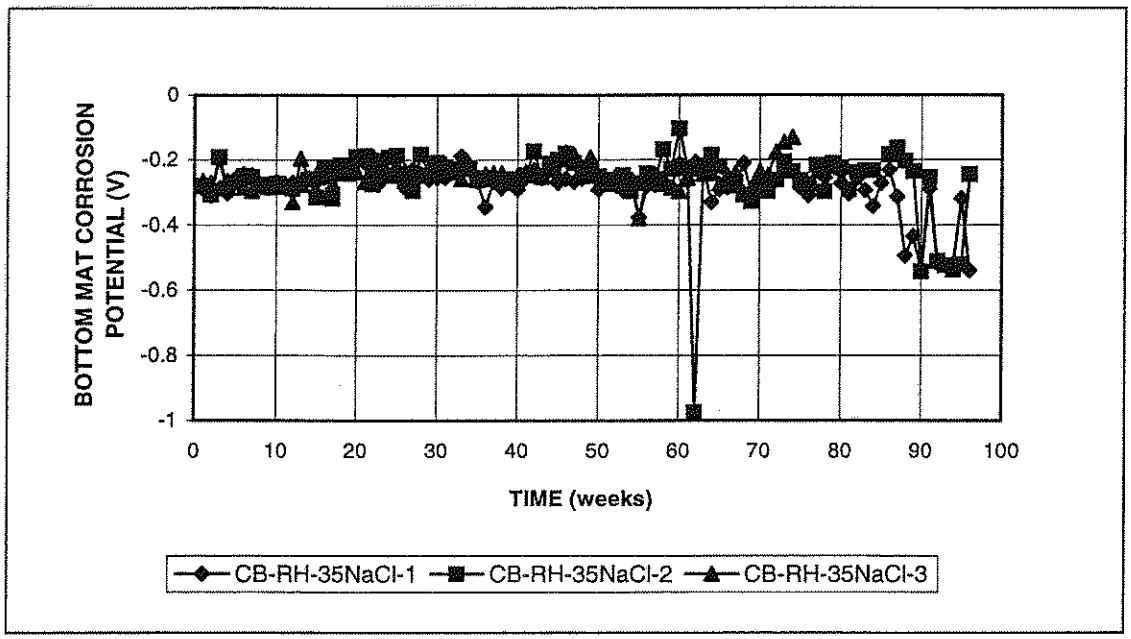

Figure C4.d Cracked Beam Test. Corrosion potential, bottom mat, conventional steel, normalized, Rheocrete, w/c=0.35, 6.04 m ion NaCl.

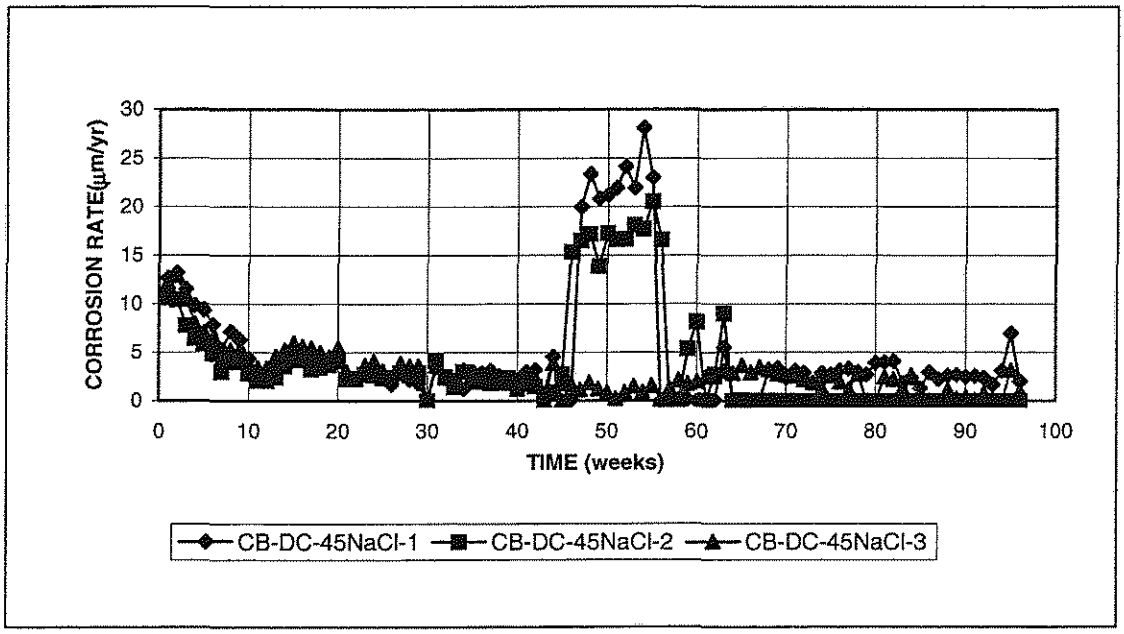

Figure C5.a Cracked Beam Test. Corrosion rate for conventional steel, normalized, DCI-S, w/c=0.45, 6.04 m ion NaCl.

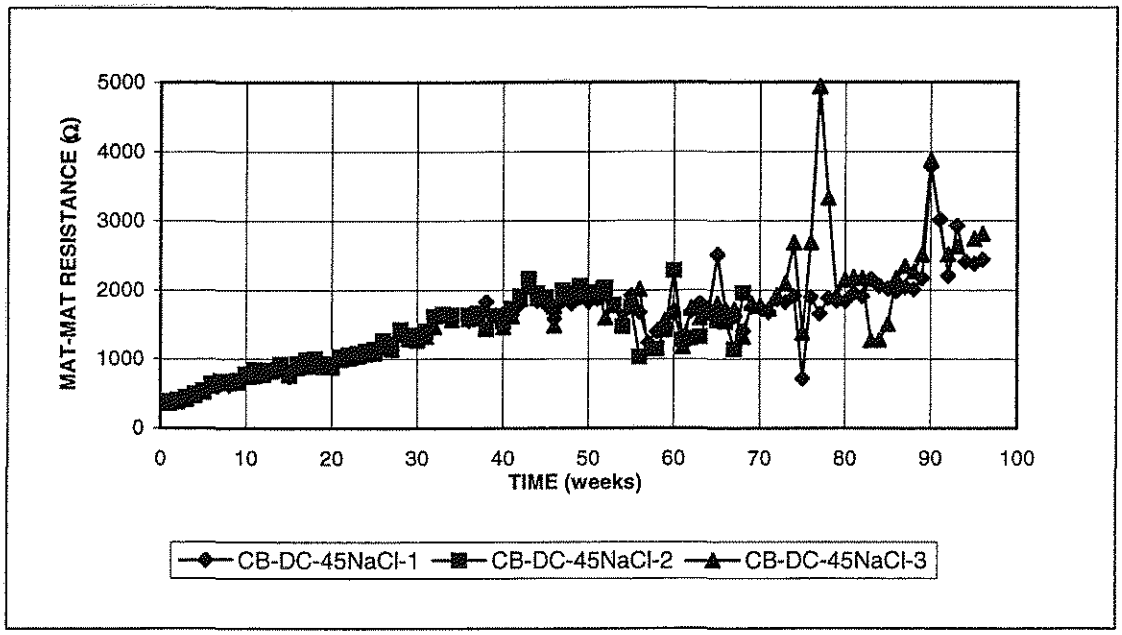

Figure C5.b Cracked Beam Test. Mat-to-mat resistance, conventional steel, normalized, DCI-S, w/c=0.45, 6.04 m ion NaCl.

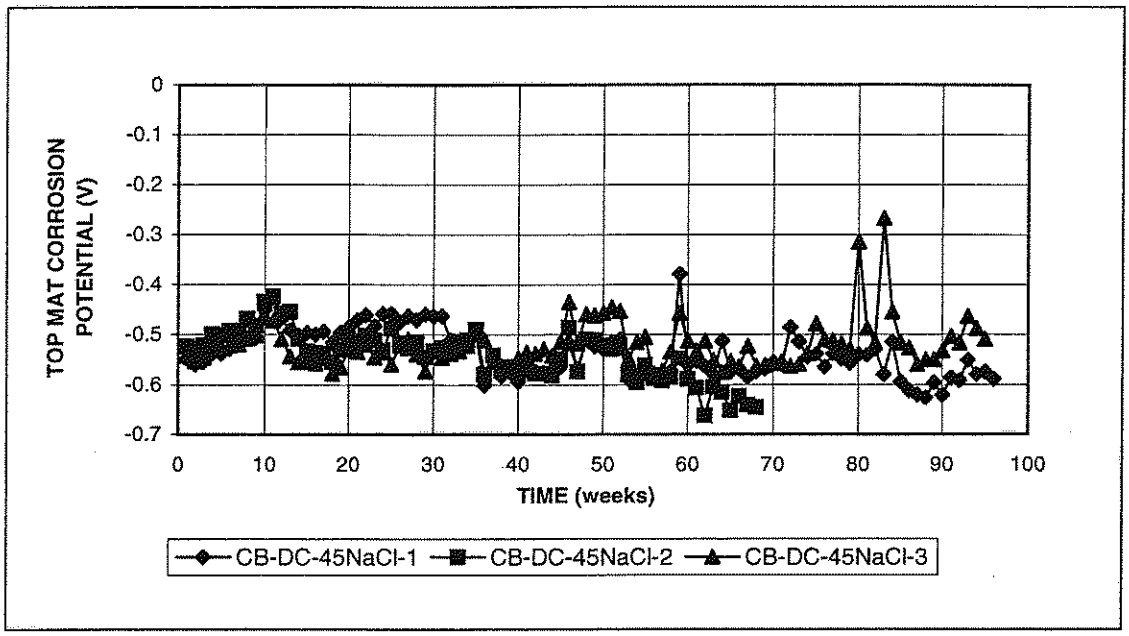

Figure C5.c Cracked Beam Test. Corrosion potential, top mat, conventional steel, normalized, DCI-S, w/c=0.45, 6.04 m ion NaCl.

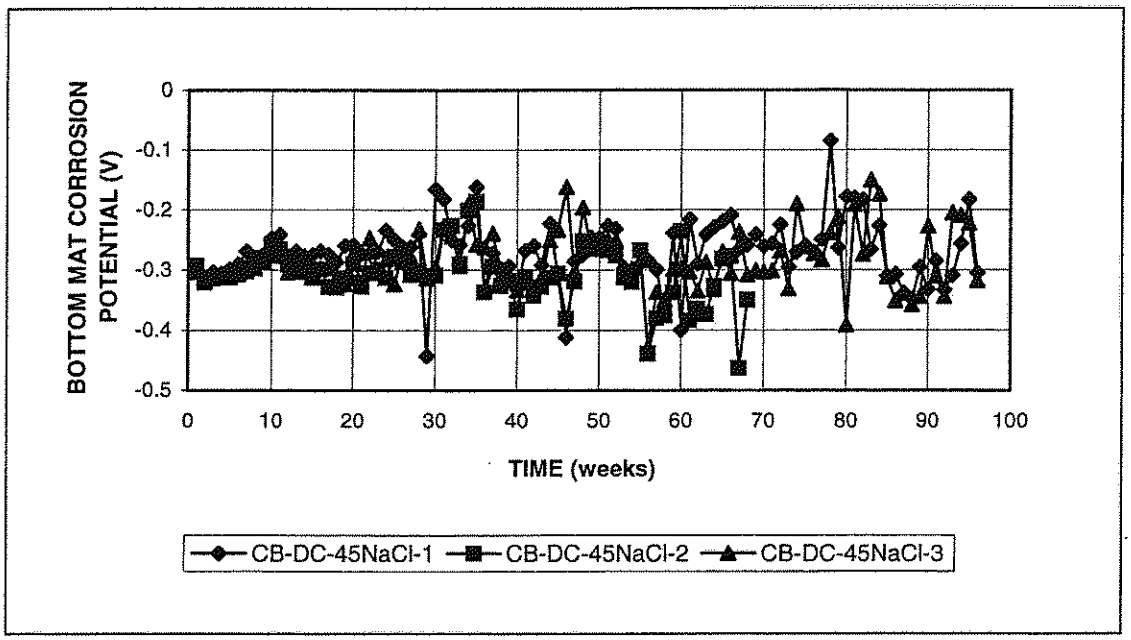

Figure C5.d Cracked Beam Test. Corrosion potential, bottom mat, conventional steel, normalized, DCI-S, w/c=0.45, 6.04 m ion NaCl.

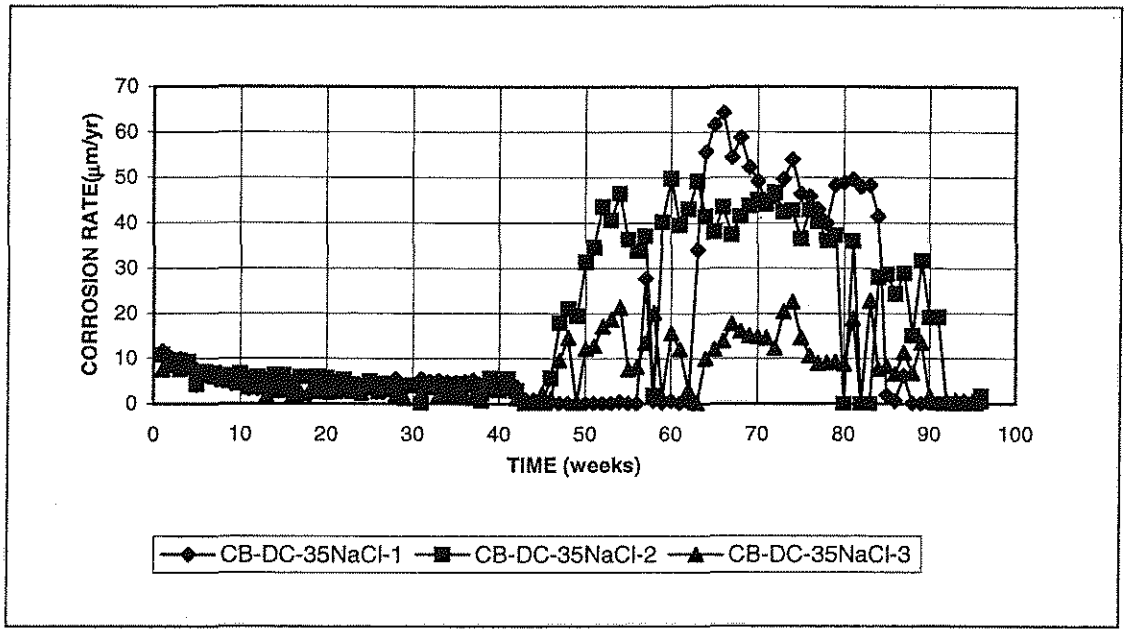

Figure C6.a Cracked Beam Test. Corrosion rate for conventional steel, normalized, DCI-S, w/c=0.35, 6.04 m ion NaCl.

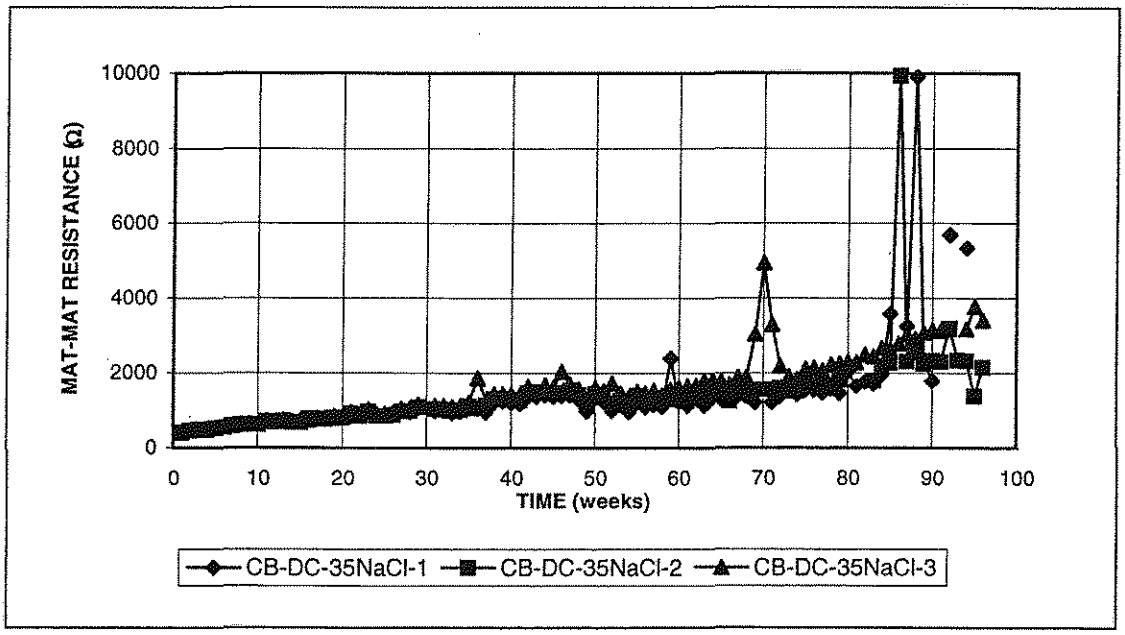

Figure C6.b Cracked Beam Test. Mat-to-mat resistance, conventional steel, normalized, DCI-S, w/c=0.35, 6.04 m ion NaCl.

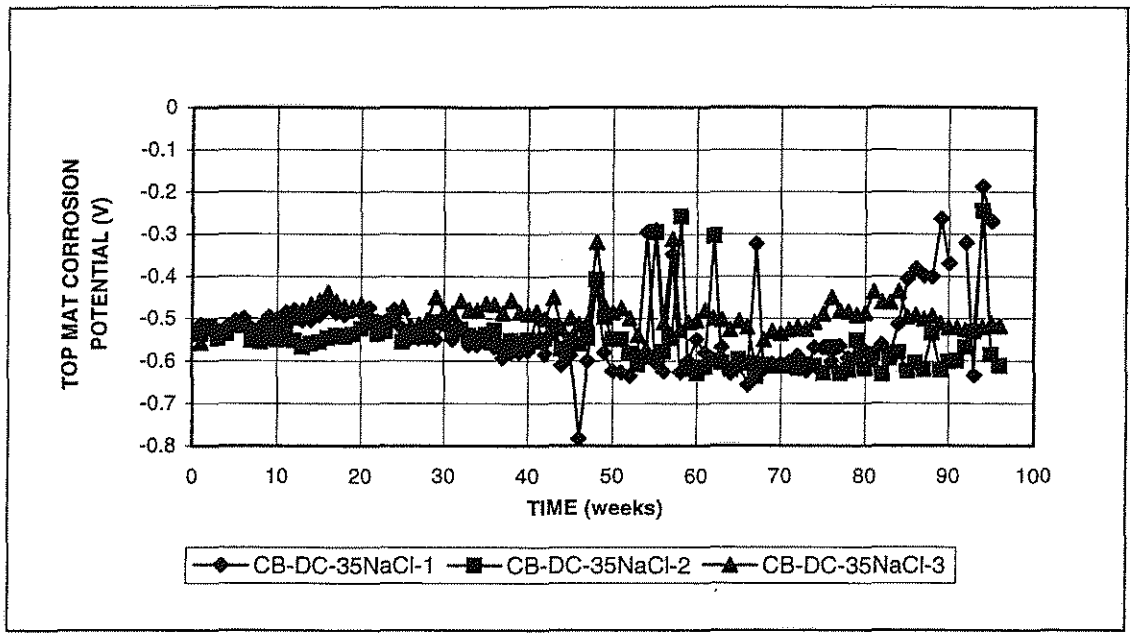

Figure C6.c Cracked Beam Test. Corrosion potential, top mat, conventional steel, normalized, DCI-S, w/c=0.35, 6.04 m ion NaCl.

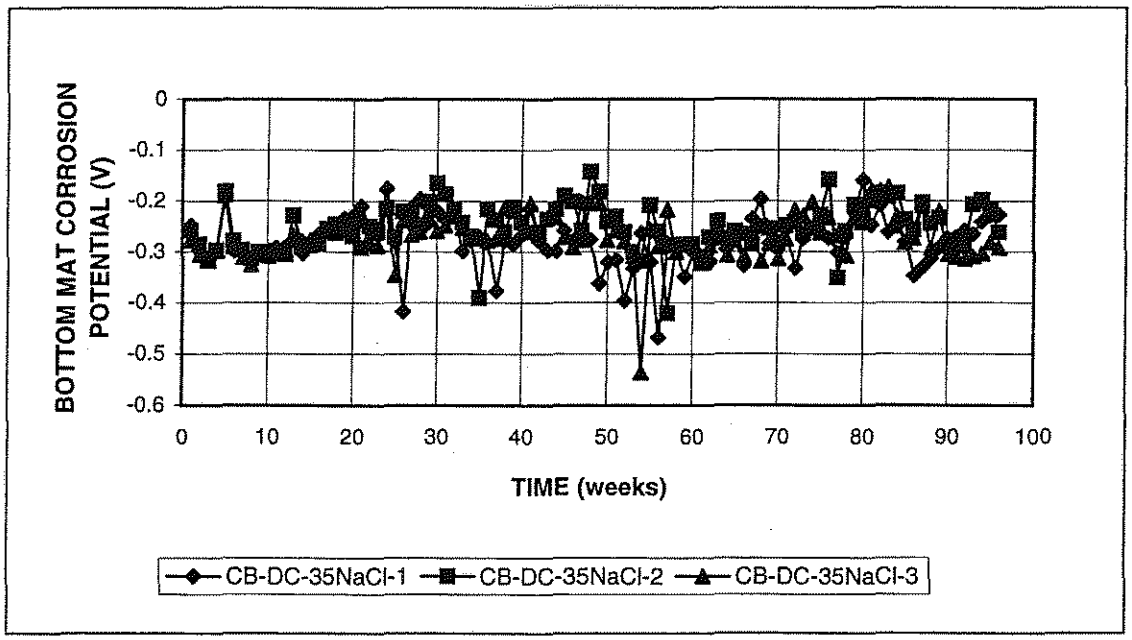

Figure C6.d Cracked Beam Test. Corrosion potential, bottom mat, conventional steel, normalized, DCI-S, w/c=0.35, 6.04 m ion NaCl.

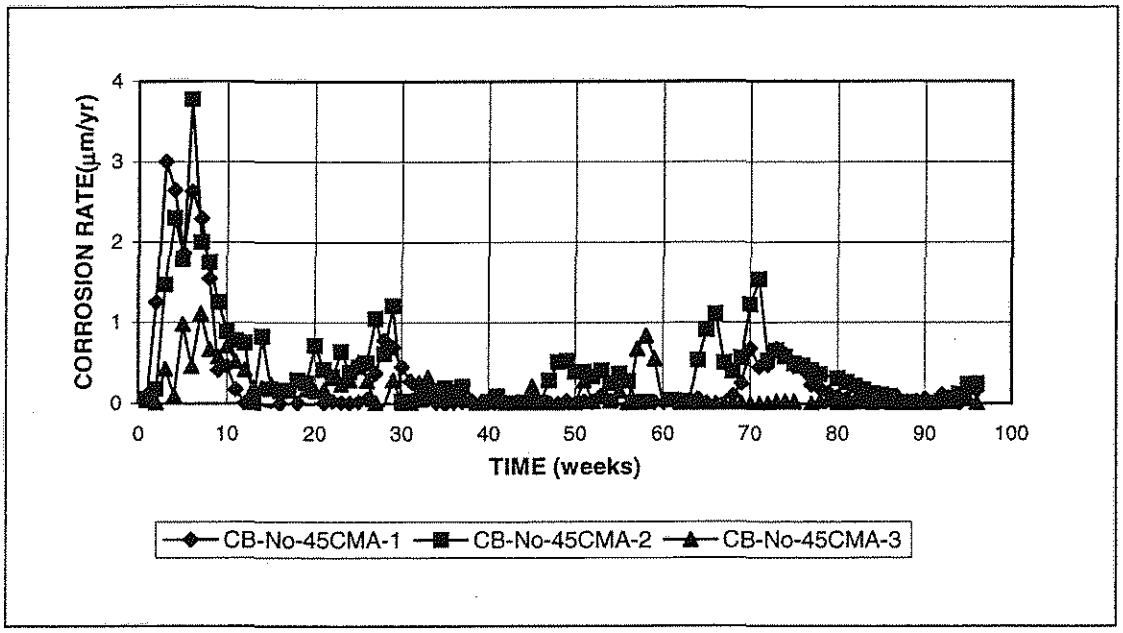

Figure C7.a Cracked Beam Test. Corrosion rate for conventional steel, normalized, no inhibitors, w/c=0.45, 6.04 m ion CMA.

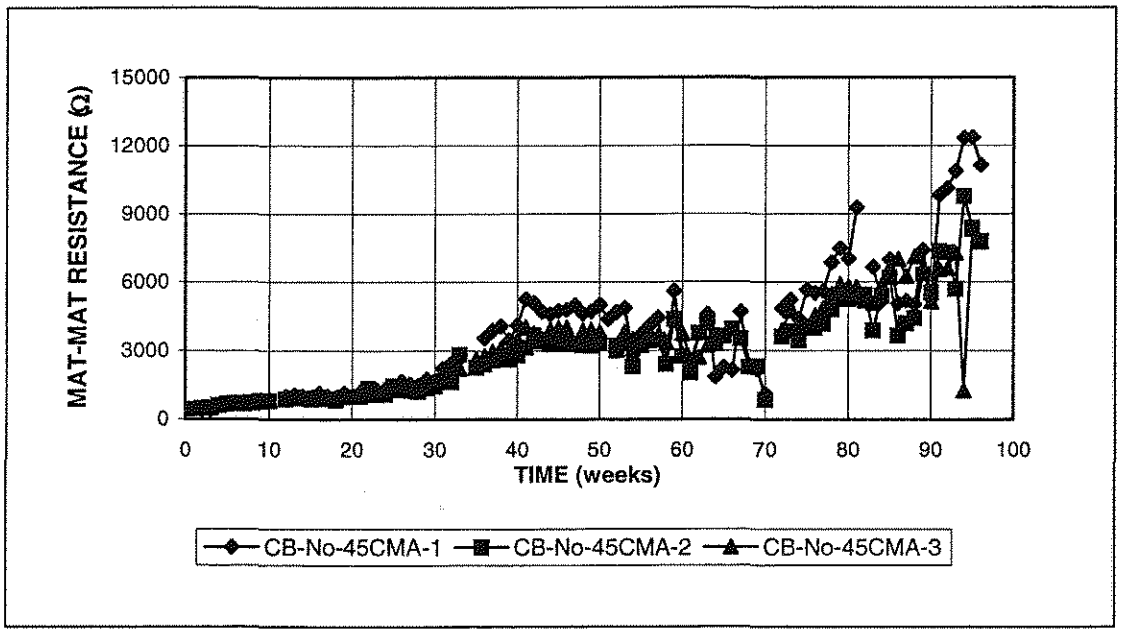

Figure C7.b Cracked Beam Test. Mat-to-mat resistance, conventional steel, normalized, no inhibitors, w/c=0.45, 6.04 m ion CMA.

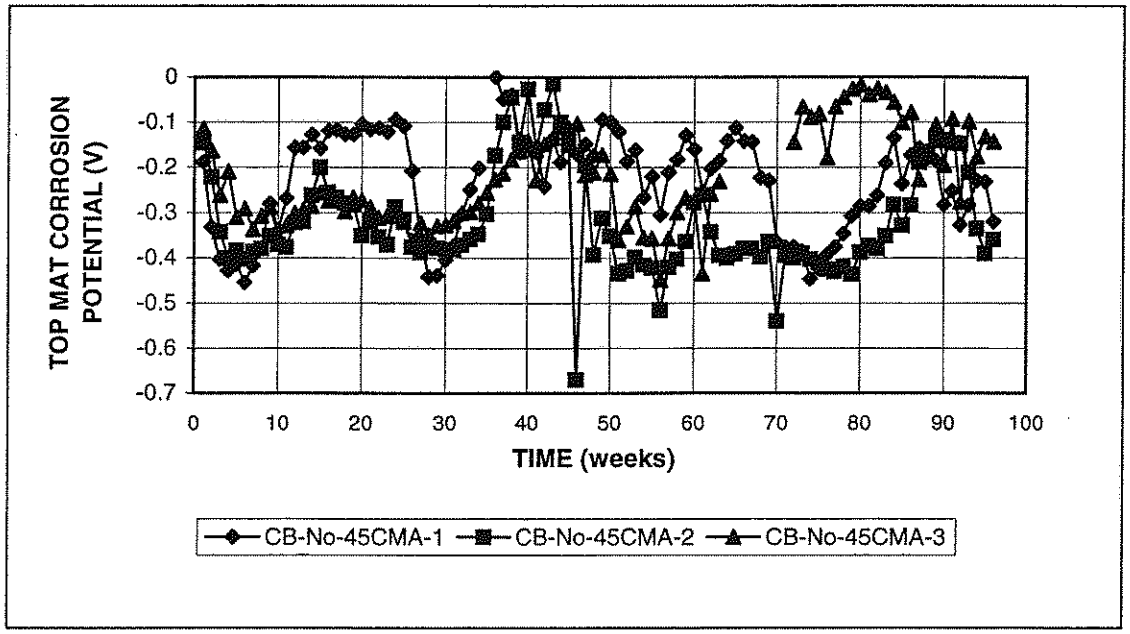

Figure C7.c Cracked Beam Test. Corrosion potential, top mat, conventional steel, normalized, no inhibitors, w/c=0.45, 6.04 m ion CMA.

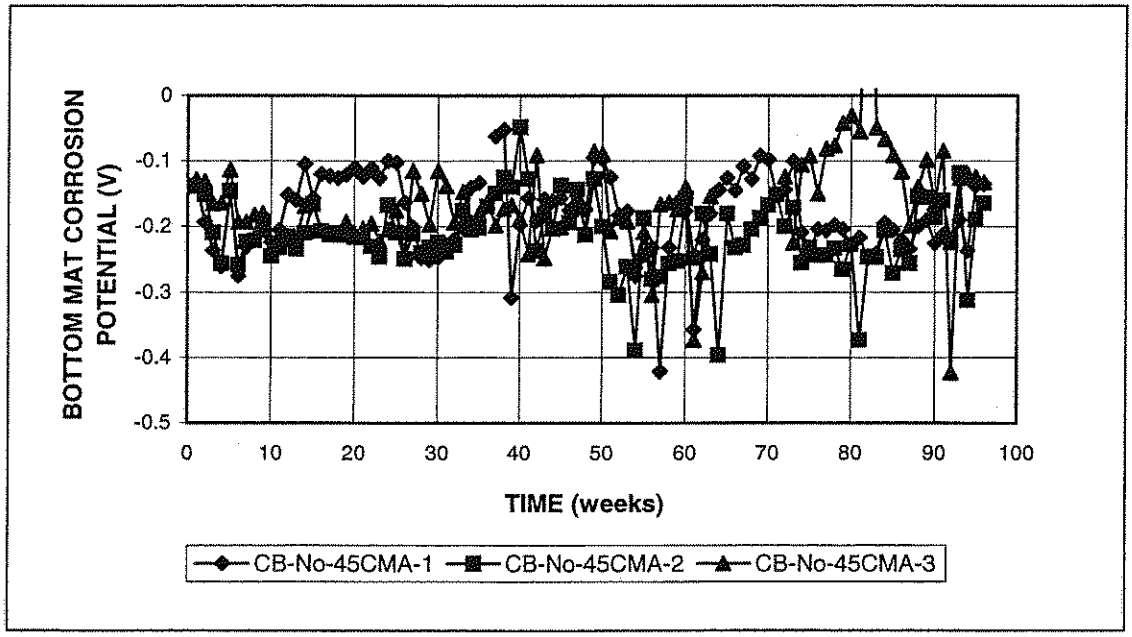

Figure C7.d Cracked Beam Test. Corrosion potential, bottom mat, conventional steel, normalized, no inhibitors, w/c=0.45, 6.04 m ion CMA.

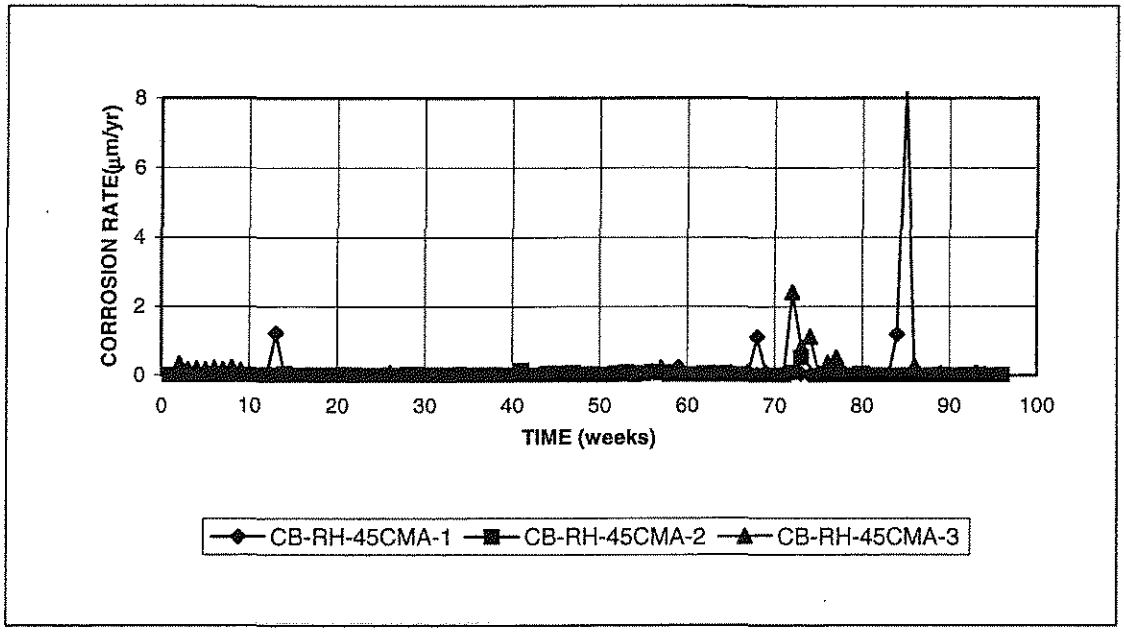

Figure C8.a Cracked Beam Test. Corrosion rate for conventional steel, normalized, Rheocrete, w/c=0.45, 6.04 m ion CMA.

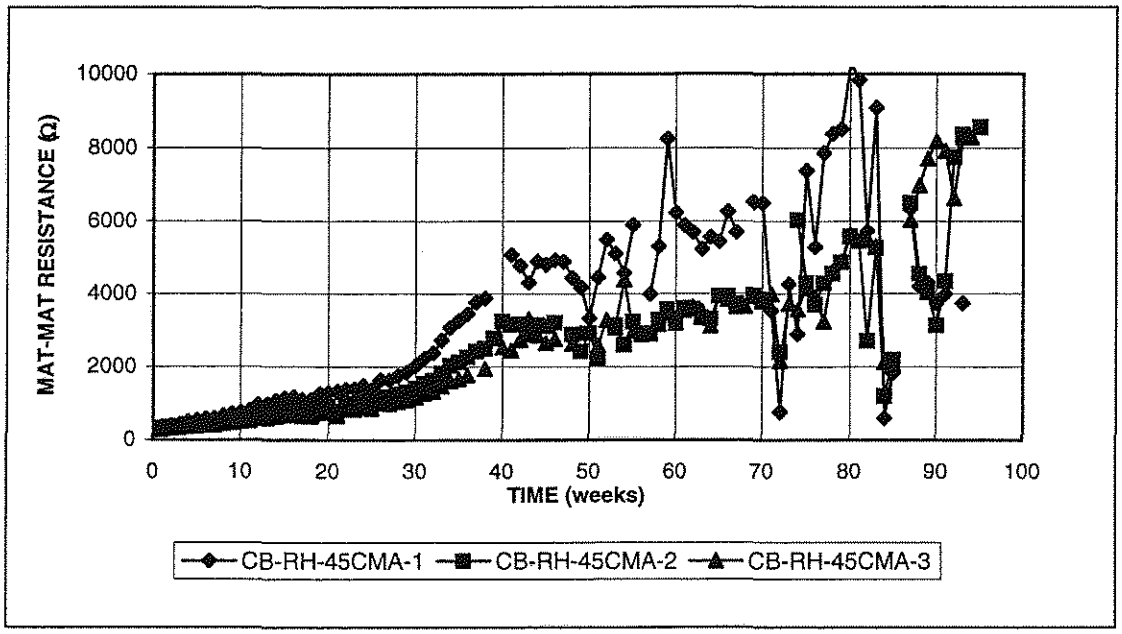

Figure C8.b Cracked Beam Test. Mat-to-mat resistance, conventional steel, normalized, Rheocrete, w/c=0.45, 6.04 m ion CMA.

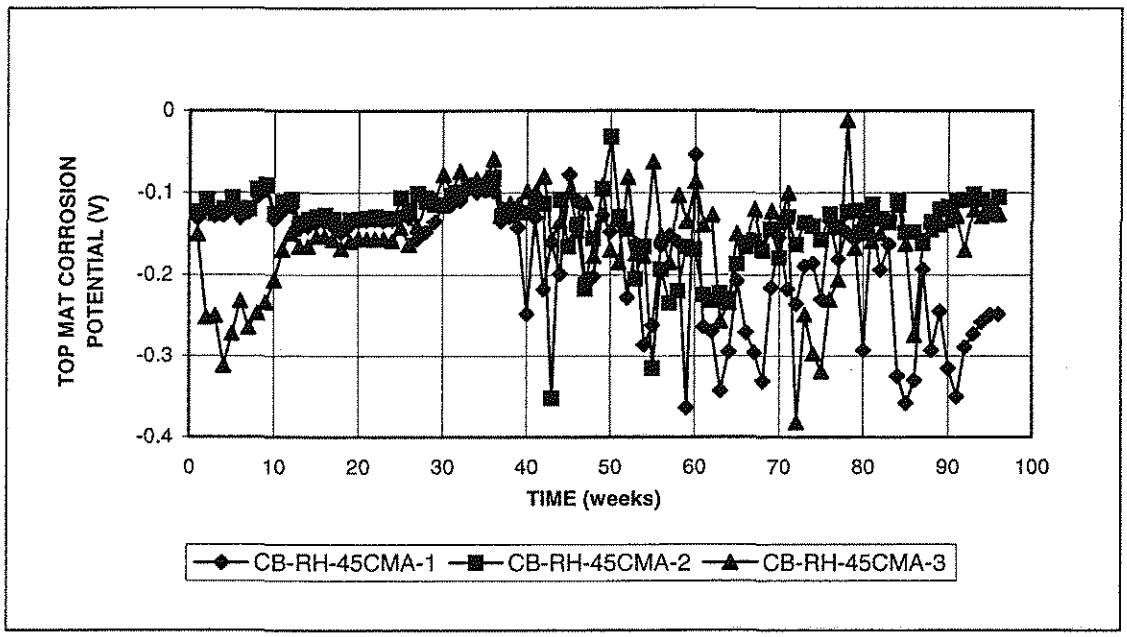

Figure C8.c Cracked Beam Test. Corrosion potential, top mat, conventional steel, normalized, Rheocrete, w/c=0.45, 6.04 m ion CMA.

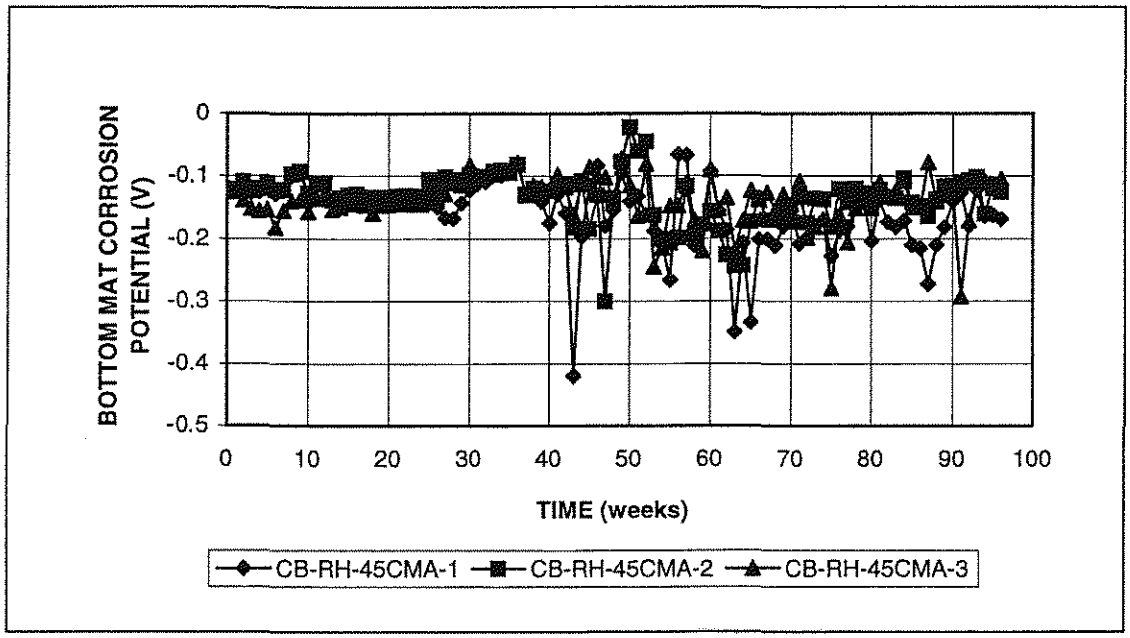

Figure C8.d Cracked Beam Test. Corrosion potential, bottom mat, conventional steel, normalized, Rheocrete, w/c=0.45, 6.04 m ion CMA.

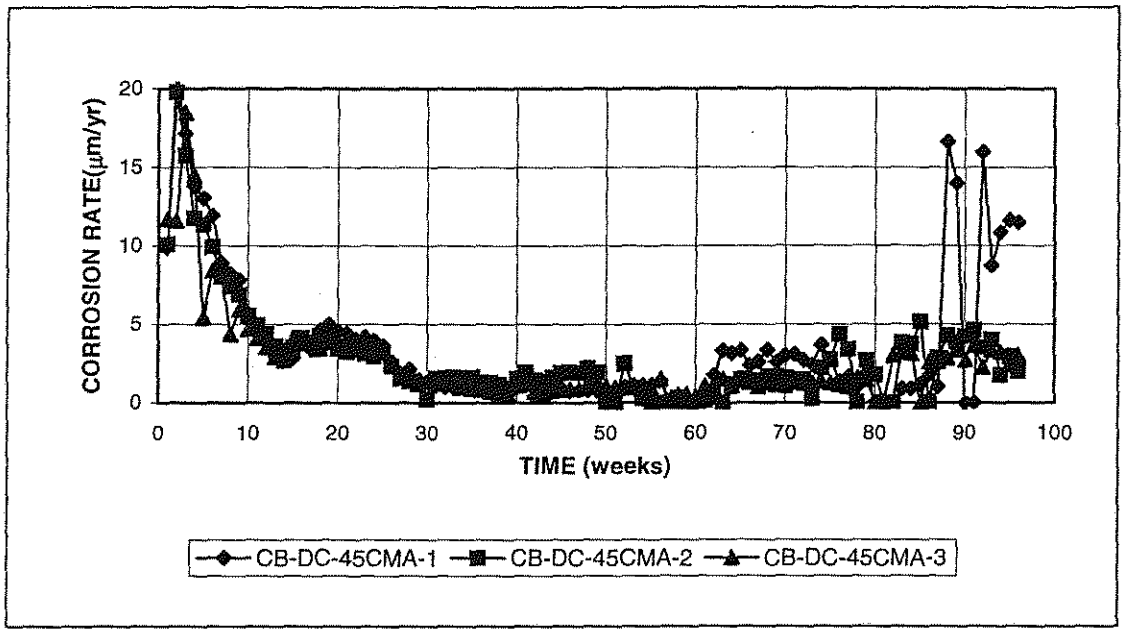

Figure C9.a Cracked Beam Test. Corrosion rate for conventional steel, normalized, DCI-S, w/c=0.45, 6.04 m ion CMA.

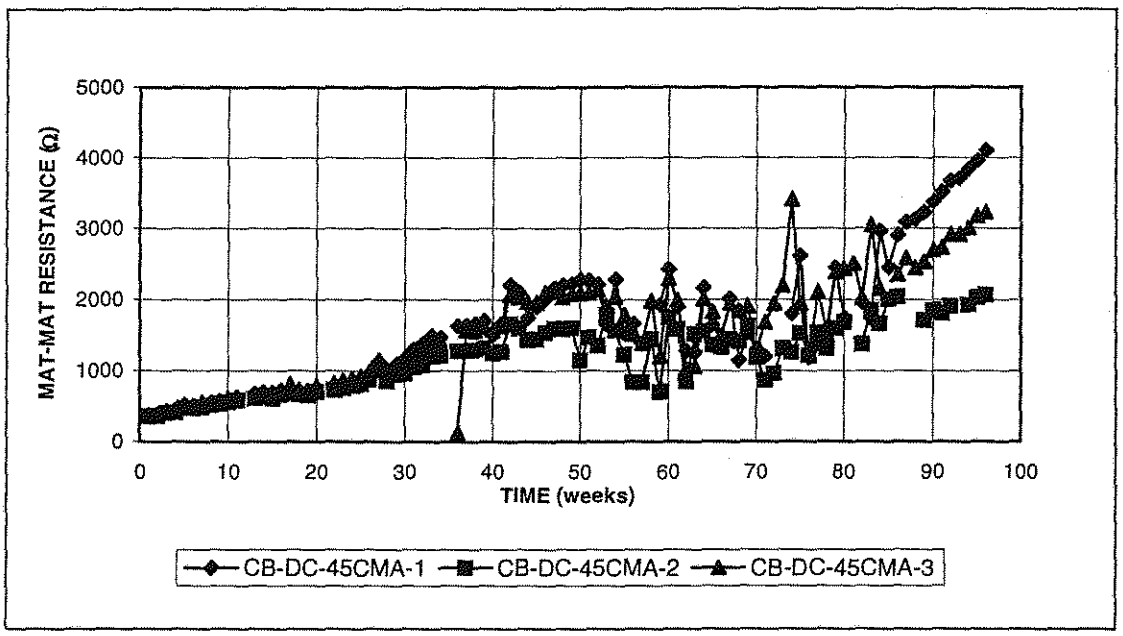

Figure C9.b Cracked Beam Test. Mat-to-mat resistance, conventional steel, normalized, DCI-S, w/c=0.45, 6.04 m ion CMA.

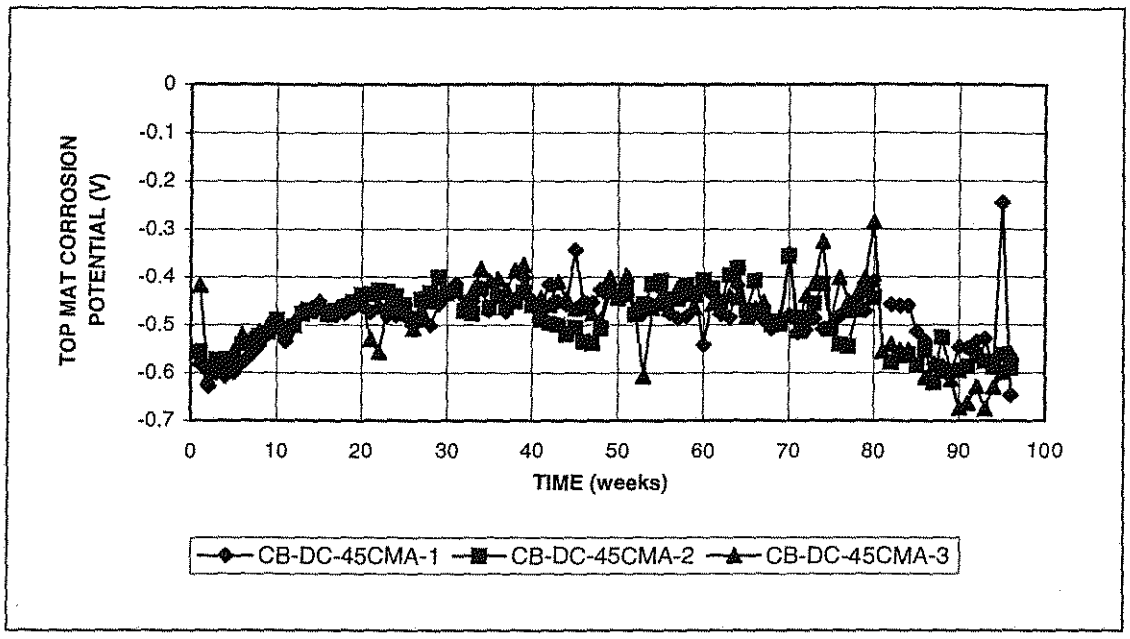

Figure C9.c Cracked Beam Test. Corrosion potential, top mat, conventional steel, normalized, DCI-S, w/c=0.45, 6.04 m ion CMA.

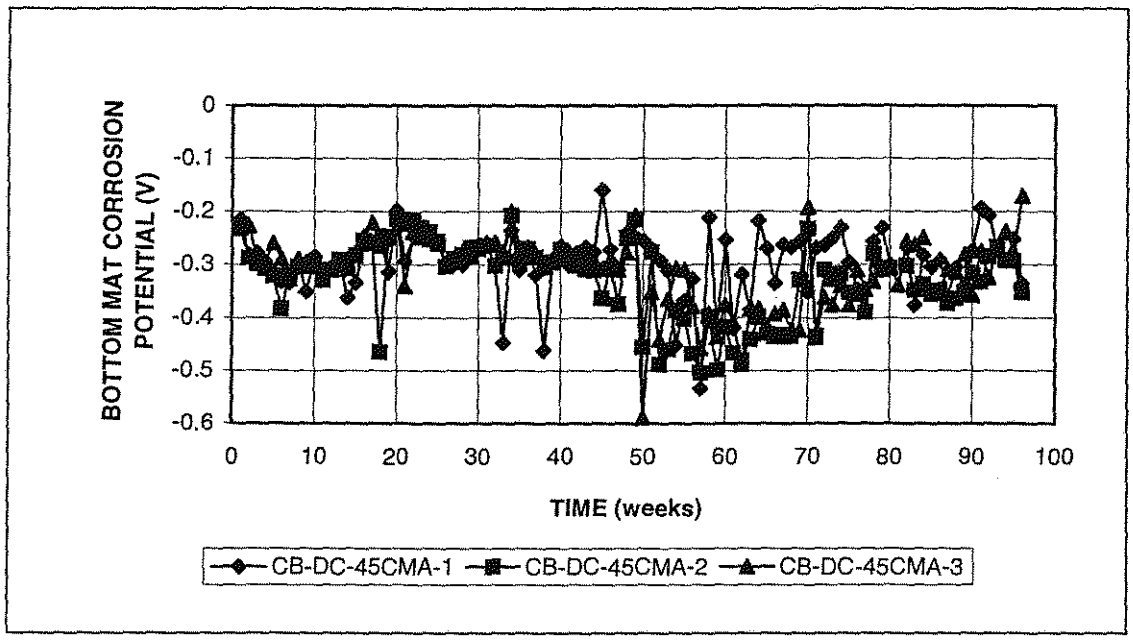

Figure C9.d Cracked Beam Test. Corrosion potential, bottom mat, conventional steel, normalized, DCI-S, w/c=0.45, 6.04 m ion CMA.